2011

SCENARIO SHAKEMAPS FOR OTTAWA, CANADA

Jalpa Davendra Pal

SCENARIO SHAKEMAPS FOR OTTAWA, CANADA

(Spine title: Scenario ShakeMaps for Ottawa, Canada)

(Thesis format: Monograph)

by

Jalpa Devendra Pal

Graduate Program in Geophysics

2

A thesis submitted in partial fulfillment of the requirements for the degree of

Master of Science

The School of Graduate and Postdoctoral Studies

The University of Western Ontario

London, Ontario, Canada

THE UNIVERSITY OF WESTERN ONTARIO

SCHOOL OF GRADUATE AND POSTDOCTORAL STUDIES

CERTIFICATE OF EXAMINATION

Supervisor	Examiners
______________________	______________________
Dr. Gail Atkinson	Dr. Gerhard Pratt
	______________________
Supervisory Committee	Dr. Robert Shcherbakov
______________________	______________________
Dr. Kristy Tiampo	Dr. Hanping Hong

The thesis by

Jalpa Devendra Pal

entitled:

Scenario ShakeMaps for Ottawa, Canada

is accepted in partial fulfilment of the
requirements for the degree of

Master of Science

Date______________   ______________________________

Chair of the Thesis Examination Board

Abstract

Ottawa ranks third among Canadian urban areas in terms of seismic risk. Variability in near surface geology plays an important role in earthquake ground shaking in the region. Scenario ShakeMaps are generated for the Ottawa region to study the expected ground-shaking intensity distribution patterns, for input to damage and risk studies. The quarter wavelength method is used to generate frequency-dependent amplification functions for typical generic soil profiles for National Earthquake Hazard Reduction Program (NEHRP) soil classes using recent data from ~17250 soil profiles. The methodology and amplifications are validated using the ground motion and "Did You Feel It" records from the 2010 **M**5 Val des Bois earthquake, which occurred 60 km from Ottawa. It is noted that the calculated amplifications for typical Ottawa soil profiles are often greater than generic "NEHRP factors" as applied in building code applications.

For a scenario corresponding to ground motions specified by the National Building Code of Canada (NBCC) for a probability level of 2%/50 years, expected Modified Mercalli Intensity (MMI) values in soft-soil areas of Ottawa would be near 7. The impact of event location on expected ground motions and intensities was tested by considering the occurrence of a scenario (a given magnitude event) at various locations in the region. The results of this study may be used as input to seismic risk studies for Ottawa.

Key words: Ottawa, ShakeMaps, amplification.

Acknowledgments

First of all, I would like to thank my supervisor Dr. Gail Atkinson for providing me with this wonderful opportunity and exemplary support throughout this project. I feel really fortunate to have you as my supervisor. All I want to say is: "You are the best".

I also want to thank Dr. Kristy Tiampo for co-supervising this thesis. I owe a deep gratitude to the members of examining committee: Dr. Lalu Mansinha, Dr. Gerhard Pratt, Dr. Robert Shcherbakov and Dr. Hanping Hong for graciously accepting to be on the examining committee, and their support. Your suggestions and comments on my thesis are indeed valuable.

Thank you also extends to Dr. Jim Hunter, Heather Crow and Dr. Dariush Motazedian for sharing the microzation data, also to Katie Ploeger and Katsu Goda who helped me get started with this project. The financial support of NSERC under the Canadian Seismic Risk Network grant is acknowledged.

A special thanks to Ranjeet Nagare, Alireza Babaie Mahani, Javad Kazemian, Karen Assatourians, Meriem Grifi and Marie Burford for helping me improve my defense presentation.

Of course I could not forget the support and help that I received from my awesome friends:

Ranjeet Nagare, who has been extremely supportive to me. Your constructive suggestions were of enormous help to me. I feel blessed to have a friend like you who actually played a role of a family member by always helping me ease my stress, especially after I had moved to a completely new environment.

Alireza Babaie Mahani, for helping me understand the concepts of engineering seismology. I greatly appreciate that you were always more than willing to answer any of my questions.

Nelson Cho and Pathikrit Bhattacharya, for sharing their knowledge with me and also for helping me with some of my MATLAB codes.

Last but not the least, I would like to take this opportunity to tell my parents Dharmika and Devendra Pal that I love you.

Table of Contents

Certificate of Examination ii

Abstract iii

Acknowledgments iv

List of Figures ix

List of Tables xiv

List of Appendices xvi

List of Acronyms xviii

CHAPTER 1

INTRODUCTION 1

1.1 Introduction to ShakeMaps 2

1.1.1. Types of Scenario ShakeMaps 9

1.2 Study Area 11

1.3 Seismicity of the Ottawa region 13

1.4 2010 M5 Val des Bois earthquake 18

1.5 Effect of local geology 20

1.6 Objectives 23

1.7 Software used 24

1.8 Structure of Thesis 24

CHAPTER 2

METHODOLOGY ... 26

2.1 Overview of Methodology ... 27

2.2 Data Collection and Grid Selection ... 28

2.3 Input Ground Motions ... 30

2.3.1 Input ground motions for ShakeMap Category I ... 31

2.3.2 Input ground motions for ShakeMap Category II and III ... 32

2.3.3 Input ground motions for Val des Bois event ... 38

2.4 Local Soil Amplification ... 40

2.4.1. NEHRP Amplification Factors ... 41

2.4.2. Profile-Specific Amplification Factors ... 44

2.4.2.1. Frequency-dependent Linear Amplification Factors ... 44

2.4.2.2. Impact of nonlinearity ... 50

2.4.3. H/V Ratio from Val des Bois event ... 51

2.5 Modified Mercalli Intensity ... 54

2.6 Epicenters for Scenarios ... 55

2.6.1. Postulated Scenario events ... 55

2.6.2. Historic events ... 57

CHAPTER 3

RESULTS AND DISCUSSION ... 60

3.1 M5 Val des Bois ShakeMaps: A Validation Exercise ... 61

3.1.1. Felt Intensities ... 61

3.1.2. Correlation of Felt Intensity and Soil Type ... 64

3.2 Category I ShakeMaps ... 69

3.3 M6 scenarios (Category II and III) ... 70

3.3.1. Local M6 Scenarios: Ground motions ... 70

3.3.2. Local M6 Scenarios: MMI ... 76

3.4 M6.5 and M7.5 Scenarios ... 81

3.5 ShakeMaps for Historic earthquakes ... 83

3.5.1. 1925 M6.2 Charlevoix earthquake ... 83

3.5.2. 1935 M6.1 Timiskaming Earthquake ... 85

3.5.3. 1944 M5.8 Cornwall Earthquake ... 87

3.6 Implications based on past earthquakes and scenarios ... 90

CHAPTER 4

SUMMARY AND CONCLUSIONS ... 92

4.1 Summary ... 93

4.2 Future Recommendations ... 95

BIBLIOGRAPHY ... 98

APPENDICES ... 104

CURRICULUM VITAE ... 171

List of Figures

Figure 1.1. Scenario ShakeMap for M9.0 Cascadia earthquake. Black star shows the epicenter. 4

Figure 1.2. Location and Vs30 map of Ottawa region. 13

Figure 1.3. Map of seismicity of Canada from 1627 to 2007 15

Figure 1.4. Approximate distribution of seismic risk in Canadian cities 16

Figure 1.5. Western Quebec Seismic Zone. 16

Figure 1.6. 13 regional earthquakes around the Ottawa region between 1830 and 2008 that had an impact on the Ottawa region. Circles with diagonal lines have uncertain location of epicenter.. 17

Figure 1.7. Felt intensities for M5 Val des Bois earthquake 18

Figure 1.8. Did You Feel It reports in and around Ottawa region for M5 Val des Bois earthquake. 19

Figure 2.1. Flowchart showing steps used to generate scenario ShakeMaps. 28

Figure 2.2. Spatial distribution of 17251 grid points having soil profile information in Ottawa region, adopted for ShakeMap application 30

Figure 2.4. Uniform hazard spectra for hard-rock sites in Ottawa (2%/50 years) as provided by Adams and Halchuk (2003) for NBCC 2005 compared with Atkinson and Boore (2006) predicted median motions for hard rock for (a) M7 at 25 km, (b) M6.5 at 20 km, (c) M6 at 15 km and (d) M6 at 10 km. 37

Figure 2.5. Fault plane with dip of 50° at 10 km below ground surface from the center of the fault plane. 38

Figure 2.6. Stations that recorded the ground motions for M5 Val des Bois earthquake; Soil sites are sites located on NEHRP C, D and E while rock sites are on NEHRP A and B. 39

Figure 2.7. Input ground motions for M5 Val des Bois event based on decay rate of AB06 (stress drop = 250 bars) 40

Figure 2.9. Density profile for given interval shear wave velocity for soil types in the Ottawa region as per equation 2.3. 45

Figure 2.10. Quality factor (Q) for given interval shear wave velocity for soil types in the Ottawa region as per equation 2.4. 46

Figure 2.11. Typical soil profiles for Ottawa region for all five NEHRP soil classes showing post-glacial, glacial and bedrock thicknesses. 48

Figure 2.12. (a) Profile-specific linear soil amplification functions developed in this study using SITE_AMP (Boore, 2000) for (b) typical representative soil profiles of Ottawa. NBCC factors Fa and Fv (relative to A) are also shown in black and grey symbols respectively. 49

Figure 2.13. Soil amplification estimated using the H/V ratios from (a) Val des Bois earthquake recorded on 7 stations in Ottawa, and (b) average H/V from multiple events for site classes, from many stations across south-eastern Canada. 53

Figure 2.14. Epicentral locations for M6 scenarios in Ottawa region, overlaid on Vs30 map. Epicenters are shown by black stars and are numbered in white circles 57

Figure 2.15. Epicentral locations for higher magnitudes at greater distances (M6.5D60 and M7.5D460), and historic event scenarios, with respect to Ottawa region 59

Figure 3.1. Felt intensities of M5 Val des Bois earthquake in Ottawa region as per "Did

You Feel It" (DYFI) reports; averaged over boxes of approx. 1.5 km^2 area, for number of reports greater than 3. 61

Figure 3.2. Vs30 Map of Ottawa region overlaid on approx. 1.5 km^2 grid 62

Figure 3.3. Felt intensities in Ottawa region as per 2412 number of DYFI reports for M5 Val des Bois earthquake averaged over boxes of approx. 1.5 km^2 grids and overlaid on the Vs30 map of Ottawa region 63

Figure 3.4. Correlation of PGV vs. Vs30 for the Ottawa region for M5 Val des Bois earthquake. 64

Figure 3.5. Predicted intensities for Val des Bois earthquake in Ottawa region for average MMI based on PSA 3, 1 and 0.5 Hz using profile-specific amplification factors. 65

Figure 3.6. Difference of felt intensities and predicted average MMI based on PSA 3, 1 and 0.5 Hz (profile-specific amplification factors) for M5 Val des Bois earthquake. 67

Figure 3.7. Error bounds for predicted MMI at (a) PSA at 3 Hz, (b) PSA at 1 Hz, (c) PSA at 0.5 Hz and (d) PSA at average of 3, 1 and 0.5 Hz 68

Figure 3.9. PSA at 3 Hz for epicenter in soft soil using the NBCC 2005 amplification factors. 71

Figure 3.10. PSA at 3 Hz for epicenter in soft soil using the site-specific amplification factors. 71

Figure 3.11. PSA at 1 Hz for epicenter in Hull area using the NBCC 2005 amplification factors. 74

Figure 3.12. PSA at 1 Hz for epicenter in Hull area using the site-specific amplification factors. 74

Figure 3.13. MMI based on PGV for **M**6 scenario located on hard rock, south of the Ottawa region using NBCC 2005 amplification factors. 77

Figure 3.14. MMI based on PGV for **M**6 scenario located on hard rock, south of the Ottawa region using site-specific amplification factors. 77

Figure 3.15. MMI based on PSA at 3 Hz for **M**6 scenario located on hard rock, south of the Ottawa region using NBCC 2005 amplification factors. 78

Figure 3.16. MMI based on PSA at 3 Hz for **M**6 scenario located on hard rock, south of the Ottawa region using site-specific amplification factors. 78

Figure 3.17. PSA at 3 Hz for **M**6.5 scenario using site-specific amplification factors. The epicenter for this event is approximately 60 km North. 82

Figure 3.18. MMI based on PGV for **M**6.5 scenario using site-specific amplification factors. 82

Figure 3.19. MMI based on PGV for **M**7.5 scenario using site-specific amplification factors. The epicenter for this event is located approximately 460 km away in Charlevoix Seismic Zone. 83

Figure 3.20. Isoseismal map for entire Eastern North America for 1925 Charlevoix earthquake.. 84

Figure 3.21. Predicted MMI based on PGV at median ground motions for 1925 Charlevoix earthquake using profile-specific amplification factors. 85

Figure 3.22. Isoseismal map for entire Eastern North America for 1935 Timiskaming earthquake.. 86

Figure 3.23. Predicted MMI based on PGV at median ground motions for 1935 Timiskaming earthquake using profile-specific amplification factors. 87

Figure 3.24. Isoseismal map for 1944 Cornwall earthquake... 88

Figure 3.25. Predicted MMI based on PGV at median ground motions for 1944 Cornwall earthquake using profile-specific amplification factors. 89

List of Tables

Table 1.1. Description of MMI.. 5

Table 1.2. NEHRP soil classification 12

Table 2.1. Input ground motion parameters for Category I ShakeMaps (AH03). The ground motions for Ottawa are given for site class C. 32

Table 2.2. Details of input ground motions, local soil amplification and MMI estimation approaches for all three categories of ShakeMaps. 36

Table 2.3. NBCC 2005 recommended NEHRP amplification factors Fa for short periods (T = 0.2s) 43

Table 2.4. NBCC 2005 recommended NEHRP amplification factors Fv for long periods (T = 1.0s) 43

Table 2.5. Coefficients of equation 2.5 for predicting frequency dependent profile-specific amplification factors for all five NEHRP soil classes. 50

Table 2.6. Coefficients of Equation 2.6 to predict MMI from Instrumental Ground-Motion Parameters 55

Table 2.7. Details of the historic earthquake studied.. 58

Table 3.1. Ground motions range for all the ground motion parameters for Epicenter 1 and 2. 73

Table 3.2. Ground Motions range for all the ground motion parameters for Epicenter 3 and 4. 75

Table 3.3. Range of predicted MMI for Epicenters 1 and 2 of ShakeMap Categories II and III based on median ground motions; intensities could be ± 1 based on one std deviation. 79

Table 3.4. Range of predicted MMI for Epicenters 3 and 4 of ShakeMap Categories II and III based on median ground motions; intensities could be ± 1 based on one std deviation. 80

Table 3.5. Comparison of felt and predicted MMI for median ground motions in the Ottawa region for historic events. 90

List of Appendices

APPENDIX I

Category I ShakeMaps: Ground motions based on NBCC 2005 104

APPENDIX II

ShakeMaps for M5 Val des Bois Earthquake 108

APPENDIX III

Category II ShakeMaps: Ground motions and MMI for Epicenter 1 112

APPENDIX IV

Category II ShakeMaps: Ground motions and MMI for Epicenter 2 118

APPENDIX V

Category II ShakeMaps: Ground motions and MMI for Epicenter 3 124

APPENDIX VI

Category II ShakeMaps: Ground motions and MMI for Epicenter 4 130

APPENDIX VII

Category III ShakeMaps: Ground motions and MMI for Epicenter 1 136

APPENDIX VIII

Category III ShakeMaps: Ground motions and MMI for Epicenter 2 142

APPENDIX IX

Category III ShakeMaps: Ground motions and MMI for Epicenter 3 148

APPENDIX X

Category III ShakeMaps: Ground motions and MMI for Epicenter 4 154

APPENDIX XI

Category III ShakeMaps: Ground motions and MMI for M6.5 and M7.5 Scenarios 160

List of Acronyms

AB06	Atkinson and Boore (2006)
AH03	Adams and Halchuk (2003)
BA08	Boore and Atkinson (2008)
BSSC	Building Seismic Safety Council
CSRN	Canadian Seismic Risk Network
DYFI	Did You Feel It?
GMPE	Ground Motion Prediction Equation
GSC	Geological Survey of Canada
H/V	Horizontal-to-vertical component ratio
M	Moment magnitude
MMI	Modified Mercalli Intensity
NAD	North American Datum
NBCC	National Building Code of Canada
NEHRP	National Earthquake Hazard Reduction Program
NRCan	Natural Resources Canada
PGA	Peak Ground Acceleration
PGV	Peak Ground Velocity
PSA	Pseudo Spectral Acceleration
PSHA	Probabilistic Seismic Hazard Analysis
Rcd	Closest distance to the fault
SITE_AMP	Boore's site amplification program
UHS	Uniform Hazard Spectrum
USGS	United States Geological Survey
V_s	Shear Wave Velocity
Vs_{avg}	Average Shear wave velocity

Vs30	Time-averaged shear wave velocity over top 30m
Q	Quality factor

CHAPTER 1

INTRODUCTION

"Out of compassion I destroy the darkness of their ignorance. From within them I light the lamp of wisdom and dispel all darkness from their lives." - Bhagvad Gita

1.1 Introduction to ShakeMaps

Earthquakes cause a lot of damage to property and life. Earthquakes result from the sudden release of stored energy in the Earth's crust which creates seismic waves that lead to ground shaking and displacement. Earthquakes can trigger slope failures, soil liquefaction, ground cracking, etc. on land and tsunamis in oceans. Most damage is caused by strong ground shaking, which can produce great damage to infrastructure (e.g., buildings, oil and water supply pipelines, roads, bridges, dams) and lead to huge loss of life. While it is difficult to predict precisely when earthquakes will strike, it is possible to predict where they will be most destructive by identifying features and areas of high risk (Lang, 1998). Earthquakes will cause most damage in metropolitan areas given the high density of population and infrastructure. The process of earthquake hazard assessment, which is the first step of risk assessment, includes determination of expected levels of earthquake induced ground shaking, including the effects of local soil amplification and the potential for liquefaction and slope instability. Hazard estimates delineated based on such analyses, need to be presented in a form easily understandable even to the untrained eye. One way of doing this is creating regional maps of ground shaking, liquefaction potential and slope stability in units to which a common observer can relate with ease.

Maps generated to graphically represent ground shaking intensity are called ShakeMaps (Wald *et al.,* 1999a). This form of representation makes it easier to relate the recorded ground motions to the expected felt and damage distribution. ShakeMaps have attained widespread usage because of their easy-to-understand format for presentation of the impact of earthquakes to varied audiences, including scientists, businesses, emergency response agencies, media, and the general public (Wald *et al.,* 1999a). ShakeMap was first developed for earthquakes in southern California as part of the TriNet Project, a joint effort by the U.S. Geological Survey (USGS), California Institute of Technology (Caltech), and the California Geological Survey (CGS) (Wald *et al.,* 1999).

ShakeMaps can be classified into real-time and scenario ShakeMaps. Real-time ShakeMaps are those that are generated within a couple of minutes of occurrence of any event. Scenario ShakeMaps are generated to predict expected ground shaking patterns for a given "scenario" earthquake, allowing inference of damage and other effects. A scenario ShakeMap is not a prediction of earthquake occurrence, but a projection of consequences for a hypothetically selected magnitude and location of a possible event. It answers questions like: what would be the damage patterns/shaking intensities if a particular magnitude of earthquake would occur at a particular location? Scenario ShakeMaps have applications in earthquake engineering, seismological research, planning for emergency response, utilities, public information and education (Wald *et al.,* 2007). While no scenario will prove accurate in detail, scenario ShakeMaps are useful for providing a regional pattern of expected damage, and to give a better understanding of earthquake hazards; this is a first step towards developing earthquake response plans. Figure 1.1 shows a sample scenario ShakeMap for the west coast of North America generated by the USGS for a moment magnitude (**M**) 9 Cascadia mega-thrust event. The map projects strong shaking over a large area, with shaking above the damage threshold Modified Mercalli Intensity (MMI) 6 (Wood and Neumann 1931; Dewey *et al.* 1995) within about 100 km of the coast line. The description of MMI and its meaning in terms of felt effects is given in Table 1.1.

-- Earthquake Planning Scenario --
ShakeMap for Casc9.0 Scenario
Scenario Date: JUL 16 2009 09:00:00 PM PST PST M 9.0 N45.00 W124.50 Depth: 10.0km

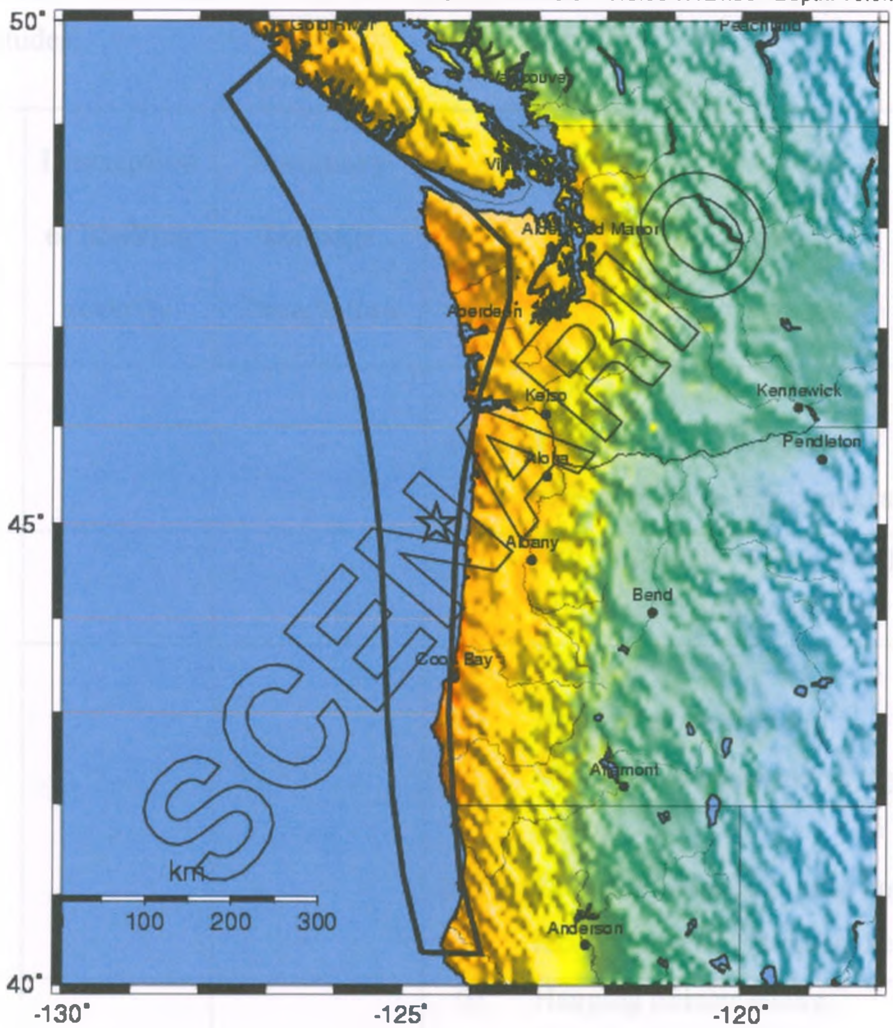

PLANNING SCENARIO ONLY -- Map Version 3 Processed Tue Sep 29, 2009 03:43:47 PM MDT

PERCEIVED SHAKING	Not felt	Weak	Light	Moderate	Strong	Very strong	Severe	Violent	Extreme
POTENTIAL DAMAGE	none	none	none	Very light	Light	Moderate	Moderate/Heavy	Heavy	Very Heavy
PEAK ACC.(%g)	<.17	.17-1.4	1.4-3.9	3.9-9.2	9.2-18	18-34	34-65	65-124	>124
PEAK VEL.(cm/s)	<0.1	0.1-1.1	1.1-3.4	3.4-8.1	8.1-16	16-31	31-60	60-116	>116
INSTRUMENTAL INTENSITY	I	II-III	IV	V	VI	VII	VIII	IX	X+

Figure 1.1. Scenario ShakeMap for M9.0 Cascadia earthquake. Black star shows the epicenter (source: http://earthquake.usgs.gov/earthquakes/shakemap/global/shake/Casc9.0_se/; accessed July 26, 2010).

Table 1.1. Description of MMI (http://www.abag.ca.gov/bayarea/eqmaps/doc/mmi.html). Note that Roman numerals are used to describe intensities in order to distinguish them from magnitudes.

MMI Value	Description of Shaking severity	Summary Damage Description	Full Description
I			(i) Not felt. (ii) Marginal and long period effects of large Earthquakes.
II			(i) Felt by persons at rest, on upper floors or favorably placed.
III			(i) Felt indoors. (ii) Hanging objects swing. Vibration like passing of light trucks. (iii) Duration estimated. May not be recognized as an earthquake.
IV			(i) Hanging objects swing. (ii) Vibration like passing of heavy trucks; or sensation of a jolt like a heavy ball striking the walls. (iii) Standing motor cars rock. (iv) Windows, dishes, doors rattle. (v) Glasses clink; Crockery clashes. (vi) In the upper range of IV, wooden walls and frame creak.
V	Light	Pictures	(i) Felt outdoors; direction

		Move	estimated. (ii) Sleepers wakened. (iii) Liquids disturbed, some spilled. (iv) Small unstable objects displaced or upset. (v) Doors swing – close and open; shutters, pictures move. (vi) Pendulum clocks stop, start, change rate.
VI	Moderate	Objects Fall	(i) Felt by all; Many frightened and run outdoors, walk unsteadily. (ii) Windows, dishes, glassware broken. (iii) Knickknacks, books, etc., off shelves; Picture off walls. (iv) Furniture moved or overturned. (v) Weak plaster and masonry D cracked. (vi) Small bells ring (church, school). (vii) Trees, bushes shaken (visibly, or heard to rustle).
VII	Strong	Nonstructural Damage	(i) Difficult to stand; Noticed by drivers of motor cars. (ii) Hanging objects quiver. (iii) Furniture broken. (iv) Damage to masonry D, including cracks; Weak chimney broken at roof line.

			(v) Fall of plaster, loose bricks, stones, tiles, cornices (also unbraced parapets and architectural ornaments). (vi) Some cracks in masonry C. (vii) Waves on ponds; water turbid with mud. (viii) Small slides and caving in along sand or gravel banks. (ix) Large bells ring. (x) Concrete irrigation ditches damaged.
VIII	Very Strong	Moderate Damage	(i) Steering of motor cars affected. (ii) Damage to masonry C; partial collapse; some damage to masonry B; none to A. (iii) Fall of stucco and some masonry walls. (iv) Twisting, fall of chimneys, factory stacks, monuments, towers, elevated tanks. (v) Frame houses moved on foundations if not bolted down; loose panel walls thrown out. (vi) Decayed piling broken off. (vii) Branches broken from trees. (viii) Changes in flow or temperature of springs and wells. (ix) Cracks in wet ground and on steep slopes.

IX	Violent	Heavy Damage	(i) General panic. (ii) Masonry D destroyed; masonry C heavily damaged, sometimes with complete collapse; masonry B seriously damaged (General damage to foundations). (iii) Frame structures if no bolted, shifted off foundations; Frames racked. (iv) Serious damage to reservoirs. (v) Underground pipes broken. (vi) Conspicuous cracks in ground. In alluvial areas sand and mud ejected, earthquake fountains, sand craters.
X	Very Violent	Extreme Damage	(i) Most of the masonry and frame structures destroyed with their foundations. (ii) Some well-built wooden structures and bridges destroyed; Serious damage to dams, dikes, embankments. (iii) Large landslides. (iv) Water thrown on banks of canals, rivers, lakes, etc. (v) Sand and mud shifted horizontally on beaches and flat land. Rails bent slightly.

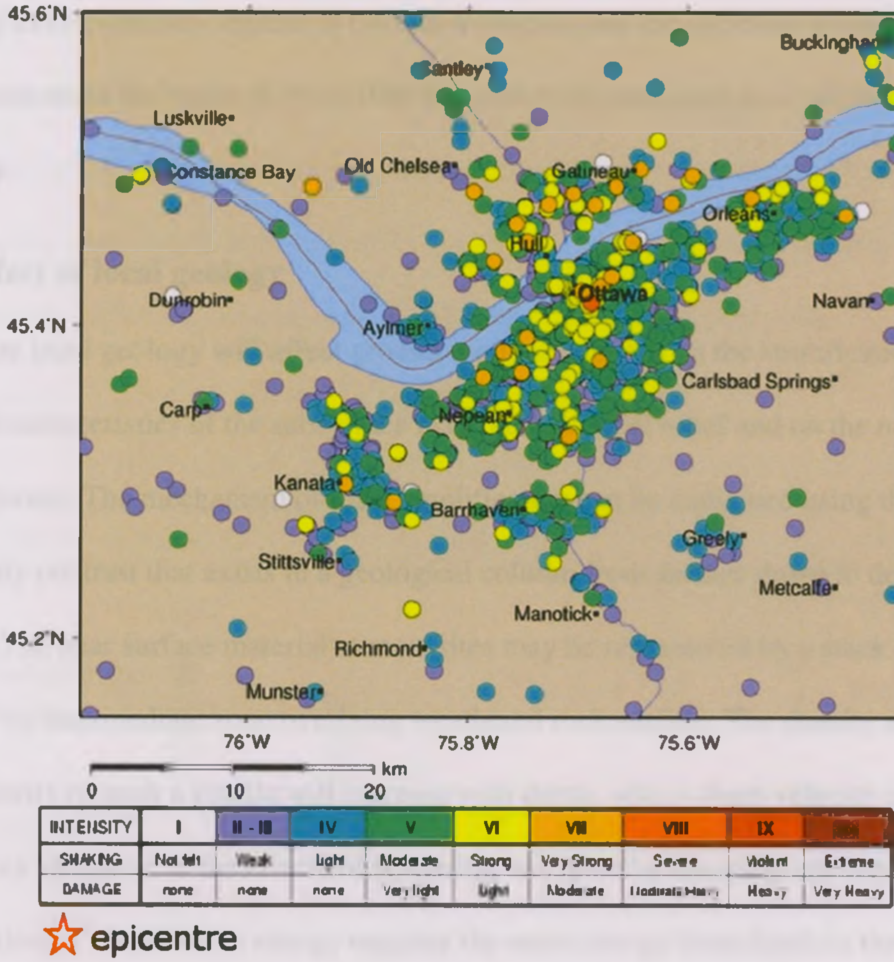

Figure 1.8. Did You Feel It reports in and around Ottawa region for M5 Val des Bois earthquake (Source: http://earthquakescanada.nrcan.gc.ca/recent_eq/2010/20100623.1741/dyfi-eng.php#OTT; accessed on 23.09.2010).

This event caused minor damage to several structures in the epicentral area, including a badly damaged church steeple, and cracked and fallen masonry (CBC news, June 23, 2010; Atkinson and Assatourians, 2010); windows were broken 60 km away in the Ottawa city hall, and many buildings were evacuated (Atkinson and Assatourians, 2010). There was also some road and bridge damage in the epicentral area. Given the dataset of DYFI intensity reports in the Ottawa region and the recorded ground motions on 111 stations in the range of 58 to 1000 km, this event was used as a validation case in this study.

1.5 Effect of local geology

How local geology will affect ground motions depends on the stratification and physical characteristics of the subsurface materials, on local relief and on the nature of seismic waves. The mechanism of local amplification can be explained using the velocity and density contrast that exists in a geological column from surface down to deep bedrock. The near surface material at most sites may be represented by a stack of soil followed by intermediate zone overlying weathered rock surface. The density and shear wave velocity of such a profile will increase with depth, with a sharp velocity contrast of the bedrock interface. If the effects of scattering and material damping are neglected, the conservation of elastic wave energy requires the wave energy from depth to the ground surface to be constant. Thus as the shear wave velocity decreases while the waves travel through the near surface materials, the waves slow down resulting in the increase of their amplitudes. The role of local site conditions in amplifying ground motions is well know from past earthquakes like the 1980 Kentucky, 1985 Mexico, 1994 Northridge and 1999 Chi Chi earthquakes (Woolery *et al.*, 2008; Seed *et al.*, 1988; Field, 1997; Huang *et al.*, 2000). For example, the magnitude 8 Mexico earthquake of 1985 caused only moderate damage in the vicinity of its epicenter but caused extensive damage at 350 km from the epicenter in the areas of deep soft soils in Mexico City (Dobry and Vucetic, 1987). Structural damage in Mexico city was highly selective; large parts of the city experienced no damage while other areas suffered pronounced damage. The greatest damage occurred in those portions of the Lake Zone, a deep soft basin, underlain by 38 to 50 m of soft soil (Stone et al., 1987), where characteristic frequencies were estimated to be 0.35 to 0.5 Hz. Within this area, damage to buildings less than five stories and modern buildings greater than 30 stories was slight; buildings of 7 – 14 storeys, with resonant frequencies matching that of the soil column, were heavily damaged (Stone et al., 1987).

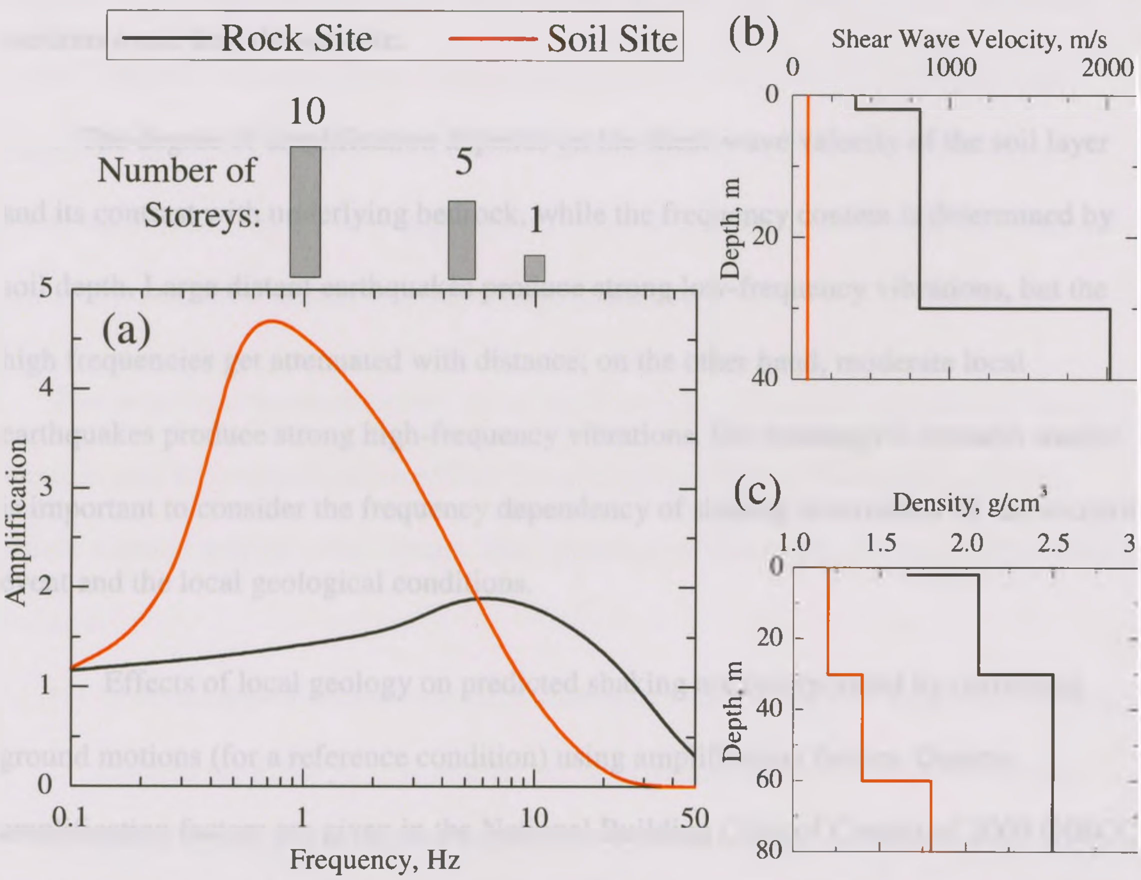

Figure 1.9. (a) An example of amplification functions of rock (stiff) and soil (soft) sites generated using SITE_AMP program (Boore, 2005). The amplification functions were developed from (b) shear wave velocity and (c) density profiles chosen for two locations in Ottawa.

Figure 1.9 shows an example amplification for a rock site and a soil site in Ottawa (Amplifications have been calculated using SITE_AMP program, discussed in detail in section 2.4; Boore, 2005). There is a difference of factor of 10 in shear wave velocities of soil site and rock, as referred to in Figure 1.9, at 30 m depth (Figure 1.9b). The differences in amplification functions of these two sites are shown in Figure 1.9a. The soil site, which is a softer material, amplifies the low frequency ground motions of the seismic waves more than the rock site, whereas the rock site amplifies the high frequency motions more than the soil site.

The degree of amplification depends on the shear-wave velocity of the soil layer and its contrast with underlying bedrock, while the frequency content is determined by soil depth. Large distant earthquakes produce strong low-frequency vibrations, but the high frequencies get attenuated with distance; on the other hand, moderate local earthquakes produce strong high-frequency vibrations. For meaningful scenario studies, it is important to consider the frequency dependency of shaking determined by the scenario event and the local geological conditions.

Effects of local geology on predicted shaking are incorporated by correcting ground motions (for a reference condition) using amplification factors. Generic amplification factors are given in the National Building Code of Canada of 2005 (NBCC 2005) based just on National Earthquake Hazard Reduction Program (NEHRP) site-class. Alternatively, frequency dependent amplification factors can be calculated for a given geology using the Quarter Wavelength method of Boore and Joyner (1997). In this study, frequency dependent amplification functions were generated using SITE_AMP program

(Boore, 2000) based on the Quarter Wavelength method as discussed in detail in Chapter 2 (section 2.4).

1.6 Objectives

Ottawa is Canada's capital city with high population density in the downtown and outlying areas. Historical buildings in Ottawa and on Parliament Hill are an integral part of Canadian heritage. The likely effects of moderate earthquakes in or close to Ottawa need to be known for emergency planning and response. Historically, a 10-50 m thick basin filled with unconsolidated deposits in downtown Ottawa has had the greatest frequency of experiencing MMI 6 and 7 (Lamontagne, 2010). However, the impact of future earthquakes on the now populated Orleans area, which mostly was farmland and sits on deep soft soil deposits, remains largely unknown.

This is the first research project to comprehensively model both expected ground motions and their amplification effects through soil profiles in the Ottawa region to obtain detailed scenario ShakeMaps. The objectives of this study can be broadly stated as follows:

(1) Generating probabilistic scenario ShakeMaps to understand the ground shaking patterns for a 2%/50 year probability of exceedance event for Ottawa region.

(2) Understanding the effect of epicentral locations (distance and type of geology) on differences in shaking intensity in the areas with high density populations (e.g., downtown Ottawa) and in the areas with soft soils (e.g., Orleans area).

(3) Comparing differences in predictions using NBCC amplification factors and frequency dependent amplification functions based on Quarter Wavelength method; the latter are specific to the types of soil profiles found in Ottawa.

(4) To study the impacts of higher magnitude events at greater distances on the downtown core and populated areas located on thick deposits of soft sediments (Orleans, Ottawa is now densely populated and sits on a 140 m thick soft sediments. It is not known how a moderate earthquake would affect this area as it was mostly farmland when the historic events occurred).

The methodology used in this study for generating ShakeMaps was validated by comparing the predicted intensities with DYFI reports of **M**5 Val des Bois event. In addition, the amplification functions developed using the Quarter Wavelength method for Ottawa were also compared with the amplification factors calculated from horizontal-to-vertical (H/V) ratio of recorded ground motions of this event.

1.7 Software used

Calculations were done in MATLAB v.2007b. Data management was done in MS Excel 2007. ShakeMaps were generated in ArcGIS 9.2.

1.8 Structure of Thesis

This thesis is structured in four chapters and 11 appendices. Chapter One introduces the ShakeMap terminology and basics pertaining to scenario ShakeMaps. The seismicity and history of earthquakes in the Ottawa region including the recent **M**5 Val des Bois event are briefly discussed. The chapter ends with a discussion on effects of local soil conditions on amplification of ground motions and objectives of the thesis.

Chapter Two opens with an overview of methodology to generate scenario ShakeMaps used in this study. Methodology used for developing (a) Category I, II and III scenario ShakeMaps, (b) ShakeMaps for **M**5 Val des Bois event, and (c) ShakeMaps for historic events is described. This is followed by discussions on input ground motions for all ShakeMaps, methodology of scenario event selection, amplification factors based on NBCC (2005), quarter wavelength method and H/V ratio method (for the Val des Bois event), introduction to and methodology for calculation of Modified Mercalli Intensity (MMI), and locations of epicenters and reasoning behind the choice of locations.

Results and discussions of predictions of ground motions and MMI for different local **M**6 scenarios, comparison between predictions based on NBCC (2005) and quarter wavelength amplification factors, scenarios of higher magnitudes (**M**6.5 and **M**7.5) at greater distances, and implications based on predicted intensities constitutes the Third Chapter in this thesis. Summary of the entire work, significant results, and recommendations for future work are given in Chapter Four. Appendix I consists of Category I ShakeMaps, Appendix II has the maps for **M**5 Val des Bois event, Appendices III to VI contain Category II ShakeMaps for four different epicenters, Appendices VII to X contain Category III ShakeMaps for four different epicenters, Appendix XI is made up of ShakeMaps for higher magnitude scenarios.

CHAPTER 2

METHODOLOGY

"Everything should be as simple as it is, but not simpler." – Albert Einstein

2.1 Overview of Methodology

To generate a scenario ShakeMap, we first define a grid of points over the region of interest. At each grid point the expected peak ground motions for a given earthquake scenario are calculated for a reference site condition. In this study, GMPEs given by Atkinson and Boore (2006) for ENA were used to relate peak ground motions to specified earthquake magnitude and distance. The peak ground motions were defined for a reference site of NEHRP Class A (hard rock). Then, amplification factors were used to correct for the local soil conditions at each grid point. Soft soils amplify motions at low frequencies, while providing damping at high frequencies, with the frequency range of the effect being dependant on soil depth. MMI was then calculated from ground motions using empirical relationships. Different empirical relations have been developed to correlate MMI with ground motions in different regions. The empirical relationships of Atkinson and Kaka (2007) were used to estimate MMI in this study.

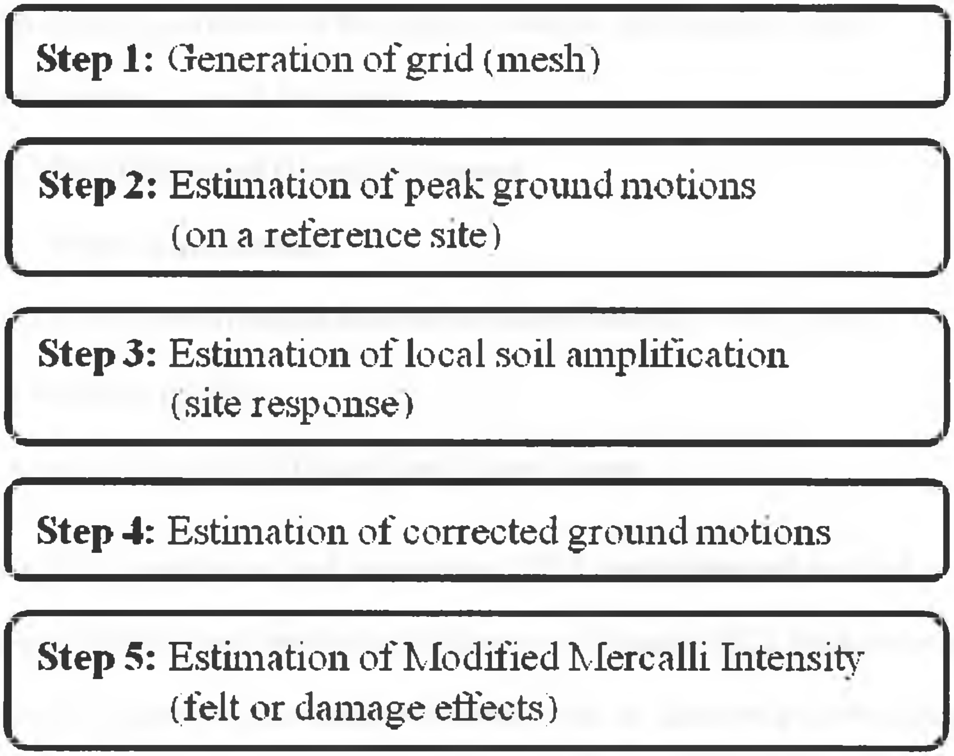

Figure 2.1. Flowchart showing steps used to generate scenario ShakeMaps.

Figure 2.1 shows the flow chart describing the methodology in general form used in this study to develop ShakeMaps. Three categories of ShakeMaps were developed in this study. The details of empirical relations used to estimate ground motions and MMI, and the approach used to correct the local soil amplification for all three categories are listed in Table 2.1 and discussed in section 2.3, 2.4, and 2.5.

ShakeMaps for the 2010 **M**5 Val des Bois event were generated following the same procedure as described above. The reports within the Ottawa region were averaged over boxes representing ~1.5 km^2 area; boxes with less than three reports were ignored.

2.2 Data Collection and Grid Selection

The following data were collected at the start of the study:

1. Geographical co-ordinates of the region of interest and boundary points.
2. Soil parameters for each data point:
    2.1 Post-Glacial and Glacial thicknesses
    2.2 Depth to the bedrock
    2.3 Travel time averaged shear wave velocity over top 30 m (Vs30)
    2.4 Density profiles
3. Location and magnitude of significant historic events.

Geographical co-ordinates, soil parameters (17251 data points) and surficial elevations were obtained from the Geological Survey of Canada (GSC). Background data in form of ArcGIS shapefiles was obtained from the Serge A. Sauer Map Library located at the University of Western Ontario (DMTI CanMap RouteLogistics v2008.3). Locations of significant historic events were obtained from National Resources Canada (2010a), Bent (2009) and Lamontagne (2010). The soil data are required to estimate the soil amplification functions (discussed in section 2.4.2). Figure 2.2 shows the 17251 data points having soil information; note the spatially non-uniform grid. These data points were obtained from the GSC and compiled from 15011 water wells, 899 boreholes and 1341 engineering logs (Hunter, per. comm., 2009; Hunter *et al.*, 2010). A grid of spatially uniform data points is generally recommended to generate ShakeMap. However, the non-uniform grid was adopted in this study because of the variability of density of data points over the entire region. Also, it was found that interpolation to generate a uniform grid created undesirable spatial distribution of soil conditions due to complex geological settings.

Figure 2.2. Spatial distribution of 17251 grid points having soil profile information in Ottawa region, adopted for ShakeMap application (Source: Hunter, per. comm.., 2009; Hunter *et al.,* 2010).

2.3 Input Ground Motions

Three parameters are used to describe the amplitude of ground shaking:

1. Peak Ground Acceleration (PGA): This is the maximum acceleration experienced by any particle on the ground during earthquake shaking.
2. Peak Ground Velocity (PGV): This is the maximum velocity experienced by any particle on the ground during earthquake shaking.

3. Pseudo-Spectral Acceleration (PSA): The maximum acceleration of a single-degree-of-freedom (SDOF) system to a particular input motion, as a function of the natural frequency and damping ratio.

Median ground motions for a given magnitude and distance were estimated using GMPEs given by AB06 to generate different types of scenarios. PSA maps were generated at frequencies of 3 Hz, 1 Hz and 0.5 Hz. Three categories of ShakeMaps were produced, as described in the following sections.

2.3.1 Input ground motions for ShakeMap Category I

Category I represents the most basic probabilistic ShakeMap application. The input ground motions for ShakeMap Category I were adopted directly from the NBCC 2005 seismic hazard maps (see Adams and Halchuk, 2003 (AH03)). Ground motion parameters given in AH03 (and NBCC 2005) were defined for a 2%/50 year probability of exceedance. The ground motions adopted from NBCC 2005 for the Ottawa region are given in Table 2.1. Note that the motions, given at the probability level of 2%/50 years are uniform over the entire region (all grid points), for a given reference ground condition.

Table 2.1. Input ground motion parameters for Category I ShakeMaps (AH03). The ground motions for Ottawa are given for site class C.

Ground motion parameter	cm/s^2
PSA (0.5 Hz)	44.15
PSA (1 Hz)	137.34
PSA (3 Hz)	470.88
PGA	412.02
PGV	176.58

2.3.2 Input ground motions for ShakeMap Category II and III

The ground motions of NBCC 2005 at 2%/50 year probability of exceedance represent a useful reference level. However, in reality, an earthquake has to occur somewhere, and ground motions will decay with distance. Thus the motions cannot in fact be constant over the region for a specific scenario. To model this reality, input ground motions for Category II and III ShakeMaps of this study were estimated by assuming a specific earthquake magnitude and location, and estimating median ground motions using the GMPEs of AB06 as given by Equation 2.1:

$$\text{Log PSA} = c_1 + c_2M + c_3M^2 + (c_4 + c_5M)\,f1 + (c_6 + c_7M)\,f2 + (c_8 + c_9M)\,f0 + c_{10}R_{cd} + S \tag{2.1}$$

where PSA is ground motion in cgs units; R_{cd} is the closest distance to the fault in km; $f_0 = \max(\log(R_0/R_{cd}),0)$; $f_1 = \min(\log R_{cd}, \log R_1)$; $f_2 = \max(\log(R_{cd}/R_2),0)$; $R_0 = 10$ km; $R_1 = 70$ km; $R_2 = 140$ km; and $S = 0$ for hard rock. The coefficients c_1 to c_{10} are frequency-dependent and are given in Table 6 (for reference site class A) and Table 9 (for reference site class B/C) of AB06.

Figure 2.3 shows a sample of predicted ground motions for hard rock based on the GMPEs of AB06 for a **M**6 event. This figure depicts how the ground motions decay with distance and may vary with vibration frequency. Also, the input ground motions in ShakeMaps are based on the median values, but the ground motions in reality will scatter according to its standard deviation.

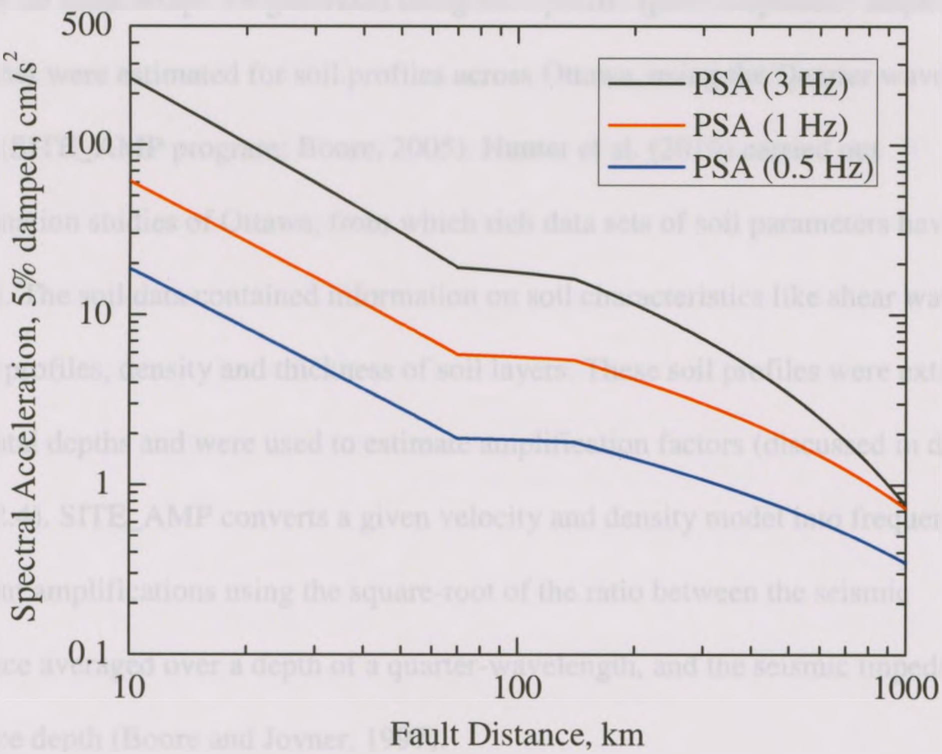

Figure 2.3. Predicted median ground motions on hard rock simulated as per GMPEs of AB06 for a **M**6 event.

Table 2.2 lists the characteristics of categories I, II and III ShakeMaps developed in this study. Category II maps use a specific magnitude and distance, but base the motions on the generic amplification factors given by NBCC 2005 for the NEHRP site class, as given by Finn and Wightman (2003). Finn and Wightman (2003) specify generic amplifications using two factors, Fa and Fv, which correspond to short and long period amplification respectively, for each NEHRP site class. These Fa and Fv factors are developed by lumping groups of similar soil profiles together so that their provisions apply to broad ranges of soil conditions within which the local conditions of a particular site of a given NEHRP class (A through E) are expected to fall.

In order to include more site-specific effects in the ShakeMap application, Category III ShakeMaps are generated using site-specific (profile-specific) amplification factors that were estimated for soil profiles across Ottawa, using the Quarter wavelength method (SITE_AMP program; Boore, 2005). Hunter et al. (2010) carried out microzonation studies of Ottawa, from which rich data sets of soil parameters have been obtained. The soil data contained information on soil characteristics like shear wave velocity profiles, density and thickness of soil layers. These soil profiles were extended to mid-crustal depths and were used to estimate amplification factors (discussed in detail in section 2.4). SITE_AMP converts a given velocity and density model into frequency-dependent amplifications using the square-root of the ratio between the seismic impedance averaged over a depth of a quarter-wavelength, and the seismic impedance at the source depth (Boore and Joyner, 1997).

Because NBCC 2005 amplification factors are based on a reference site C condition, median ground motions for Category II maps were calculated using the AB06 coefficients for B/C boundary conditions (Vs30 = 760 m/s) and the amplification factors were adjusted for B/C boundary when correcting the ground motions. Ground motions for Category III maps were calculated based on a reference site condition of A using the coefficients in Table 6 of AB06, then amplified over the entire site profile.

For purposes of scenario selection in terms of magnitude and distance equivalent to 2%/50 year probability of exceedance, as per NBCC 2005, the predicted median ground motions as per AB06 for many sets of combinations of magnitude and distance were compared with the expected ground motions as per NBCC 2005 for 2%/50 year probability of exceedance, 5% damping (Figure 2.4). The NBCC 2005 2%/50 year Uniform Hazard Spectrum (UHS) is very similar in shape to the AB06 median prediction for an event of moment magnitude (**M**) 6 at distance (D) 15 km (Figure 2.4c). By scaling the median **M**6D15 ground motions up by a factor of 1.4 which is equivalent to 0.4 standard deviations, the NBCC 2005 2%/50 year ground motions for Ottawa region matched very closely with the AB06 predictions. Based on this close match, a local **M**6 event was selected for the 2%/50 year scenario earthquake.

Table 2.2. Details of input ground motions, local soil amplification and MMI estimation approaches for all three categories of ShakeMaps.

Type of ShakeMap	**Estimation of input ground motions (PGA, PGV and PSA)**	**Local soil amplification correction (amplification factors)**	**Estimation of MMI**
Category I	Uniform ground motions over entire region as per NBCC 2005 for reference site C (Adams and Halchuk, 2003).	Soil amplification factors as prescribed by NBCC 2005; reference site C (Finn and Wightman, 2003).	Using empirical relations of Atkinson and Kaka (2007).
Category II	Ground motions as per Atkinson and Boore (2006) for reference site C.	Soil amplification factors as prescribed by NBCC 2005; reference site C (Finn and Wightman, 2003).	Using empirical relations of Atkinson and Kaka (2007).
Category III	Ground motions as per Atkinson and Boore (2006) for reference site A.	Linear soil amplification using Quarter wavelength method (Boore and Joyner, 1997; Boore, 2000); Non linear soil response using empirical equations of Boore and Atkinson (2008) reference site A.	Using empirical relations of Atkinson and Kaka (2007).

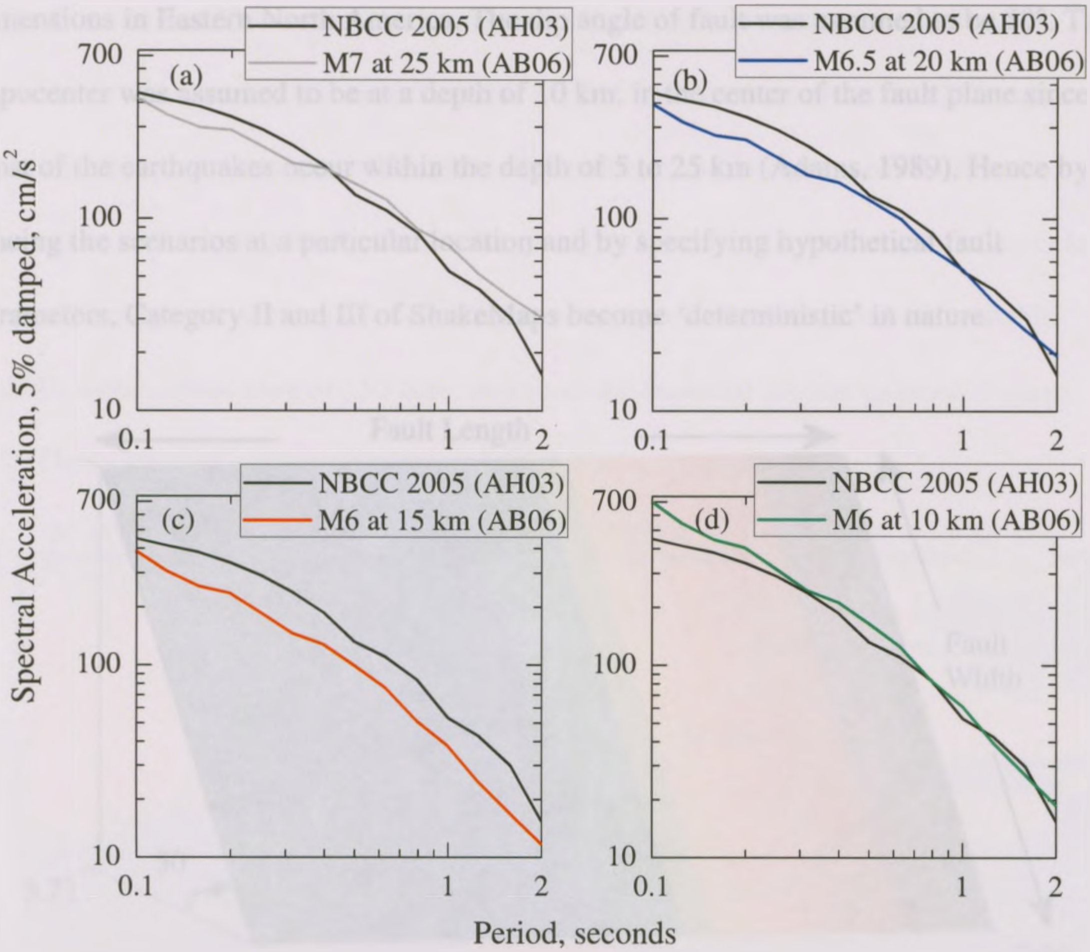

Figure 2.4. Uniform hazard spectra for hard-rock sites in Ottawa (2%/50 years) as provided by Adams and Halchuk (2003) for NBCC 2005 (black line) compared with Atkinson and Boore (2006) predicted median motions for hard rock for (a) **M**7 at 25 km, (b) **M**6.5 at 20 km, (c) **M**6 at 15 km and (d) **M**6 at 10 km.

The **M**6D15 scenario assumes that the epicentral distance is always 15 km from any point in the region of interest. But in reality the earthquake has to happen somewhere, so hypothetical epicenters were selected in and around the city, which also helped to study the impact of location on different soil types. Fault dimensions for these epicenters were estimated using the empirical relationships of Wells and Coppersmith (1994). The fault dimensions for the **M**6 event were obtained as 12.6 x 8.12 km, but each dimension was scaled by 60% as per Atkinson and Boore (2006), to account for smaller fault dimensions in Eastern North America. The dip angle of fault was assumed to be 50°. The hypocenter was assumed to be at a depth of 10 km, in the center of the fault plane since most of the earthquakes occur within the depth of 5 to 25 km (Adams, 1989). Hence by placing the scenarios at a particular location and by specifying hypothetical fault parameters, Category II and III of ShakeMaps become 'deterministic' in nature.

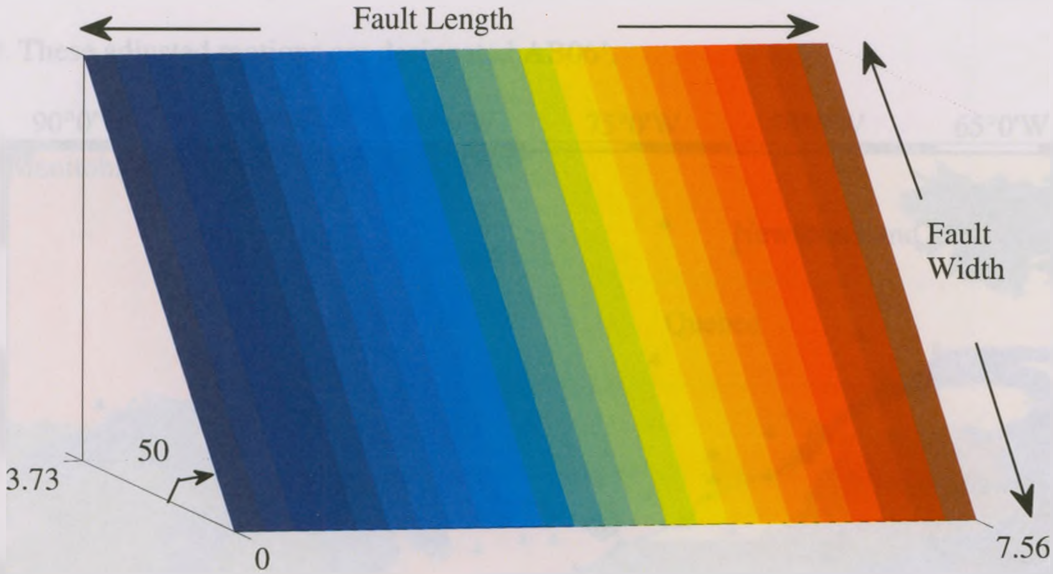

Figure 2.5. Fault plane with dip of 50° at 10 km below ground surface from the center of the fault plane.

2.3.3 Input ground motions for Val des Bois event

Ground motions for the M5 Val des Bois earthquake were recorded on 111 stations, ranging in distance from 22 to 1167 km (see Figure 2.6); 77 stations were located on NEHRP class A, 6 on B, 19 on C, 7 on D, and 2 stations on E. The processed recorded ground motion data for these 111 stations was obtained from the engineering seismology toolbox website (http://www.seismotoolbox.ca/ValDesBois.html). There were 5 stations in the Ottawa region, located in the range of 58 to 69 km (Ottawa region limits from 40 to 100 km from the epicenter). The default stress drop value in AB06 equation is 140 bars, but the stress drop for the **M**5 Val des Bois event was 250 bars (Atkinson and Assatourians, 2010). Hence the stress drop parameters of AB06 were adjusted to 250 bars to provide the median predicted motions for this event. In order to estimate the ground motions for the entire Ottawa region, the decay rate of the AB06 GMPE, with a stress drop of 250 bars, was fit to the recorded ground motions (Figure 2.7). These adjusted motions are designated AB06'.

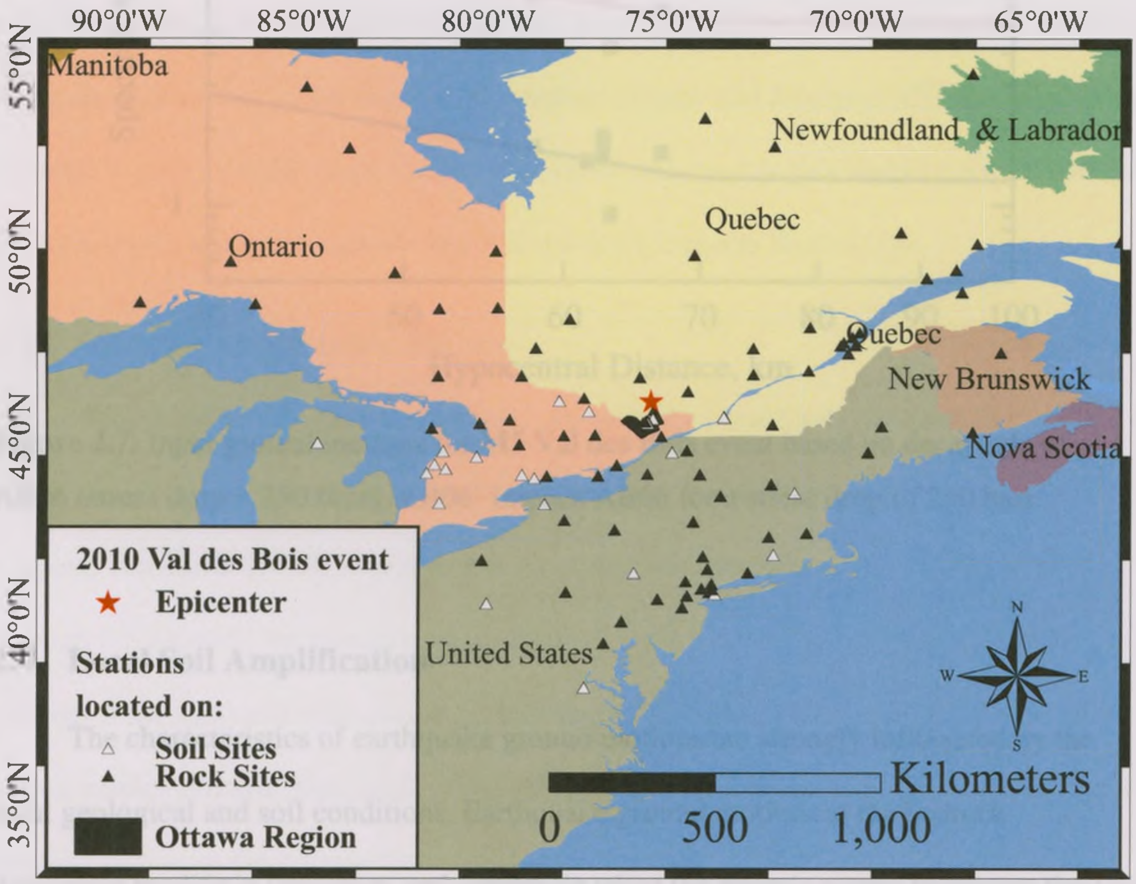

Figure 2.6. Stations that recorded the ground motions for **M**5 Val des Bois earthquake; Soil sites are sites located on NEHRP C, D and E while rock sites are on NEHRP A and B.

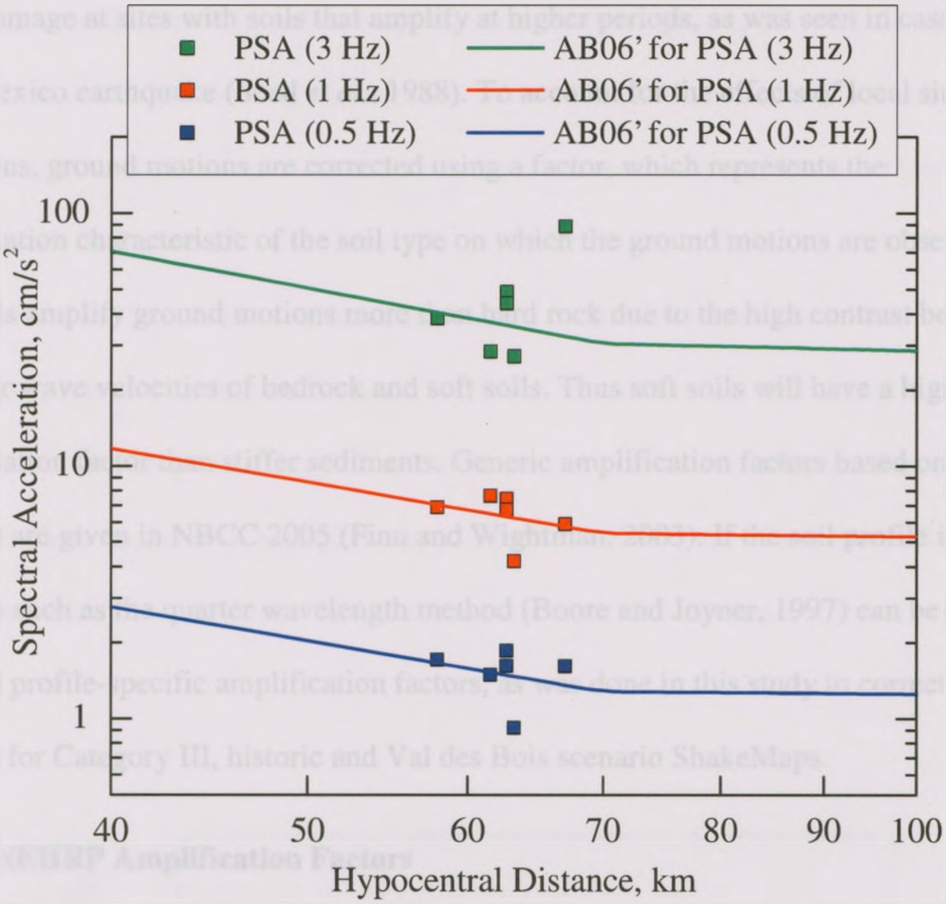

Figure 2.7. Input ground motions for M5 Val des Bois event based on decay rate of AB06 (stress drop = 250 bars). AB06' implies AB06 for a stress drop of 250 bars.

2.4 Local Soil Amplification

The characteristics of earthquake ground motions are strongly influenced by the local geological and soil conditions. Earthquake ground motions at the bedrock drastically modify in frequency and amplitude when the seismic waves propagate through a soil column. Hence, site conditions have strong influence on amplification of ground motions. Severe damage can be inflicted if the natural frequency of the buildings matches the frequency of ground shaking during an earthquake. This is why distant earthquakes cause damage at sites with soils that amplify at higher periods, as was seen in case of e.g., 1985 Mexico earthquake (Seed *et al.*, 1988). To account for the effects of local site conditions, ground motions are corrected using a factor, which represents the amplification characteristic of the soil type on which the ground motions are observed. Soft soils amplify ground motions more than hard rock due to the high contrast between the shear wave velocities of bedrock and soft soils. Thus soft soils will have a higher amplification factor than stiffer sediments. Generic amplification factors based only on stiffness are given in NBCC 2005 (Finn and Wightman, 2003). If the soil profile is know, methods such as the quarter wavelength method (Boore and Joyner, 1997) can be used to estimate profile-specific amplification factors, as was done in this study to correct ground motions for Category III, historic and Val des Bois scenario ShakeMaps.

2.4.1. NEHRP Amplification Factors

The NEHRP site class coefficients are part of a simplified procedure to characterize free-field spectral demands that account for local soil conditions. For this purpose, Borcherdt (1994) averaged site amplification factors over the short-period (0.1 through 0.5 second), intermediate-period (0.5 through 1.5 seconds), mid-period (0.4 through 2 seconds) and long-period (1.5 through 5 seconds) bands using the Loma Prieta strong-motion records. Borcherdt proposed that the four period bands be collapsed to two because factors in the intermediate-, mid- and long-period bands were similar. The NEHRP site class coefficients Fa and Fv were established from averages of the site amplification estimates in the short- and mid-period bands, respectively. NBCC 2005 uses generic amplification factors specified at two spectral periods to correct ground motions for site effects as based on the work of Borcherdt (1994). As described by Finn and Wightman (2003), Fa specifies amplification for short-periods (T = 0.2 s), while Fv specifies amplification for long periods (T = 1.0 s) spectral accelerations. The response spectra specified application of these factors for a reference site condition is shown schematically in Figure 2.8. The factors Fa and Fv are listed in Table 2.3 and 2.4 respectively. The factors are amplitude dependent to account for soil non-linearity. The formulation is based on that developed by NEHRP for the western U.S. (BSSC, 1997; Borcherdt, 2002). Note these amplification factors are given for a reference firm soil (NEHRP Class C), hence the amplification factors for class C are 1, less than 1 for materials harder (A and B) than C, and are greater than 1 for materials softer (D and E) than C.

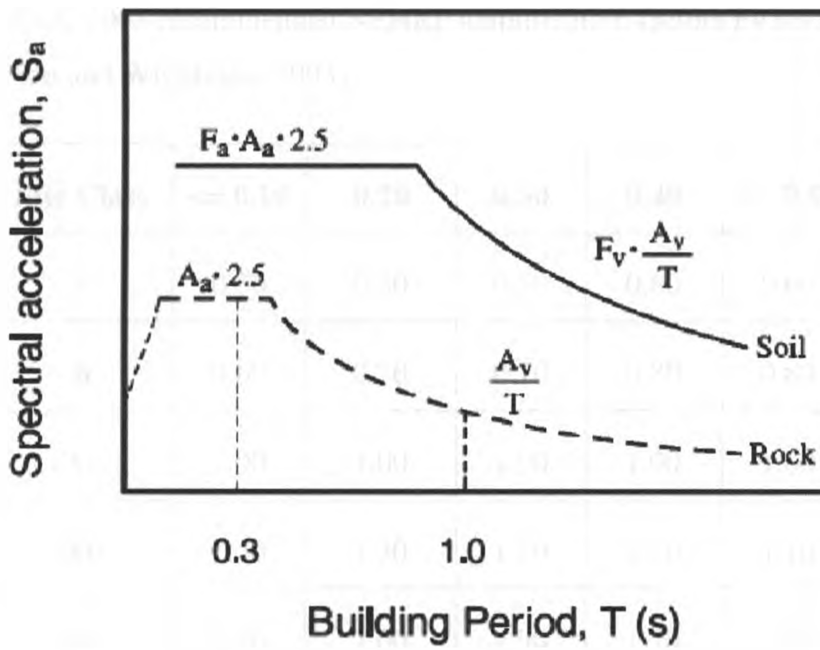

Figure 2.8. Design spectra based on period-dependent site amplification factors (Source: Finn and Wightman, 2003).

Table 2.3. NBCC 2005 recommended NEHRP amplification factors Fa for short periods (T = 0.2s), (Finn and Wightman, 2003).

Site Class	<= 0.25	0.50	0.75	1.00	>= 1.25
A	0.70	0.70	0.80	0.80	0.80
B	0.80	0.80	0.90	1.00	1.00
C	1.00	1.00	1.00	1.00	1.00
D	1.30	1.20	1.10	1.10	1.00
E	2.10	1.40	1.10	0.90	0.90

Table 2.4. NBCC 2005 recommended NEHRP amplification factors Fv for long periods (T = 1.0s), (Finn and Wightman, 2003).

Site Class	<= 0.10	0.20	0.30	0.40	>= 0.50
A	0.50	0.50	0.50	0.60	0.60
B	0.60	0.70	0.70	0.80	0.80
C	1.00	1.00	1.00	1.00	1.00
D	1.40	1.30	1.20	1.10	1.10
E	2.10	2.00	1.90	1.70	1.70

2.4.2. Profile-Specific Amplification Factors

2.4.2.1. Frequency-dependent Linear Amplification Factors

In this study, we consider profile-specific amplification factors for sites across the Ottawa region, and how they might differ from the generic factors as specified in the building code. The profile-specific factors were calculated using Boore's SITE_AMP program (Boore, 2000), which is based on the quarter wavelength method (Boore and Joyner, 1997). SITE_AMP converts a given velocity and density model into frequency-dependent amplifications using the square-root of the ratio between the seismic impedance averaged over a depth of a quarter-wavelength, and the seismic impedance at the source depth (Boore and Joyner, 1997). Representative velocity and density profiles were compiled for approximately 17, 250 locations in Ottawa, as given by Hunter et al. (2010); all profiles were extended from near-surface to mid-crustal depths. To generate and extend the profiles, the time averaged shear wave velocity (Vs_{av}) for the surficial layer of post-glacial sediments was first calculated using Equation 2.2, developed based on compiled soil-profile data across Ottawa (Hunter *et al.*, 2010):

$$Vs_{av} = 0.88*z + 123.9 \,, \tag{2.2}$$

where Vs_{av} is in m/s and z is the thickness in m down to the base of the post-glacial layer. z ranges from 0 to 144 m. Equation (1) models the post-glacial material as a single layer of constant velocity. The interval velocity of the glacial materials underlying the post-glacial deposits is 580 +/- 174 m/s, and for bedrock it is 2700 +/- 680 m/s (Hunter *et al.*, 2010).

The density at each point was estimated as a function of the interval shear wave velocity as given by Hunter *et al.* (2010):

$$\text{Density} = 0.8477 * V_s^{0.1446} \quad (2.3)$$

where Density is in g/cm^3 and V_s is the interval shear wave velocity in m/s. Density varies from 1.67 to 2.8 g/cm^3 for soft soil to hard rock respectively as shown in Figure 2.9.

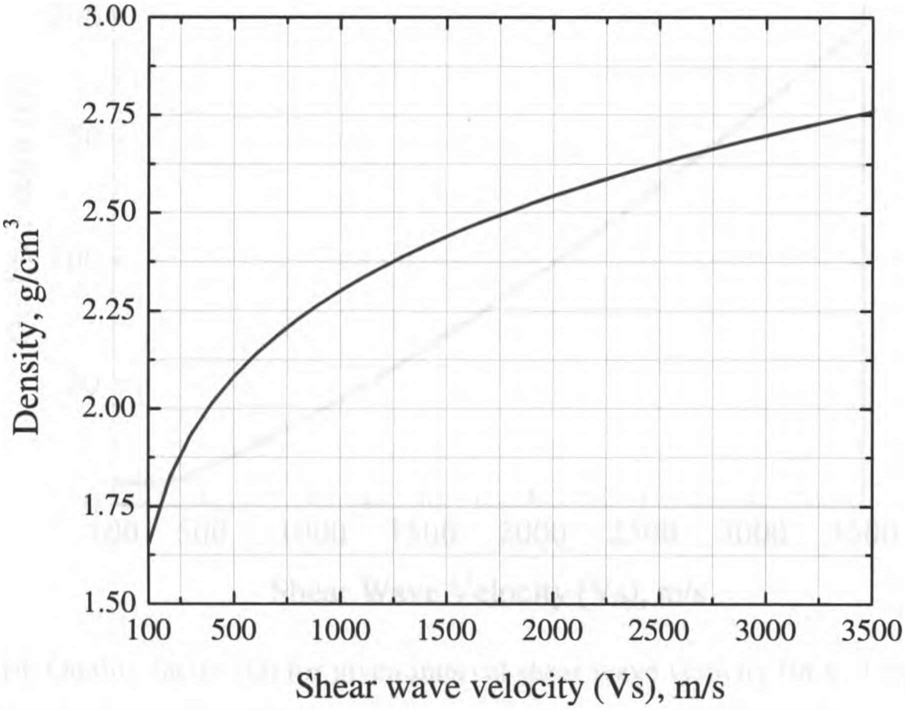

Figure 2.9. Density profile for given interval shear wave velocity for soil types in the Ottawa region as per equation 2.3.

The quarter-wavelength amplification effects must be corrected for high-frequency attenuation, as calculated from the Quality factor (Q) values of the soil (Wald and Mori, 2000). The Quality factor was estimated from Campbell (2009):

$$Q = 10, \qquad V_s \leq 366 \text{ m/s}$$

$$Q = 0.00382 \times V_s^{(1.33)}, \quad V_s > 366 \text{ m/s} \quad (2.4)$$

Q varies from 10 to 212 for soft soils to very hard rock as shown in Figure 2.10.

Source velocity and density were taken to be 3700 m/s and 2.8 g/cm^3 respectively (Atkinson and Boore, 2006).

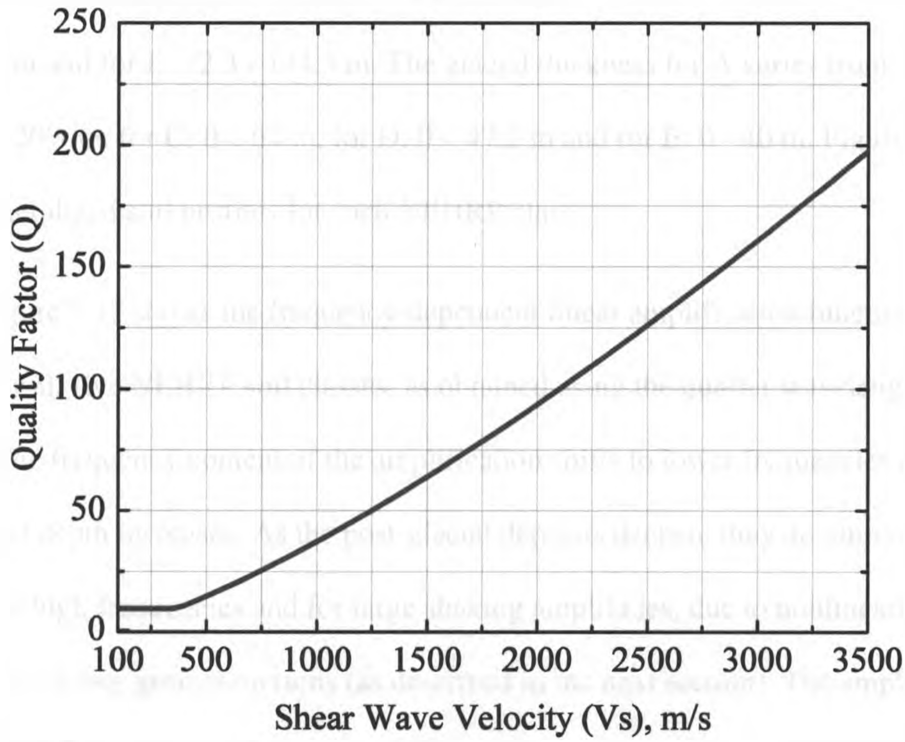

Figure 2.10. Quality factor (Q) for given interval shear wave velocity for soil types in the Ottawa region as per equation 2.4.

Typical profiles are those which have varying thicknesses of post-glacial and glacial sediments, all underlain by bedrock. These profiles were initially divided into many broad classes based upon post-glacial and glacial thicknesses. Glacial units are soft compared to the underlying hard rock, but stiff compared to the overlying post-glacial sediments. It was a challenge to obtain generic classes of differing post-glacial to glacial thicknesses. Amplification factors are sensitive to post-glacial thickness due to their low shear wave velocity, while being sometimes sensitive to glacial thickness, for cases in which the post-glacial thickness is thin. The level of amplification is generally governed by the shear wave velocity of the soil, while the frequency of response is governed by the depth of the sediment. By NEHRP classes across the region, the post-glacial thickness for NEHRP class A deposits varies from 0 - 4.8 m, for B: 0 - 3.7 m, for C: 0 - 10.1 m, for D: 6.1 - 23.8 m and for E: 22.3 - 144.3 m. The glacial thickness for A varies from: 0 – 6.7 m, for B: 0 – 20.4 m, for C: 0 – 64 m, for D: 0 – 47.2 m and for E: 0 - 40 m. Figure 2.11 shows generalized soil profiles for each NEHRP class.

Figure 2.12 shows the frequency-dependent linear amplification functions for the profiles for all five NEHRP soil classes, as obtained using the quarter wavelength method. The frequency content of the amplification shifts to lower frequencies as the post-glacial depth increases. As the post-glacial deposits deepen, they de-amplify ground motions, at high frequencies and for large shaking amplitudes, due to nonlinearity of response for strong ground motions (as described in the next section). The amplification for the NEHRP class E profile peaks at 1 Hz with a maximum value of 5.5. The maximum value of amplification for NEHRP class A is approximately 1.2, and occurs at 10 Hz, when there is a very thin layer of post-glacial sediment overlying the bedrock, or for profiles in which bedrock is exposed at the surface. For reference, the generic NEHRP amplification factors Fa and Fv from the NBCC are also shown (all for linear soil response). To simplify the application of the frequency-dependent amplification functions (amp(f)) for the Ottawa region, we developed empirical equations for each NEHRP soil class, of the form:

$$amp(f) = \frac{p_0 + p_1\omega + p_2\omega^2 + p_3\omega^3 + p_4\omega^4}{q_0 + q_1\omega + q_2\omega^2 + q_3\omega^3} \tag{2.5}$$

where $\omega = \log_{10}(f) - n$ and f is frequency in Hertz. The coefficients p, q and n for each NEHRP soil class were determined by regression of the linear amplification, and are given in Table 2.5. Note that PGA correlates to PSA at 10 Hz and PGV to PSA at 2 Hz. Hence, the amplification factors for estimation of corrected PGA were assumed as those of PSA at 10 Hz and corrected PGV as PSA at 2 Hz.

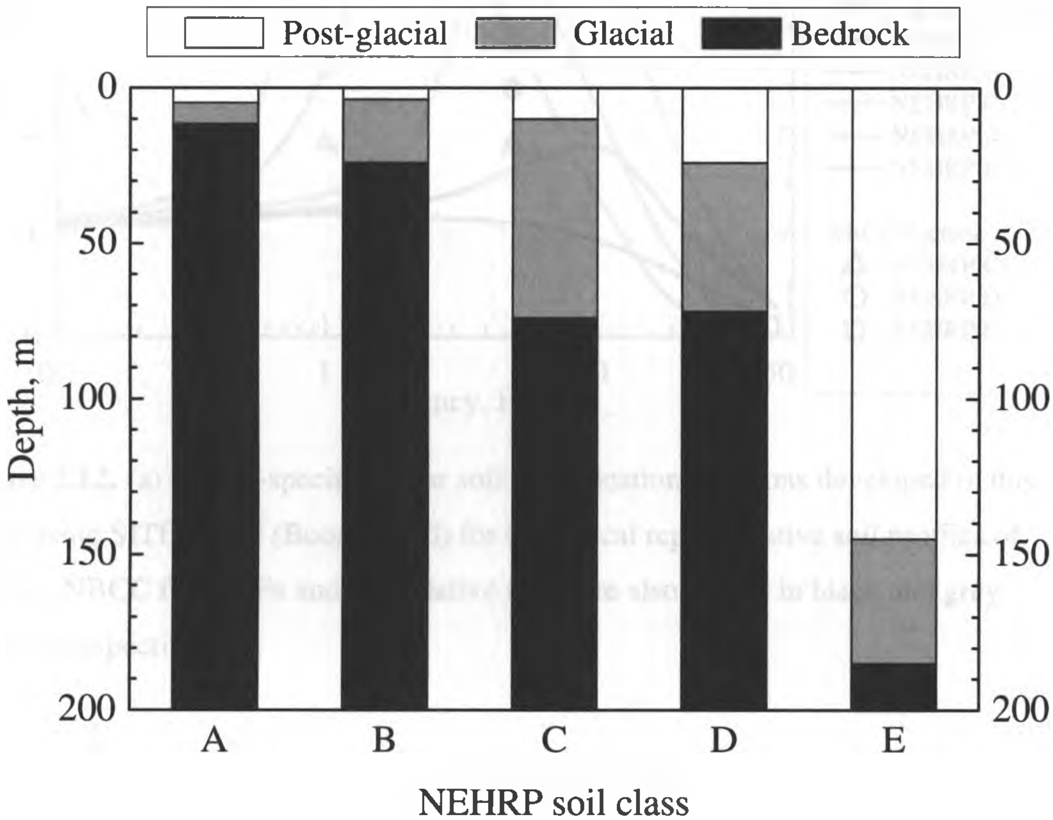

Figure 2.11. Typical soil profiles for Ottawa region for all five NEHRP soil classes showing post-glacial, glacial and bedrock thicknesses.

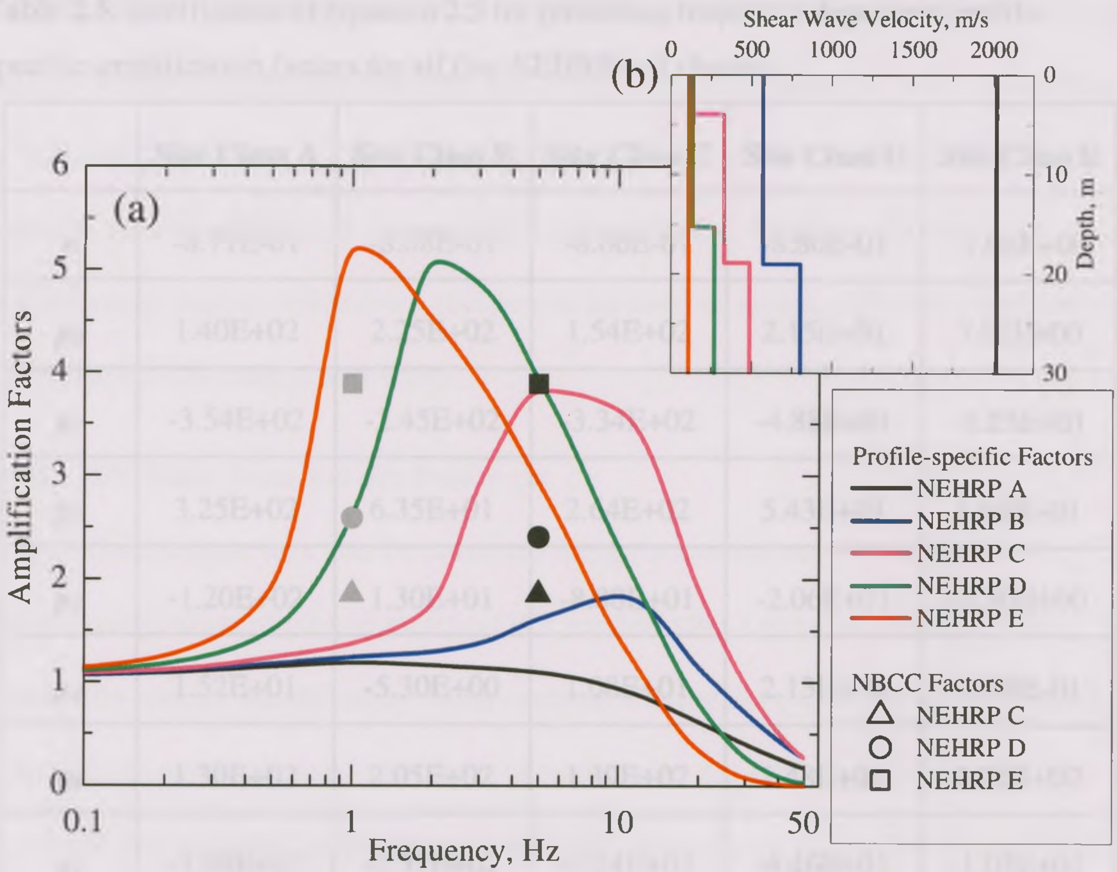

Figure 2.12. (a) Profile-specific linear soil amplification functions developed in this study using SITE_AMP (Boore, 2000) for (b) typical representative soil profiles of Ottawa. NBCC factors Fa and Fv (relative to A) are also shown in black and grey symbols respectively.

Table 2.5. Coefficients of equation 2.5 for predicting frequency dependent profile-specific amplification factors for all five NEHRP soil classes.

	Site Class A	Site Class B	Site Class C	Site Class D	Site Class E
n	-8.71E-01	-8.08E-01	-8.00E-01	-8.80E-01	-1.06E+00
p_0	1.40E+02	2.25E+02	1.54E+02	2.15E+01	3.93E+00
p_1	-3.54E+02	-2.45E+02	-3.34E+02	-4.88E+01	-1.23E+01
p_2	3.25E+02	6.35E+01	2.64E+02	5.43E+01	1.64E+01
p_3	-1.20E+02	1.30E+01	-8.88E+01	-2.06E+01	-2.50E+00
p_4	1.52E+01	-5.30E+00	1.08E+01	2.13E+00	-8.79E-01
q_0	1.30E+02	2.05E+02	1.39E+02	1.48E+01	2.75E+00
q_1	-3.38E+02	-2.53E+02	-3.24E+02	-4.46E+01	-1.05E+01
q_2	3.22E+02	9.43E+01	2.78E+02	5.18E+01	1.43E+01
q_3	-1.24E+02	-2.34E+00	-1.01E+02	-2.34E+01	-5.61E+00

2.4.2.2. Impact of nonlinearity

For the weak ground motions accompanying small earthquakes, the amplification due to sediments is well understood in terms of linear elasticity (Hooke's law). However, Hooke's law breaks down at the larger strains associated with strong ground motions causing a reduced (nonlinear) amplification (Field *et al.*, 1997). Nonlinear effects include an increase in damping and reduction in shear wave velocity as the excitation strength increases. Nonlinearity is considerable in cohesionless soils, but may be negligible in stiff soils. The SITE_AMP program does not consider the non-linearity effects directly. In this study, we used the empirical nonlinear factors of Boore and Atkinson (2008) to account for the non-linear effects of shaking. According to BA08, a non-linear amplification function, which multiplies the linear amplification function to obtain the total amplification, may be defined as a function of the level of shaking (PGA on reference site condition: B/C boundary) and Vs30.

2.4.3. H/V Ratio from Val des Bois event

Site-response may also be estimated using the spectral ratio of horizontal-to-vertical components of ground motions (H/V method after Lermo and Chavez, 1993). The profile-specific amplification factors estimated using the quarter wavelength method (Figure 2.12) were compared with those obtained using the H/V method. Figure 2.13 shows the amplification factors for each NEHRP class inferred using H/V for the **M**5 Val des Bois event, along with the average H/V ratios for multiple sites and events in south-eastern Canada. The data for the **M**5 Val des Bois were recorded on 7 stations that were located in Ottawa, (Engineering Seismology Toolbox, 2010). Out of the 7 stations in Ottawa, three are located on NEHRP class A, two on NEHRP B and one each on NEHRP C and D. Amplification factors were calculated by taking ratio of the geometric mean of the two horizontal components to the vertical component at each station at frequencies from 0.1 Hz to 50 Hz. Kolos (2010) studied the H/V ratios for 579 events recorded on 81 stations across south-eastern Canada. The stations used by Kolos (2010) were grouped into 4 NEHRP classes (A to D) based on the Vs30 of the stations. An average curve for each class was estimated by taking the log averages of H/V ratios for all events recorded on all stations.

Based on Figure 2.13, we observe that the implied amplification effects at lower frequencies (about a factor of 3 from hard to soft sites; Figure 2.13b) are in general agreement with those calculated for the typical profiles as shown in Figure 2.12 (when one considers that there is likely some amplification of the vertical component and thus H/V may underestimate amplification of the horizontal component). However, it is also apparent that H/V is not a reliable index of site-response, especially when based on single-event observation (compare Figures 2.13a vs. 2.13b).

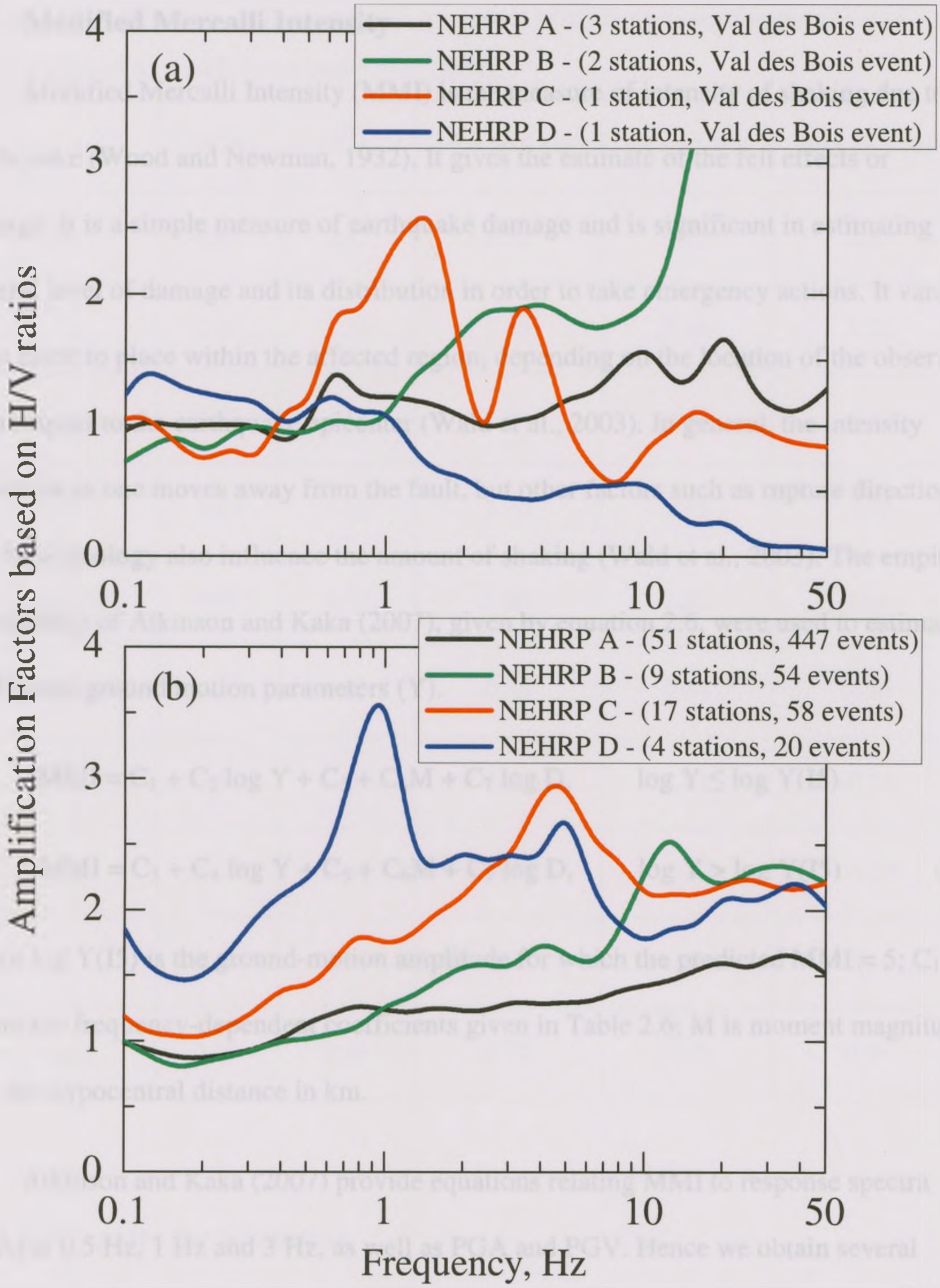

Figure 2.13. Soil amplification estimated using the H/V ratios from (a) Val des Bois earthquake recorded on 7 stations in Ottawa, and (b) average H/V from multiple events for site classes, from many stations across south-eastern Canada.

2.5 Modified Mercalli Intensity

Modified Mercalli Intensity (MMI) is the measure of intensity of shaking due to earthquake (Wood and Newman, 1932). It gives the estimate of the felt effects or damage. It is a simple measure of earthquake damage and is significant in estimating general level of damage and its distribution in order to take emergency actions. It varies from place to place within the affected region, depending on the location of the observer with respect to the earthquake epicenter (Wald et al., 2003). In general, the intensity decreases as one moves away from the fault, but other factors such as rupture direction and local geology also influence the amount of shaking (Wald et al., 2003). The empirical relationship of Atkinson and Kaka (2007), given by equation 2.6, were used to estimate MMI from ground motion parameters (Y).

$$MMI = C_1 + C_2 \log Y + C_5 + C_6 M + C_7 \log D, \qquad \log Y \leq \log Y(I5)$$

$$MMI = C_3 + C_4 \log Y + C_5 + C_6 M + C_7 \log D, \qquad \log Y > \log Y(I5) \qquad (2.6)$$

where log Y(I5) is the ground-motion amplitude for which the predicted MMI = 5; C_1 to C_7 are the frequency-dependent coefficients given in Table 2.6; M is moment magnitude; D is the hypocentral distance in km.

Atkinson and Kaka (2007) provide equations relating MMI to response spectra (PSA) at 0.5 Hz, 1 Hz and 3 Hz, as well as PGA and PGV. Hence we obtain several estimates of MMI, based on different ground motion frequencies. This may provide some insight into the frequency associated with the felt effects. The coefficients are reproduced in Table 2.6.

Table 2.6. Coefficients of Equation 2.6 to predict MMI from Instrumental Ground-Motion Parameters (Atkinson and Kaka, 2007).

Y	PGV	PGA	PSA (0.5 Hz)	PSA (1 Hz)	PSA (3.3 Hz)
C_1	4.37	2.65	3.72	3.23	2.40
C_2	1.32	1.39	1.29	1.18	1.36
C_3	3.54	-1.91	1.99	0.57	-1.83
C_4	3.03	4.09	3.00	2.95	3.56
log Y(I5)	0.48	1.69	1.00	1.50	1.92
σ_{1MMI}	0.80	1.01	0.86	0.84	0.88
C_5	0.47	-1.96	2.24	1.92	-0.11
C_6	-0.19	0.02	-0.33	-0.39	-0.20
C_7	0.26	0.98	-0.31	0.04	0.64
σ_{MMI}	0.76	0.89	0.72	0.73	0.79

2.6 Epicenters for Scenarios

2.6.1. Postulated Scenario events

Different epicentral locations were postulated to investigate the effects of soil conditions and epicentral distance on predicted intensities. Four epicenters were chosen for the local **M**6 scenarios, one each on the North, South, East and West sides of the region, and were located within different soil types (Figure 2.14). For example, the epicenter in the east is located within the 140 m thick basin sediments under the Orleans area, while the epicenter to the south is located on hard rock. Such differences allowed studying the impact of geology and distancing on predicted ground motions and intensities for these scenarios. While I chose locations on different soil types for local scenarios, scenarios with higher magnitudes (**M**6.5 and **M**7.5) were located based upon the history of earthquakes in the region. The epicentral location of the 2010 **M**5 Val des Bois earthquake was used for the **M**6.5 scenario, whereas the **M**7.5 event was assumed to be situated ~460 km northeast, in the Charlevoix region (Figure 2.15). These higher magnitude scenarios give an idea as to how the ground motions and intensities will be if a large magnitude earthquake, either near the location of the **M**5 Val des Bois earthquake, or farther away in the Charlevoix Seismic Zone.

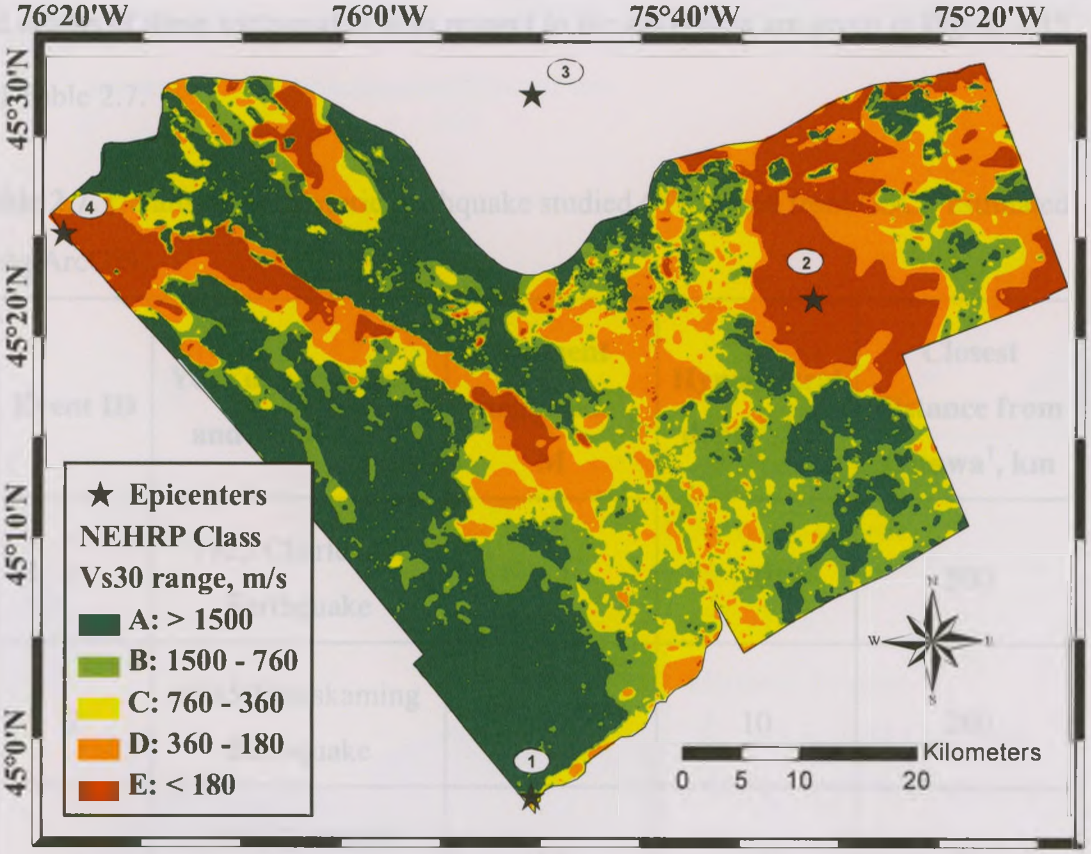

Figure 2.14. Epicentral locations for M6 scenarios in Ottawa region, overlaid on Vs30 map. Epicenters are shown by black stars and are numbered in white circles.

2.6.2. Historic events

The intensity levels in the Ottawa region for previous historic earthquakes are not very well understood. In particular, the Orleans area, which sits on 40 to 140 m thick soft sediments, was not heavily populated until the last few decades. To study how these areas will be affected if the historic large magnitude earthquakes were to occur today, scenarios were generated for three major historic events. These include the 1925 Charlevoix (M6.2), 1935 Timiskaming (M6.1) and 1944 Cornwall (M5.8) earthquakes that occurred at approximately 500 km, 260 km and 50 km respectively from Ottawa. The locations and details of these earthquakes with respect to the study area are given in Figure 2.15 and Table 2.7.

Table 2.7. Details of the historic earthquake studied (§Obtained from GSC, †estimated using ArcGIS).

Event ID	Year of occurrence and event name	Moment magnitude§, M	Hypocentral depth§, km	Closest distance from Ottawa†, km
1	1925 Charlevoix Earthquake	6.2	10	500
2	1935 Timiskaming Earthquake	6.1	10	260
3	1944 Cornwall Earthquake	5.8	20	50

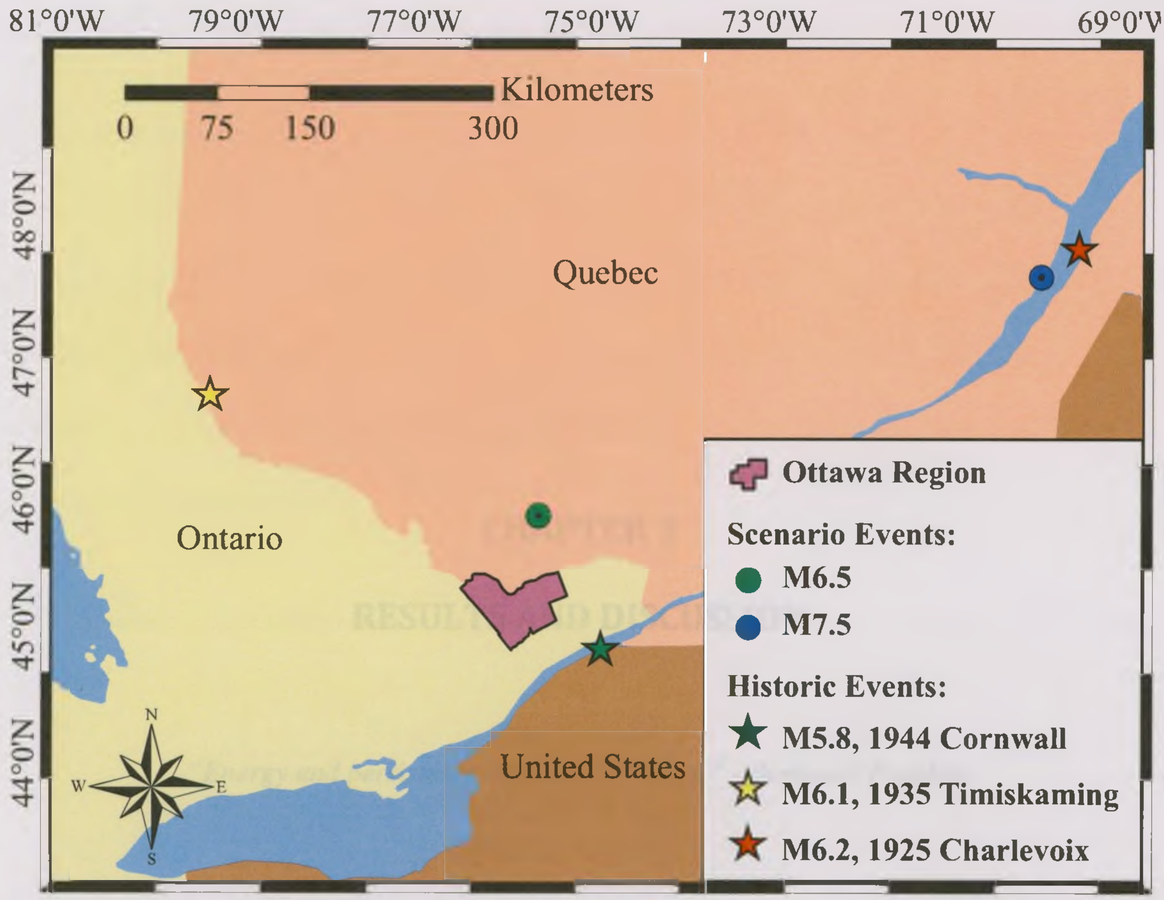

Figure 2.15. Epicentral locations for higher magnitudes at greater distances (M6.5D60 and M7.5D460), and historic event scenarios, with respect to Ottawa region.

CHAPTER 3

RESULTS AND DISCUSSION

"Energy and persistence conquer all things." - *Benjamin Franklin*

3.1 M5 Val des Bois ShakeMaps: A Validation Exercise

3.1.1. Felt Intensities

The reported intensities from 2412 DYFI reports in the Ottawa region were averaged over "boxes" of approximately 1.5 km^2, and plotted in a grid pattern. The averages were taken only in boxes that had three or more DYFI reports. The felt intensities and Vs30 map overlaid on such a grid for Ottawa region are shown in Figures 3.1 and 3.2 respectively.

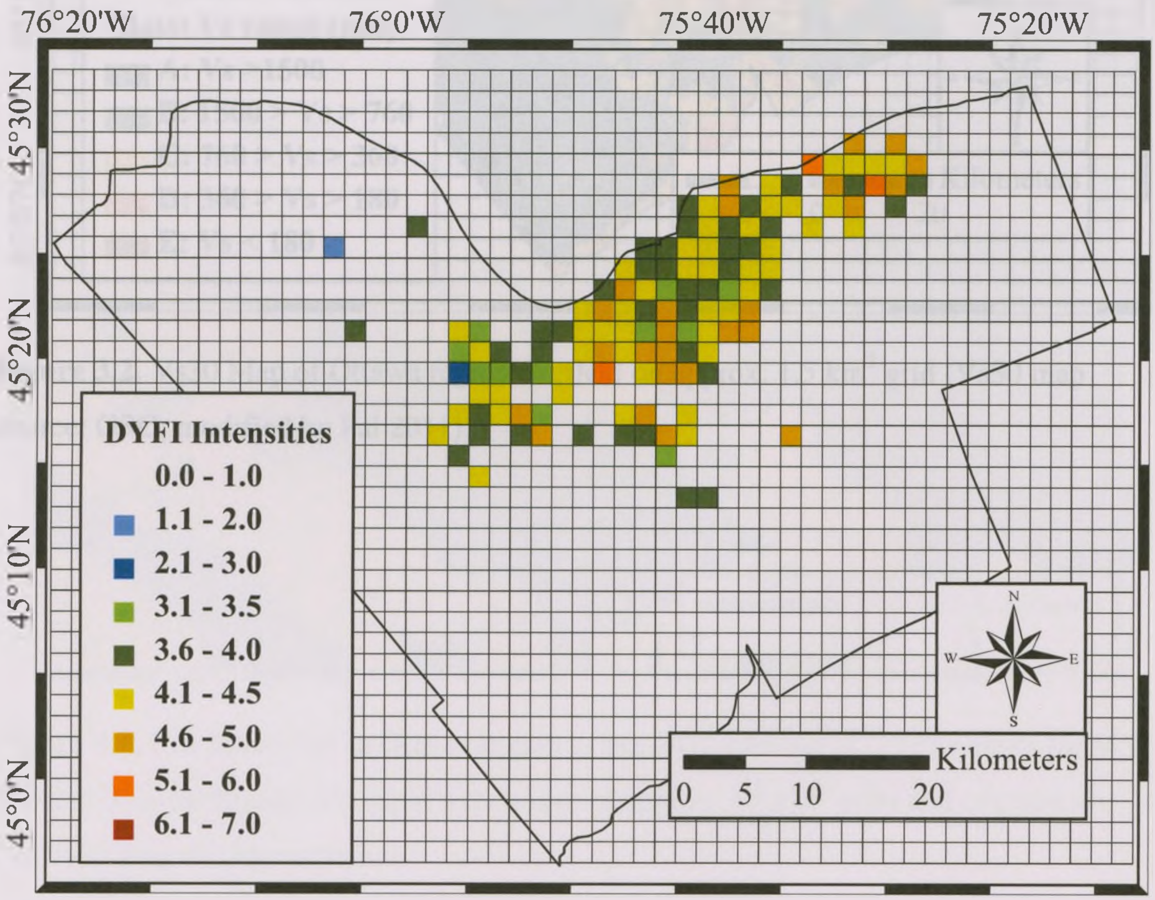

Figure 3.1. Felt intensities of M5 Val des Bois earthquake in Ottawa region as per "Did You Feel It" (DYFI) reports; averaged over boxes of approx. 1.5 km^2 area, for number of reports greater than 3.

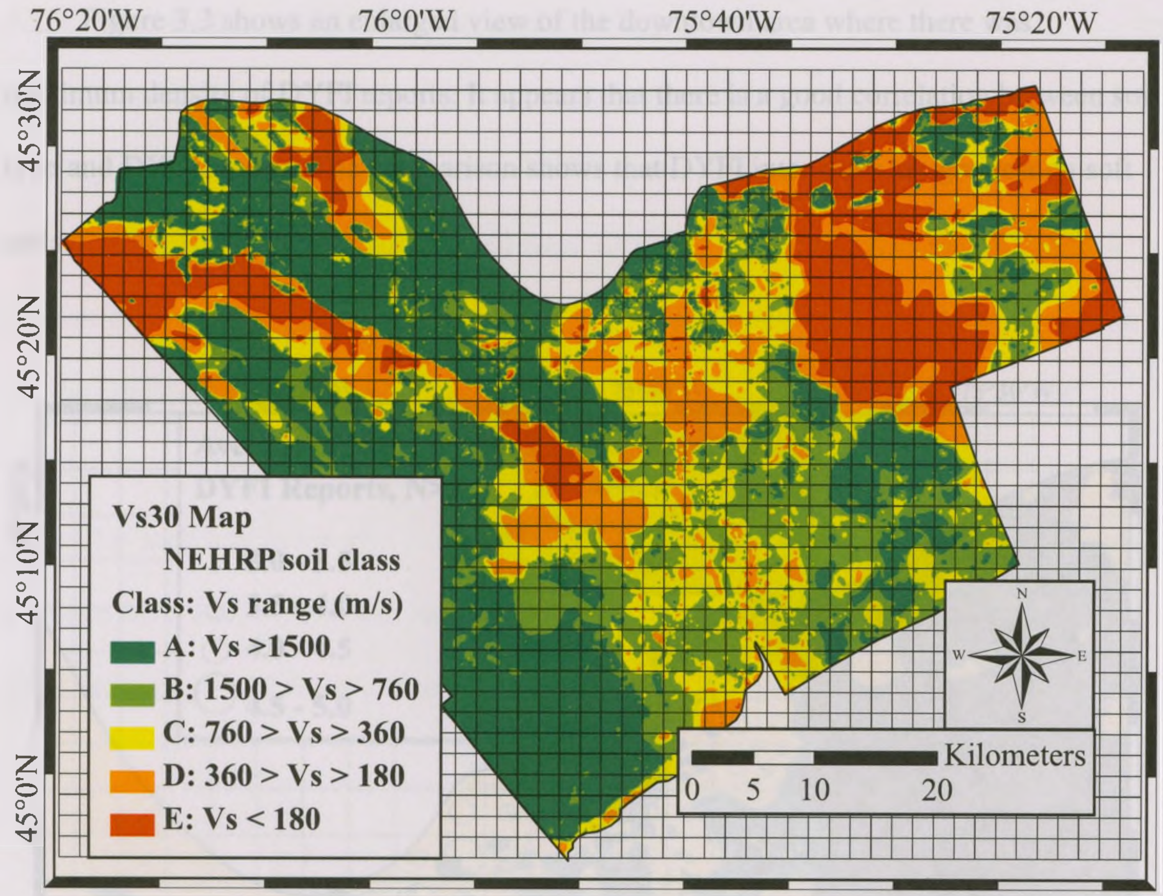

Figure 3.2. Vs30 Map of Ottawa region overlaid on approx. 1.5 km^2 grid (Vs30 map source: GSC; modified by Pal 2011).

Figure 3.3 shows an enlarged view of the downtown area where there was maximum density of DYFI reports. It appears that there is a good correlation between soil type and DYFI reports. The comparison shows that DYFI intensities are greatest on soft soils.

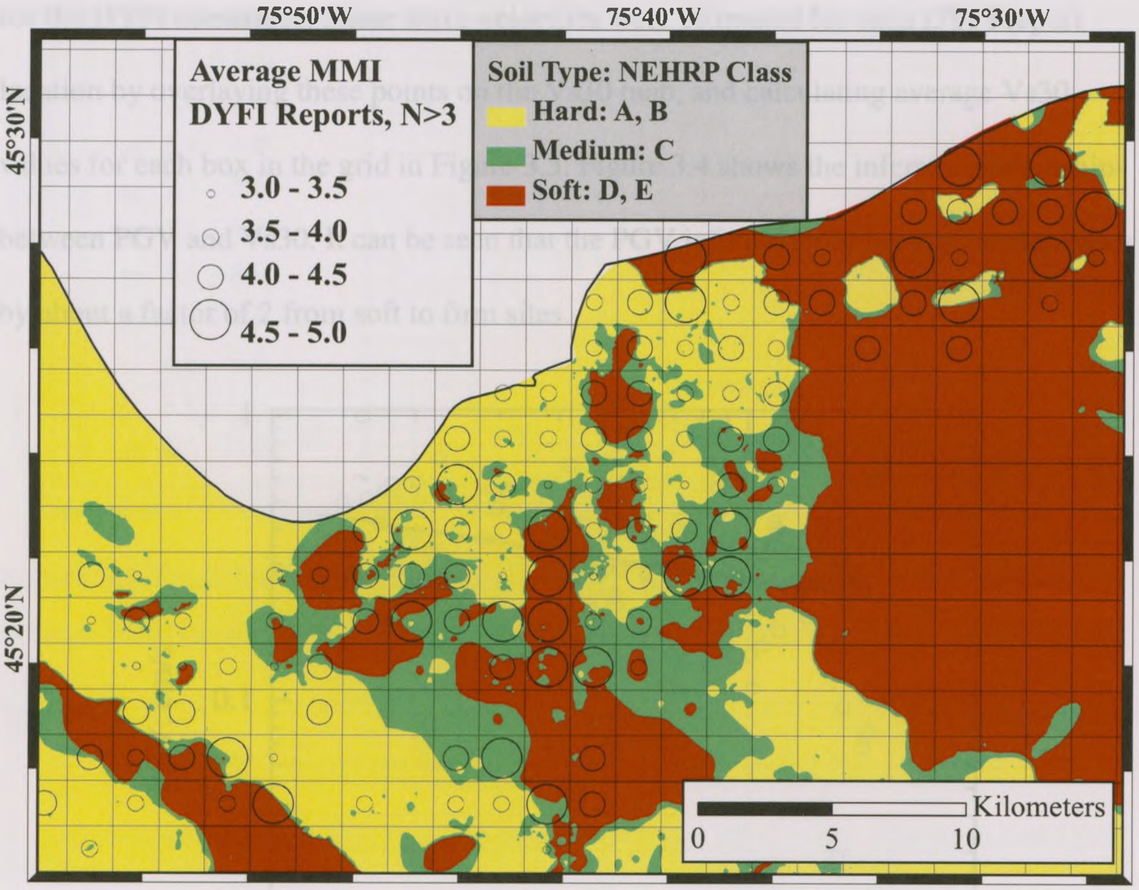

Figure 3.3. Felt intensities in Ottawa region as per 2412 number of DYFI reports for M5 Val des Bois earthquake averaged over boxes of approx. 1.5 km^2 grids and overlaid on the Vs30 map of Ottawa region.

3.1.2. Correlation of Felt Intensity and Soil Type

To quantify the correlation between soil type and reported intensity, peak ground velocity (PGV) was calculated for each DYFI report location (2412 reports) using the empirical relationships of Atkinson and Kaka (2007). The calculated PGV from the felt intensities were averaged in boxes over the grid shown in Figure 3.3, in the same way as for the DYFI intensities. Shear wave velocities were estimated for each DYFI report location by overlaying these points on the Vs30 map, and calculating average Vs30 values for each box in the grid in Figure 3.3. Figure 3.4 shows the inferred relationships between PGV and Vs30. It can be seen that the PGV inferred from felt reports decreases by about a factor of 2 from soft to firm sites.

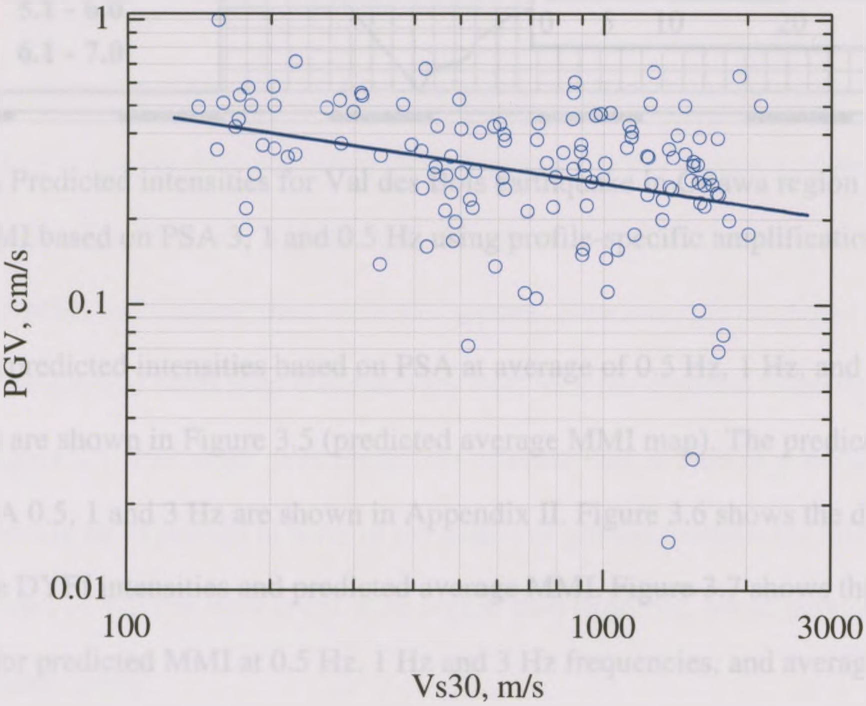

Figure 3.4. Correlation of PGV vs. Vs30 for the Ottawa region for M5 Val des Bois earthquake. The equation of the line is: *log PGV = -0.25*log Vs30 + 0.18*. The slope of the trend line is -0.25 (± 0.12).

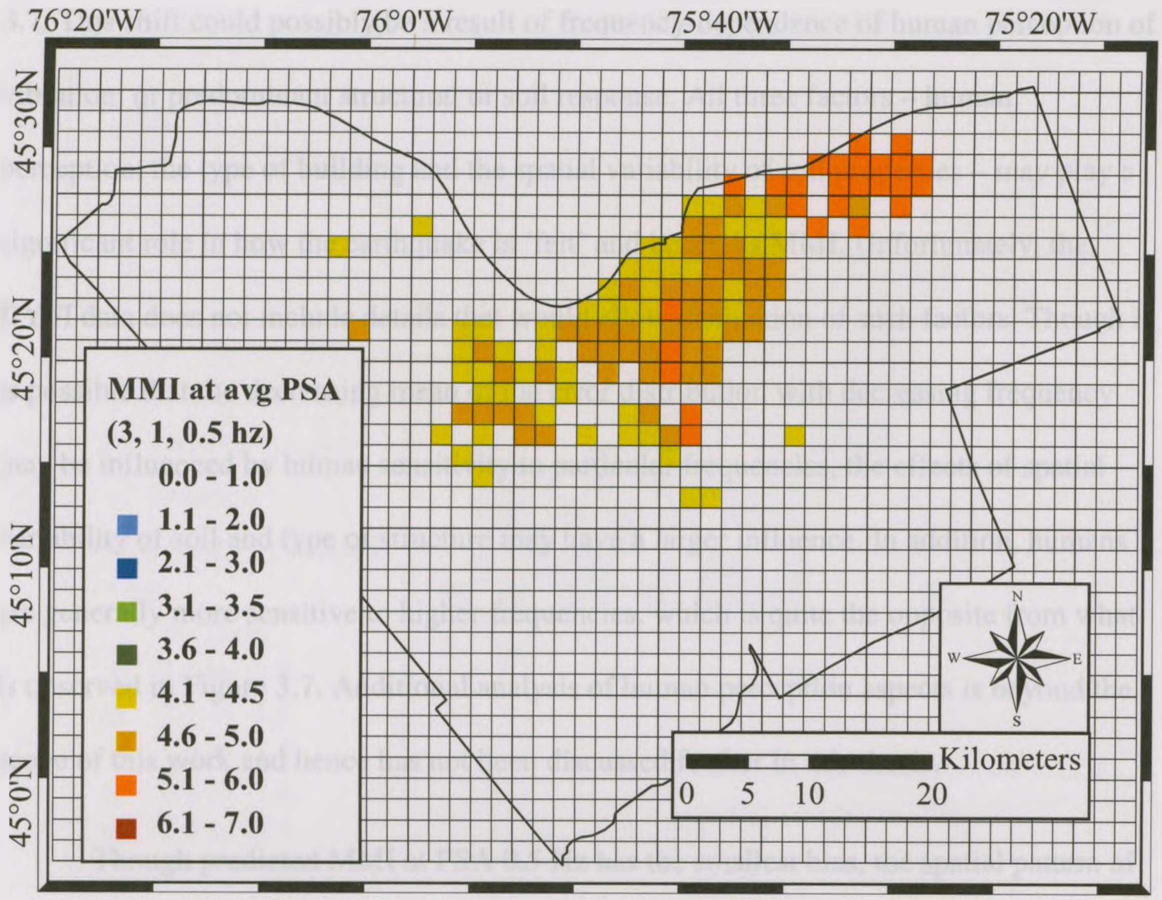

Figure 3.5. Predicted intensities for Val des Bois earthquake in Ottawa region for average MMI based on PSA 3, 1 and 0.5 Hz using profile-specific amplification factors.

The predicted intensities based on PSA at average of 0.5 Hz, 1 Hz, and 3 Hz frequencies are shown in Figure 3.5 (predicted average MMI map). The predicted MMI maps at PSA 0.5, 1 and 3 Hz are shown in Appendix II. Figure 3.6 shows the difference between the DYFI intensities and predicted average MMI. Figure 3.7 shows the error histogram for predicted MMI at 0.5 Hz, 1 Hz and 3 Hz frequencies, and average of all frequencies.

It is interesting how the distribution of error between observed and predicted intensities shifts towards zero mean with decreasing frequency (3 to 0.5 Hz) in Figure

3.7. This shift could possibly be a result of frequency-dependence of human perception of vibration, or predominant structural or soil response. All three factors – human perception, the type of building and the spatial variability of soil properties – may play a significant role in how the earthquake is 'felt' and hence its MMI. Unfortunately, the DYFI data does not include details that would allow distinction of such factors. Though it is possible that the decreasing mean of the error distribution with decreasing frequency may be influenced by human sensitivity to particular frequencies, the effects of spatial variability of soil and type of structure may have a larger influence. In addition, humans are generally more sensitive to higher frequencies, which is quite the opposite from what is observed in Figure 3.7. Additional analysis of human perception aspects is beyond the scope of this work and hence has not been discussed further in this thesis.

Though predicted MMI at PSA 0.5 Hz has the smallest bias, the spatial pattern of predicted MMI at 0.5 Hz does not match as well with the DYFI reports as does predicted MMI for the average PSA (see Appendix II). The predicted MMI (based on PSA average) is biased 0.5 MMI units higher than the DYFI reports. However, the predicted intensity pattern for the average MMI map matches very well with the reported intensity pattern shown in Figure 3.1. The slight over-prediction of intensities at median ground motions in this case could be explained in form of the nature of ground motions for this event. The ground motions of Val des Bois event were higher than expected, while shaking intensity was surprisingly lower.

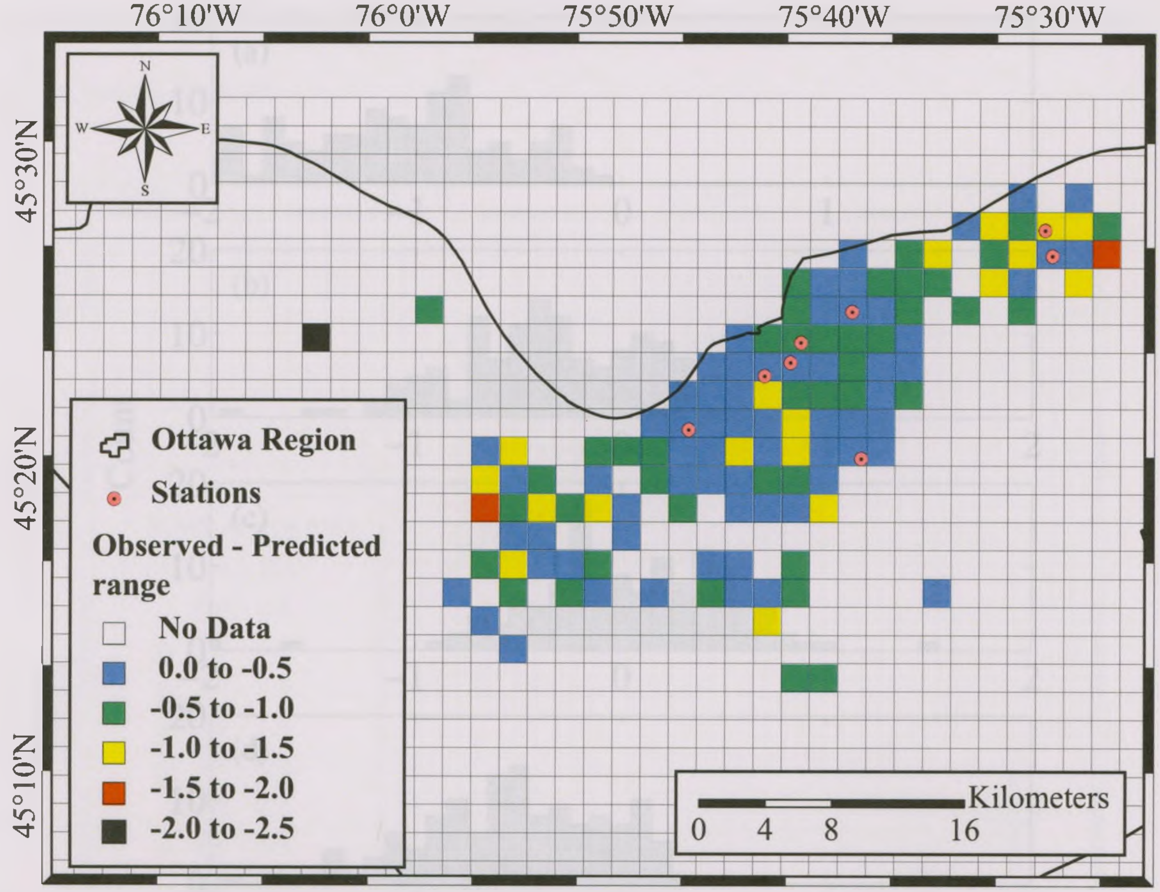

Figure 3.6. Difference of felt intensities and predicted average MMI based on PSA 3, 1 and 0.5 Hz (profile-specific amplification factors) for **M**5 Val des Bois earthquake.

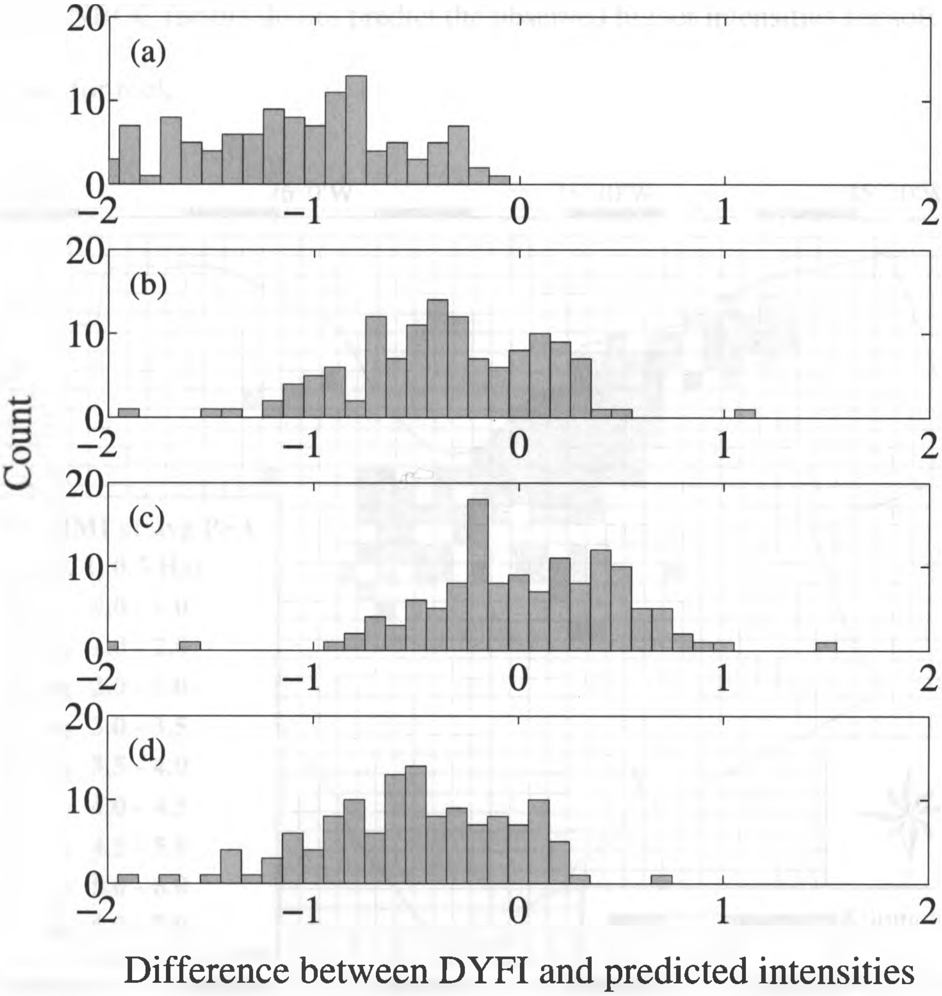

Figure 3.7. Error bounds for predicted MMI at (a) PSA at 3 Hz, (b) PSA at 1 Hz, (c) PSA at 0.5 Hz and (d) PSA at average of 3, 1 and 0.5 Hz.

For a comparison of predictions based on profile-specific amplification factors and NBCC 2005 amplification factors, MMI were also estimated using NBCC 2005 amplification factors. A similar procedure of averaging over approximately 1.5 km^2 area was carried out to generate this map (Figure 3.8), using the same ground motions, but with the NBCC 2005 amplification factors instead of the profile-specific factors. It can be seen that the NBCC factors do not predict the observed higher intensities for soft soil and lower values for rock.

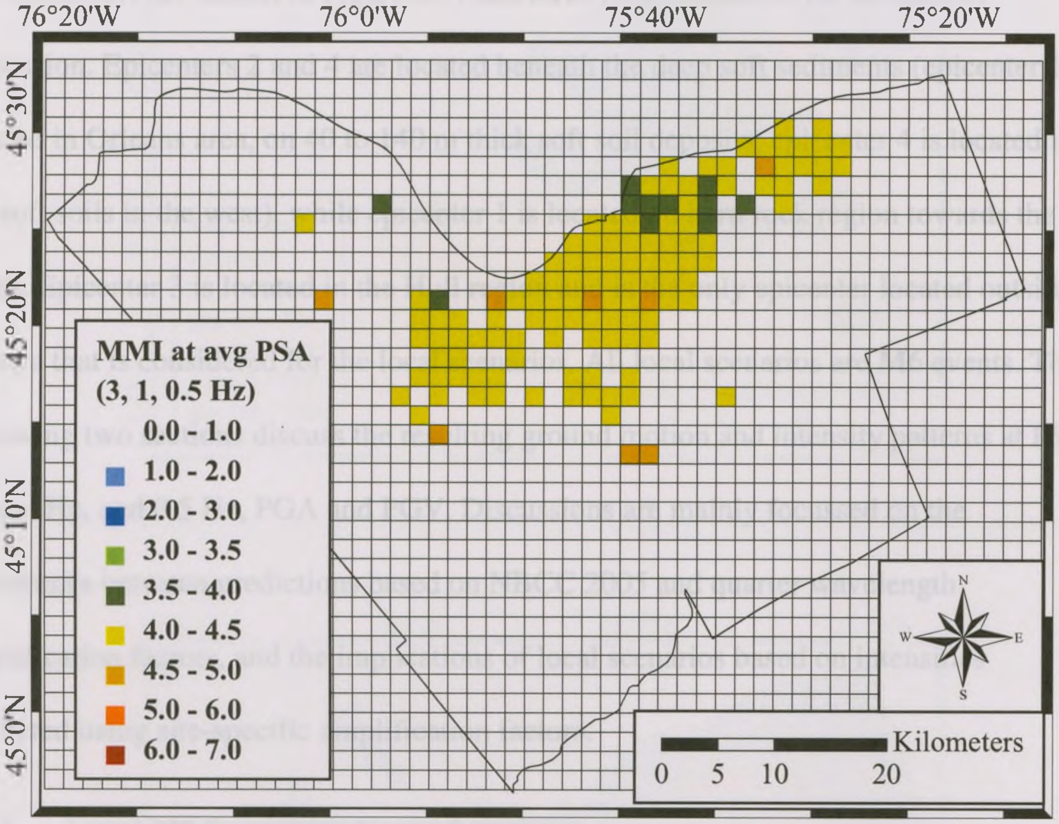

Figure 3.8. Predicted intensities for **M5** Val des Bois earthquake in Ottawa region for average MMI based on PSA 3, 1 and 0.5 Hz using NBCC 2005 amplification factors.

3.2 Category I ShakeMaps

For category I ShakeMaps, the ground motion pattern is exactly the same as the pattern of the Vs30 map, because the ground motions are assumed to be uniform for the entire Ottawa region as per NBCC 2005 (maps are shown in Appendix I).

3.3 M6 scenarios (Category II and III)

Four epicenters were considered in and around Ottawa region for local scenarios. The epicenters are shown in Figure 2.11 and have been numbered for the sake of discussion. Epicenters 2 and 4 are located beneath the deep soft sediments (epicenter 2 is located in Orleans area, on 40 to 140 m thick soft soil deposits; epicenter 4 is located in the soft soils in the west), while epicenter 1 is located on hard rock region towards the south. Epicenter 3 is located in the Hull region and is the only epicenter located outside Ottawa that is considered for the local scenarios. All local scenarios are M6 events. The following two sections discuss the resulting ground motion and intensity patterns at PSA 3 Hz, 1Hz, and 0.5 Hz, PGA and PGV. Discussions are mainly focussed on the differences between predictions based on NBCC 2005 and quarter wavelength amplification factors, and the implications of local scenarios based on intensities predicted using site-specific amplification factors.

3.3.1. Local M6 Scenarios: Ground motions

Figures 3.9 and 3.10 show the PSA 3 Hz maps generated for the epicenter in the soft soil patch in the Orleans area (epicenter 2) using the NBCC 2005 and the site-specific amplification factors respectively. The predicted ground motions for the NBCC 2005 amplification factors decrease with distance, with maximum values occurring close to the epicenter (Figure 3.9). In comparison, the maps generated using site-specific amplification factors (Figure 3.10) show a de-amplification effect near source due to the non-linearity effect associated with strong ground motions, and the frequency dependence of the amplifications at higher frequencies. The ground motions are larger outside the soft soil patch as they propagate through stiffer soils of NEHRP classes B, C and D

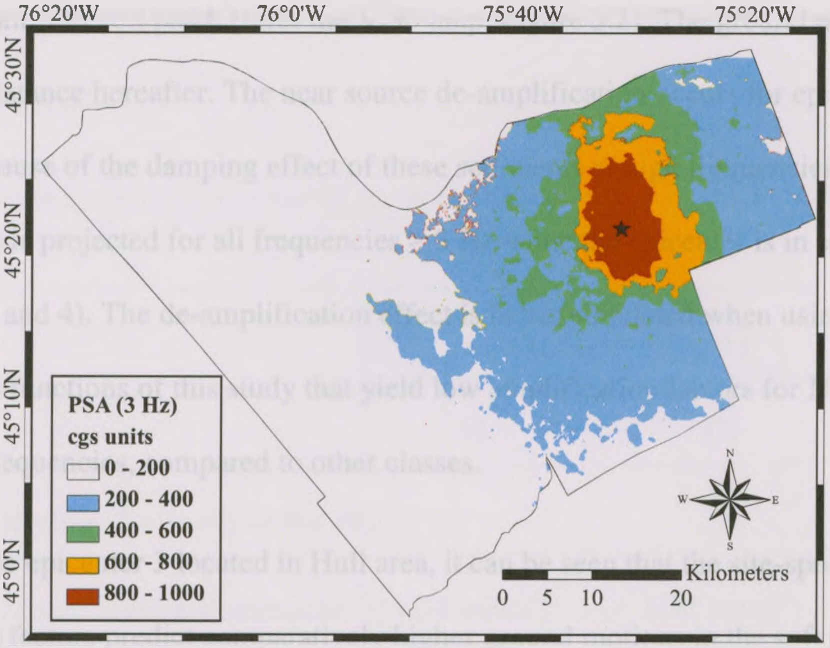

Figure 3.9. PSA at 3 Hz for epicenter in soft soil using the NBCC 2005 amplification factors.

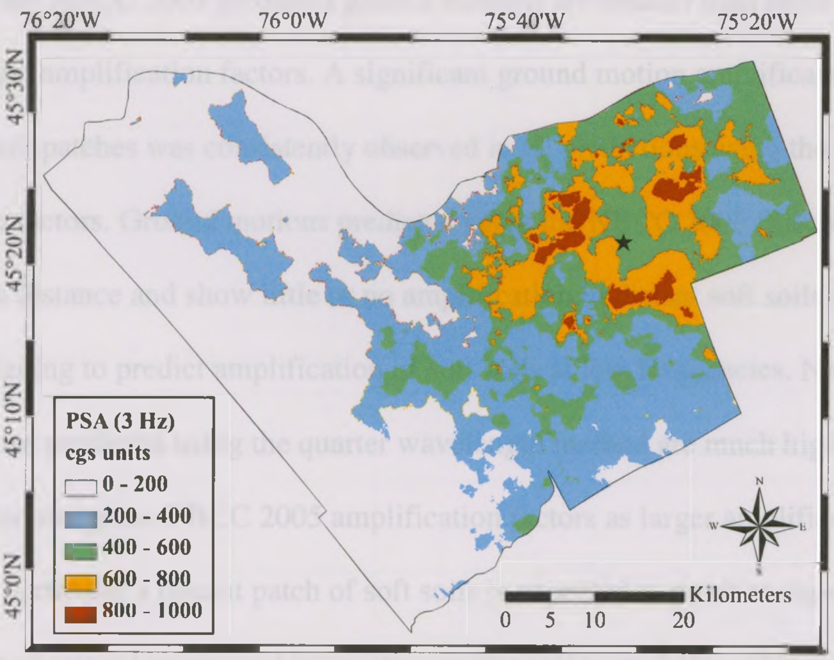

Figure 3.10. PSA at 3 Hz for epicenter in soft soil using the site-specific amplification factors.

surrounding the soft soil patch (refer the V_s30 map, Figure 3.2). The ground motions decay with distance hereafter. The near source de-amplification occurs for epicenters in soft soils because of the damping effect of these sediments at high frequencies. De-amplification is projected for all frequencies $\geq$ 3 Hz when the epicenter is in soft soils (epicenters 2 and 4). The de-amplification effect is better simulated when using amplification functions of this study that yield low amplification factors for NEHRP class E at higher frequencies, compared to other classes.

For the epicenter 3 located in Hull area, it can be seen that the site-specific amplification factors predict comparatively higher ground motions in the soft patch of soils in Orleans area (Figures 3.11 and 3.12). This can also be seen in the western soft patch where the NBCC 2005 predicted ground motions are smaller than those predicted by site-specific amplification factors. A significant ground motion amplification effect in distant soft soil patches was consistently observed in all predictions using the site-specific amplification factors. Ground motions predicted using the NBCC 2005 factors continue to decay with distance and show little or no amplification in distant soft soils for all cases considered, failing to predict amplification of soft soils at low frequencies. Near-source ground motions predicted using the quarter wavelength method are much higher than those predicted using the NBCC 2005 amplification factors as larger amplifications are predicted; in particular a distant patch of soft soils is expected to produce significant amplification of ground motions at lower frequencies (1Hz and 3 Hz). This is because higher frequencies get attenuated with distance and at lower frequencies soft soils amplify motions. Overall, I speculate that the NBCC 2005 factors under predict the ground motions in basin sediments at distance. Tables 3.1 and 3.2 give the ground motion ranges for Epicenters 1 and 2, and Epicenters 3 and 4 respectively for ShakeMap Categories II and III.

Table 3.1. Ground motions range for all the ground motion parameters for Epicenter 1 and 2.

	ShakeMap Category	
	II	**III**
Epicenter 1 - South of the city		
Ground Motion Parameter	**GM (cm/s^2)**	**GM (cm/s^2)**
PSA at 3 Hz	27 - 718	35 - 1053
PSA at 1 Hz	7 - 139	11 - 140
PSA at 0.5 Hz	2 - 42	2 - 39
PGA	13 - 668	1 - 2464
PGV	0.5 - 22	1 - 40
Epicenter 2 - Orleans area		
Ground Motion Parameter	**GM (cm/s^2)**	**GM (cm/s^2)**
PSA at 3 Hz	37- 923	38 – 1066
PSA at 1 Hz	7 - 262	12 - 221
PSA at 0.5 Hz	2 - 80	3 - 38
PGA	21 - 887	29 - 1800
PGV	1 - 34	1 - 48

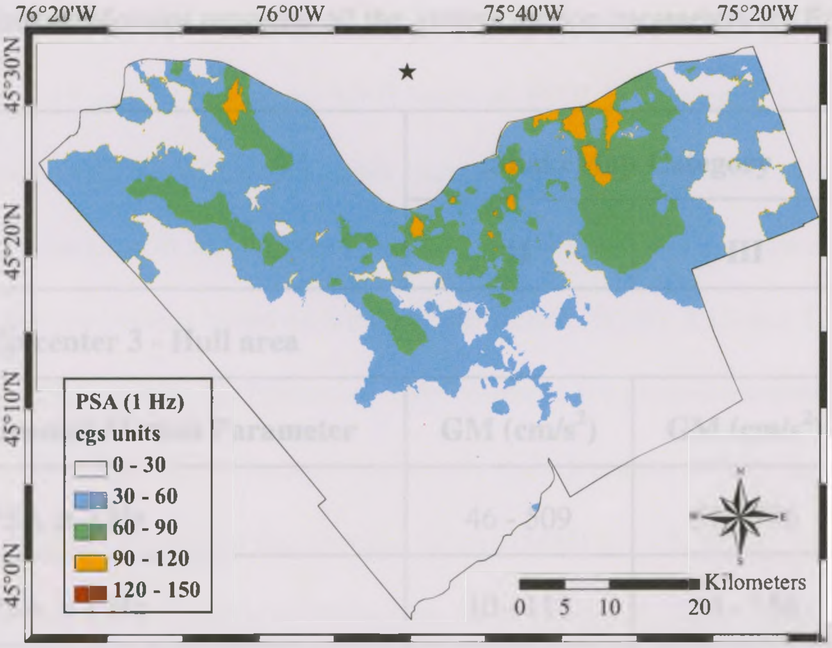

Figure 3.11. PSA at 1 Hz for epicenter in Hull area using the NBCC 2005 amplification factors.

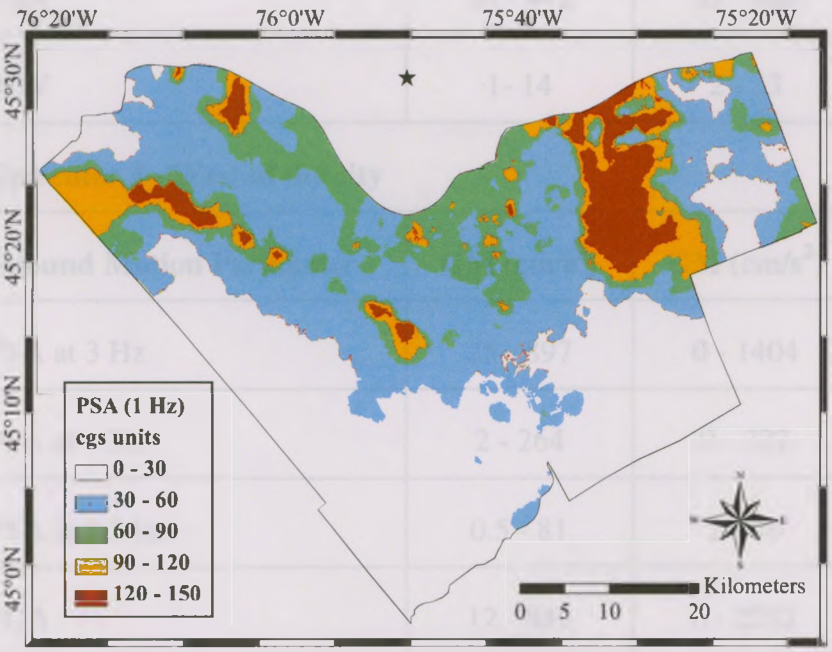

Figure 3.12. PSA at 1 Hz for epicenter in Hull area using the site-specific amplification factors.

Table 3.2. Ground Motions range for all the ground motion parameters for Epicenter 3 and 4.

	ShakeMap Category	
	II	**III**
Epicenter 3 - Hull area		
Ground Motion Parameter	**GM (cm/s^2)**	**GM (cm/s^2)**
PSA at 3 Hz	46 - 509	51 - 776
PSA at 1 Hz	10 - 117	14 - 156
PSA at 0.5 Hz	3 - 36	4 - 23
PGA	26 - 442	43 - 986
PGV	1- 14	2 - 33
Epicenter 4 - West of the city		
Ground Motion Parameter	**GM (cm/s^2)**	**GM (cm/s^2)**
PSA at 3 Hz	25 - 897	0 - 1404
PSA at 1 Hz	2 - 264	0 - 222
PSA at 0.5 Hz	0.5 - 81	2 - 40
PGA	12 - 885	6 - 2292
PGV	0.5 - 35	0 - 50

3.3.2. Local M6 Scenarios: MMI

Figure 3.13 and 3.14 show the MMI based on PGV for Epicenter 1 using NBCC 2005 and site-specific amplification factors respectively. Predicted MMI using NBCC 2005 factors in distant soft soil patches is approximately one MMI unit lower as compared to the predictions based on site-specific factors. Figure 3.15 and 3.16 show the MMI based on PSA at 3 Hz for Epicenter 2. As observed for ground motions, there is de-amplification when epicenter is located below soft soils. Because of this effect, the near-source predicted MMI based on site-specific factors (MMI = 7 - 8, Figure 3.16) is less than that predicted by the generic amplification factors given by NBCC 2005 (MMI = 8 - 9, Figure 3.15). However, in distant soft soil patches the site-specific factors predict higher MMI in comparison to NBCC 2005 predictions. Tables 3.3 and 3.4 show the predicted MMI range for ShakeMap Categories II and III for Epicenters 1 and 2, and Epicenters 3 and 4 respectively. All the other maps for MMI for all the epicenters considered are attached in Appendices III to X.

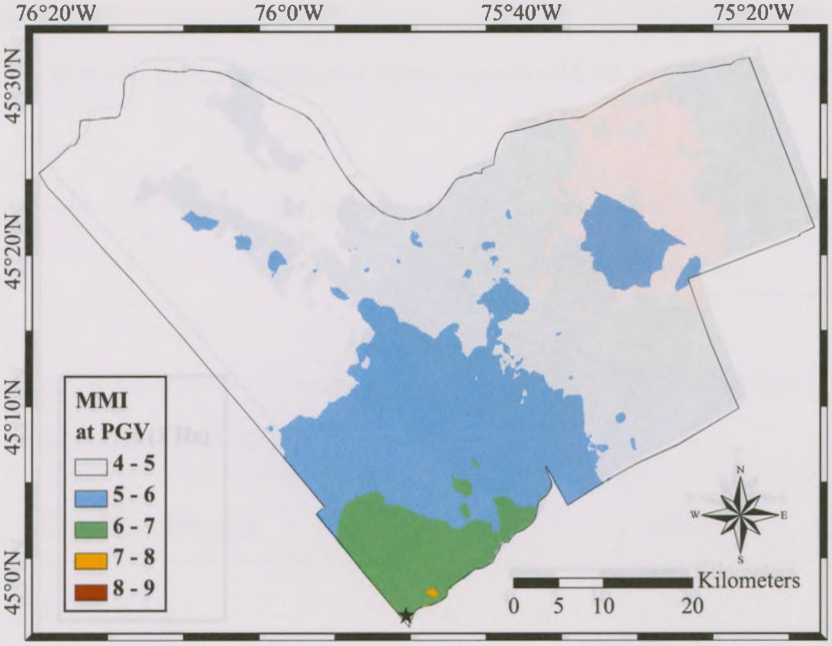

Figure 3.13. MMI based on PGV for **M**6 scenario located on hard rock, south of the Ottawa region using NBCC 2005 amplification factors.

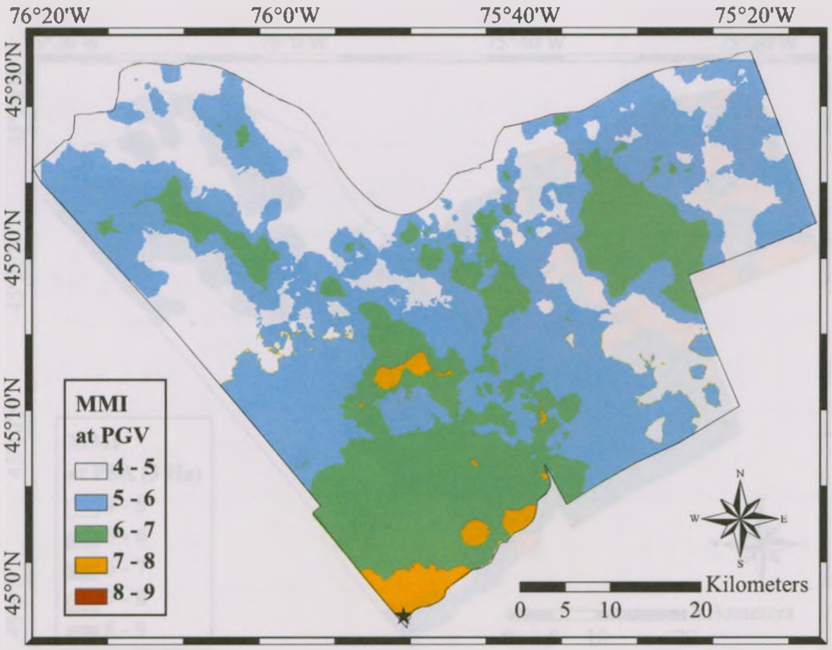

Figure 3.14. MMI based on PGV for **M**6 scenario located on hard rock, south of the Ottawa region using site-specific amplification factors.

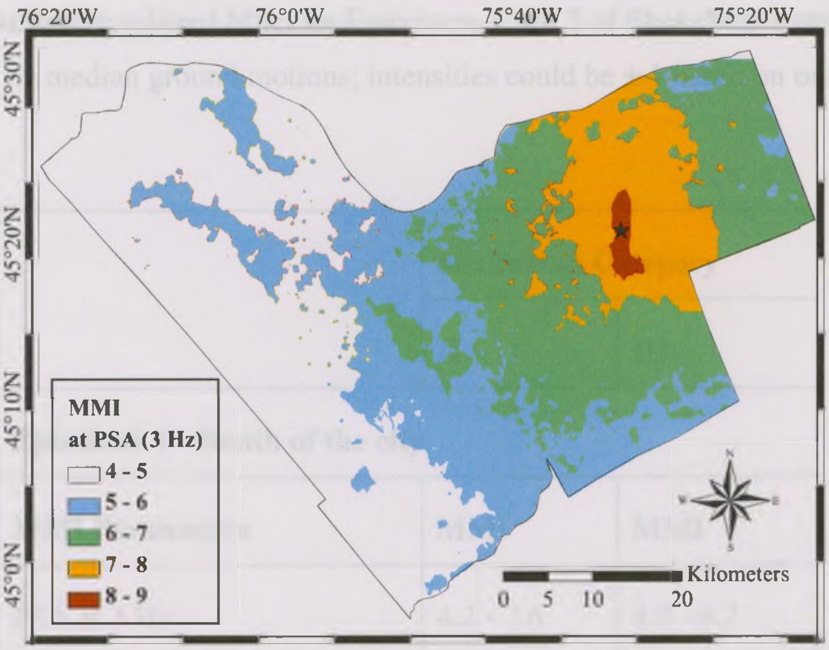

Figure 3.15. MMI based on PSA at 3 Hz for **M6** scenario located on hard rock, south of the Ottawa region using NBCC 2005 amplification factors.

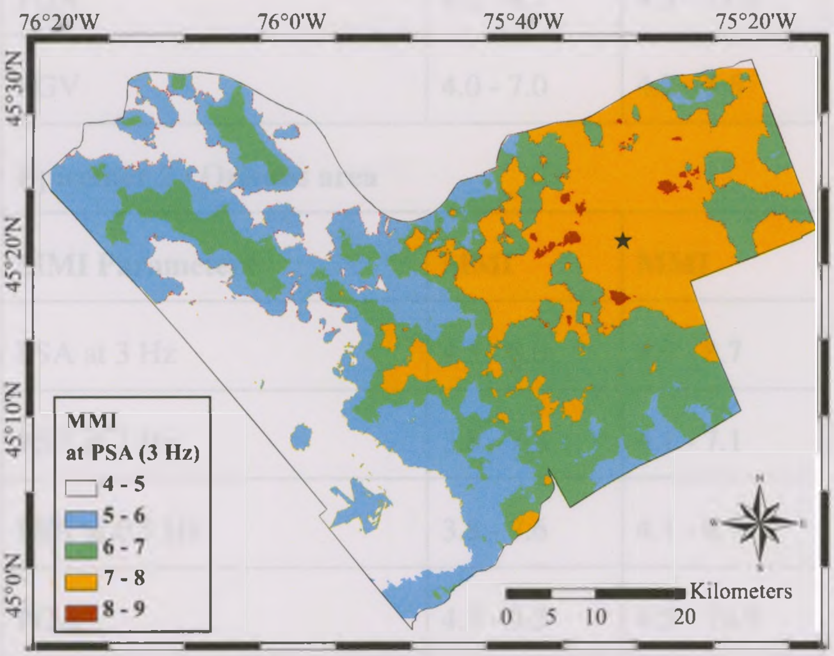

Figure 3.16. MMI based on PSA at 3 Hz for **M6** scenario located on hard rock, south of the Ottawa region using site-specific amplification factors.

Table 3.3. Range of predicted MMI for Epicenters 1 and 2 of ShakeMap Categories II and III based on median ground motions; intensities could be ± 1 based on one std deviation.

	ShakeMap Category	
	II	**III**
Epicenter 1 – South of the city		
MMI Parameters	**MMI**	**MMI**
PSA at 3 Hz	4.2 - 7.6	4.3 - 8.7
PSA at 1 Hz	3.8 - 6.4	4.1 - 6.9
PSA at 0.5 Hz	3.8 - 6.7	4.1 - 6.7
PGA	4.2 - 8.7	4.5 - 11.0
PGV	4.0 - 7.0	4.2 - 8.6
Epicenter 2 - Orleans area		
MMI Parameters	**MMI**	**MMI**
PSA at 3 Hz	4.3 - 8.0	4.4 - 8.7
PSA at 1 Hz	3.8 - 7.3	4.1 - 7.1
PSA at 0.5 Hz	3.8 - 7.6	4.1 - 6.7
PGA	4.3 - 9.3	4.5 - 10.9
PGV	4.0 - 7.8	4.3 - 8.6

Table 3.4. Range of predicted MMI for Epicenters 3 and 4 of ShakeMap Categories II and III based on median ground motions; intensities could be ± 1 based on one std deviation.

	ShakeMap Category	
	II	**III**
Epicenter 3 - Hull area		
MMI Parameters	**MMI**	**MMI**
PSA at 3 Hz	4.4 - 7.2	4.5 - 7.9
PSA at 1 Hz	4.0 - 6.2	4.2 - 6.7
PSA at 0.5 Hz	4.0 - 6.5	4.2 - 5.9
PGA	4.4 - 8.2	4.7 - 9.6
PGV	4.2 - 7.0	4.4 - 7.7
Epicenter 4 – East of the city		
MMI Parameters	**MMI**	**MMI**
PSA at 3 Hz	4.2 - 8.0	4.3 - 8.3
PSA at 1 Hz	3.6 - 7.3	3.7 - 7.1
PSA at 0.5 Hz	3.5 - 7.6	3.9 - 6.7
PGA	4.2 - 9.2	4.0 - 10.9
PGV	3.9 - 7.7	3.7 - 8.6

3.4 M6.5 and M7.5 Scenarios

What would have happened in Ottawa if the **M**5 Val des Bois event had been of larger magnitude? This was tested by selecting a **M**6.5 event at the epicenter of the Val des Bois earthquake. Figure 3.17 shows PSA at 3 Hz for this scenario event. For the Val des Bois event, the range of PSA at 3 Hz was 30 to 70 cm/s^2. In case of a **M**6.5 event, the range of PSA at 3 Hz would be 30 to 300 cm/s^2. Hence the ground motions would be considerably higher, and so will be the intensities. Figure 3.18 shows the predicted MMI based on PGV for this **M**6.5 scenario. The intensities would be in range of 4.5 to 6.5 for entire Ottawa region. The core of downtown Ottawa would experience intensity range of 4.5 to 6 while Orleans would experience MMI between 6 and 6.5.

Another large magnitude scenario was tested, assuming a maximum-magnitude event in the distant Charlevoix seismic zone (**M**7.5 at 460 km). The predicted intensities would range from 3.5 to 7 for median ± 1 standard deviation motions. The maximum MMI of 7 would be felt in the Orleans area. This shows that the soft soil patch (over which Orleans area is located) is vulnerable to strong distant earthquakes. Downtown Ottawa would experience a wide range of intensities, between 4.5 and 6.5. Figure 3.19 shows the MMI based on PGV for the **M**7.5 scenario. All other maps for **M**6.5 and **M**7.5 are attached in Appendix XI.

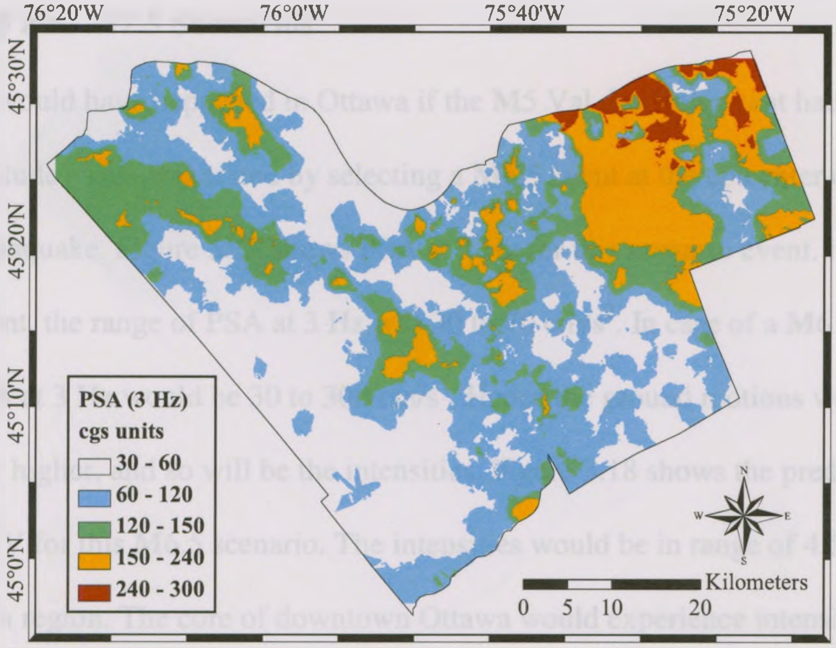

Figure 3.17. PSA at 3 Hz for M6.5 scenario using site-specific amplification factors. The epicenter for this event is approximately 60 km North.

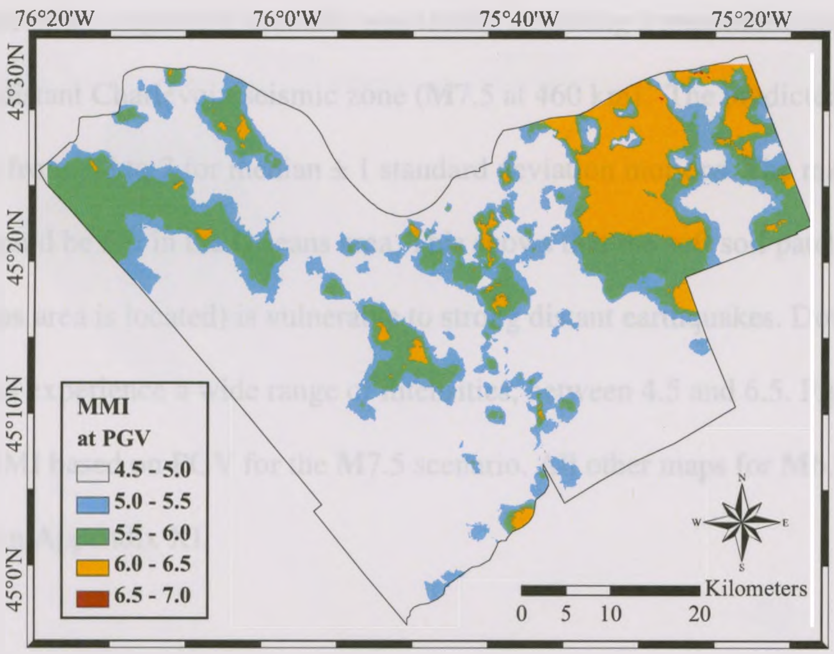

Figure 3.18. MMI based on PGV for M6.5 scenario using site-specific amplification factors.

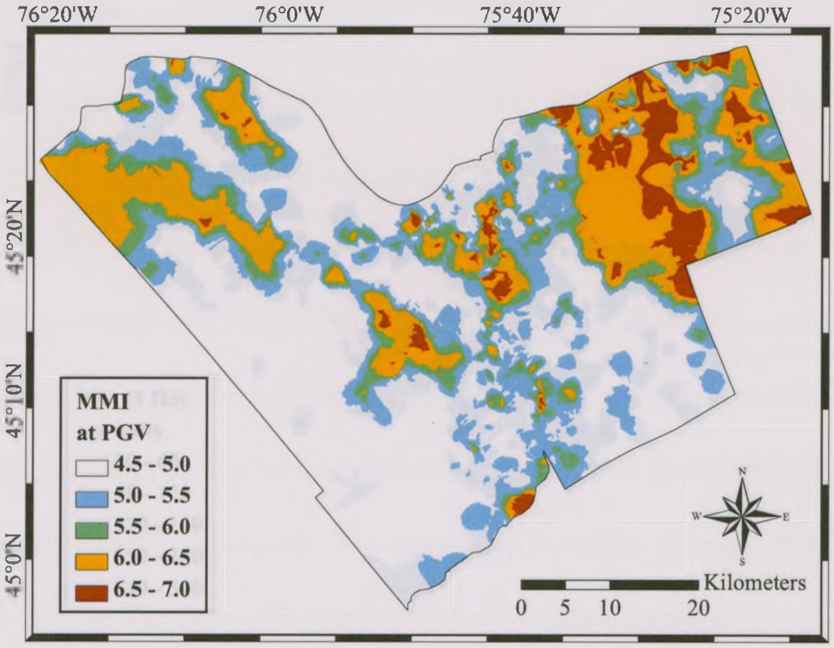

Figure 3.19. MMI based on PGV for **M**7.5 scenario using site-specific amplification factors. The epicenter for this event is located approximately 460 km away in Charlevoix Seismic Zone.

3.5 ShakeMaps for Historic earthquakes

What happened in the past reflects what could happen in the future. To increase the understanding of the effects of distant strong earthquakes, three historic earthquakes with **M**>5.5 and located at three different distances were considered. The 1925 Charlevoix, 1935 Timiskaming and 1944 Cornwall earthquakes were studied for which the moment magnitudes and epicentral distances region are given in Table 2.7 and the summary of intensities are given in Table 3.5.

3.5.1. 1925 M6.2 Charlevoix earthquake

The **M**6.2 Charlevoix earthquake occurred on 28 February 1925 in Charlevoix-Kamouraska region and widely felt more than 1000 km (Figure 3.20). Downtown Ottawa experienced strong shaking, as evidenced by felt reports from key buildings like the Auditorium, the Canadian Museum of Nature and the Lisgar Collegiate Institute (Lamontagne, 2010). There were some reports of cracks in plaster, and damage to brick walls and chimneys in the Ottawa region, with a maximum reported intensity of 6 (Lamontagne, 2010). Now when the population and infrastructure of Ottawa have considerably increased as compared to 1925, what would happen if similar earthquake were to occur today? Figure 3.21 shows the predicted MMI based on PGV for 1925 Charlevoix Earthquake. According to the ShakeMap predictions, for a similar event today, the range of MMI in Ottawa would be 3.5 to 5 for median ground motions, or 2.5 to 6 for ±1 standard deviation about the median predicted motions.

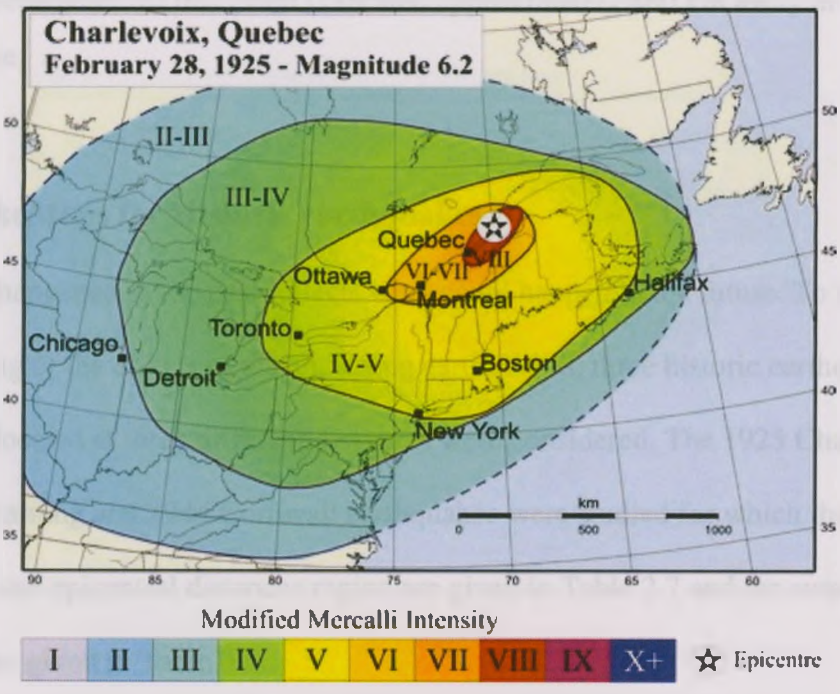

Figure 3.20. Isoseismal map for entire Eastern North America for 1925 Charlevoix earthquake. (Source: http://earthquakescanada.nrcan.gc.ca/histor/20th-eme/1925/intensitew-eng.php; accessed on 26.09.2010).

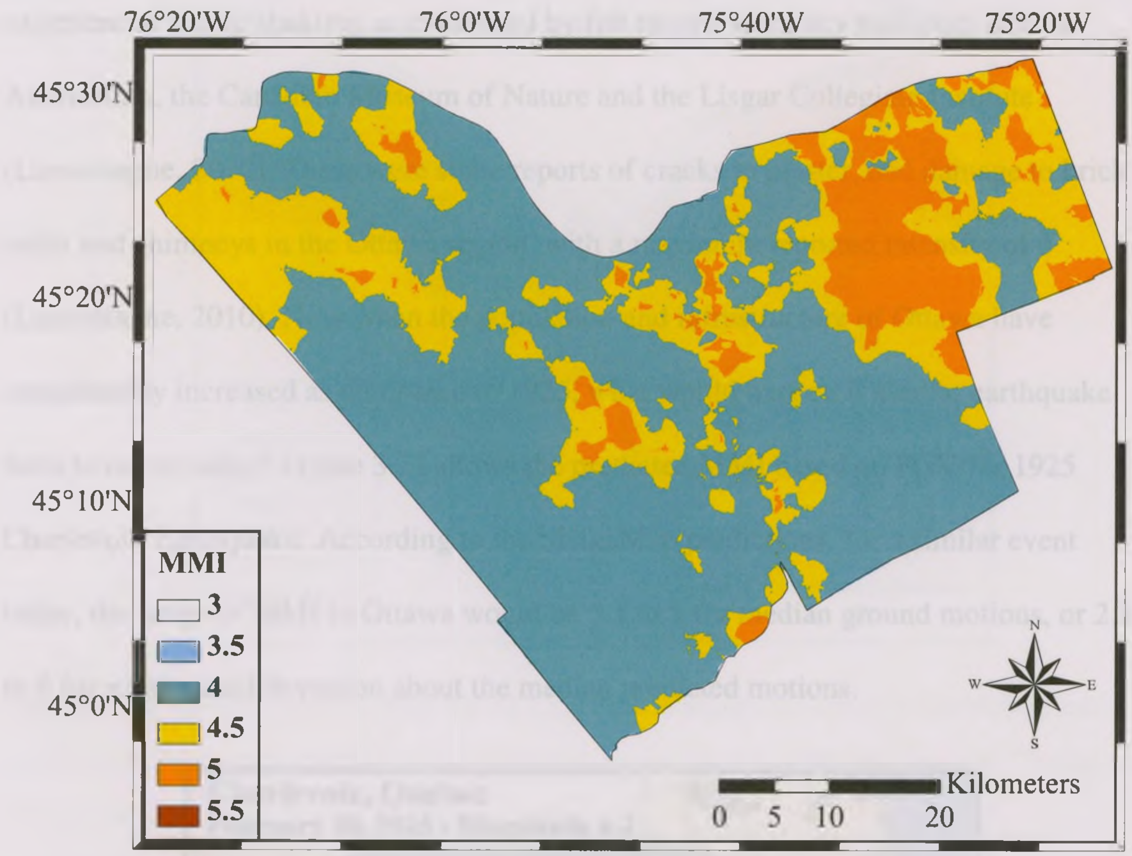

Figure 3.21. Predicted MMI based on PGV at median ground motions for 1925 Charlevoix earthquake using profile-specific amplification factors.

3.5.2. 1935 M6.1 Timiskaming Earthquake

The M6.1 Timiskaming earthquake occurred on 1st November 1935 approximately 10 km east of Timiskaming and 260 km north-east of Ottawa. The shaking was felt as far as 800 km away in New York and Detroit and damage was reported to distances as far as 70 km (Bruneau and Lamontagne, 1994). In Timiskaming, 80% of all chimneys were damaged on basis of which a maximum intensity 7 was assigned near the epicentral area (Hodgson,1936a, 1936b; Lamontagne, 2010; See Figure 3.22). If a similar earthquake were to occur today, the intensity in the Ottawa region would range from 3 to 5 based on median ground motions (See Figure 3.23), with the maximum occurring in the soft soil.

This implies that actual intensity could range from 2 to 7 considering typical ground-motion variability of about a factor of 2 (e.g. Atkinson and Boore, 2006).

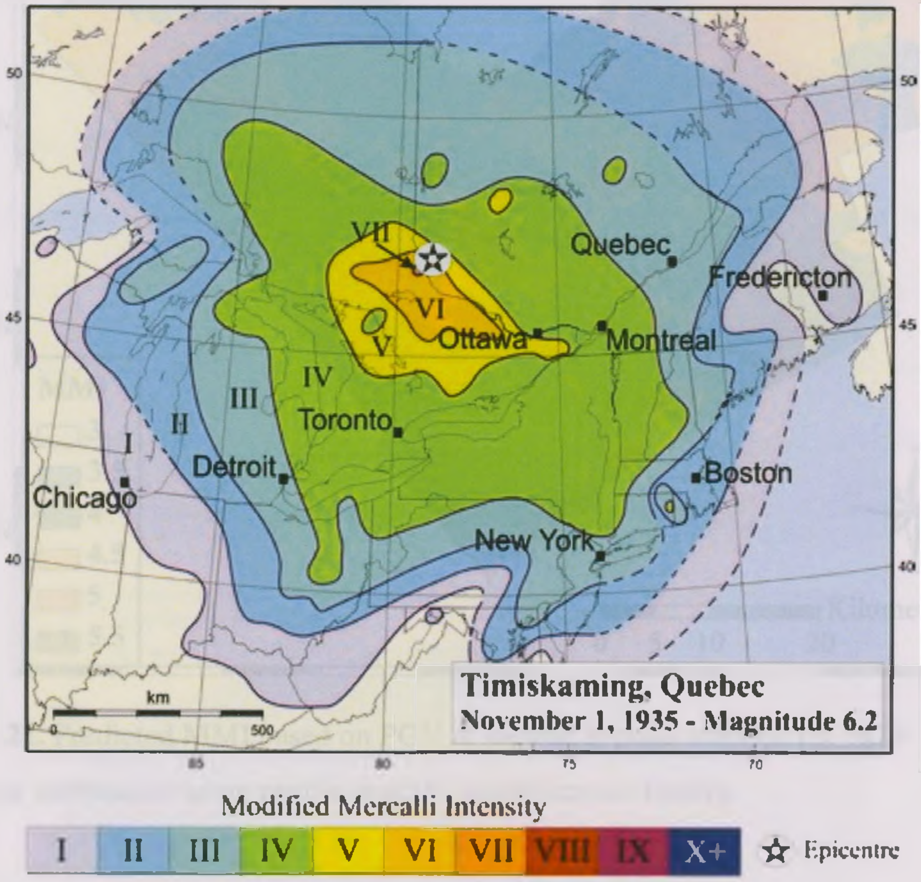

Figure 3.22. Isoseismal map for entire Eastern North America for 1935 Timiskaming earthquake. (Source: http://earthquakescanada.nrcan.gc.ca/histor/20th-eme/1935/1935-eng.php; accessed on 26.09.2010).

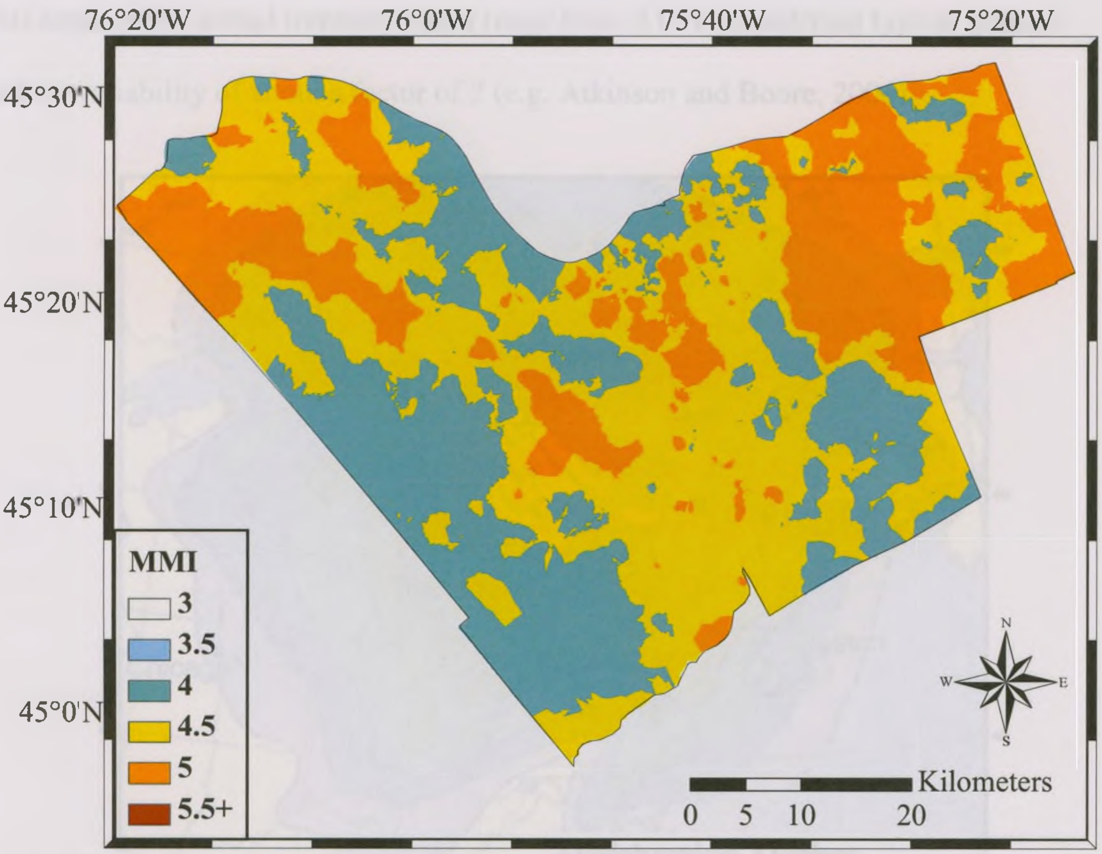

Figure 3.23. Predicted MMI based on PGV at median ground motions for 1935 Timiskaming earthquake using profile-specific amplification factors.

3.5.3. 1944 M5.8 Cornwall Earthquake

The epicenter for this **M**5.8 event that occurred on 5th September 1944, was located approximately 50 km south-east of Ottawa. Shaking was felt to 500 km but damage was restricted to within 50 km. Figure 3.24 shows the isoseismal map of Cornwall earthquake. Most of the damage was in unreinforced masonry buildings, due to out-of-plane failures; around 2000 chimneys were damaged/collapsed in the Cornwall area (Bruneau and Lamontagne, 1994). The average estimated intensity in the Ottawa region was 5, with a maximum intensity of 7. This earthquake was strongly felt in Ottawa with instances of fall of light objects, cracks in plaster of walls, and fallen masonry and also electrical blackout during the earthquake. Figure 3.25 shows the prediction of MMI based on PGV for Cornwall earthquake. If a similar earthquake were to occur today, the intensity in Ottawa region would range from 4 to 6 for median ground motions, or 3 to 7 considering one standard deviation, with the peak MMI in the downtown reaching 5 to 6 based on the profile-specific amplification factors. This could cause some damage to unreinforced masonry, to tall and slender structures like chimneys if they are old or weak, and minor damage like cracks in plasters or walls in some structures.

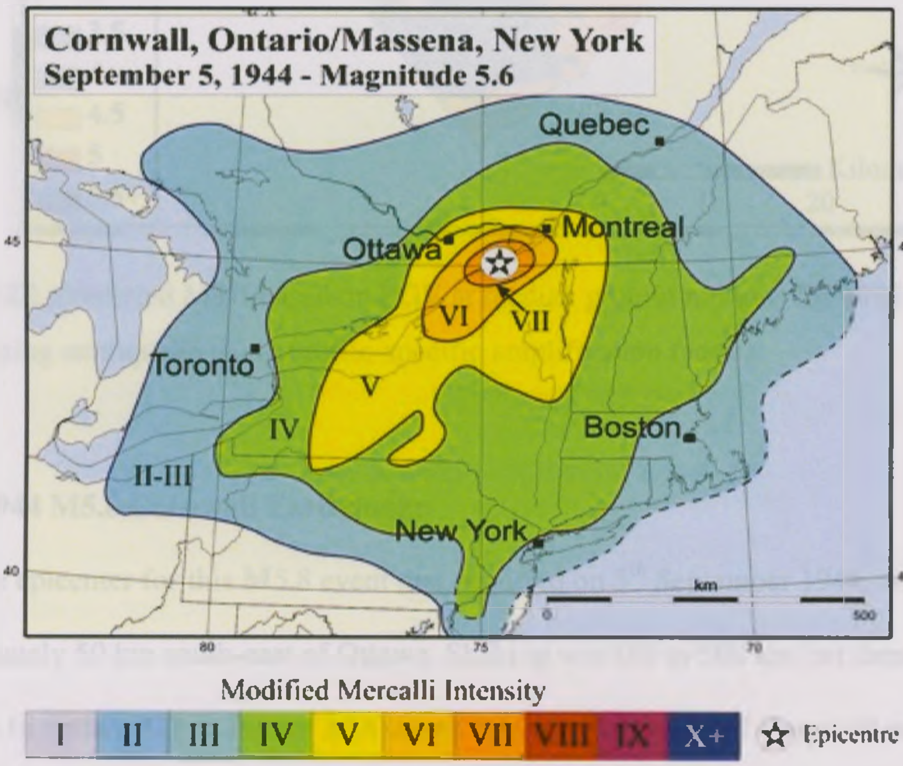

Figure 3.24. Isoseismal map for 1944 Cornwall earthquake. (Source: http://earthquakescanada.nrcan.gc.ca/histor/20th-eme/1944-eng.php; accessed on 26.09.2010).

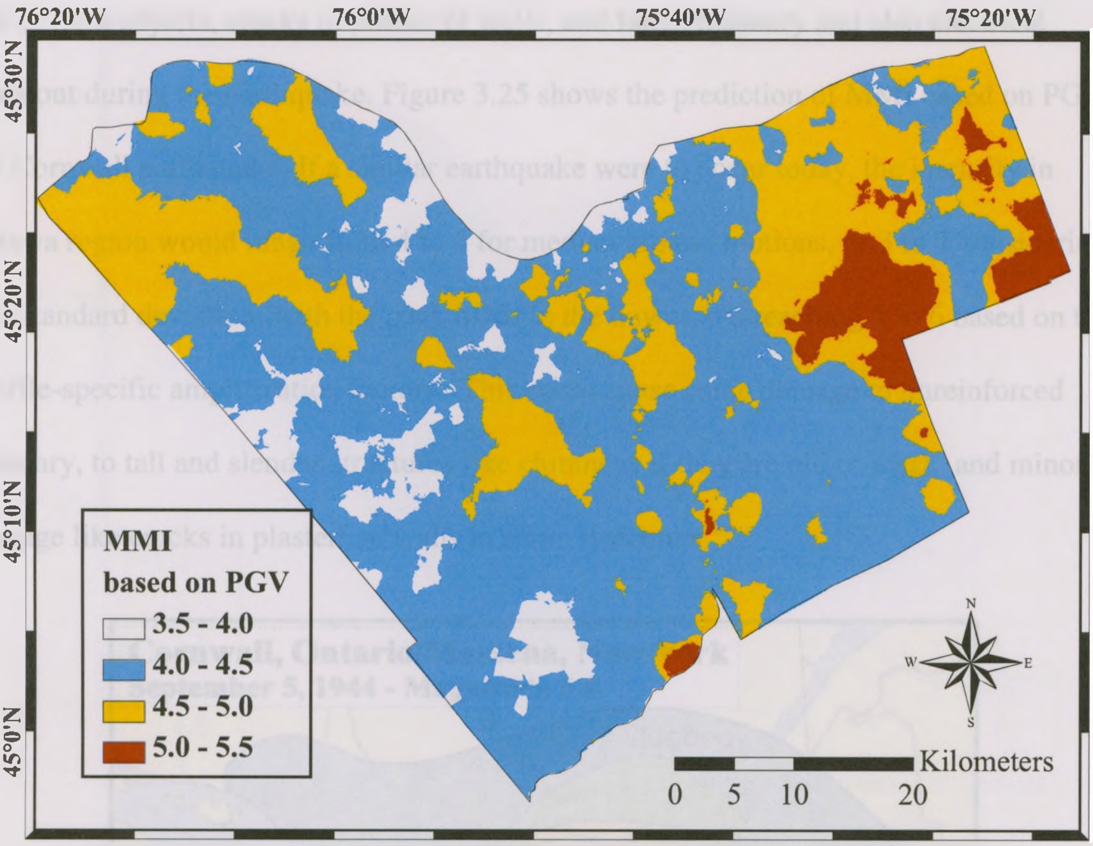

Figure 3.25. Predicted MMI based on PGV at median ground motions for 1944 Cornwall earthquake using profile-specific amplification factors.

Table 3.5. Comparison of felt (Lamontagne, 2010) and predicted (using profile-specific amplification factors) MMI for median ground motions in the Ottawa region for historic events.

Details	**Modified Mercalli Intensity**				
	Felt Intensity (Avg; Max)	Prediction as per profile-specific amplification factors for median ground motions (note that MMI could be ±1 unit for 1 std deviation of the GMPE)			
		PSA (3 Hz)	PSA (1 Hz)	PGA	PGV
M6.1, 1935 Timiskaming EQ	4; 7	4 - 5	4 - 5	4 - 5.5	4 - 5
M5.8, 1944 Cornwall EQ	5; 7	4 - 6	4 - 5.5	4 - 6.5	4 - 5
M6.2, 1925 Charlevoix EQ	3; 6	4 - 5	3.5 - 5	4 - 5	3.5 - 5

3.6 Implications based on past earthquakes and scenarios

The 2%/50 year motions of a local earthquake for Ottawa are consistent with the occurrence of an event of **M**6 in or near the city. In general, the intensity pattern would depend on the location of the event. In the case of an **M**6 event in the city, the eastern part of Ottawa could experience a maximum MMI of 8. In parts of the downtown, 3 to 5 storey buildings could be vulnerable due to the frequency of site-response. In Orleans, high-rise buildings could experience strong shaking due to site amplification at long periods, resulting in moderate damage. If the epicenter is located in Hull area, 3 to 5 storey buildings in the downtown and high-rise in the Orleans area would experience moderate to strong shaking, with limited damage such as to non-structural elements, or to poorly constructed masonry buildings. In both the scenarios, weak/old chimneys and old brick structures could be subjected to major damage or complete collapse. Distant strong earthquakes (i.e. M7.5, D>400 km), could strongly shake Ottawa with MMI range of 3 to 7, with no damage expected to structures, except in unusual circumstances. Note that buildings constructed to current code requirements should not sustain life-threatening damage.

CHAPTER 4

SUMMARY AND CONCLUSIONS

"Always bear in mind that your own resolution to success is more important than any other one thing." - Abraham Lincoln

4.1 Summary

The ShakeMaps of this study give a preliminary overview of the earthquake hazard in the Ottawa region from moderate local and strong distant events, and provide a general guide to ground motion and intensity distribution. Local scenario events (M6) based on 2% / 50 year exceedance probability motions, as well as historical events were modelled to understand the impact on:

(i) The Ottawa downtown because of the important structures and population density.

(ii) The Orleans area because of the deep soft sediments that underlie this area.

Two different sets of amplification factors were used in this study. ShakeMaps were generated using: (i) the amplification factors of NBCC 2005; and (ii) site- specific amplification factors generated based on local soil conditions, using the quarter wavelength method. It appears likely that the NBCC amplification factors under predict ground motions and shaking intensities in distant soft soil patches. In addition, these amplification factors do not model the potential for near source de-amplification effects associated with strong ground motions on soft soils at high frequencies. The near source de-amplification effect is seen when the epicenter is located in soft soil using profile-specific amplification factors. This is an interesting result as it suggests that soft soils may de-amplify high-frequency ground motions near-source, because of high-frequency damping of soft sediments due to strong ground motions. Profile-specific amplification factors appear to predict ground motions according to the changing site conditions with ground motions decaying with distance and amplifying in the distant basin sediments.

Both the NBCC 2005 and profile-specific amplification factors used in this study are frequency dependent, but the profile-specific factors feature larger variations in soil amplification at different frequencies. This is clearly seen in the differences in average predicted intensities using different sets of amplification factors in downtown Ottawa for Val des Bois event.

Of all the scenarios modelled, local scenarios pose the maximum hazard in the Ottawa region. The maximum expected damage for 2%/50 year ground motions, in the intensity range 6 to 8, might be experienced in low-to-moderate rise buildings, with the possibility of moderate to high damage to non-structural elements and in some cases also low to moderate damage to structural elements of buildings. The soft soil deposits in the region, especially Orleans, would play an important role in amplifying the risk to infrastructure if such an earthquake were to occur. Epicenters in the Orleans area or Hull area pose maximum damage out of the chosen four local scenario locations. For distant earthquake scenarios of higher magnitudes, felt effects in Orleans would be maximum, with more moderate motions in downtown. Note that buildings constructed to current code requirements should not sustain life-threatening damage.

The results of this study help identify:

(1) The hazard potential of hypothetical local earthquakes based on (a) 2% / 50 year exceedance probability motions and (b) historical earthquake scenarios. This information can be used by city of Ottawa and general public as a guide to city and emergency response planning. The results of this study can be used as a guide

to design (a) a public awareness program to the possible earthquake hazards, and (b) earthquake hazard mitigation.

(2) Differences in ground motion and intensity distributions arising from different locations in and around Ottawa for 2% / 50 year exceedance probability scenarios. This information is helpful to researchers in understanding the effect of epicenter location (geographical and geological) on hazard pattern for given regional geological conditions.

(3) Differences in ground motion and intensity distributions arising from use of different amplification factors. This information is useful to researchers to understand the local site effects and is a step forward in understanding how to improve NBCC 2005 amplification factors.

This study is based on detailed microzonation of Ottawa region carried out by Hunter *et al.* (2010). Detailed soil information helps in reducing uncertainty in the resulting ShakeMaps. Yet, the results of this study are subjected to significant uncertainty based on magnitude and location of potential future earthquakes. This study also shows that detailed ShakeMap investigations and earthquake hazard estimation are possible using geographical information systems.

4.2 Future Recommendations

Ploeger (2008) conducted a broad earthquake risk assessment for the downtown area of Ottawa, using HAZUS-MH to evaluate loss estimation wherein areas most physically and socially vulnerable to ground shaking were studied. The soil information for the study was based on just a few borehole investigations in the downtown area. The

HAZUS-MH earthquake model uses Geographic Information System (GIS) software and scientifically developed algorithms to calculate, map, and display earthquake loss data for hypothetical earthquakes (Hansen and Bausch, 2007). Ploeger (2008) used different earthquake scenarios to estimate the earthquake risk in Ottawa downtown core by interpreting the output of HAZUS-MH based on building inventory and demographic tally. The current study was done after a detailed microzonation of Ottawa and therefore gives a more comprehensive hazard assessment for the entire Ottawa region. It is now possible to combine these two studies to provide an improved risk assessment.

The following steps can be taken to mitigate the possible earthquake risks identified in the Ottawa area:

(1) Earthquake-specific emergency response plan can be prepared, based on the ShakeMaps of this study and updated risk assessment.

(2) As a part of a program to lower the risk, weak structures in strong shaking areas as delineated in ShakeMaps can be strengthened and public awareness programs initiated.

(3) One way of increasing public awareness is to publish the ShakeMaps of this study.

(4) Buildings that are greater risk by virtue of occupancy, e.g. schools in daytime need special attention and schools in high hazard areas as delineated by the ShakeMaps of this study can be inspected and structurally upgraded, if necessary.

The site specific amplification factors used in this study show the importance of typical eastern north American soil profiles in amplifying ground motions, as demonstrated by the example of the **M**5 Val des Bois event.

Amplification factors for Eastern North America should be revised to better model these effects. Finally, the amplification factors of this study could also be used in real-time ShakeMap applications for the Ottawa region.

BIBLIOGRAPHY

Adams, J. (1989) Seismicity and seismotectonics of southeastern Canada, Ann N Y Acad Sci. **558**, 40–53.

Adams, J., and P. Basham (1989). The seismicity and seismotectonics of Canada east of the Cordillera. *Geoscience Canada.* **16**, 16 pp.

Adams, J., Rogers, G., Halchuk, S., et. al.,. (2002). The case for an advanced national earthquake monitoring system for Canada's cities at risk. In Proceedings of the 7th U.S. National Conference on Earthquake Engineering, Boston, Massachusetts.

Adams, J., and S. Halchuk (2003). Fourth generation seismic hazard maps of Canada: values for over 650 Canadian localities intended for the 2005 National Building Code of Canada. Geol. Surv. of Can. Open-File Rept. 4459, 155 pp.

Atkinson, G. M., and K. Assatourians (2010). Attenuation and Source Characteristics of June 23, 2010 M5.0 Val des Bois, Quebec earthquake, *Bull. Seism. Soc. Am.,***81**, 849 - 860.

Atkinson, G. M., and D. M. Boore (2006). Earthquake Ground-Motion Prediction Equations for Eastern North America, *Bull. Seism. Soc. Am.* **96,** 2181-2205.

Atkinson, G. M., and S. I. Kaka (2007). Relationships between felt intensity and instrumental ground motion in the central United States and California, *Bull. Seism. Soc. Am.* **97,** 497-510.

Bent, A.L. (2009). A moment magnitude catalog for the 150 largest eastern Canadian earthquakes, *Geological Survey of Canada,* Open File 6080.

Beresnev, I. A., and K. L. Wen (1996). Nonlinear soil response - A reality? *Bull. Seism. Soc. Am.* **86,** 1964-1978.

Boore, D. M., and W. B. Joyner (1997). Site amplifications for generic rock sites, *Bull. Seism. Soc. Am.* **87,** 327-341.

Boore, D.M. (2000). SMSIM -- Fortran programs for simulating ground motions from earthquakes: version 2.0 --- A revision of OFR 96-80-A, U.S. Geological Survey Open-File
Report OF 00-509, 53 pp.

Boore, D. M., and G. M. Atkinson (2008). Ground-motion prediction equations for the average horizontal component of PGA, PGV, and 5%-damped PSA at spectral periods between 0.01 s and 10.0 s, *Earthquake Spectra* **24,** 99-138.

*Borcherdt, R. D. (1994). Estimates of site-dependent response spectra for design (methodology and justification), Earthquake Spectra, **10**, 617-654.*

Borcherdt. R. D. (2002). Empirical Evidence of Acceleration-Dependent Amplification Factors, *Bull. Seism. Soc. Am.* **92,** 761-782.

Bruneau, M., and M. Lamontagne (1994). Damage from 20th century earthquakes in eastern Canada and seismic vulnerability of unreinforced masonry buildings. *Canadian Journal of Civil Engineering.* **21**, 643-662.

Building Seismic Safety Council (1997). NEHRP recommended provisions for seismic regulations for new buildings, Part 1 Provision. FEMA 302. Federal Emergency Management Agency, Washington D.C., pp 290.

Campbell, K. W. (2009). Estimates of Shear-Wave Q and kappa(0) for Unconsolidated and Semiconsolidated Sediments in Eastern North America, *Bull. Seism. Soc. Am.* **99,** 2365-2392.

Cornell, C. A. (1968). Engineering seismic hazard analysis, *Bull. Seismol. Soc. Am.* **59** (1968) (5), pp. 1583–1606.

DMTI CanMap RouteLogistics v2008.3. [Computer file]. Markham, Ontario: DMTI Spatial Inc., 2008.

Dobry, R., and M. Vucetic (1987). Dynamic properties and seismic response of soft clay deposits. Proc. International Symposium on Geotechnical Engineering of Soft Soils, Mexico City, Vol. 2, 51-87.

Engineering Seismology Toolbox (2010). Response Spectra for M5 Val des Bois event - Processed Data Tables, http://www.seismotoolbox.ca/ValDesBois.html.

Field, E. H., P. A. Johnson, I. A. Beresnev, and Y. H. Zeng (1997). Nonlinear ground-motion amplification by sediments during the 1994 Northridge earthquake, *Nature* **390,** 599-602.

Finn, W. D. L., and A. Wightman (2003). Ground motion amplification factors for the proposed 2005 edition of the National Building Code of Canada, *Can.J.Civ.Eng.* **30,** 272-278.

Hanks T. C. and H. Kanamori (1979). A moment magnitude scale, *J. Geophys. Res.* **84**, 2348-2350.

Hansen, R., and D. Bausch (2007). A GIS-based methodology for exporting the Hazards U.S. (HAZUS) earthquake model for global applications. http://www.hazus.org/HUG%20DOCUMENTS/Global_HAZUS.pdf.

Hodgson, E.A. (1936a). Preliminary report of the earthquake of November 1, 1935. Earthquake Notes, **7**, 1-4.

Hodgson, E.A. (1936b). The Timiskaming earthquake of November 1st, 1935. The location of epicenter and determination of focal depth. Royal Astronomical Society of Canada Journal, **30**, 113- 123.

Hu, Y, S. C. Liu, and W. Dong (1996). Earthquake Engineering. E & FN Spon, Chapman and Hall.

Huang, B. S., K. C. Chen, W. G. Huang, J. H. Wang, T. M. Chang, R. D. Hwang, H. C. Chiu, and C. C. P. Tsai (2000). Characteristics of strong ground motion across a thrust fault tip from the September 21, 1999, Chi-Chi, Taiwan earthquake, *Geophys.Res.Lett.* **27,** 2729-2732.

Hunter, J.A., H.L. Crow, G.R. Brooks, M. Pyne, D. Motazedian, M. Lamontagne, A.J.-M. Pugin, S.E. Pullan, T. Cartwright, M. Douma, R.A. Burns, R. L. Good, K. Kaheshi-Banab, R. Caron, M. Kolaj, I. Folahan, L. Dixon, K. Dion, Duxbury, A. Landriault, V. Ter-Emmanuil, A. Jones, G. Plastow, and D. Muir (2010). Seismic site classification and site period mapping in the Ottawa area using geophysical methods, *Geol. Surv. of Can., Open File Report 6273.*

Kaka, S. I. (2006). Development of Ontario ShakeMaps, Ph.D. Thesis, Carleton University, Canada.

Kolos, D. (2010). Using Horizontal-to-Vertical Spectral Ratios to Estimate Shear Wave Velocities of Soil at South-Eastern Canadian Seismological Stations, Master Thesis, The University of Western Ontario, Canada.

Lang, L. (1998). Managing Natural Resources with GIS. ESRI Press, 132 pp.

Lamontagne, M., M. Sheshpari, and K. Khan (2008). Earthquake damage in the Ottawa-Gatineau region between 1830 and 2008, *Geological Survey of Canada,* Open File 5908.

Lamontagne, M. (2010). Historical Earthquake Damage in the Ottawa-Gatineau Region, Canada, *Seismol.Res.Lett.* **81,** 129-139.

Lermo J., F.J. Chavez-Garcia (1993). Site effect evaluation using spectral ratios with only one station, *Bull. Seism. Soc. Am.* 1993; 83(5): 1574-1594.

Ma, S., and D. W. Eaton (2007). Western Quebec seismic zone (Canada): clustered, midcrustal seismicity along a Mesozoic hot spot track. *Journal of Geophysical Research.* 112: B06306, doi:10.1029/2006JB004827.

Motazedian, D., and Hunter, J. (2008). Development of a NEHRP map for the Orleans suburb of Ottawa, Ontario, *Can. Geotech. J.* **45**, 1180-1188.

Natural Resources Canada (2010). http://earthquakescanada.nrcan.gc.ca/zones/eastcan-eng.php

Natural Resources Canada (2010a). http://earthquakescanada.nrcan.gc.ca/histor/20th-eme/e_damaging-eng.php

Ploeger, S. K. (2008). Applying the HAZUS-MH software tool to assess seismic hazard and vulnerability in downtown Ottawa, Canada. Master Thesis, Carleton University, Canada.

Stone, W.C., F.Y. Yokel, M. Celebi, T. Hanks, and E.V. Leyendecker (1987). Engineering aspects of the September 19, 1985 Mexico earthquake. NBS Building Science Series 165, National Bureau of Standards, Washington, D.C., 207 p.

Wald, D. L., L. Wald, B. Worden and J Goltz (2007). USGS ShakeMap- A tool for earthquake response, *U.S. Geol. Surv. Fact Sheet* 087-03-508, 4 p.

Wald, L. A., and J. Mori (2000). Evaluation of methods for estimating linear site-response amplifications in the Los Angeles region, *Bull. Seism. Soc. Am.* **90,** S32-S42.

Wald, D., V. Quitoriano, L. Dengler, and J. Dewey (1999a). Utilization of the Internet for rapid community intensity maps. *Seismological Research Letters* 70, 680–697.

Wells, D.L., and K.J. Coppersmith (1994). New empirical relationships among magnitude, rupture length, rupture width, rupture area, and surface displacement. *Bulletin of the Seismological Society of America.* **84**, 974-1002.

Woolery, E. W., T. Lin, Z. Wang, and B. Shi (2008). The Role of Local Soil-Induced Amplification in the 27 July 1980 Northeastern Kentucky Earthquake, *Environ. & Engg. Geoscience.* **14,** 267-280.

Wood, H. O., and F. Neumann (1931). Modified Mercalli Intensity Scale of 1931, *Bull. Seism. Soc. Am.* **21**, 277 – 283.

APPENDICES

APPENDIX I

Category I ShakeMaps: Ground motions based on NBCC 2005

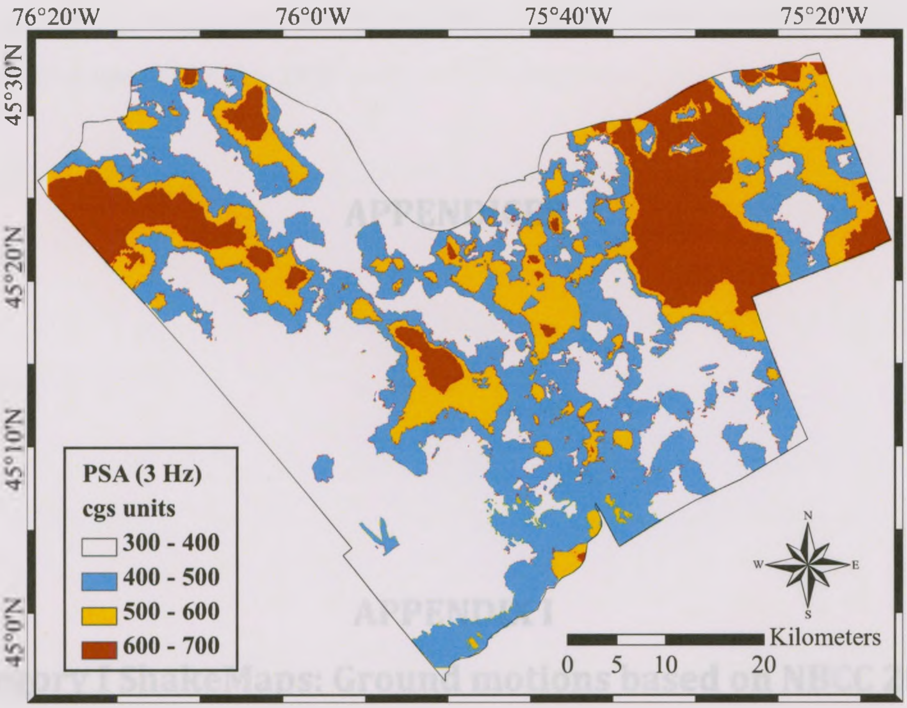

Figure A1.1. PSA at 3 Hz for uniform hazard spectrum using amplification factors based on NBCC 2005 for the Ottawa region.

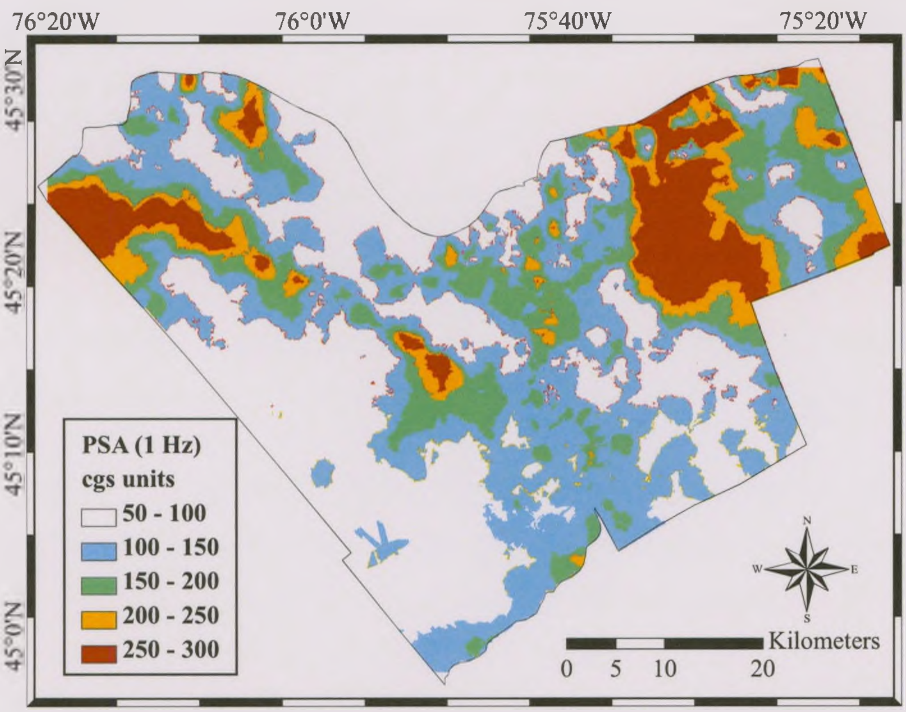

Figure A1.2. PSA at 1 Hz for uniform hazard spectrum using amplification factors based on NBCC 2005 for the Ottawa region.

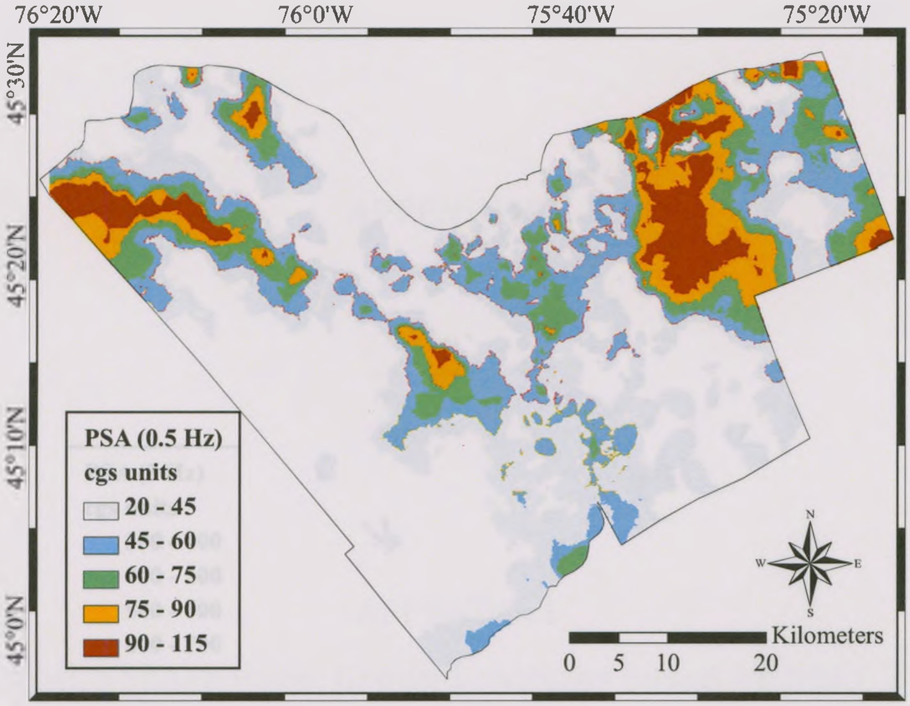

Figure A1.3. PSA at 0.5 Hz for uniform hazard spectrum using amplification factors based on NBCC 2005 for the Ottawa region.

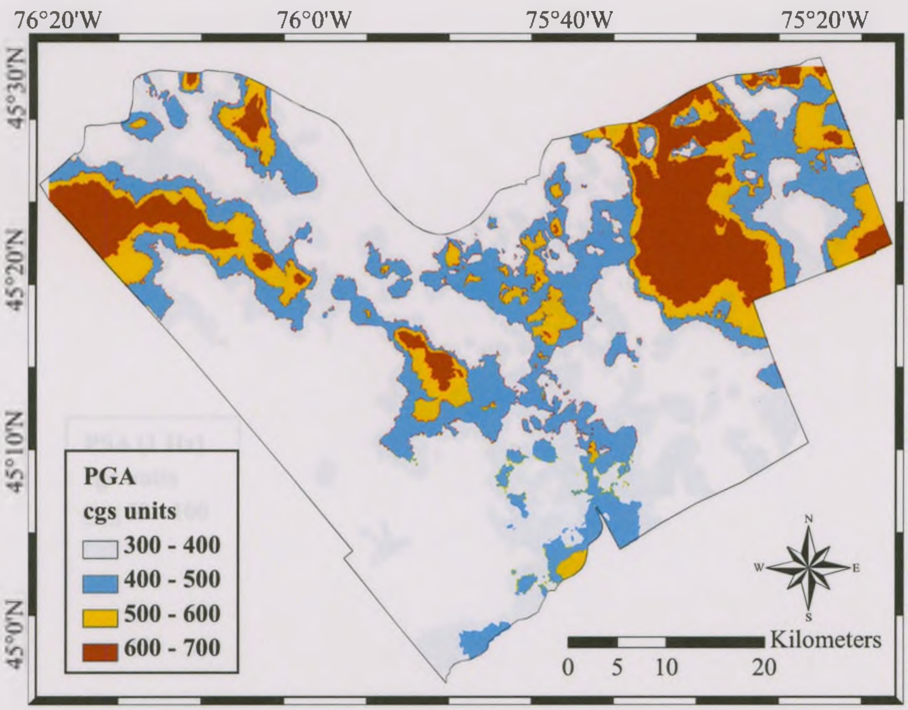

Figure A1.4. PGA for uniform hazard spectrum using amplification factors based on NBCC 2005 for the Ottawa region.

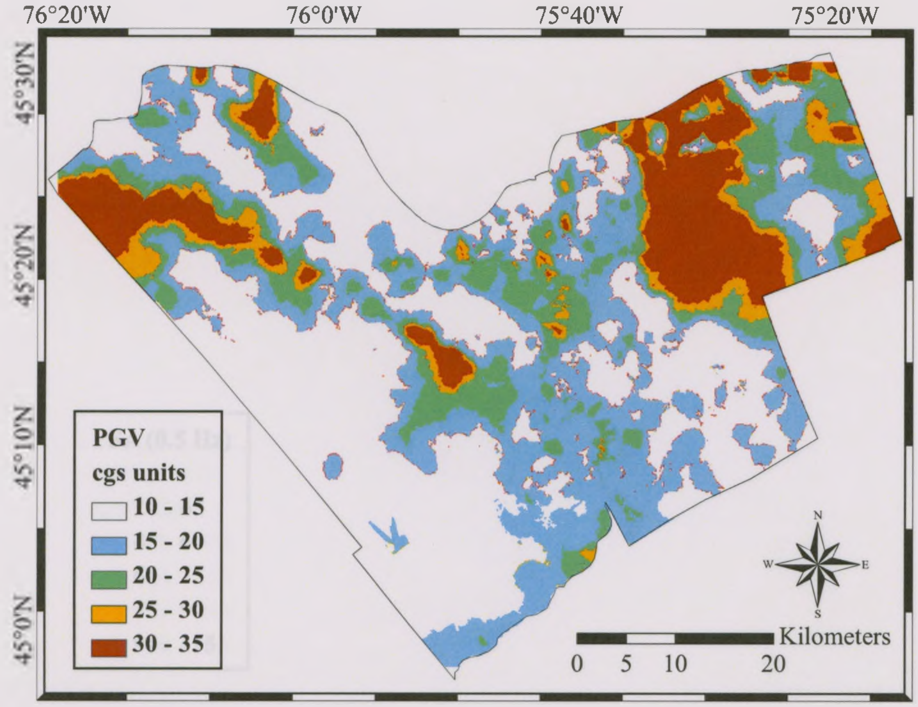

Figure A1.5. PGV for uniform hazard spectrum using amplification factors based on NBCC 2005 for the Ottawa region.

APPENDIX II

ShakeMaps for M5 Val des Bois Earthquake

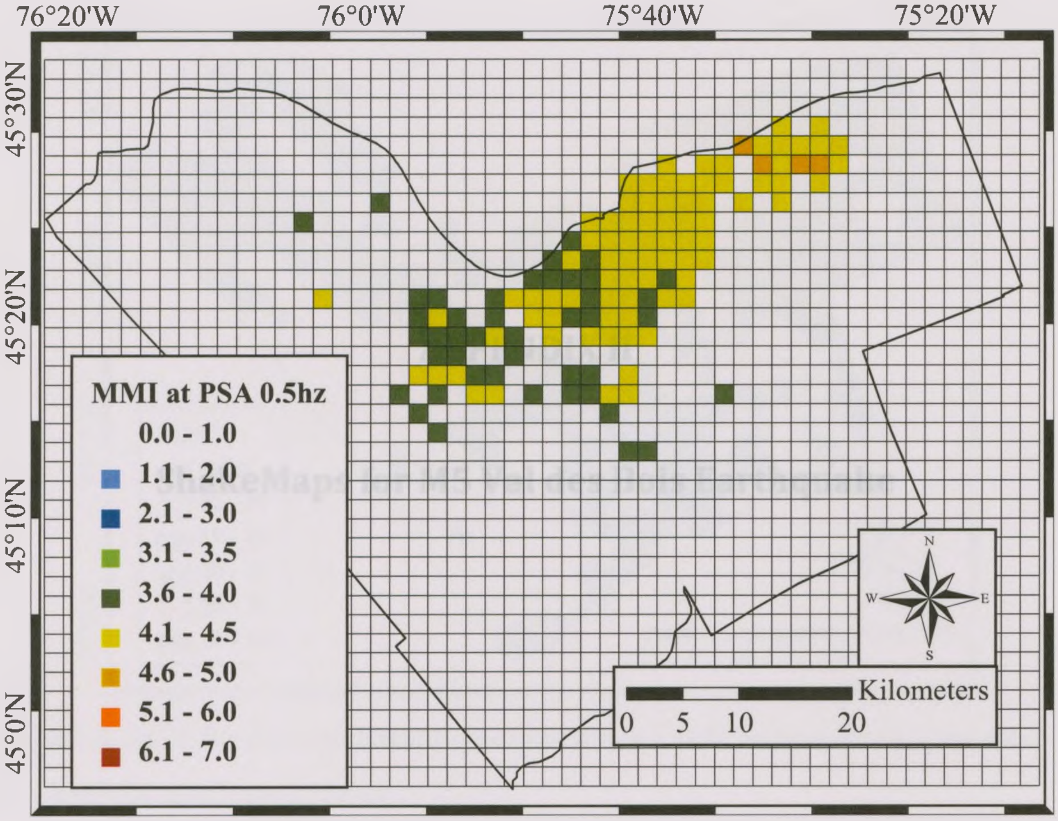

Figure A2.1. Predicted MMI based on PSA at 0.5 Hz for M5 Val des Bois earthquake averaged over boxes of approx. 1.5 km^2 grids for number of reports $\geq$ 3 in each box.

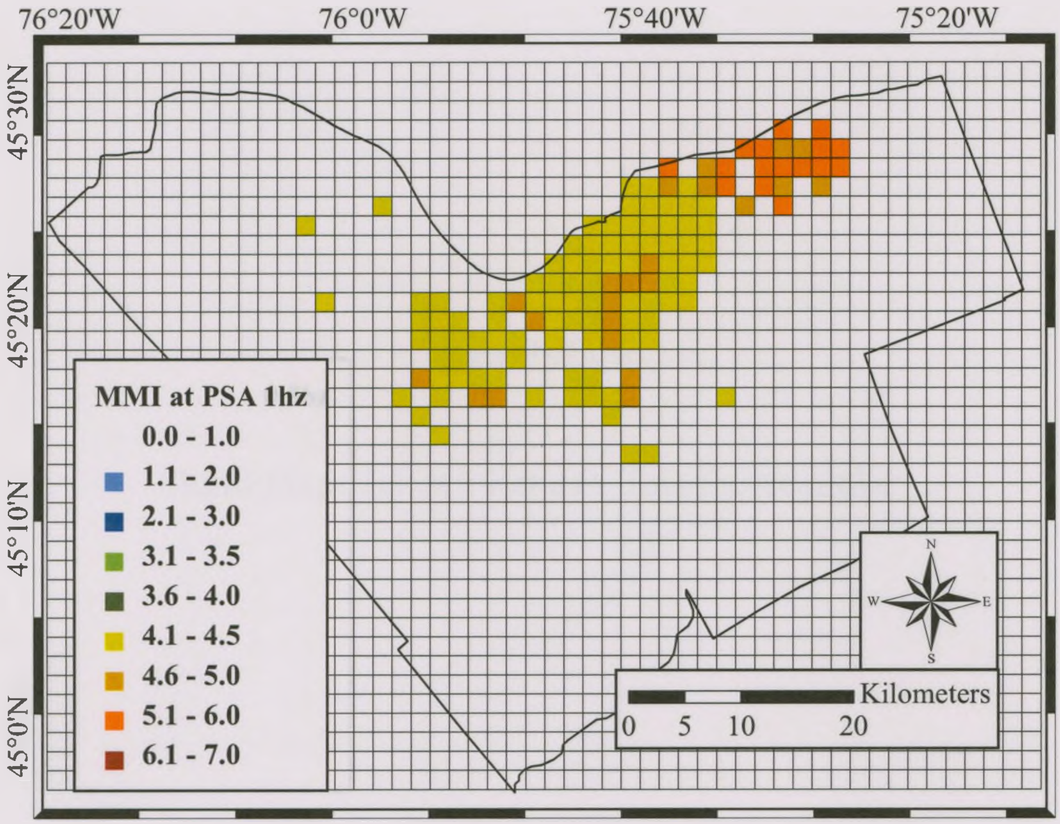

Figure A2.2. Predicted MMI based on PSA at 1 Hz for M5 Val des Bois earthquake averaged over boxes of approx. 1.5 km^2 grids for number of reports ≥ 3 in each box.

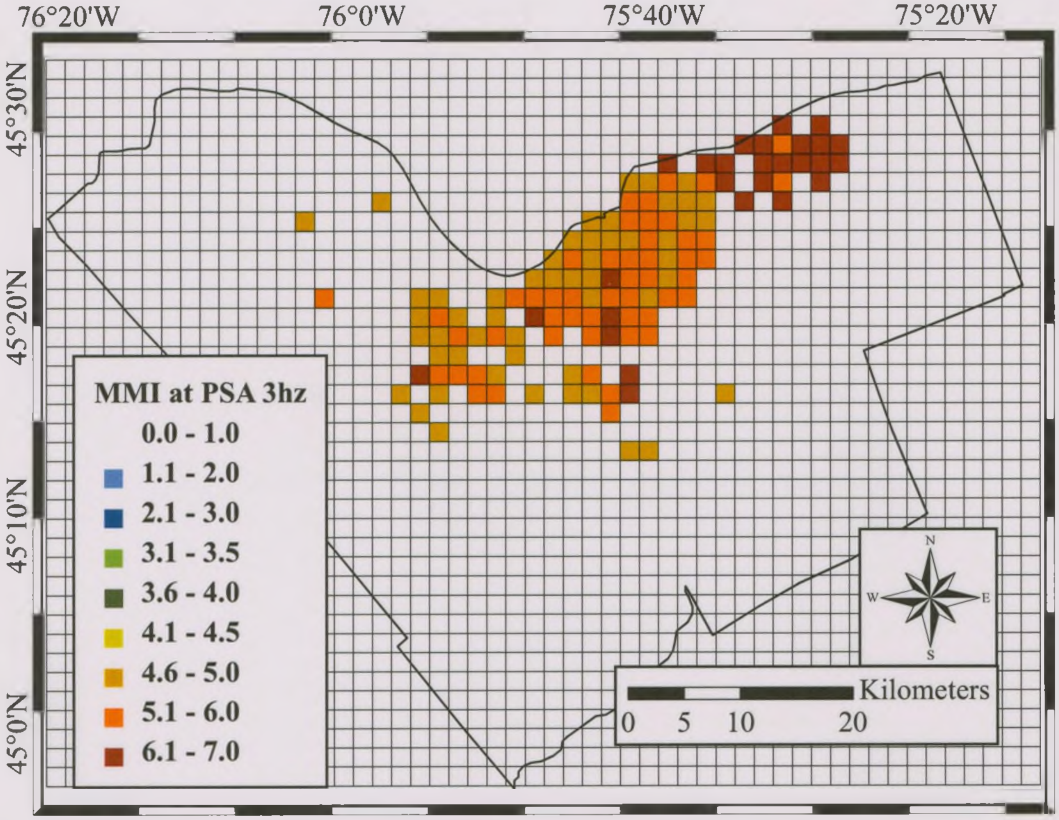

Figure A2.3. Predicted MMI based on PSA at 3 Hz for M5 Val des Bois earthquake averaged over boxes of approx. 1.5 km^2 grids for number of reports $\geq$ 3 in each box.

APPENDIX III

Category II ShakeMaps: Ground motions and MMI for Epicenter 1

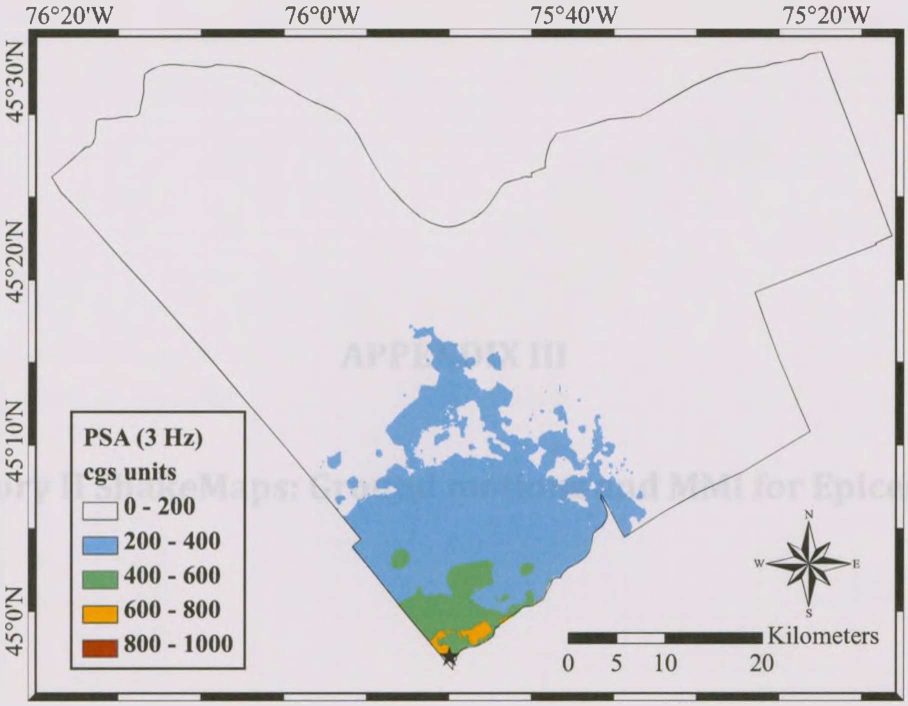

Figure A3.1. PSA at 3 Hz for M6 event using amplification factors based on NBCC 2005 for epicenter located on hard rock.

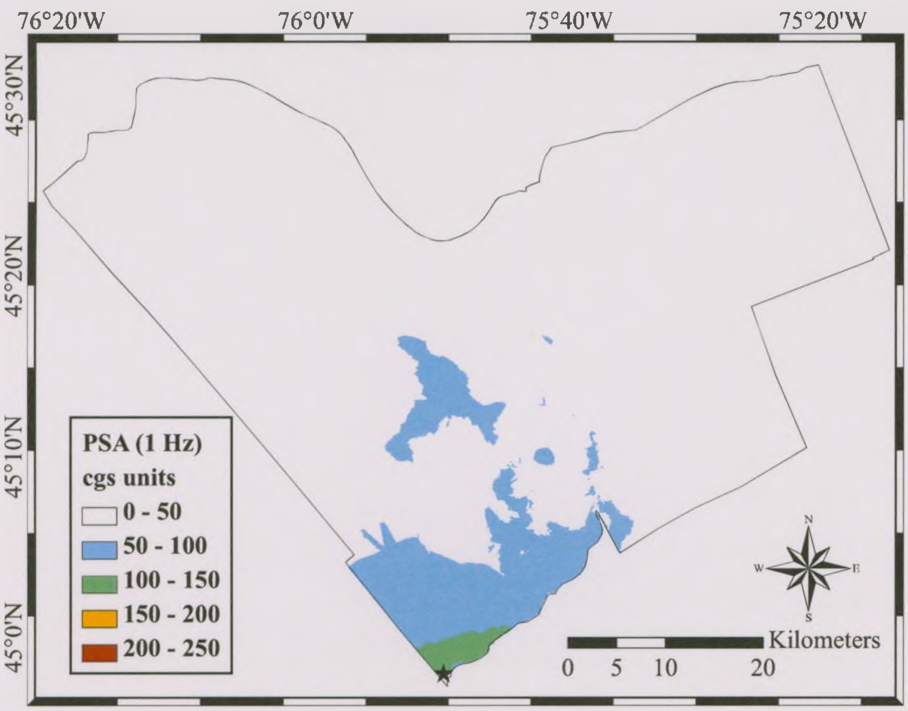

Figure A3.2. PSA at 1 Hz for M6 event using amplification factors based on NBCC 2005 for epicenter located on hard rock.

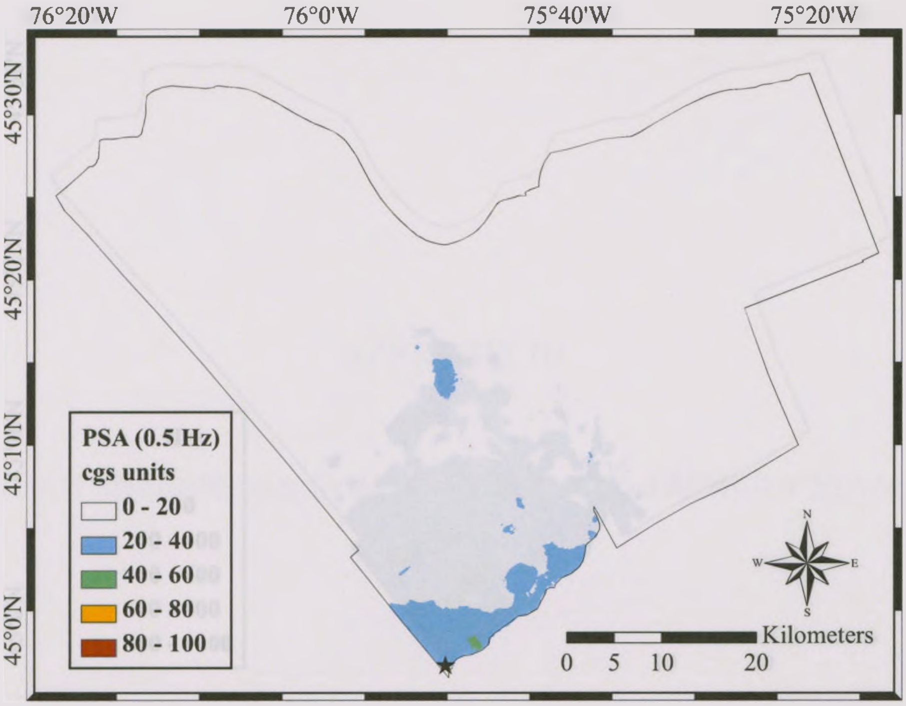

Figure A3.3. PSA at 0.5 Hz for M6 event using amplification factors based on NBCC 2005 for epicenter located on hard rock.

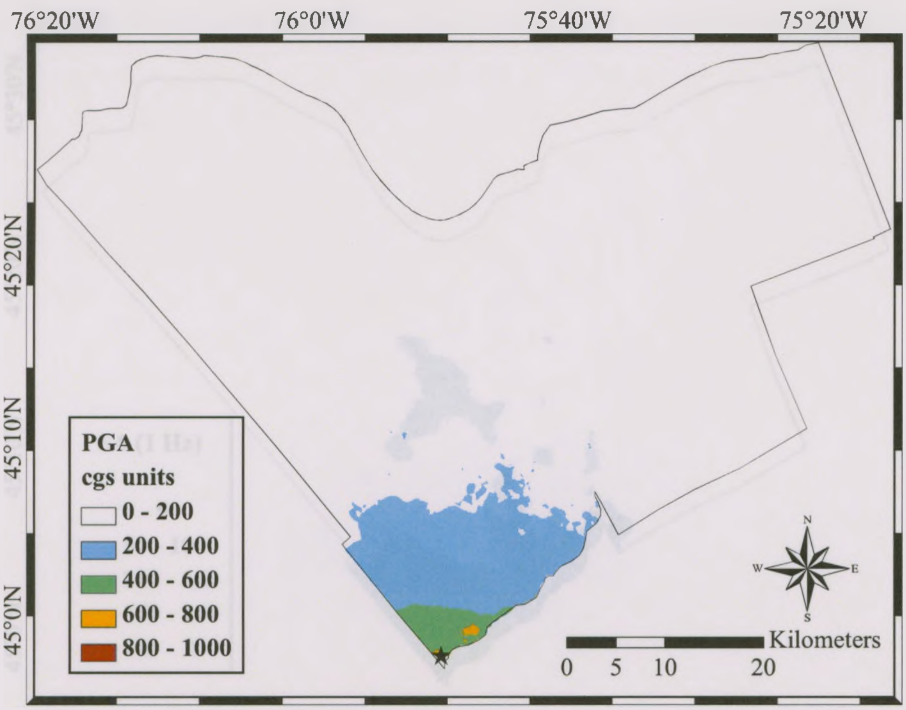

Figure A3.4. PGA for M6 event using amplification factors based on NBCC 2005 for epicenter located on hard rock.

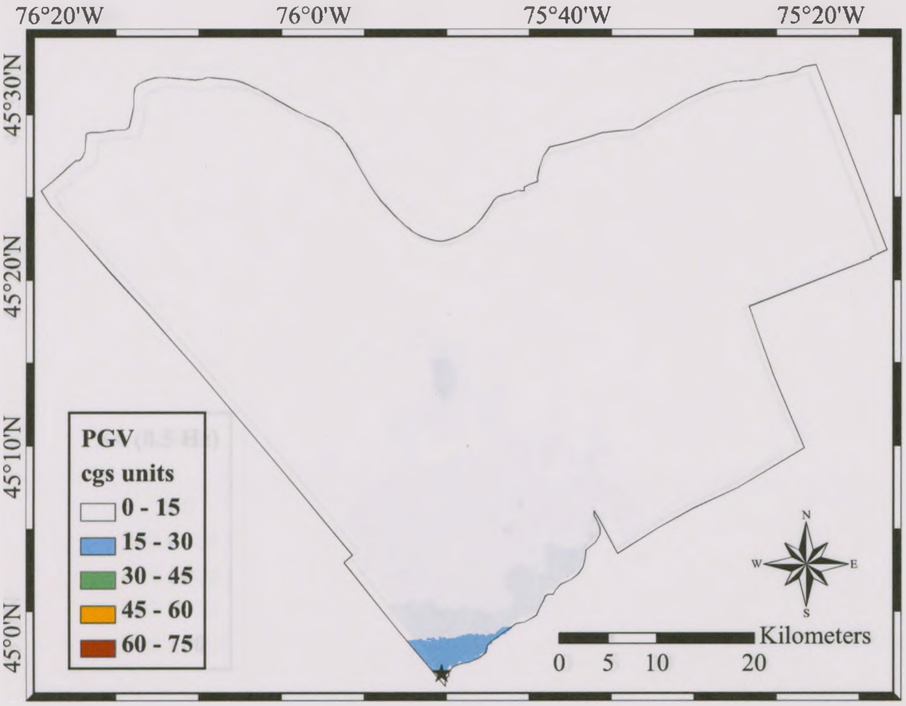

Figure A3.5. PGV for M6 event using amplification factors based on NBCC 2005 for epicenter located on hard rock.

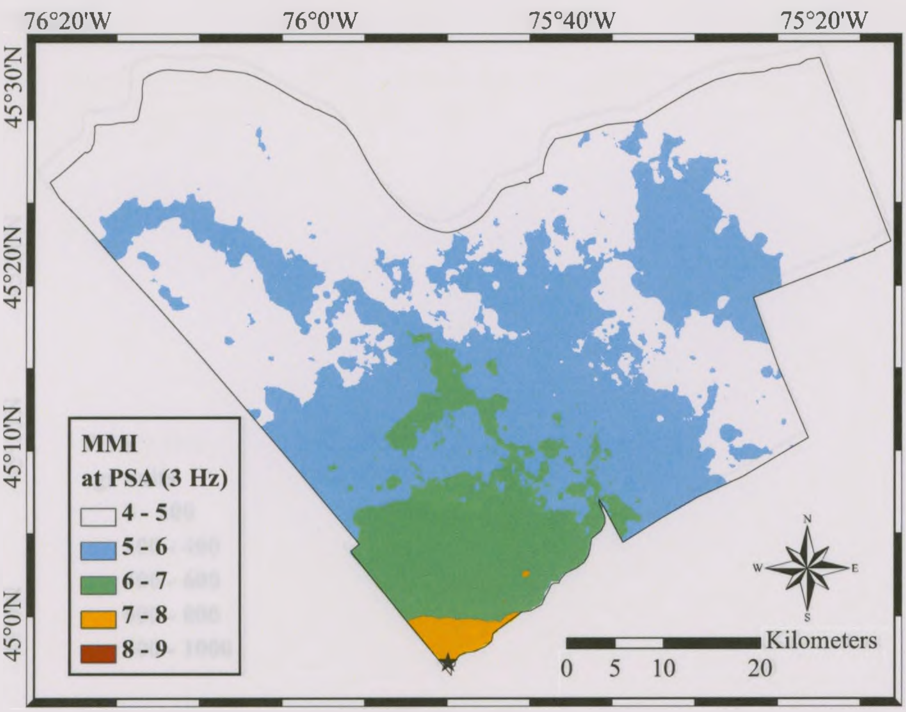

Figure A3.6. MMI based on PSA at 3 Hz for M6 event using amplification factors based on NBCC 2005 for epicenter located on hard rock.

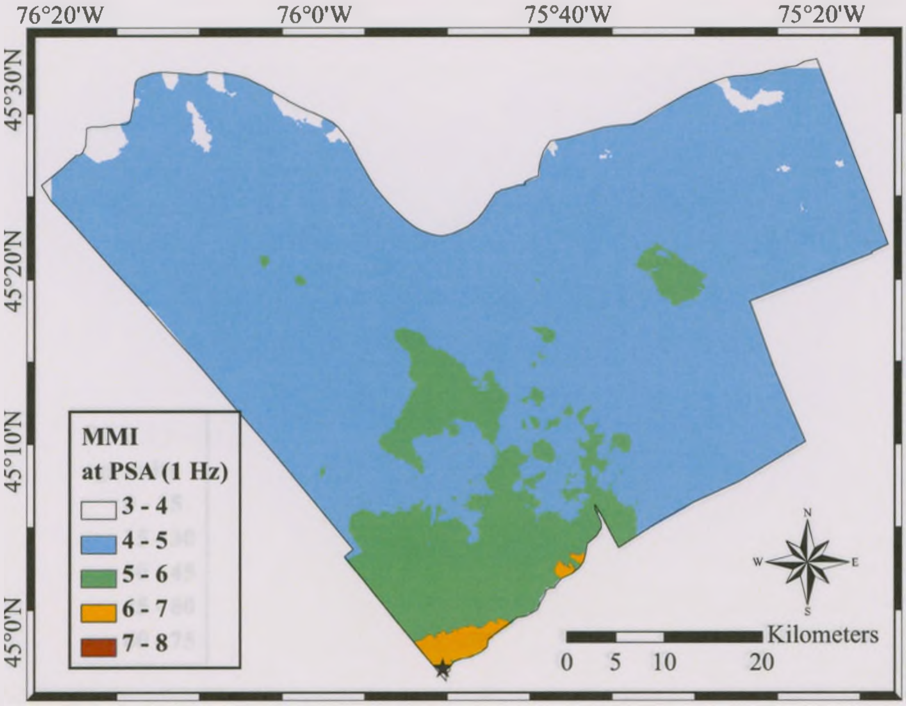

Figure A3.7. MMI based on PSA at 1 Hz for M6 event using amplification factors based on NBCC 2005 for epicenter located on hard rock.

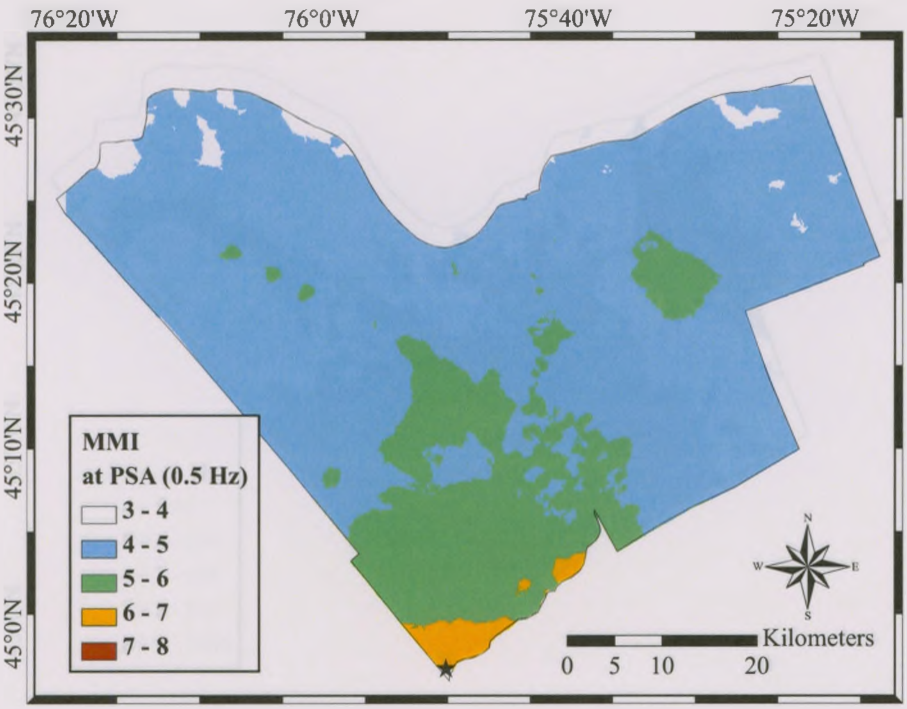

Figure A3.8. MMI based on PSA at 0.5 Hz for M6 event using amplification factors based on NBCC 2005 for epicenter located on hard rock.

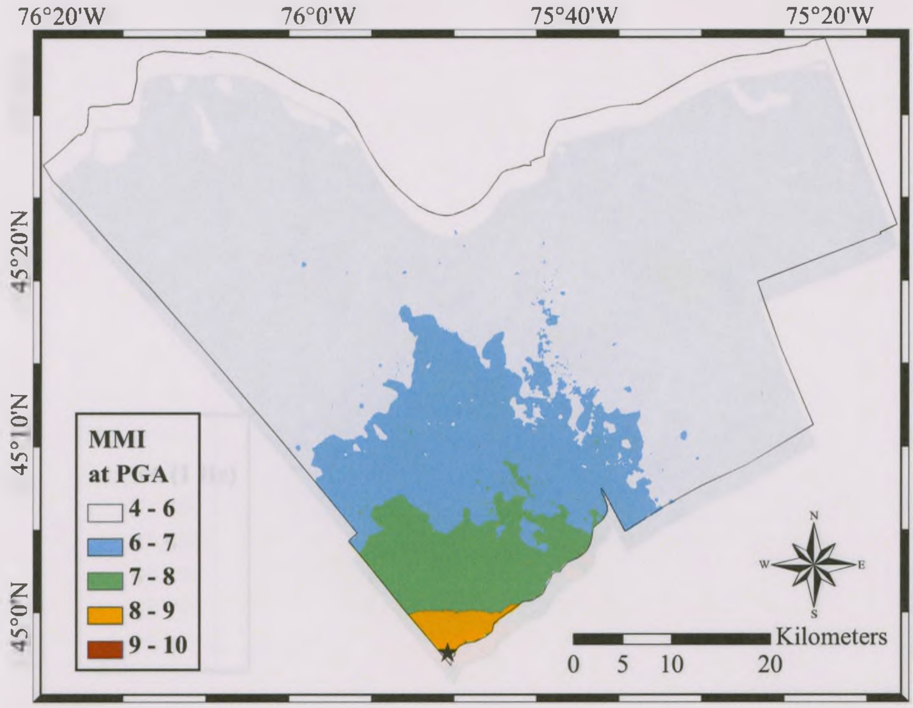

Figure A3.9. MMI based on PGA for M6 event using amplification factors based on NBCC 2005 for epicenter located on hard rock.

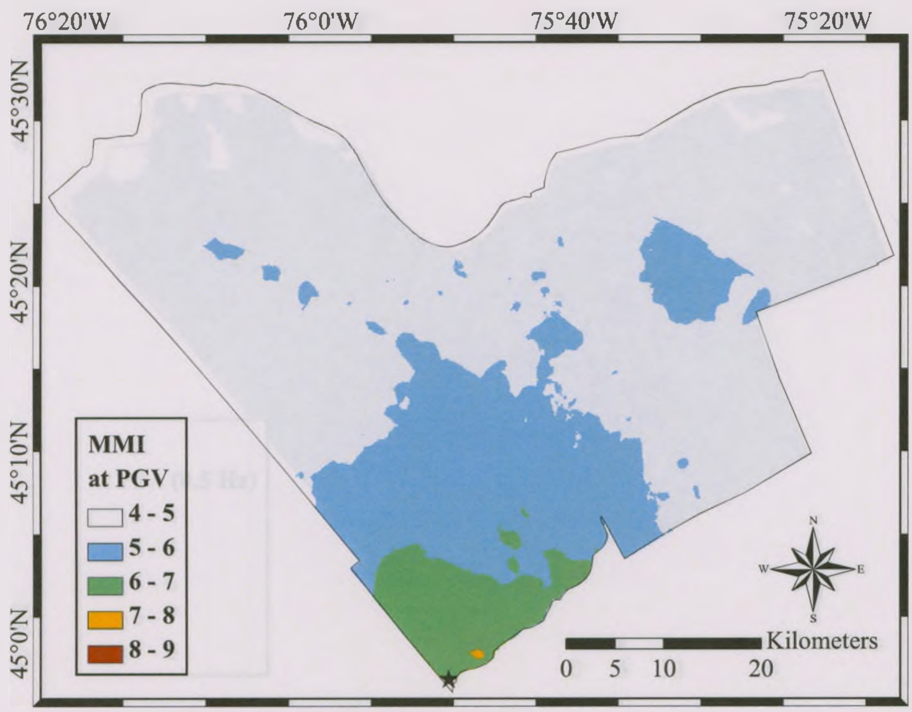

Figure A3.10. MMI based on PGV for M6 event using amplification factors based on NBCC 2005 for epicenter located on hard rock.

APPENDIX IV

Category II ShakeMaps: Ground motions and MMI for Epicenter 2

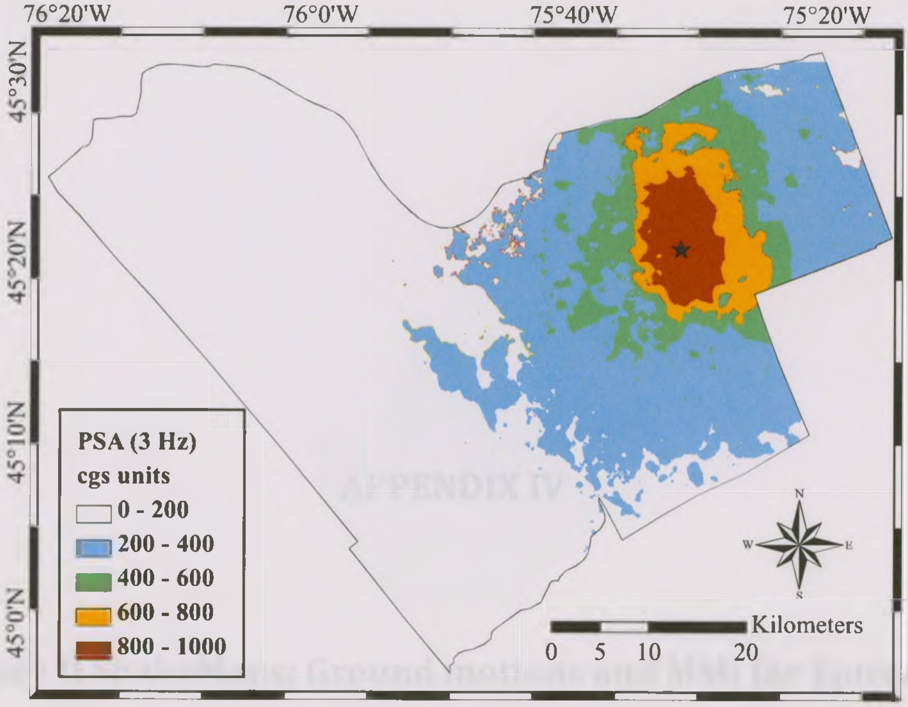

Figure A4.1. PSA at 3 Hz for M6 event using amplification factors based on NBCC 2005 for epicenter located in soft soil.

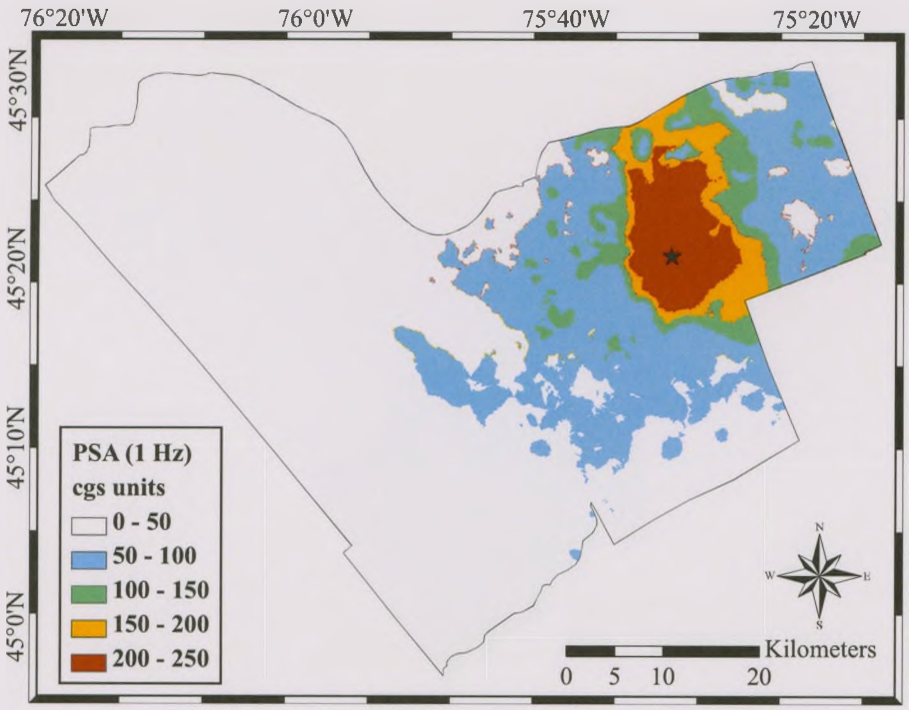

Figure A4.2. PSA at 1 Hz for M6 event using amplification factors based on NBCC 2005 for epicenter located in soft soil.

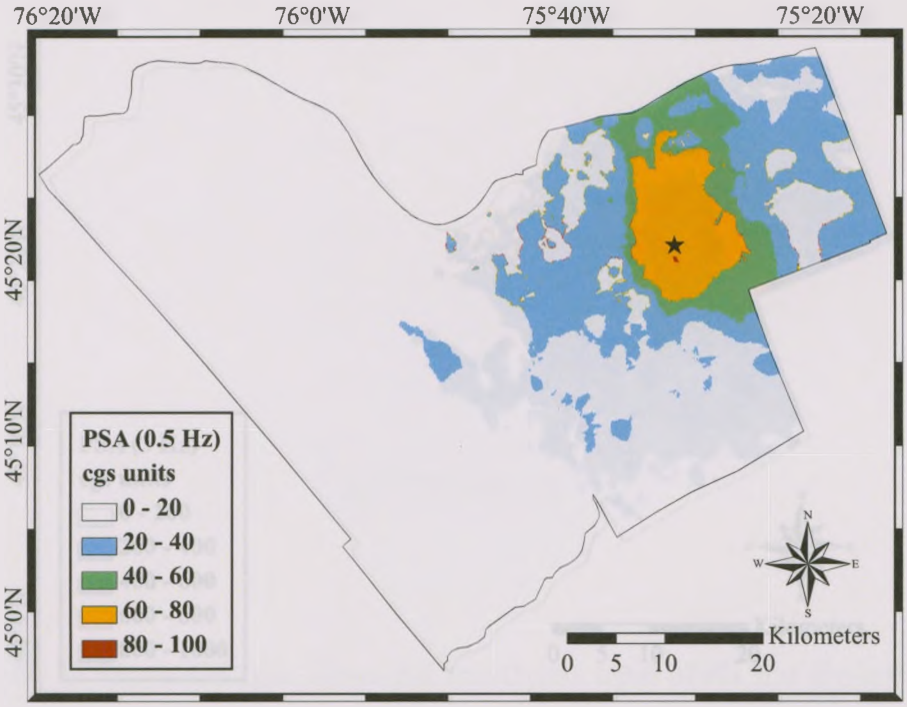

Figure A4.3. PSA at 0.5 Hz for M6 event using amplification factors based on NBCC 2005 for epicenter located in soft soil.

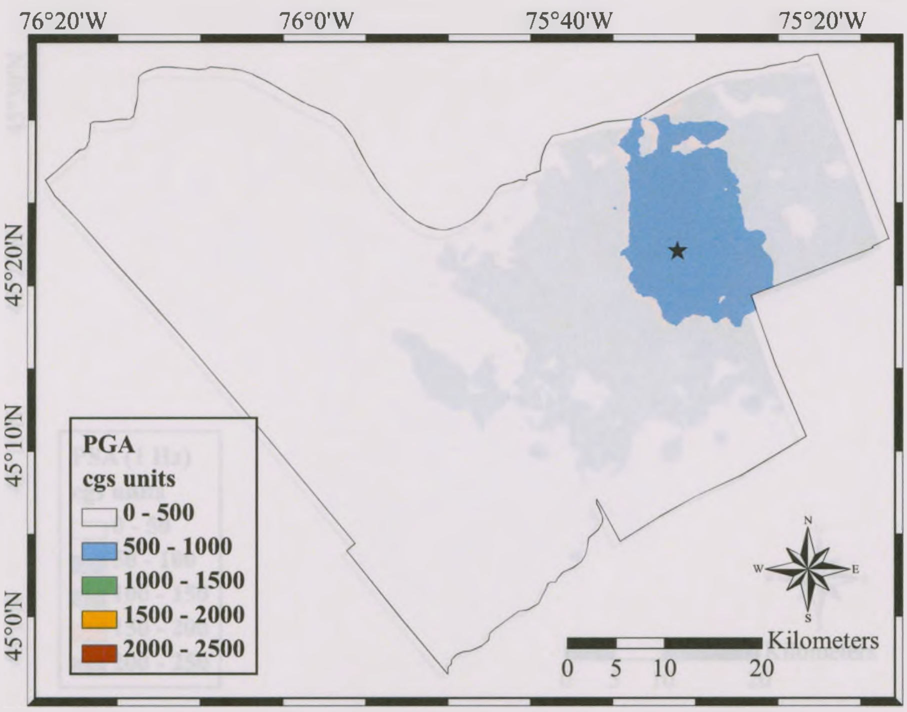

Figure A4.4. PGA for M6 event using amplification factors based on NBCC 2005 for epicenter located in soft soil.

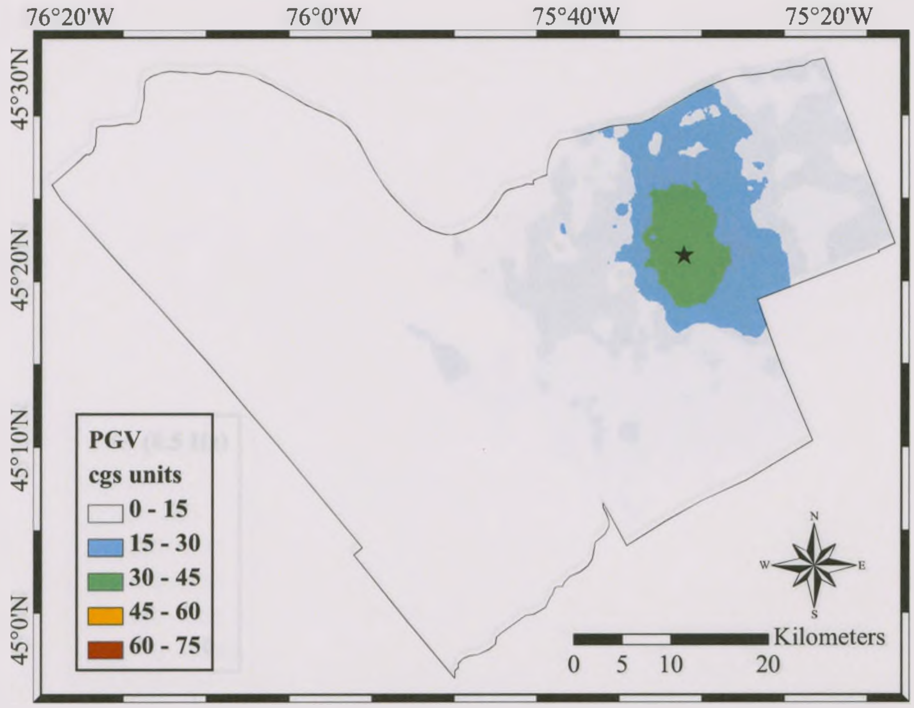

Figure A4.5. PGV for M6 event using amplification factors based on NBCC 2005 for epicenter located in soft soil.

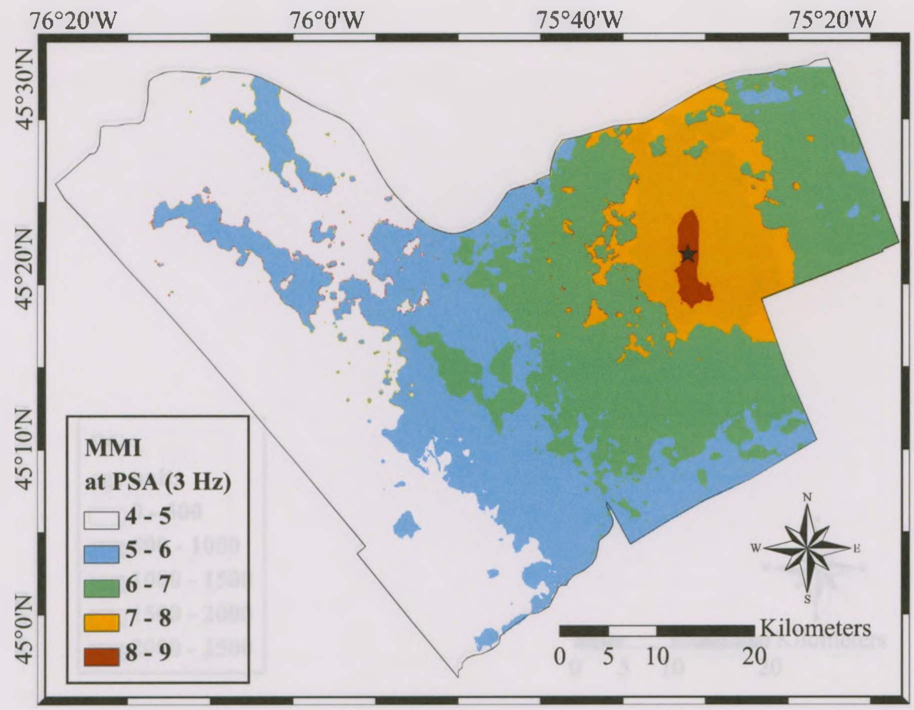

Figure A4.6. MMI based on PSA at 3 Hz for M6 event using amplification factors based on NBCC 2005 for epicenter located in soft soil.

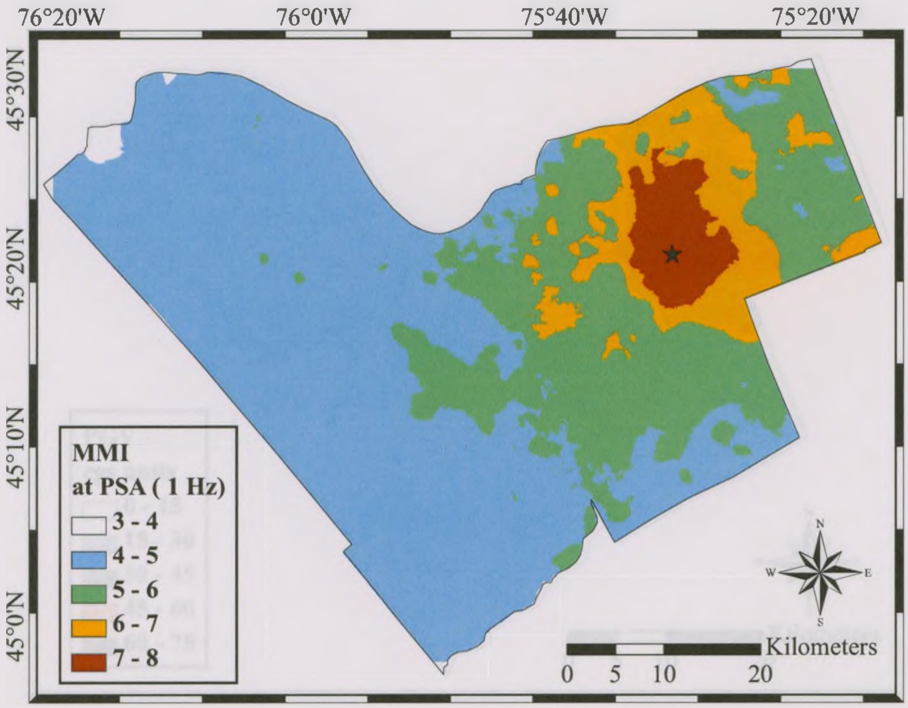

Figure A4.7. MMI based on PSA at 1 Hz for M6 event using amplification factors based on NBCC 2005 for epicenter located in soft soil.

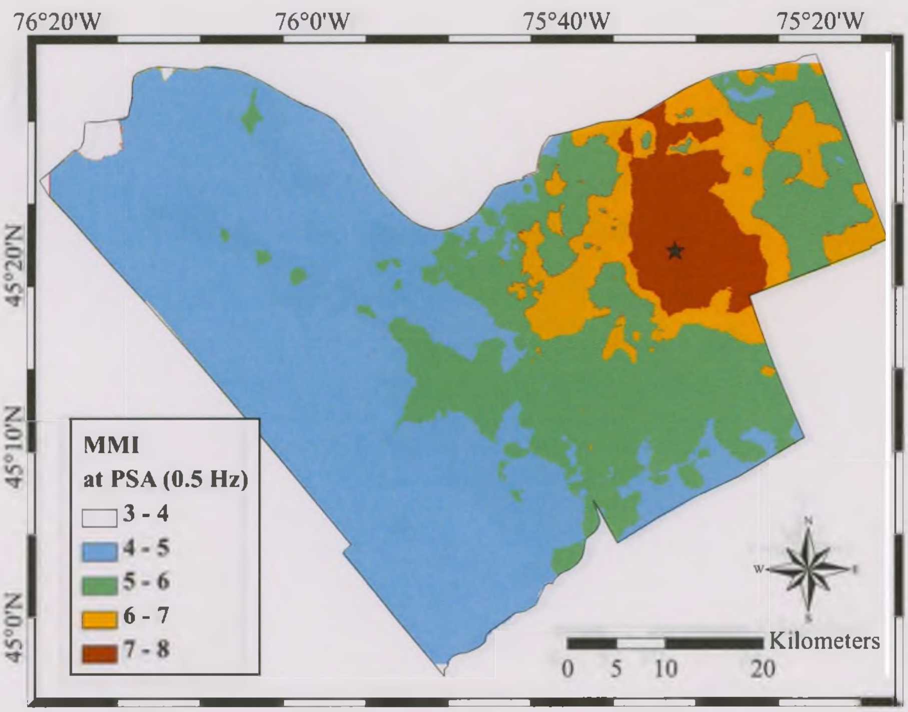

Figure A4.8. MMI based on PSA at 0.5 Hz for M6 event using amplification factors based on NBCC 2005 for epicenter located in soft soil.

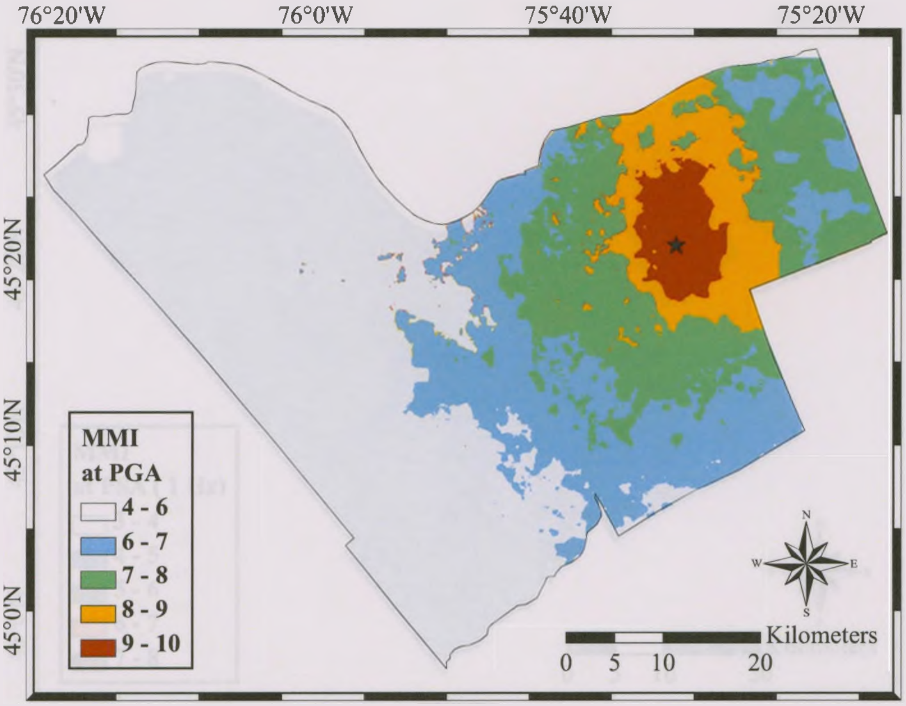

Figure A4.9. MMI based on PGA for M6 event using amplification factors based on NBCC 2005 for epicenter located in soft soil.

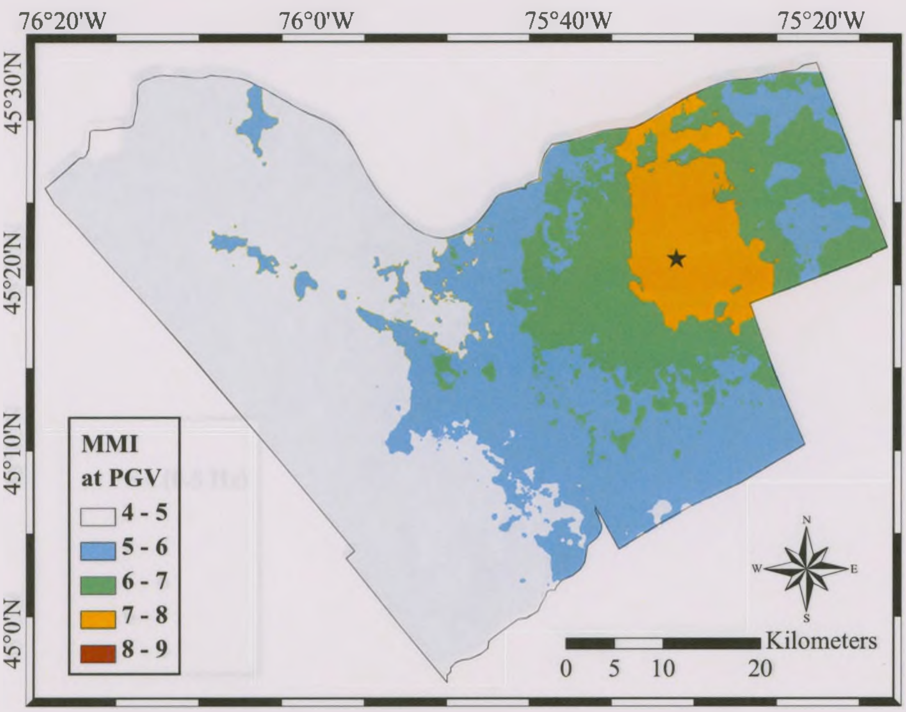

Figure A4.10. MMI based on PGV for M6 event using amplification factors based on NBCC 2005 for epicenter located in soft soil.

APPENDIX V

Category II ShakeMaps: Ground motions and MMI for Epicenter 3

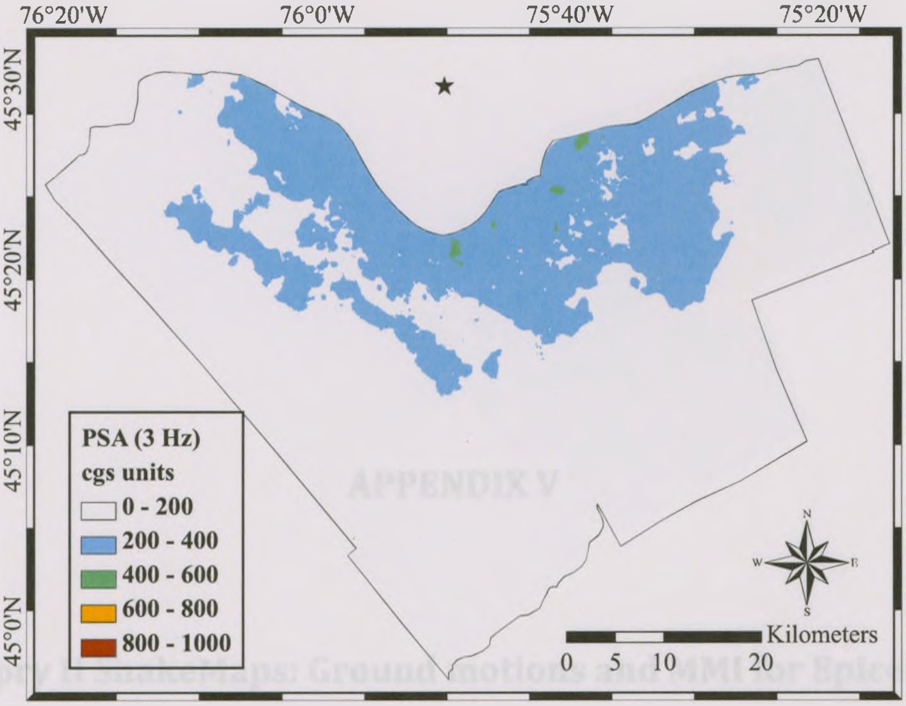

Figure A5.1. PSA at 3 Hz for M6 event using amplification factors based on NBCC 2005 for epicenter located in Hull area.

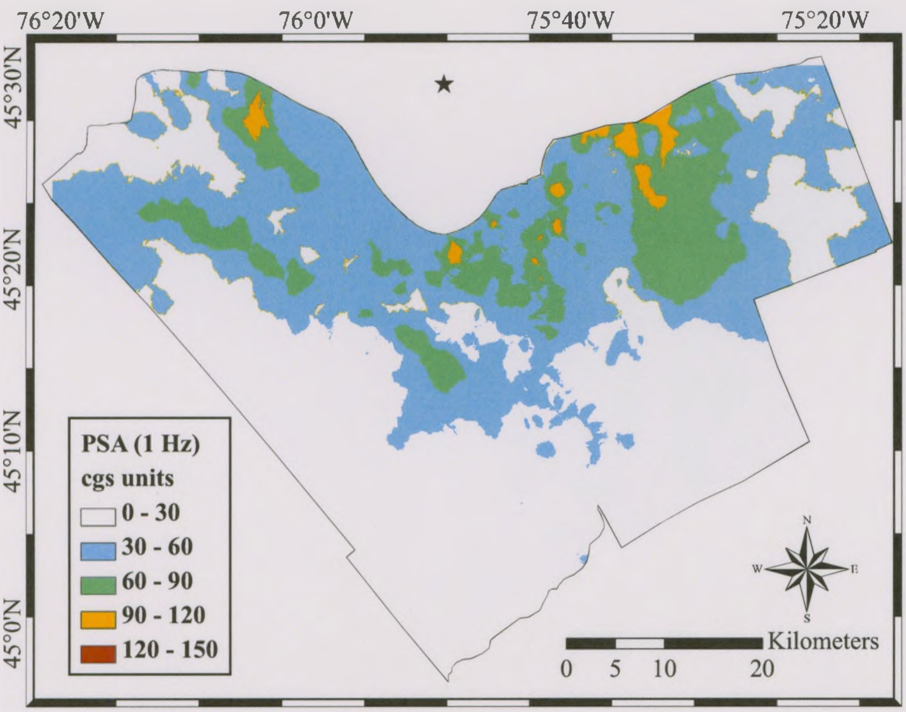

Figure A5.2. PSA at 1 Hz for M6 event using amplification factors based on NBCC 2005 for epicenter located in Hull area.

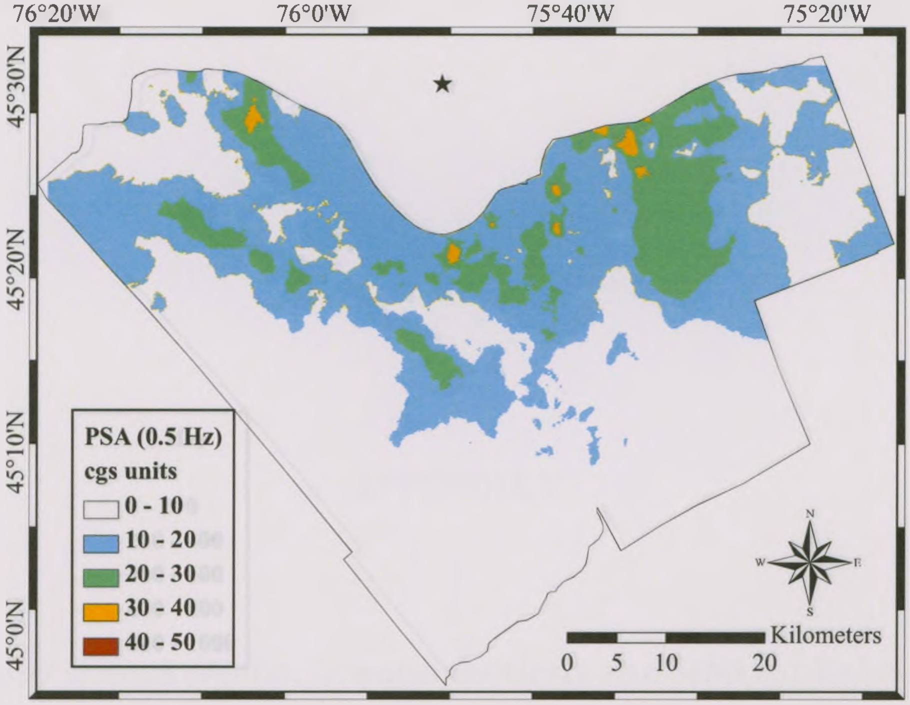

Figure A5.3. PSA at 0.5 Hz for M6 event using amplification factors based on NBCC 2005 for epicenter located in Hull area.

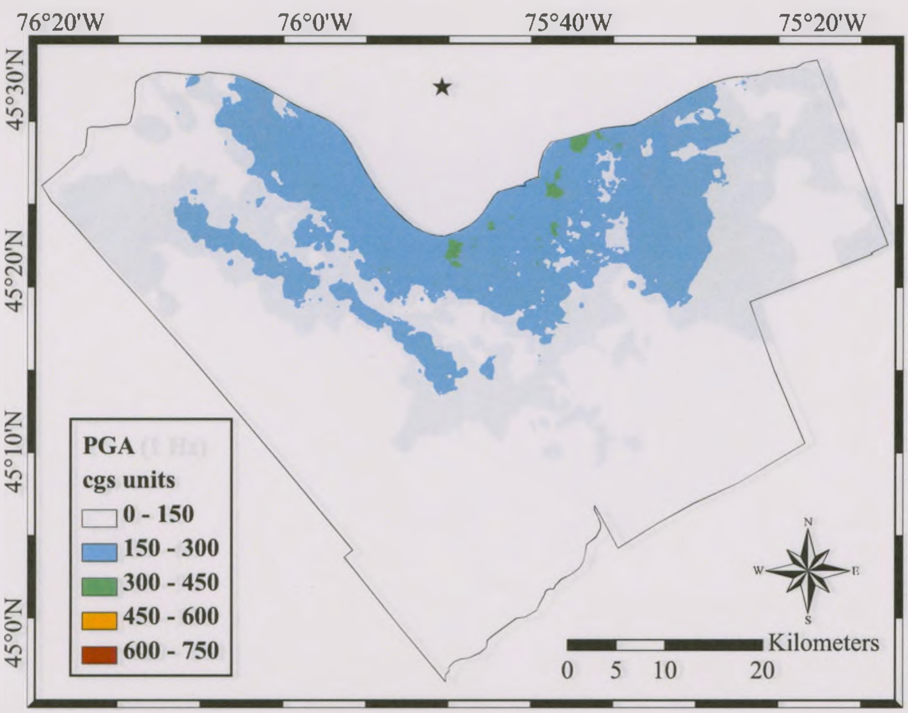

Figure A5.4. PGA for M6 event using amplification factors based on NBCC 2005 for epicenter located in Hull area.

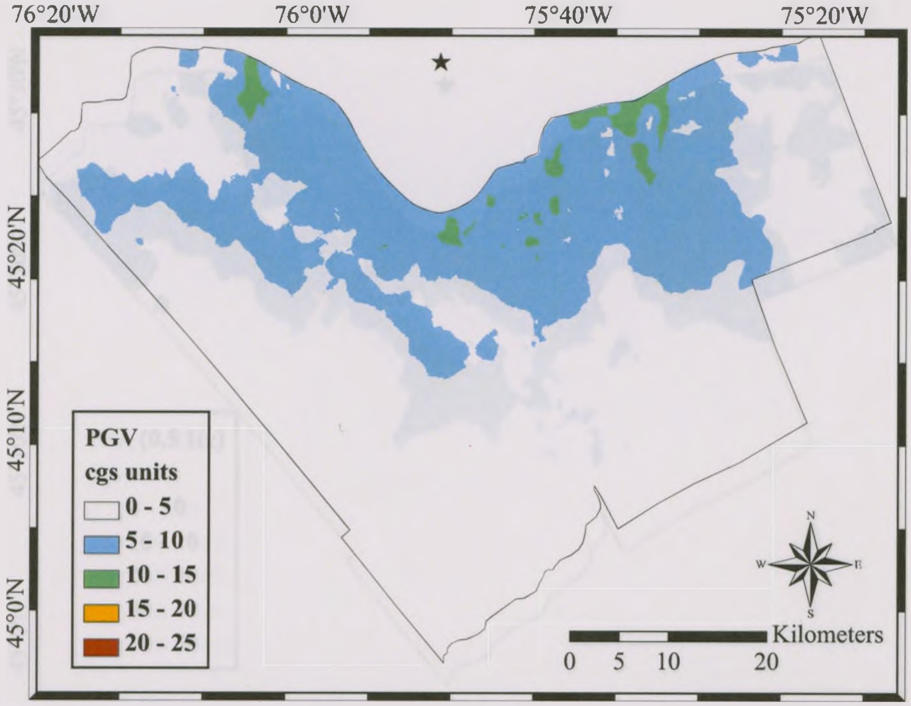

Figure A5.5. PGV for M6 event using amplification factors based on NBCC 2005 for epicenter located in Hull area.

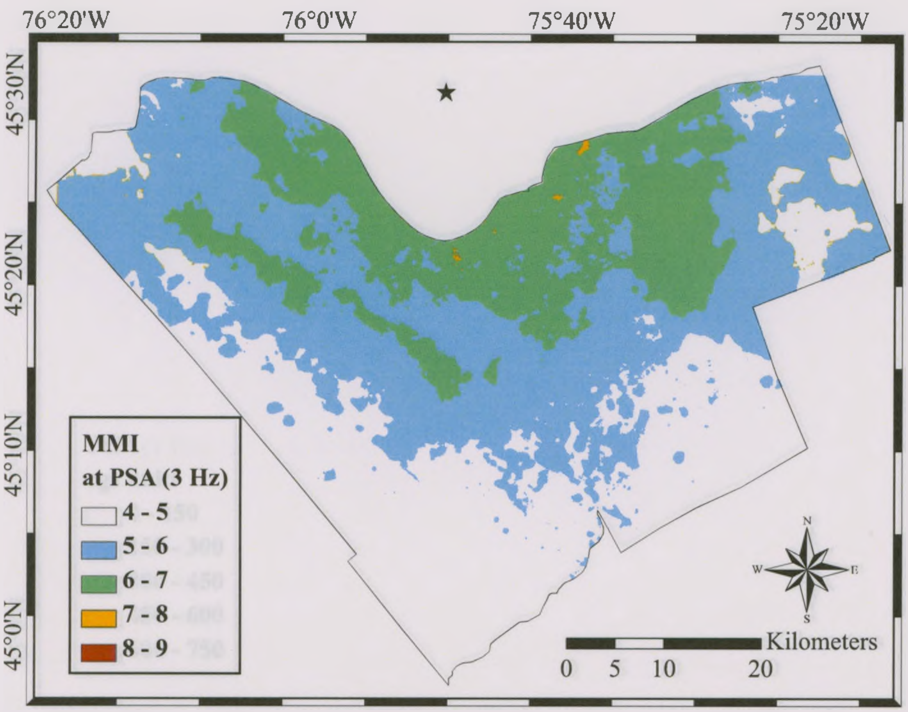

Figure A5.6. MMI based on PSA at 3 Hz for M6 event using amplification factors based on NBCC 2005 for epicenter located in Hull area.

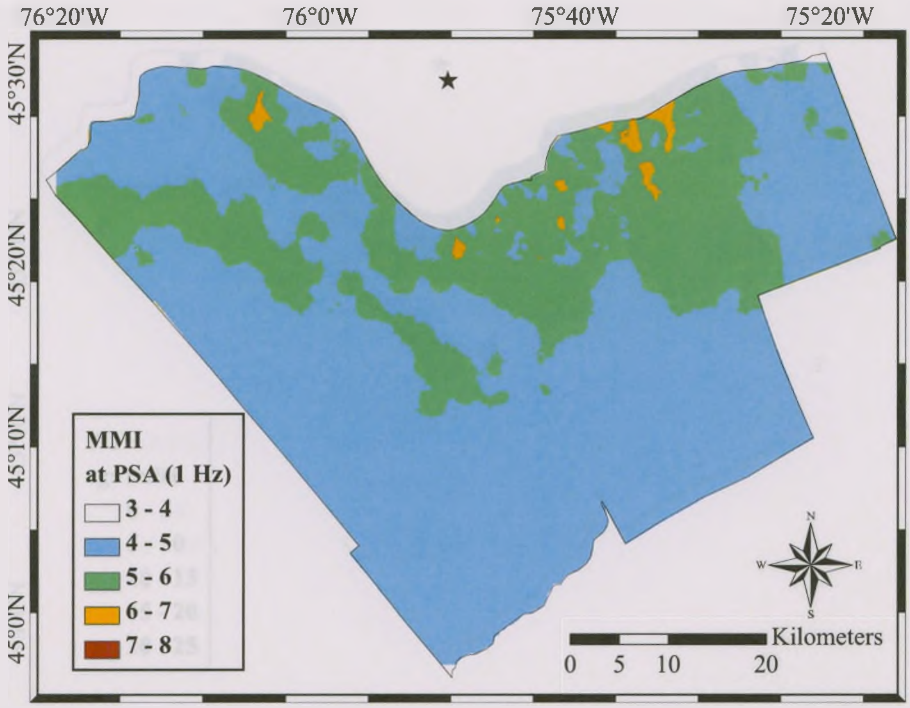

Figure A5.7. MMI based on PSA at 1 Hz for M6 event using amplification factors based on NBCC 2005 for epicenter located in Hull area.

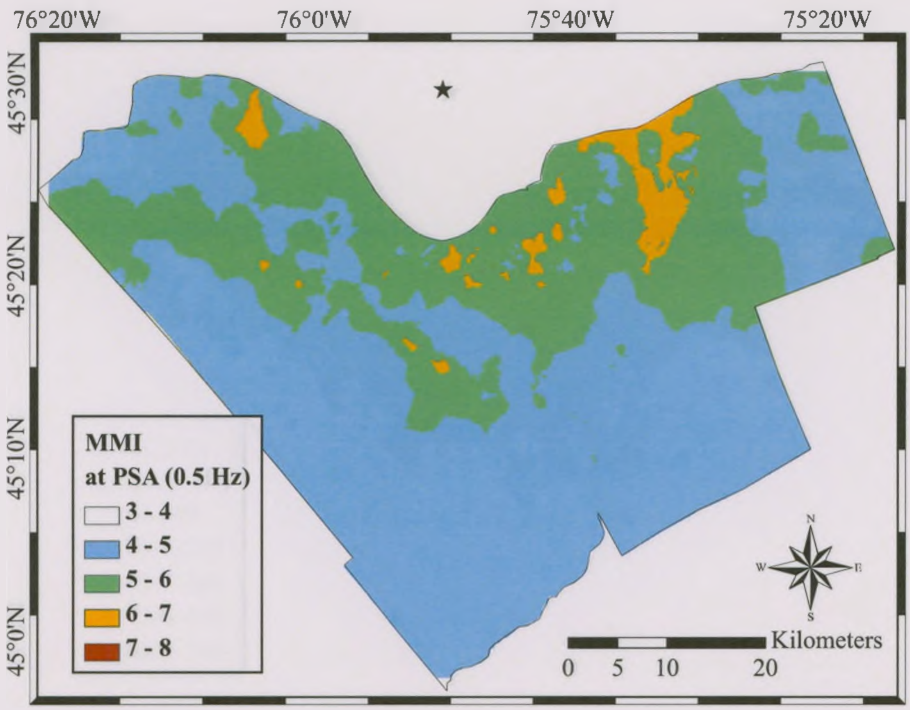

Figure A5.8. MMI based on PSA at 0.5 Hz for M6 event using amplification factors based on NBCC 2005 for epicenter located in Hull area.

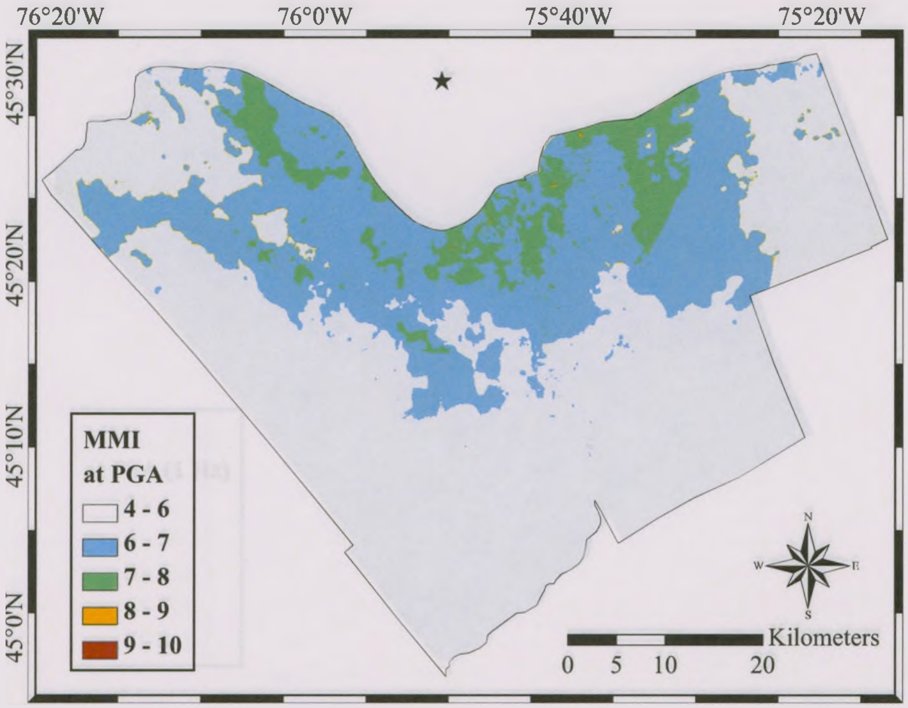

Figure A5.9. MMI based on PGA for M6 event using amplification factors based on NBCC 2005 for epicenter located in Hull area.

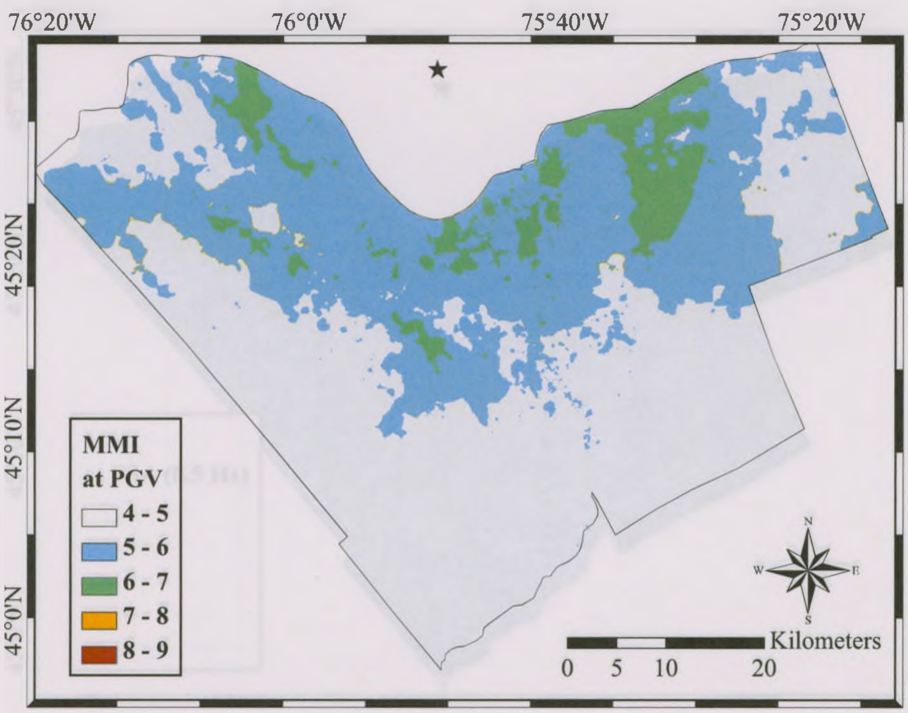

Figure A5.10. MMI based on PGV for M6 event using amplification factors based on NBCC 2005 for epicenter located in Hull area.

APPENDIX VI

Category II ShakeMaps: Ground motions and MMI for Epicenter 4

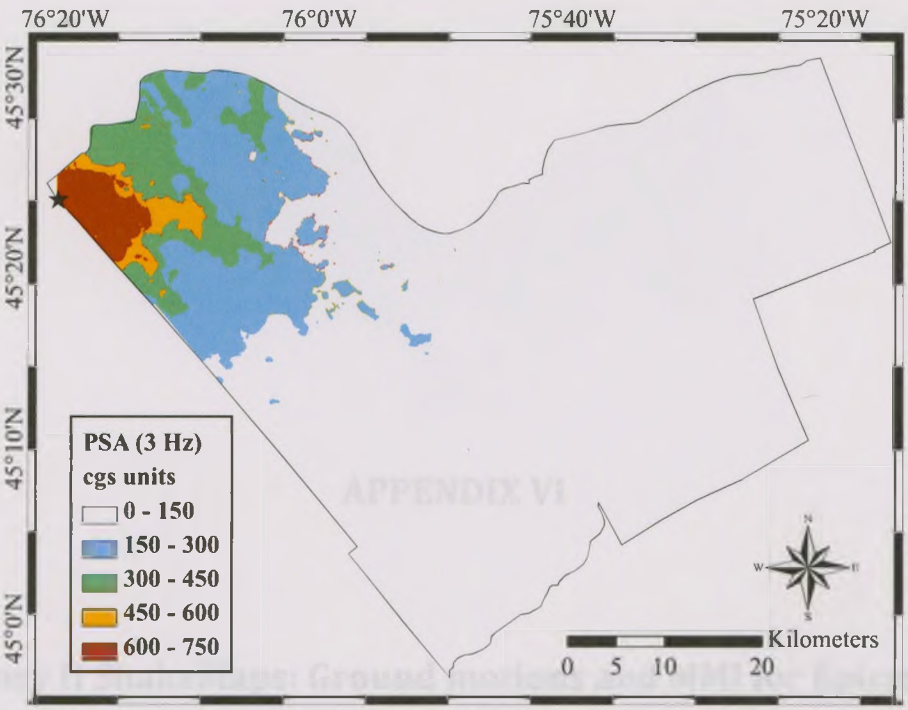

Figure A6.1. PSA at 3 Hz for M6 event using amplification factors based on NBCC 2005 for epicenter located in west.

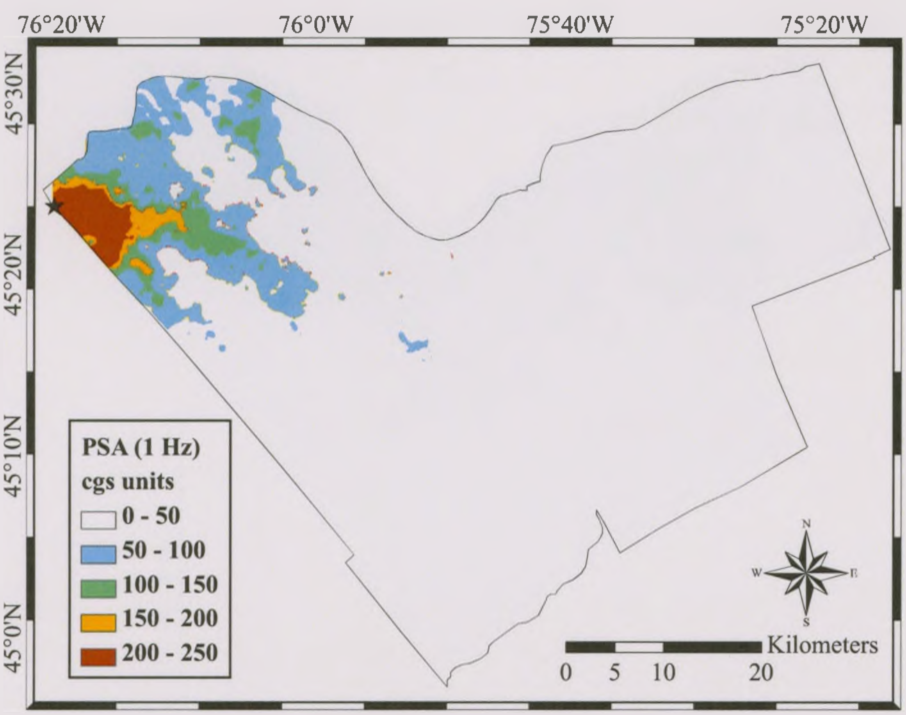

Figure A6.2. PSA at 1 Hz for M6 event using amplification factors based on NBCC 2005 for epicenter located in west.

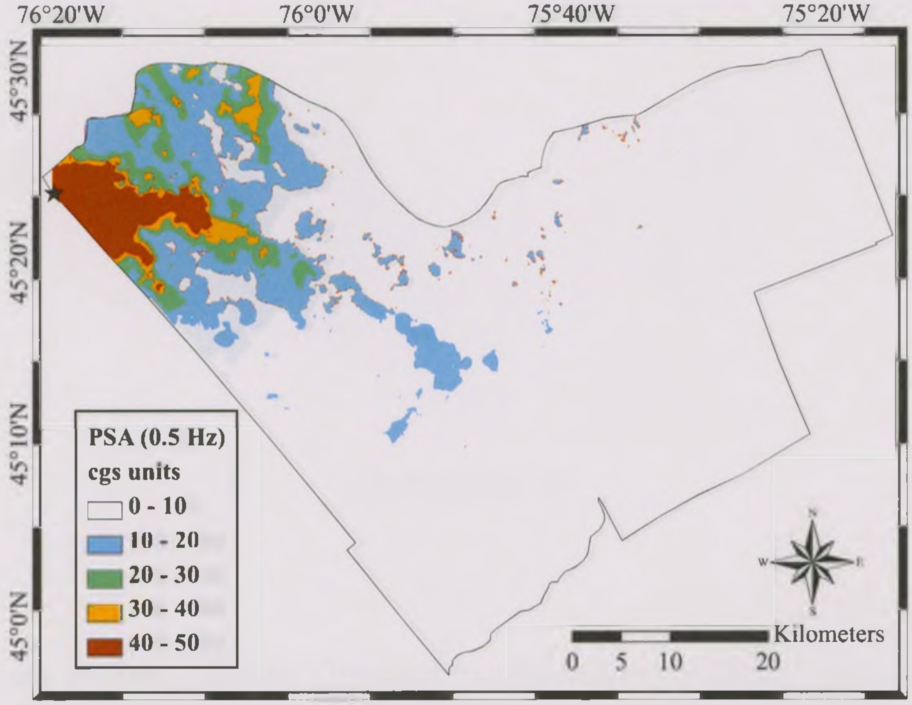

Figure A6.3. PSA at 0.5 Hz for M6 event using amplification factors based on NBCC 2005 for epicenter located in west.

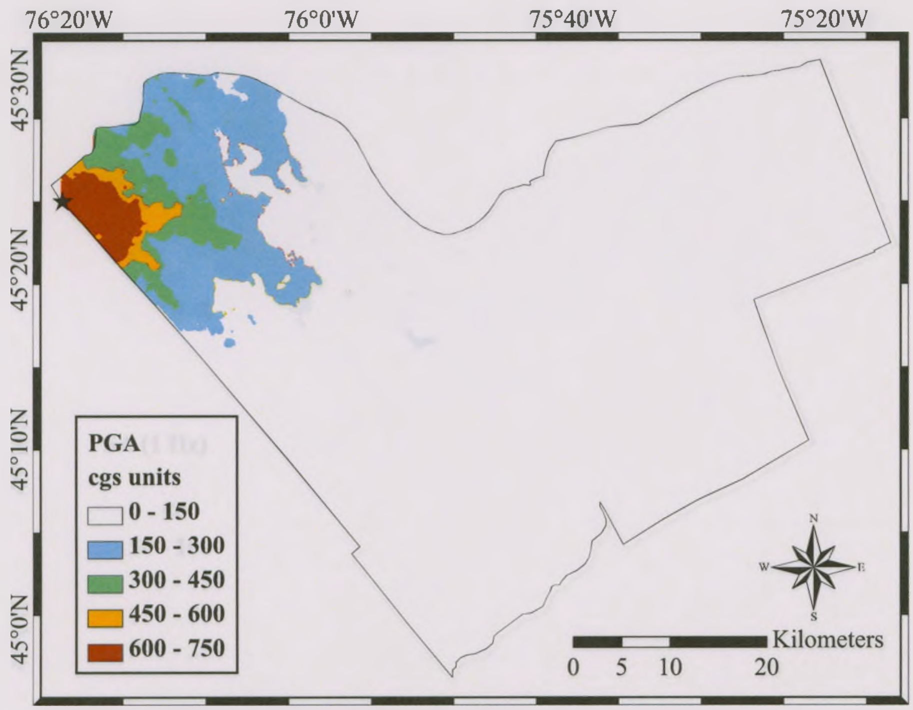

Figure A6.4. PGA for M6 event using amplification factors based on NBCC 2005 for epicenter located in west.

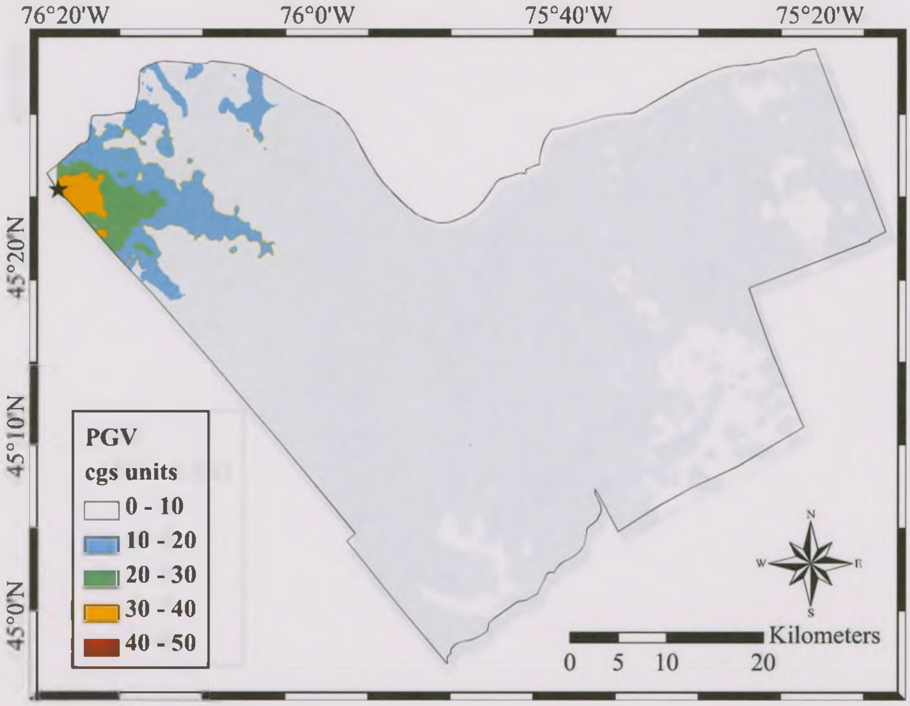

Figure A6.5. PGV for M6 event using amplification factors based on NBCC 2005 for epicenter located in west.

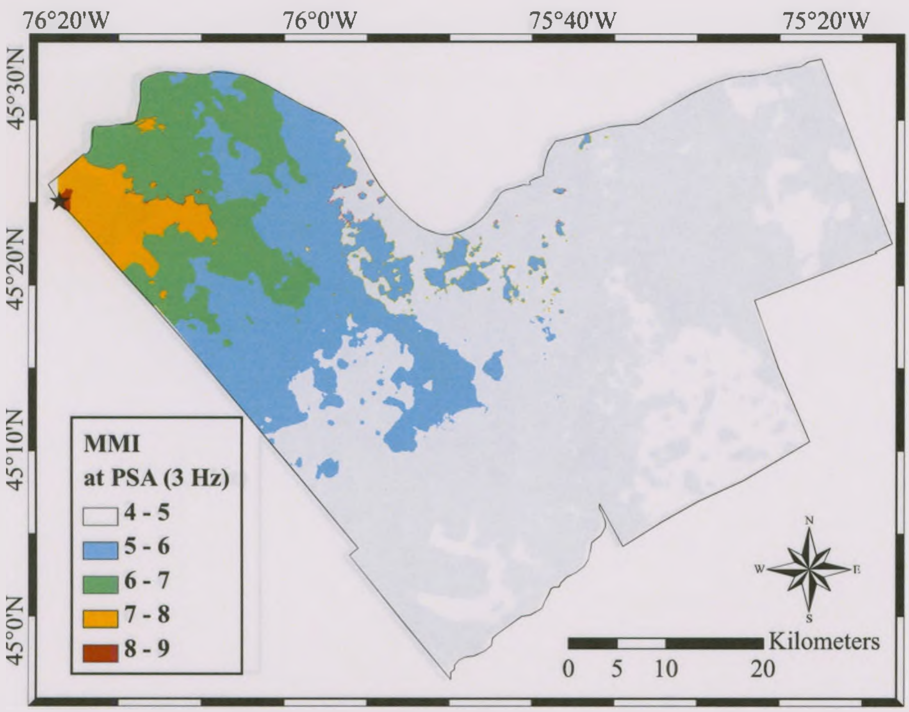

Figure A6.6. MMI based on PSA at 3 Hz for M6 event using amplification factors based on NBCC 2005 for epicenter located in west.

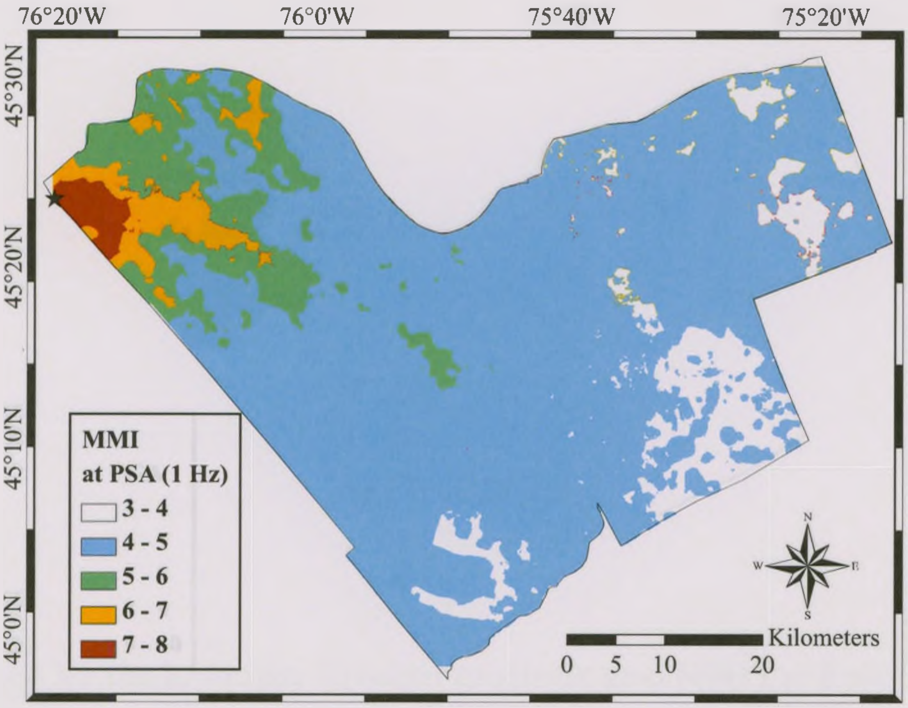

Figure A6.7. MMI based on PSA at 1 Hz for M6 event using amplification factors based on NBCC 2005 for epicenter located in west.

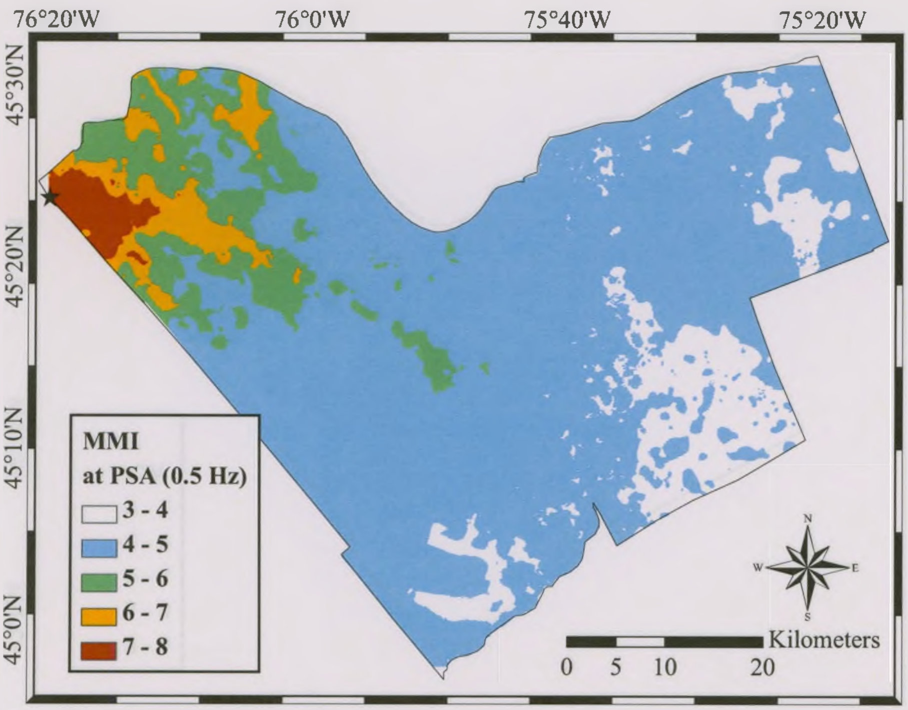

Figure A6.8. MMI based on PSA at 0.5 Hz for M6 event using amplification factors based on NBCC 2005 for epicenter located in west.

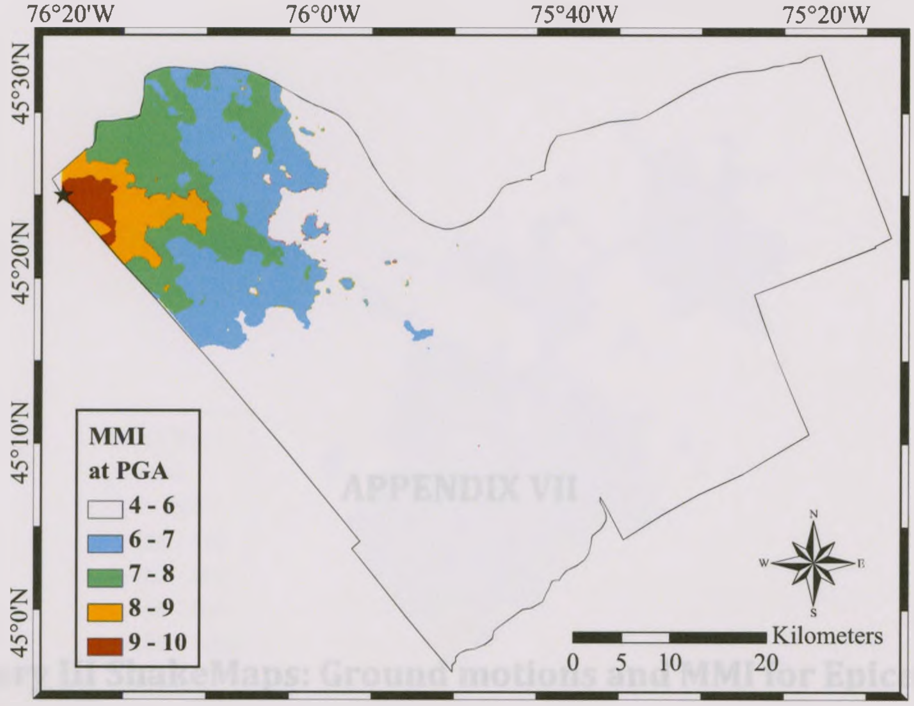

Figure A6.9. MMI based on PGA for M6 event using amplification factors based on NBCC 2005 for epicenter located in west.

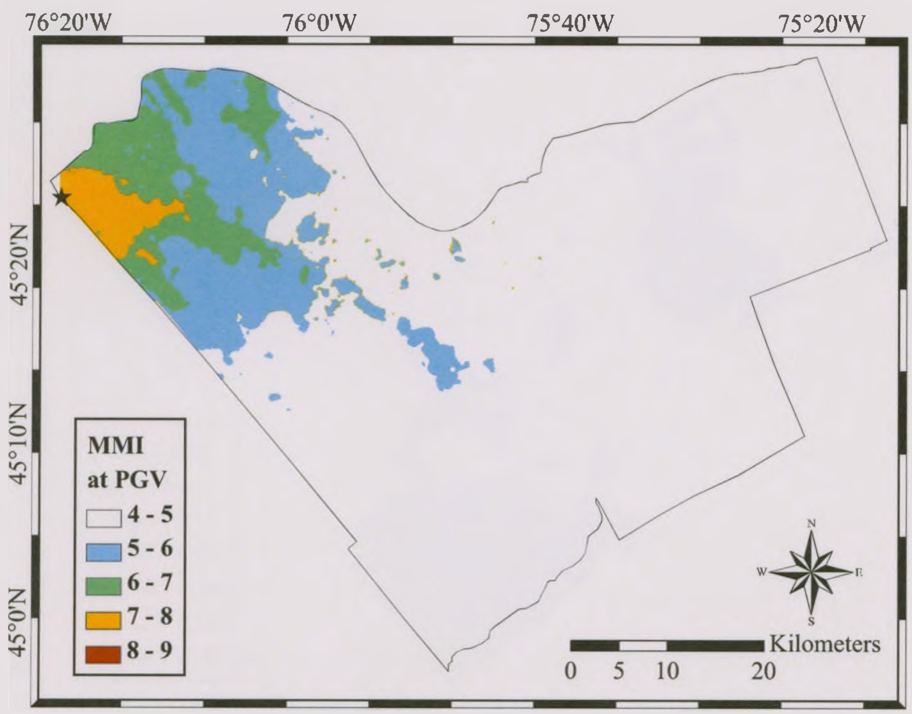

Figure A6.10. MMI based on PGV for M6 event using amplification factors based on NBCC 2005 for epicenter located in west.

APPENDIX VII

Category III ShakeMaps: Ground motions and MMI for Epicenter 1

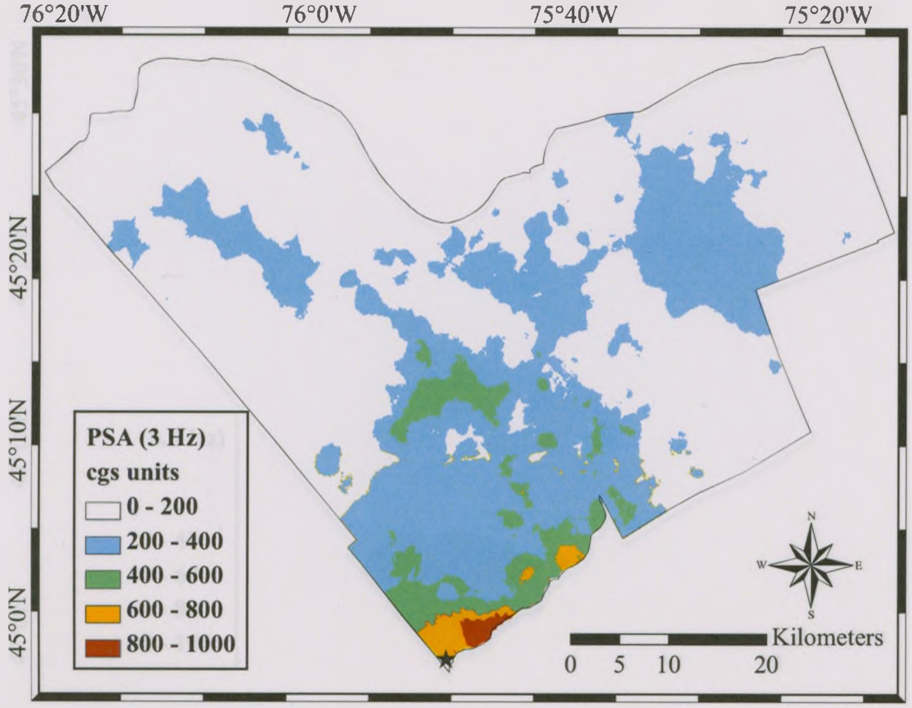

Figure A7.1. PSA at 3 Hz for M6 event using amplification factors based on Quarter wavelength method for epicenter located on hard rock.

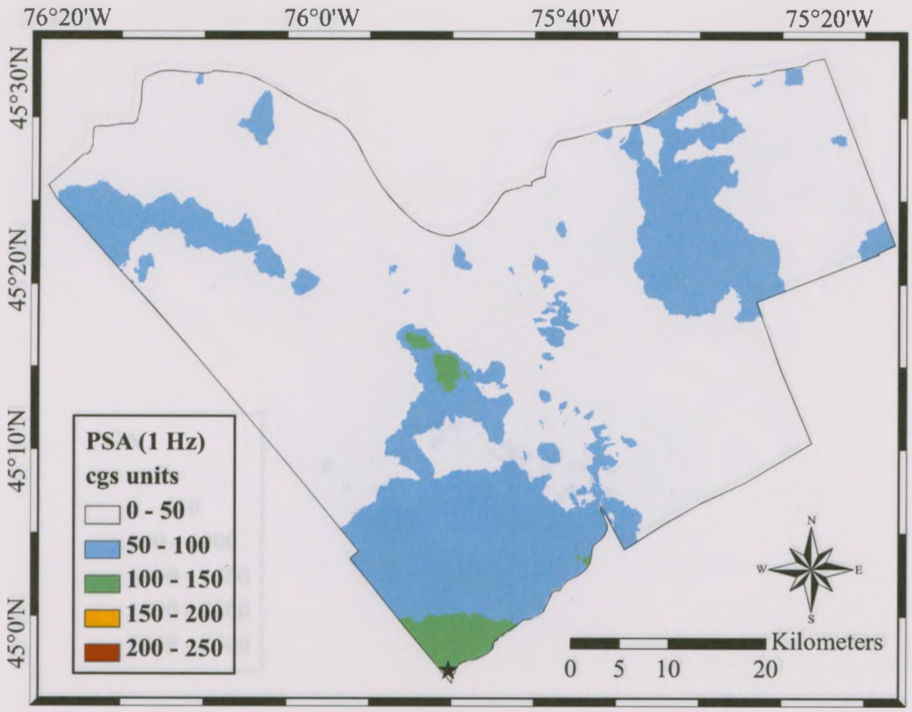

Figure A7.2. PSA at 1 Hz for M6 event using amplification factors based on Quarter wavelength method for epicenter located on hard rock.

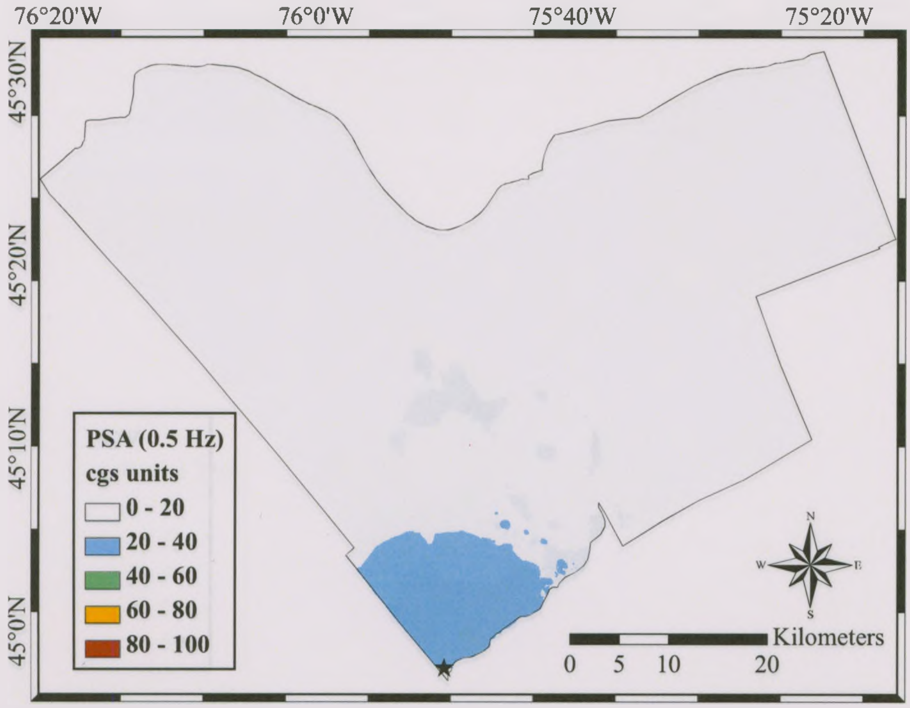

Figure A7.3. PSA at 0.5 Hz for M6 event using amplification factors based on Quarter wavelength method for epicenter located on hard rock.

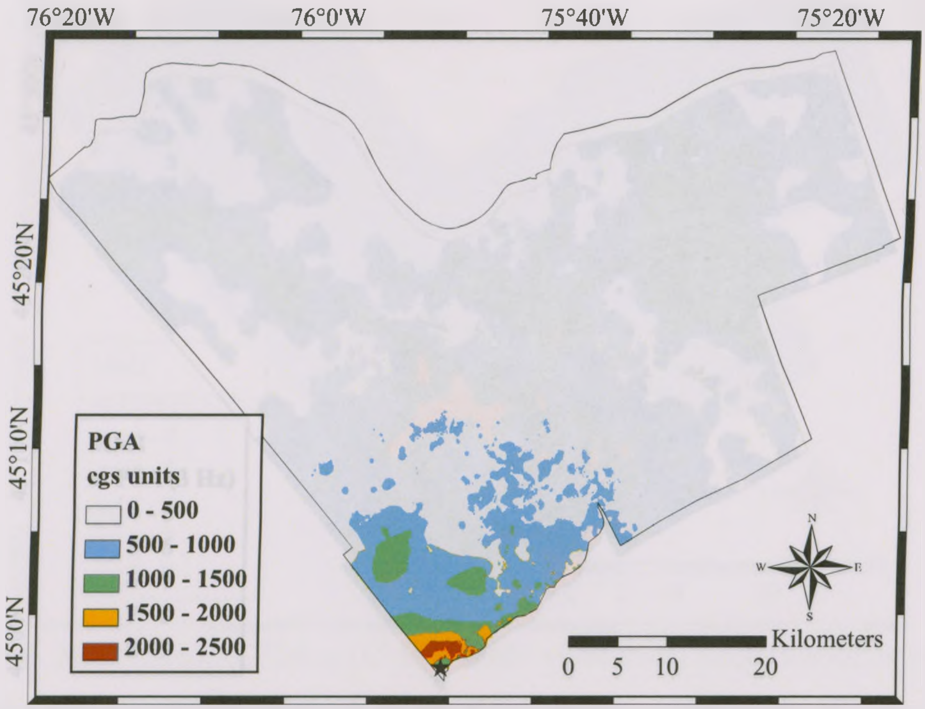

Figure A7.4. PGA for M6 event using amplification factors based on Quarter wavelength method for epicenter located on hard rock.

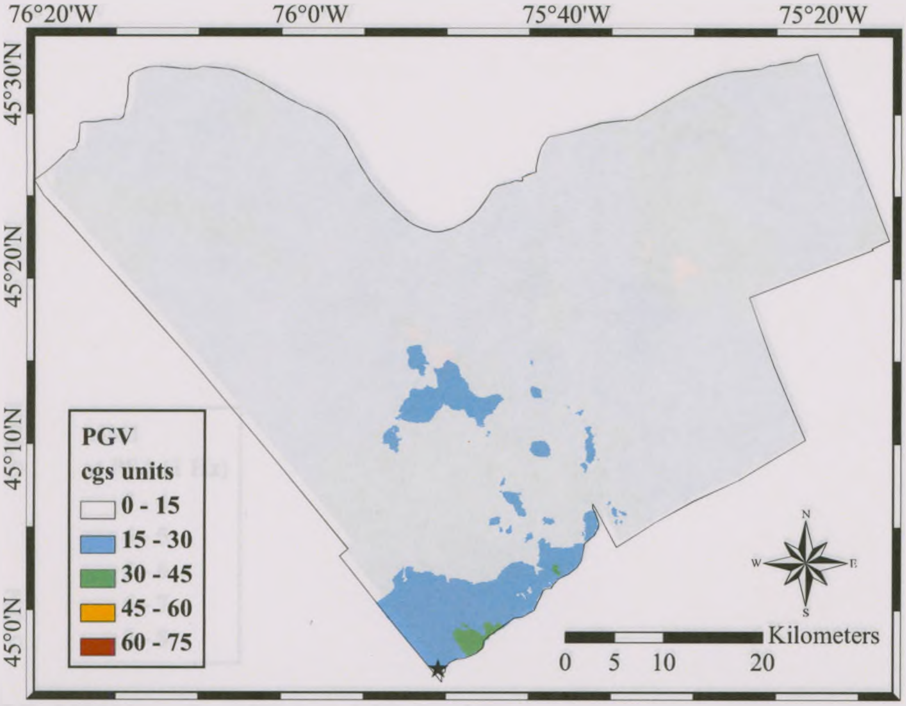

Figure A7.5. PGV for M6 event using amplification factors based on Quarter wavelength method for epicenter located on hard rock.

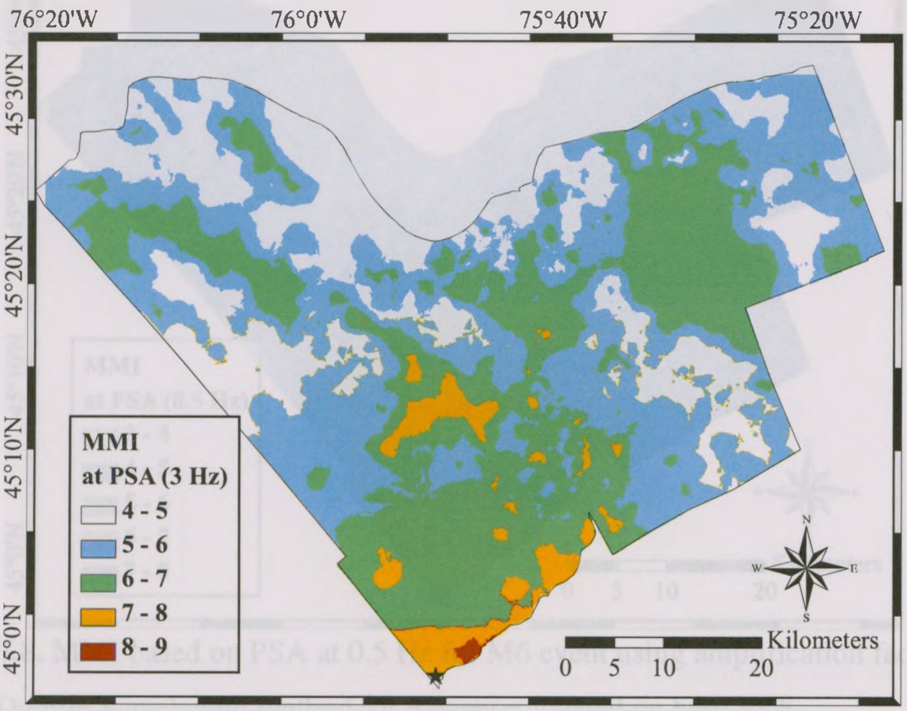

Figure A7.6. MMI based on PSA at 3 Hz for M6 event using amplification factors based on Quarter wavelength method for epicenter located on hard rock.

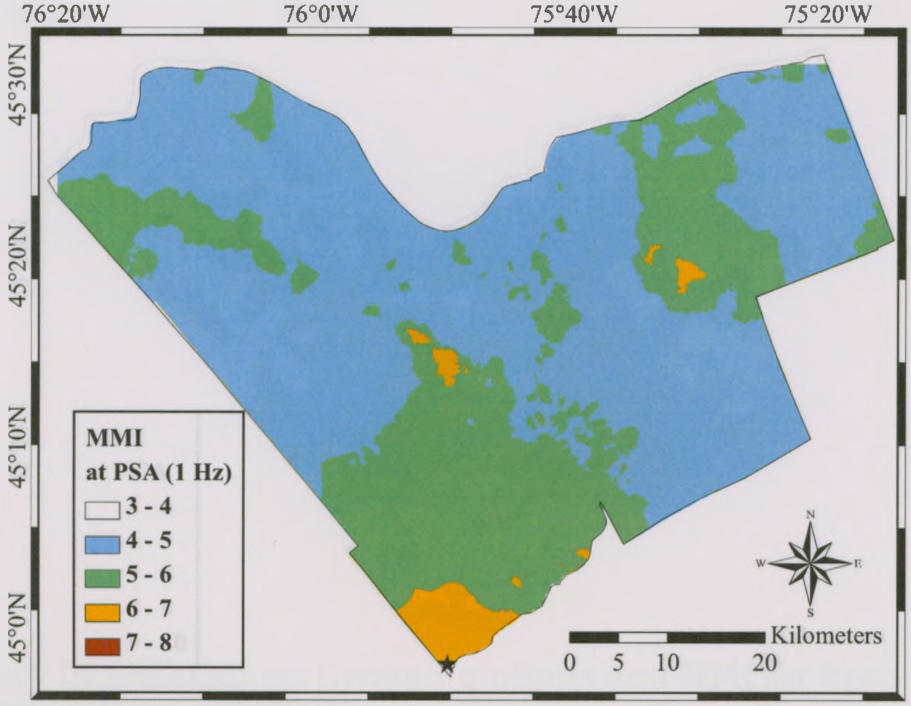

Figure A7.7. MMI based on PSA at 1 Hz for M6 event using amplification factors based on Quarter wavelength method for epicenter located on hard rock.

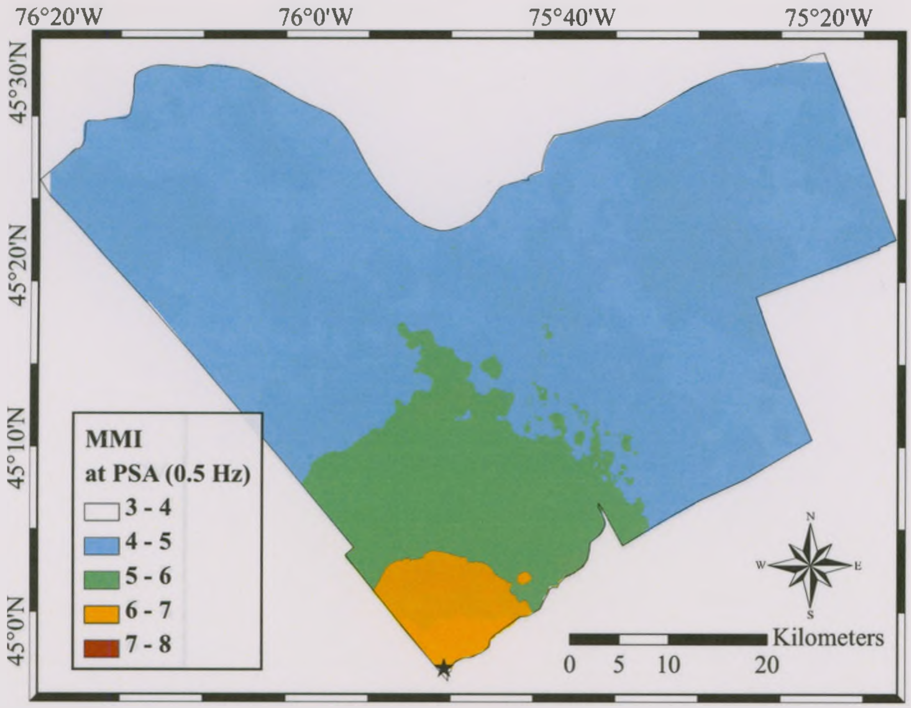

Figure A7.8. MMI based on PSA at 0.5 Hz for M6 event using amplification factors based on Quarter wavelength method for epicenter located on hard rock.

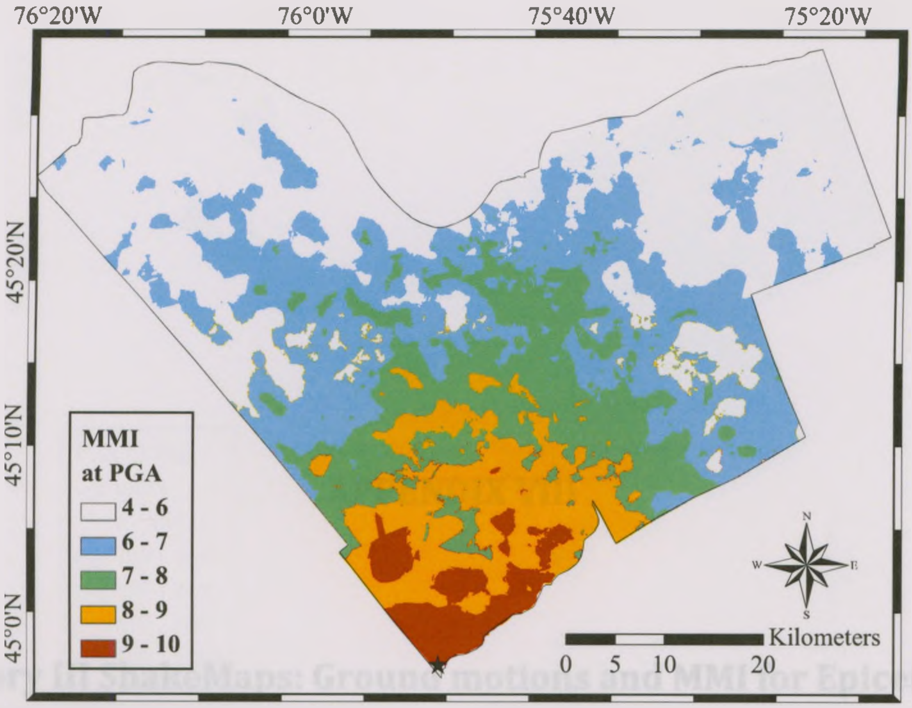

Figure A7.9. MMI based on PGA for M6 event using amplification factors based on Quarter wavelength method for epicenter located on hard rock.

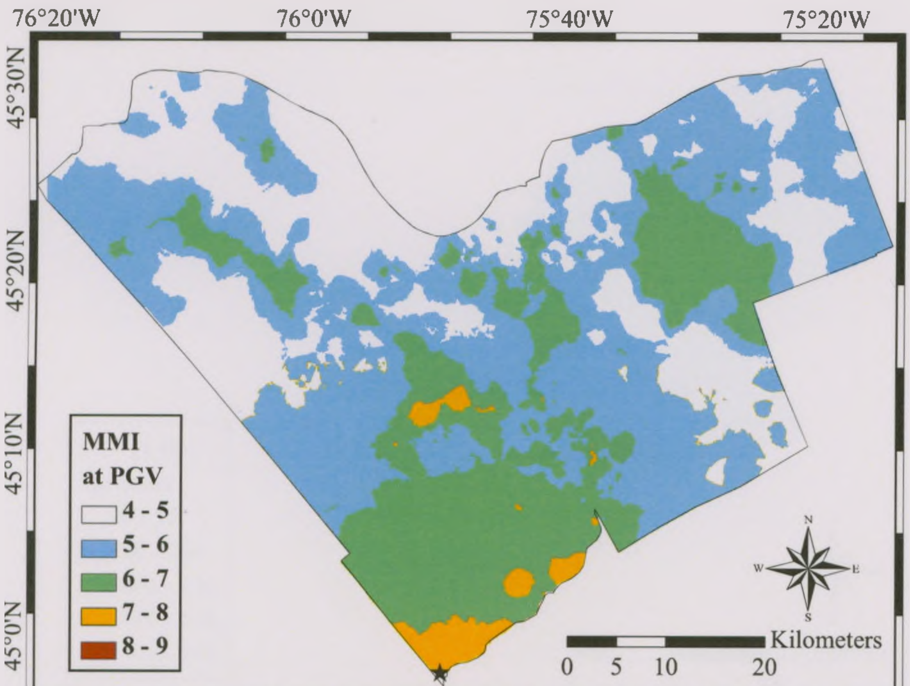

Figure A7.10. MMI based on PGV for M6 event using amplification factors based on Quarter wavelength method for epicenter located on hard rock.

APPENDIX VIII

Category III ShakeMaps: Ground motions and MMI for Epicenter 2

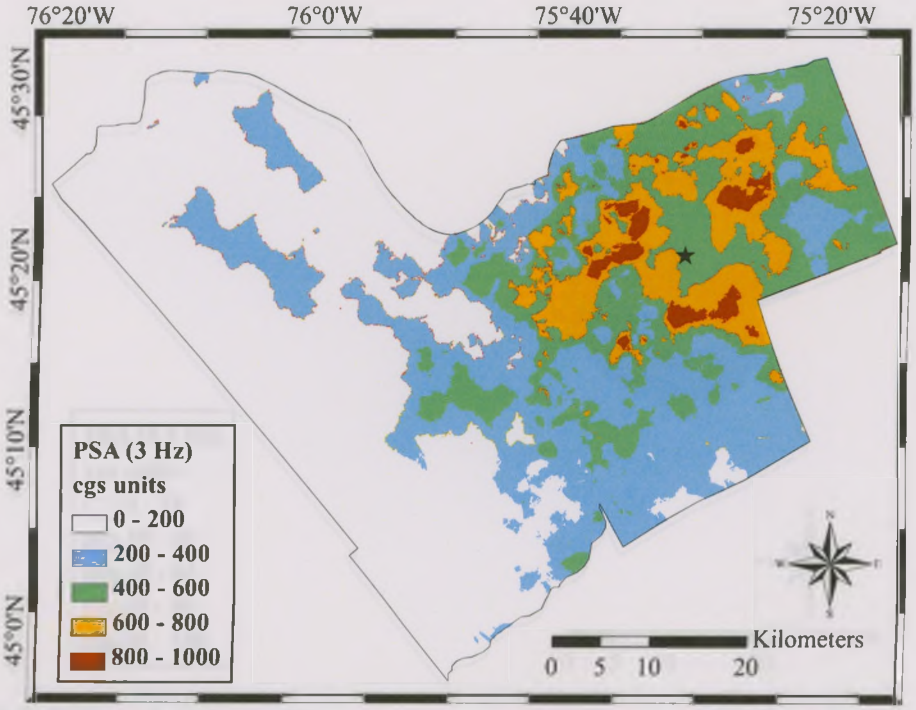

Figure A8.1. PSA at 3 Hz for M6 event using amplification factors based on Quarter wavelength method for epicenter located in soft soil.

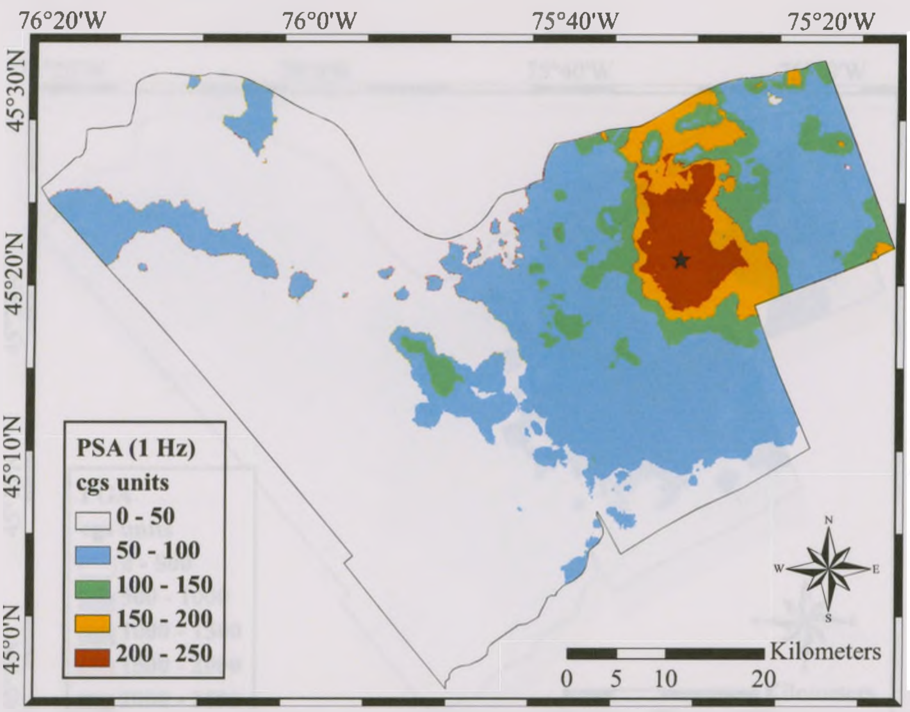

Figure A8.2. PSA at 1 Hz for M6 event using amplification factors based on Quarter wavelength method for epicenter located in soft soil.

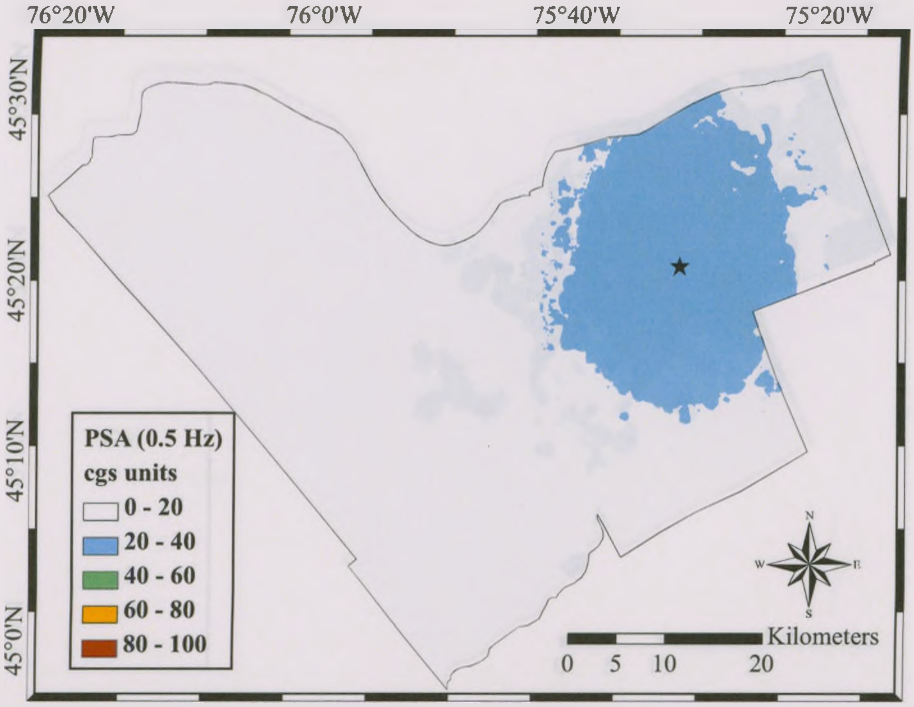

Figure A8.3. PSA at 0.5 Hz for M6 event using amplification factors based on Quarter wavelength method for epicenter located in soft soil.

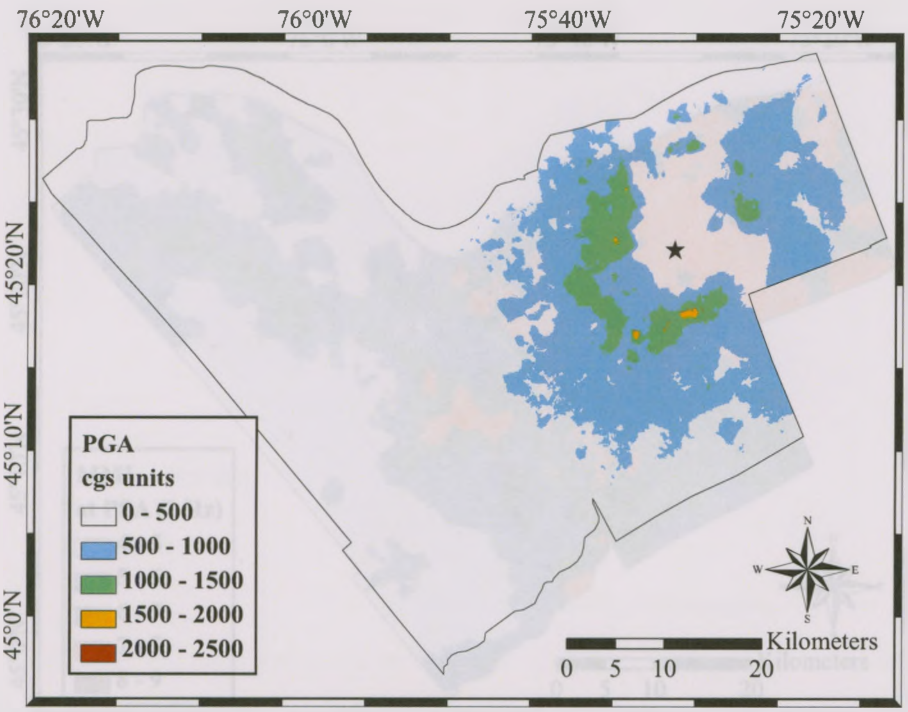

Figure A8.4. PGA for M6 event using amplification factors based on Quarter wavelength method for epicenter located in soft soil.

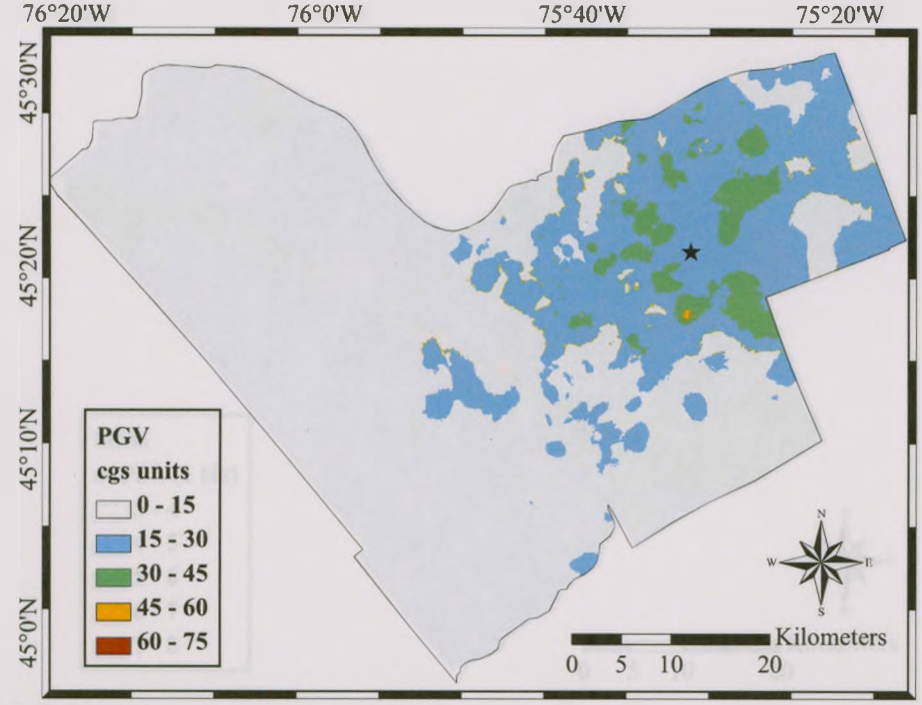

Figure A8.5. PGV for M6 event using amplification factors based on Quarter wavelength method for epicenter located in soft soil.

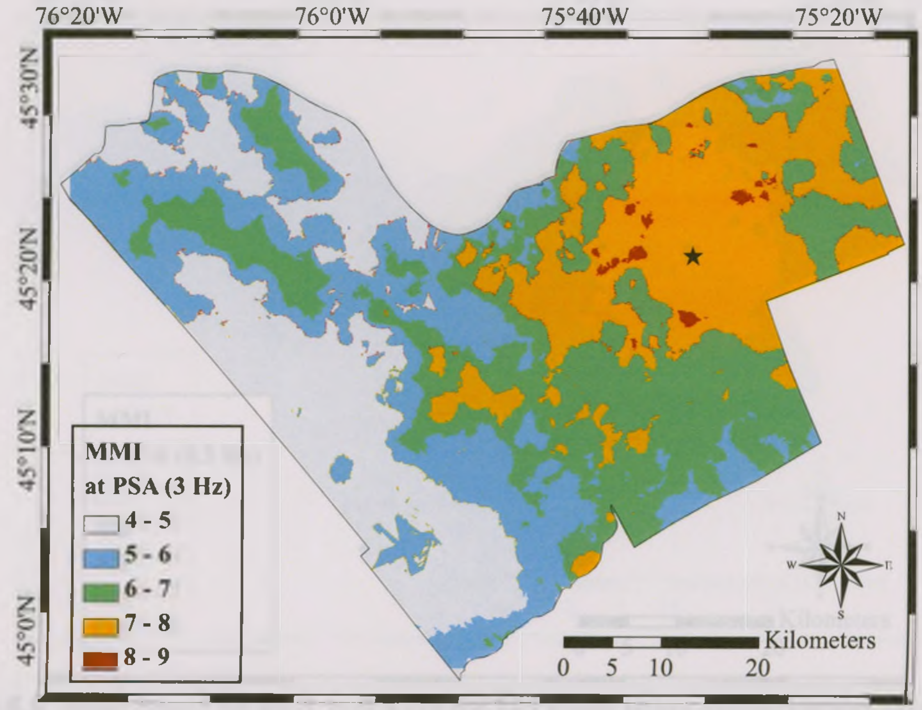

Figure A8.6. MMI based on PSA at 3 Hz for M6 event using amplification factors based on Quarter wavelength method for epicenter located in soft soil.

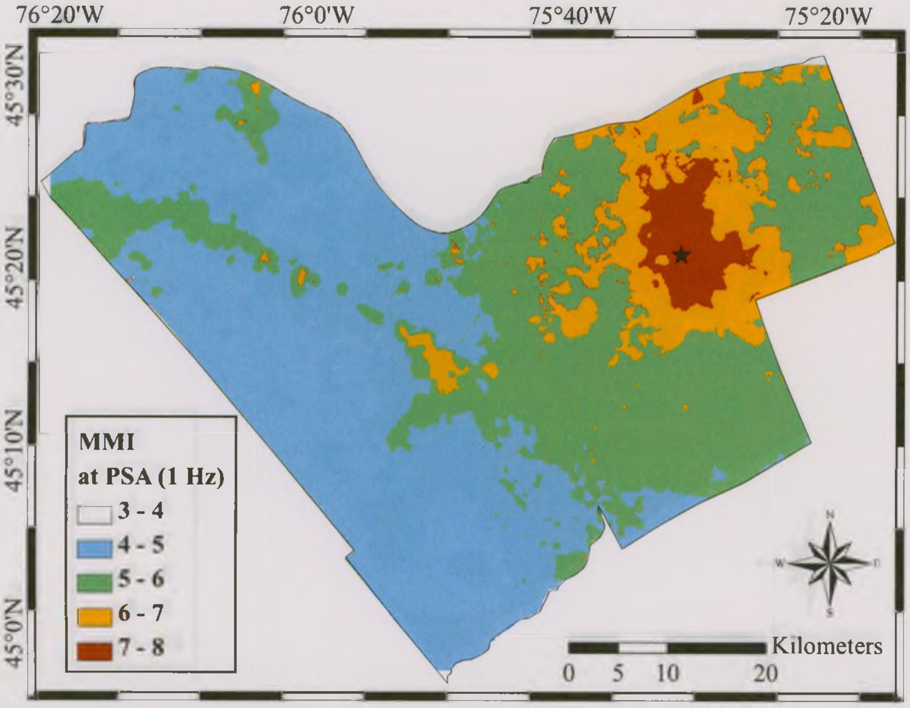

Figure A8.7. MMI based on PSA at 1 Hz for M6 event using amplification factors based on Quarter wavelength method for epicenter located in soft soil.

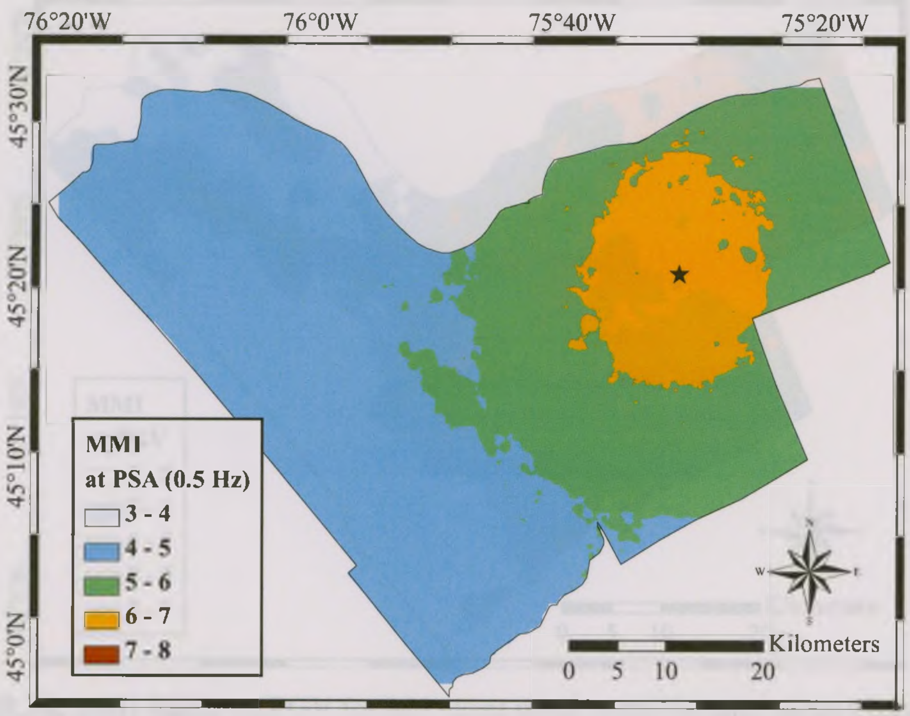

Figure A8.8. MMI based on PSA at 0.5 Hz for M6 event using amplification factors based on Quarter wavelength method for epicenter located in soft soil.

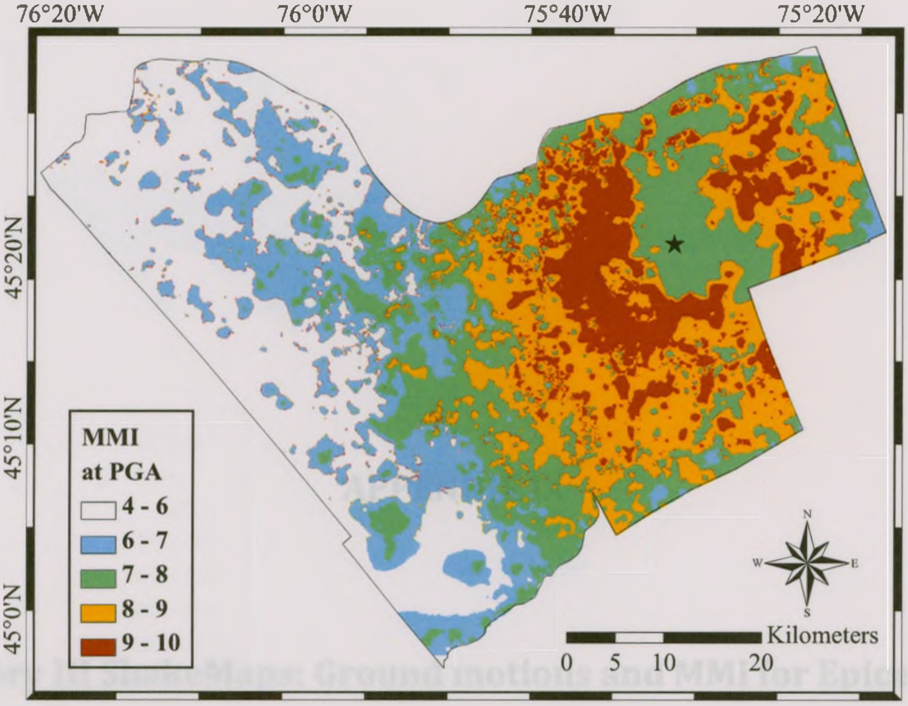

Figure A8.9. MMI based on PGA for M6 event using amplification factors based on Quarter wavelength method for epicenter located in soft soil.

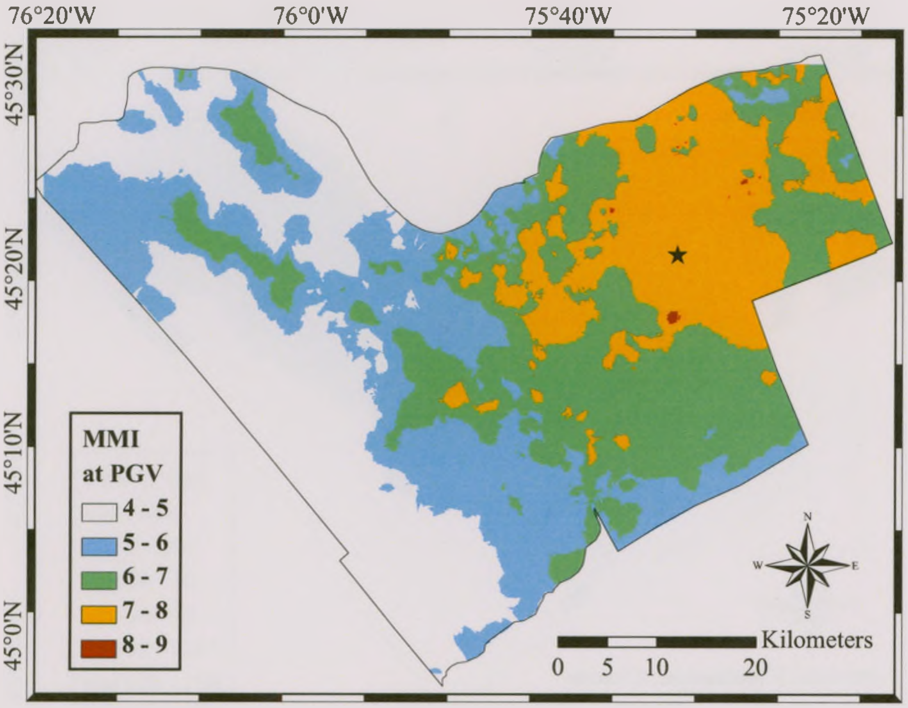

Figure A8.10. MMI based on PGV for M6 event using amplification factors based on Quarter wavelength method for epicenter located in soft soil.

APPENDIX IX

Category III ShakeMaps: Ground motions and MMI for Epicenter 3

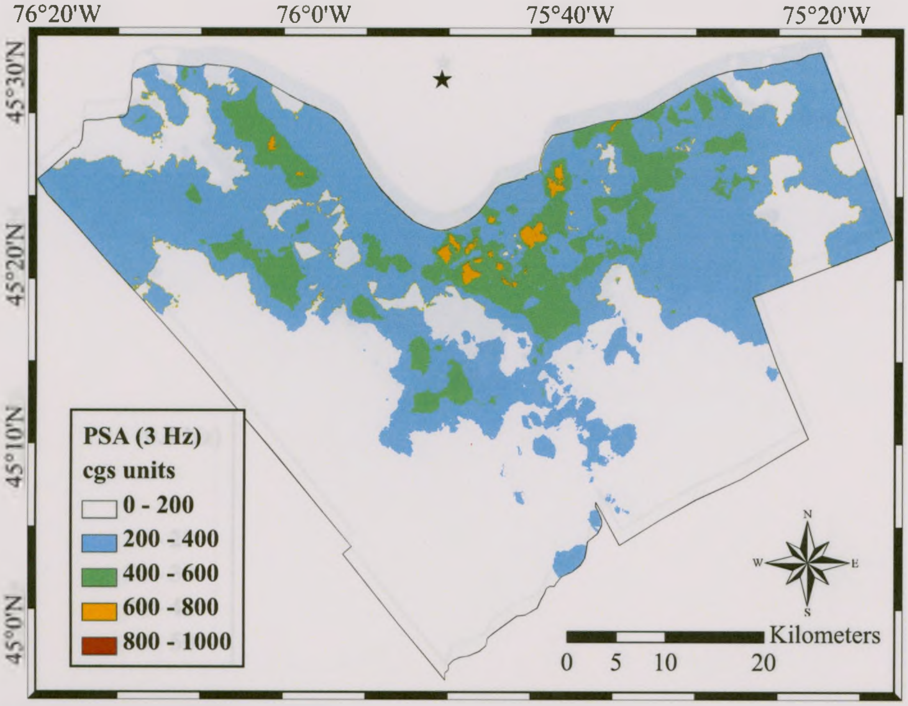

Figure A9.1. PSA at 3 Hz for M6 event using amplification factors based on Quarter wavelength method for epicenter located in Hull region.

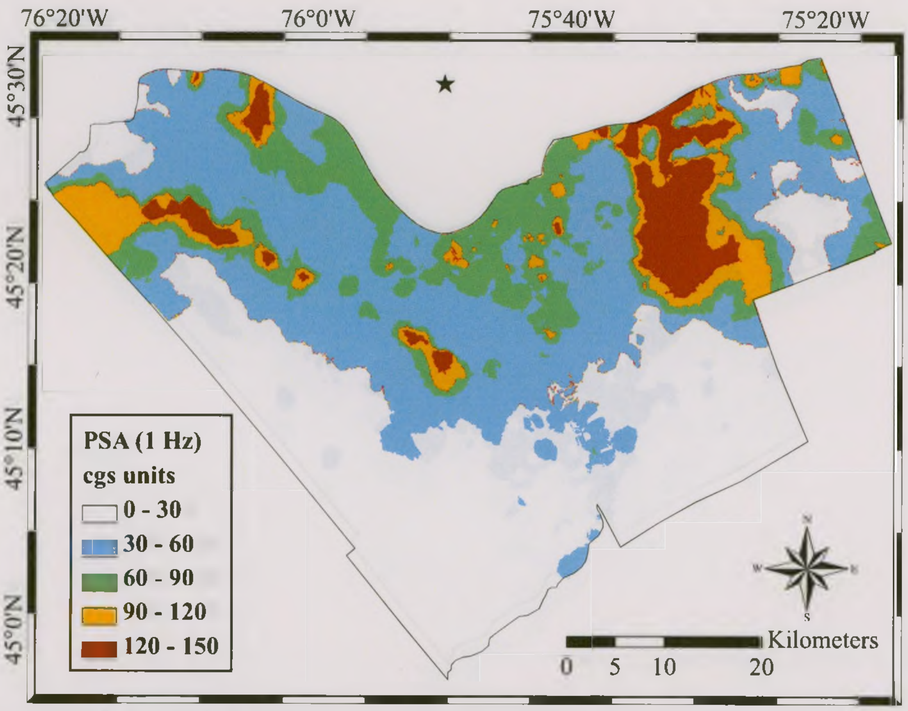

Figure A9.2. PSA at 1 Hz for M6 event using amplification factors based on Quarter wavelength method for epicenter located in Hull region.

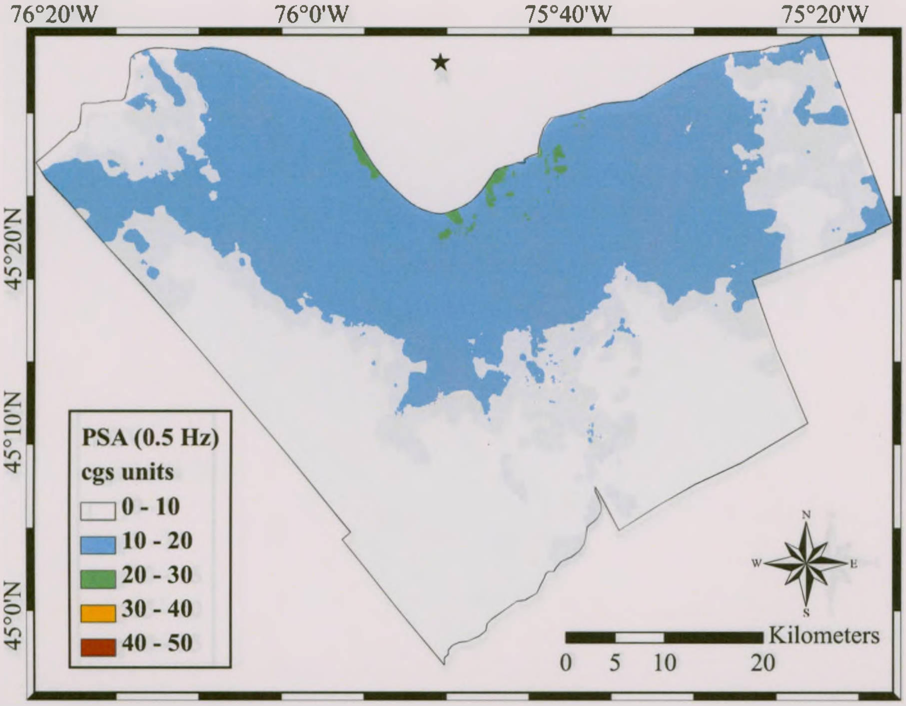

Figure A9.3. PSA at 0.5 Hz for M6 event using amplification factors based on Quarter wavelength method for epicenter located in Hull region.

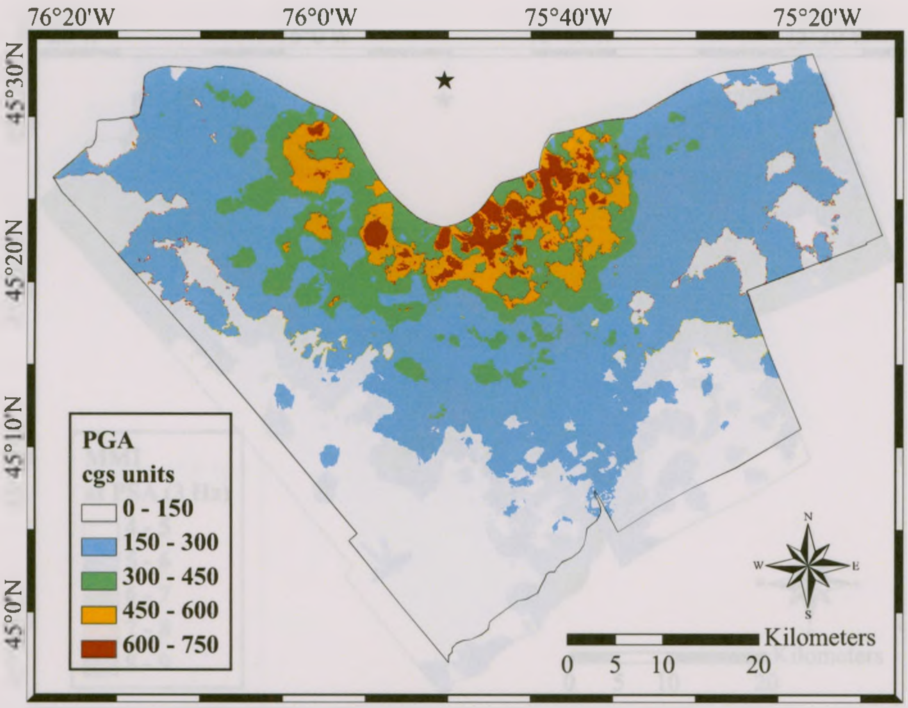

Figure A9.4. PGA for M6 event using amplification factors based on Quarter wavelength method for epicenter located in Hull region.

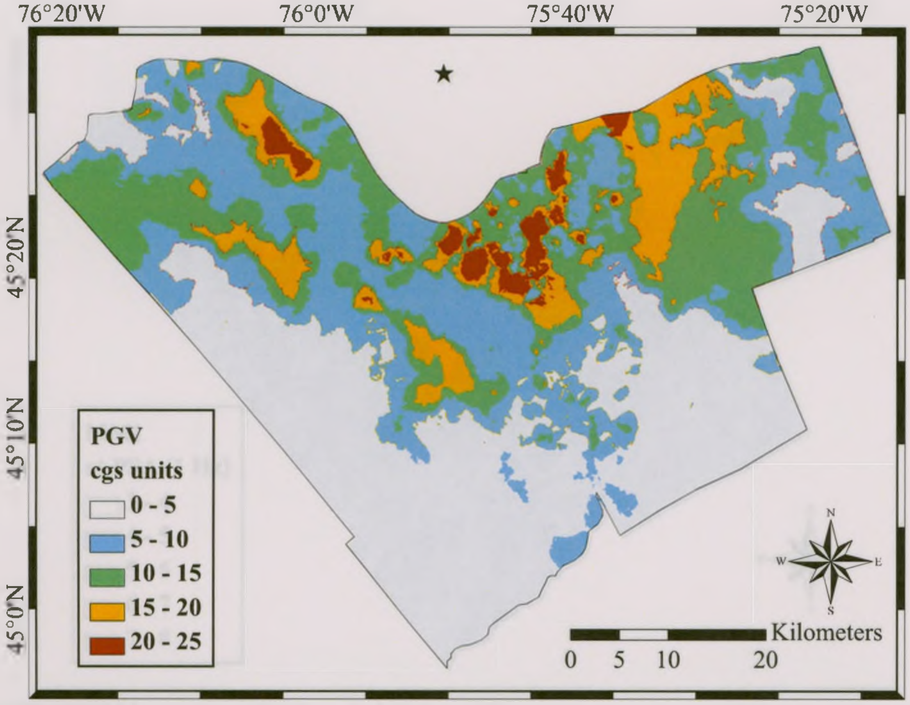

Figure A9.5. PGV for M6 event using amplification factors based on Quarter wavelength method for epicenter located in Hull region.

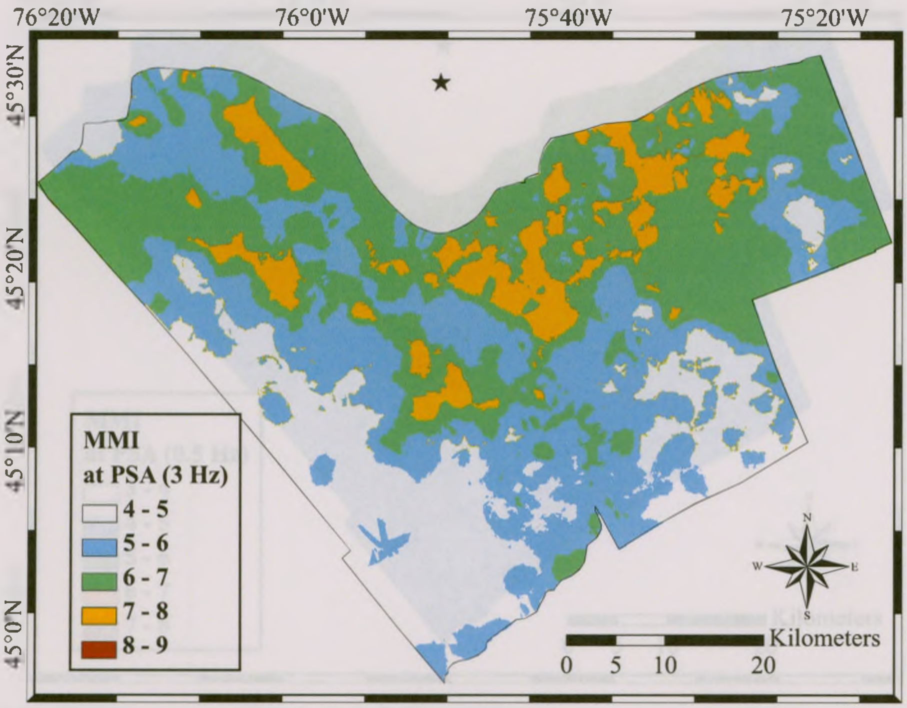

Figure A9.6. MMI based on PSA at 3 Hz for M6 event using amplification factors based on Quarter wavelength method for epicenter located in Hull region.

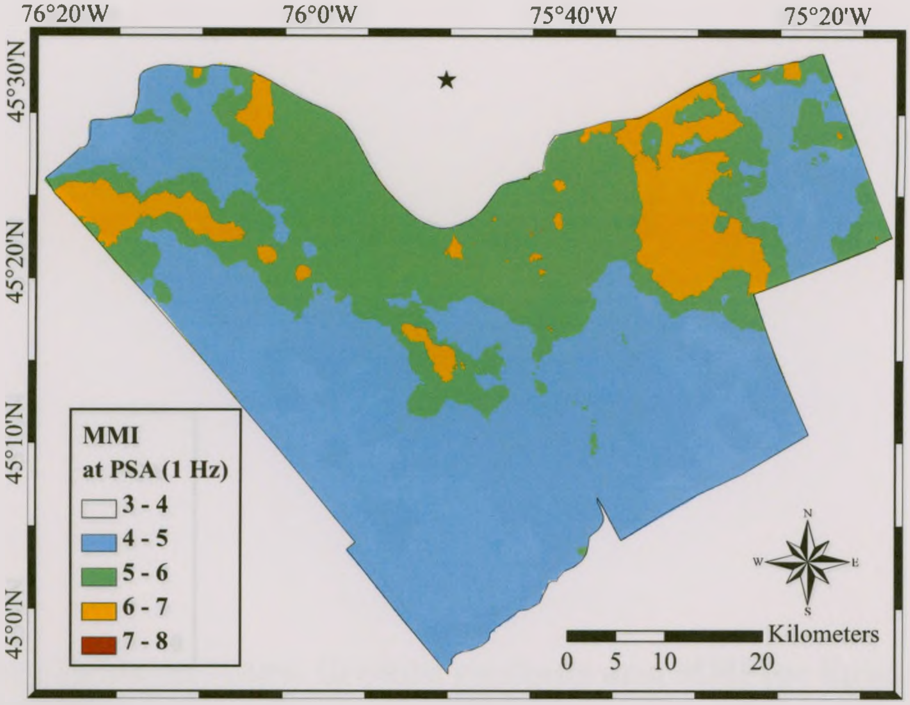

Figure A9.7. MMI based on PSA at 1 Hz for M6 event using amplification factors based on Quarter wavelength method for epicenter located in Hull region.

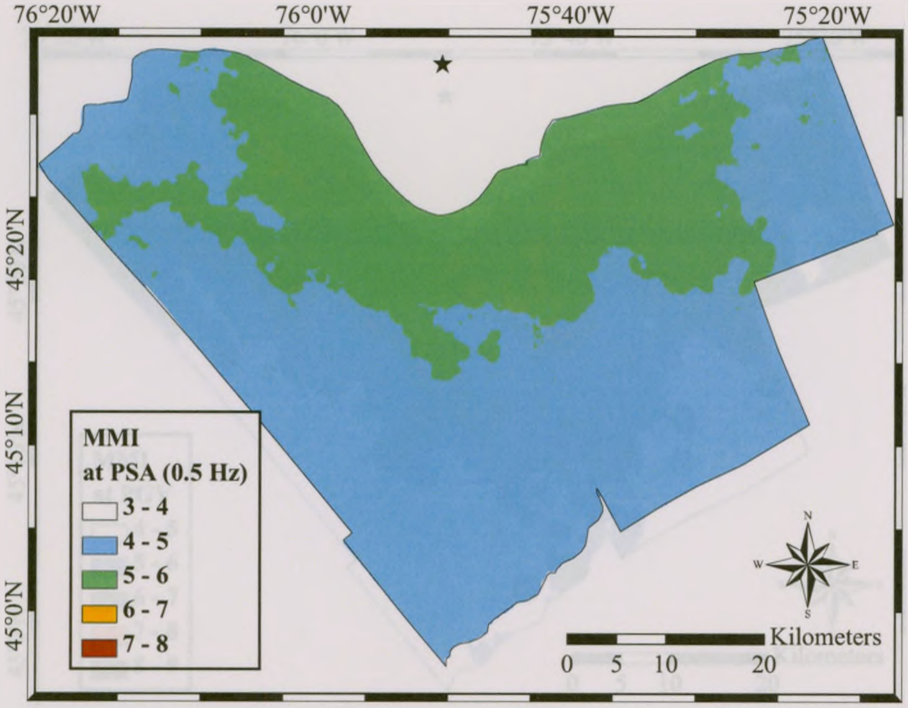

Figure A9.8. MMI based on PSA at 0.5 Hz for M6 event using amplification factors based on Quarter wavelength method for epicenter located in Hull region.

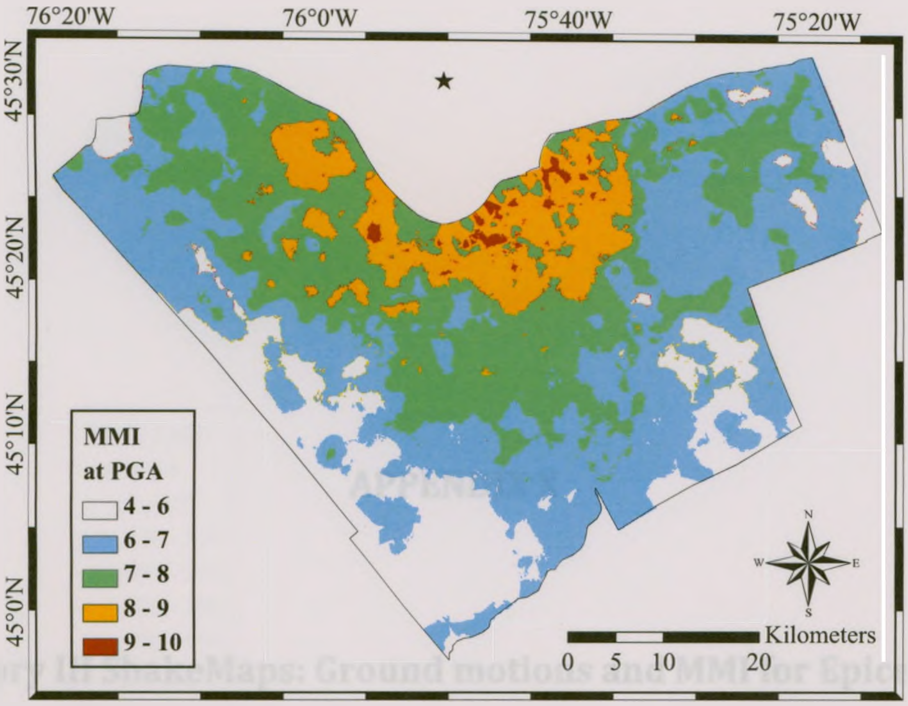

Figure A9.9. MMI based on PGA for M6 event using amplification factors based on Quarter wavelength method for epicenter located in Hull region.

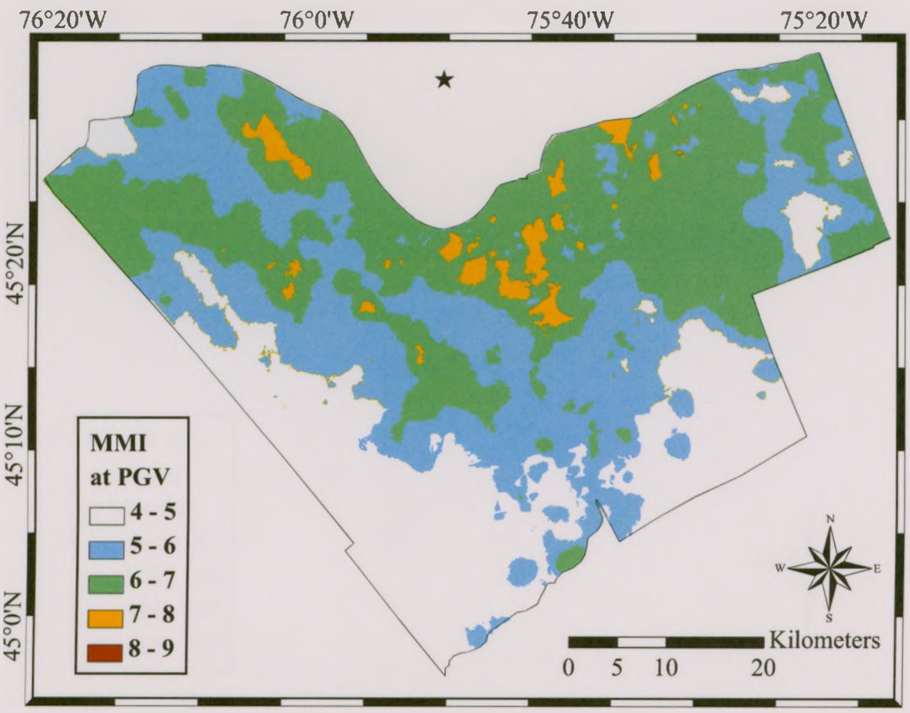

Figure A9.10. MMI based on PGV for M6 event using amplification factors based on Quarter wavelength method for epicenter located in Hull region.

APPENDIX X

Category III ShakeMaps: Ground motions and MMI for Epicenter 4

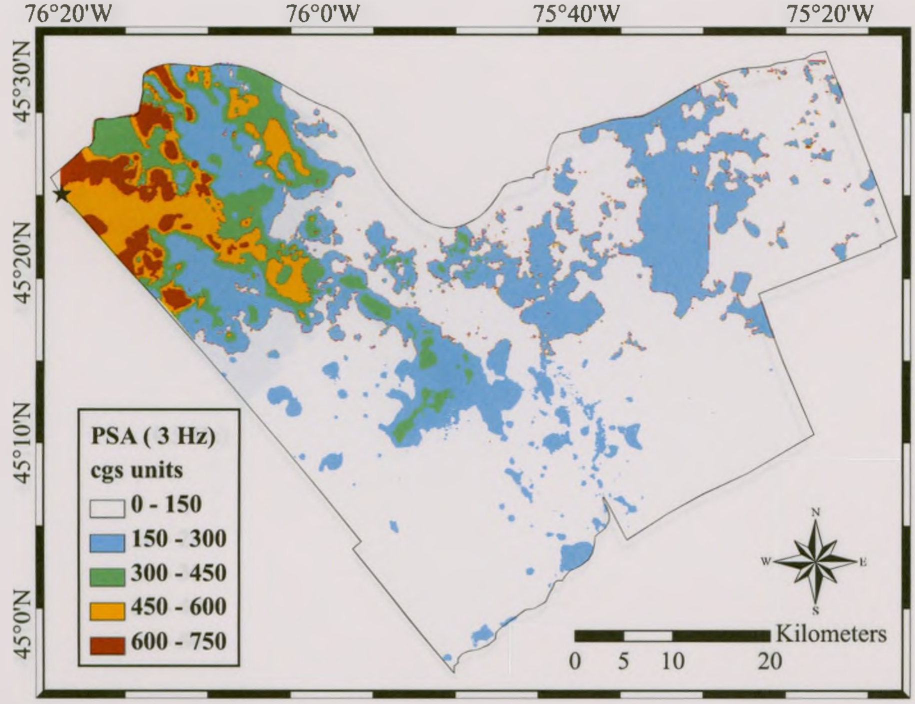

Figure A10.1. PSA at 3 Hz for M6 event using amplification factors based on Quarter wavelength method for epicenter located in west.

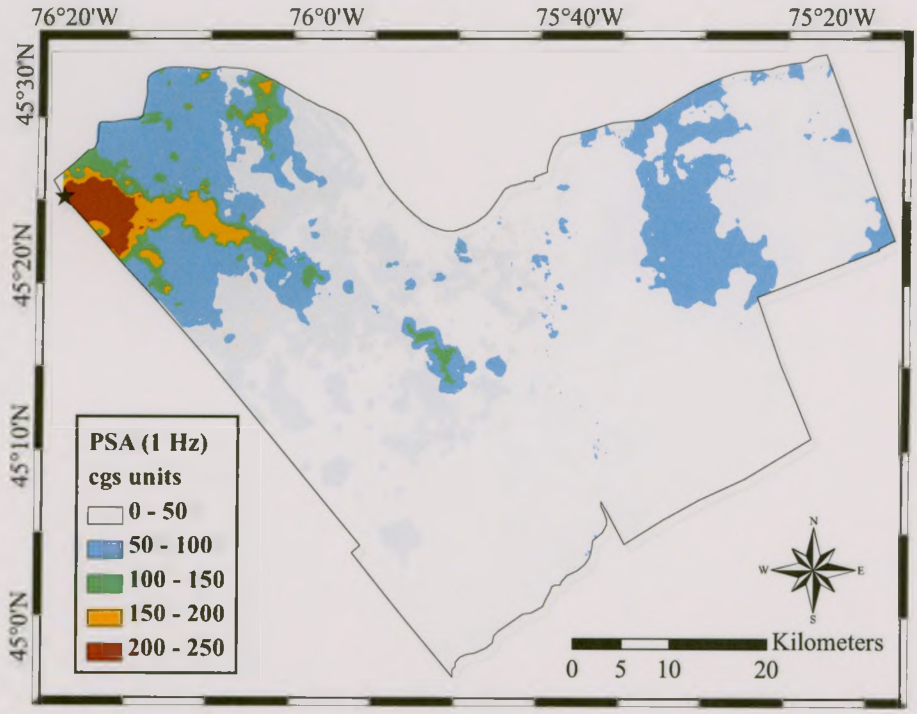

Figure A10.2. PSA at 1 Hz for M6 event using amplification factors based on Quarter wavelength method for epicenter located in west.

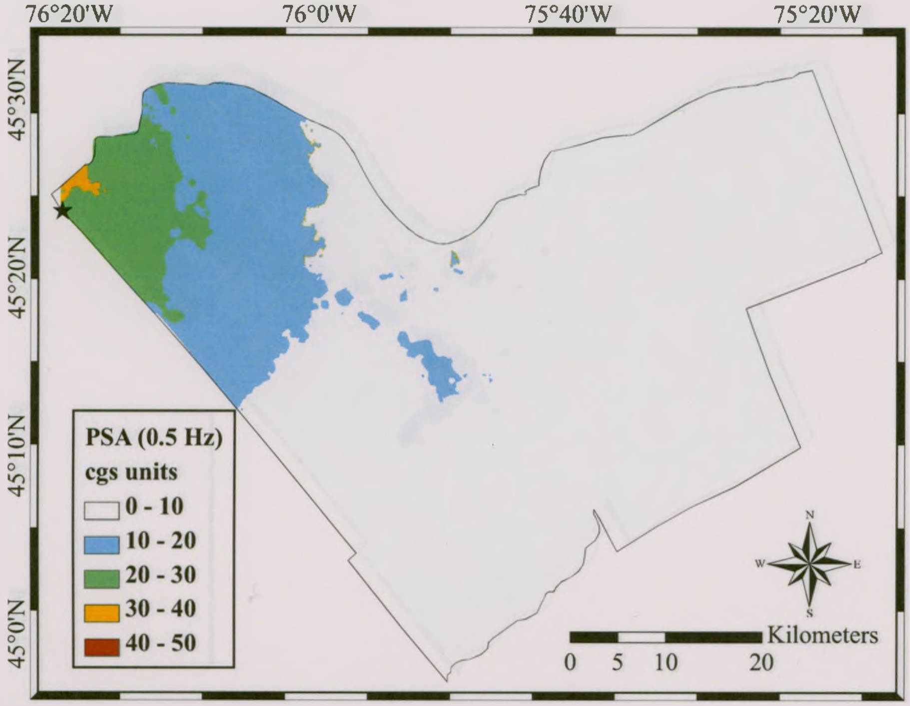

Figure A10.3. PSA at 0.5 Hz for M6 event using amplification factors based on Quarter wavelength method for epicenter located in west.

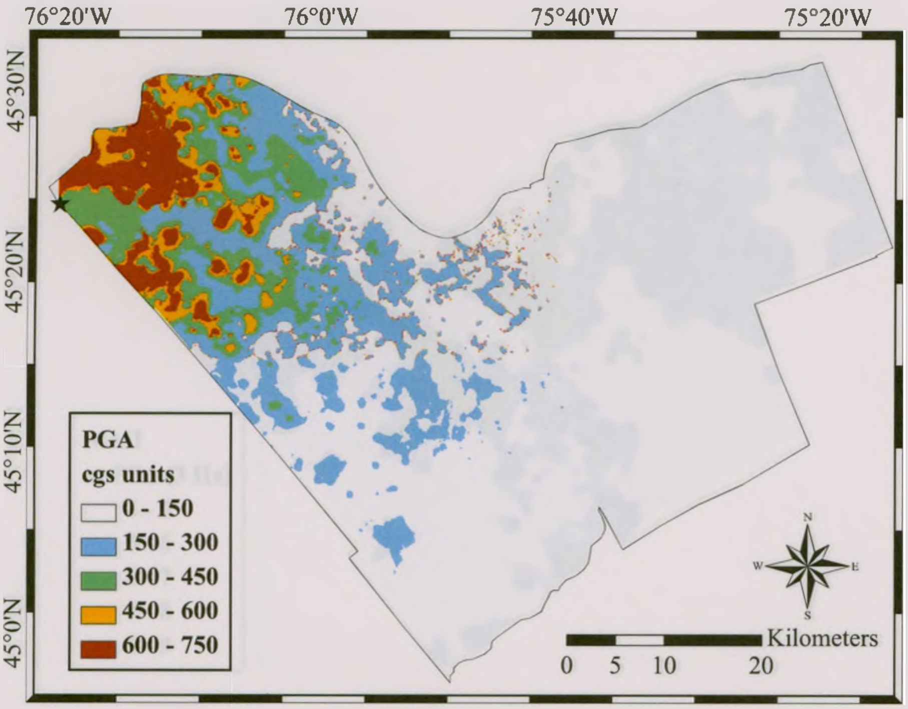

Figure A10.4. PGA for M6 event using amplification factors based on Quarter wavelength method for epicenter located in west.

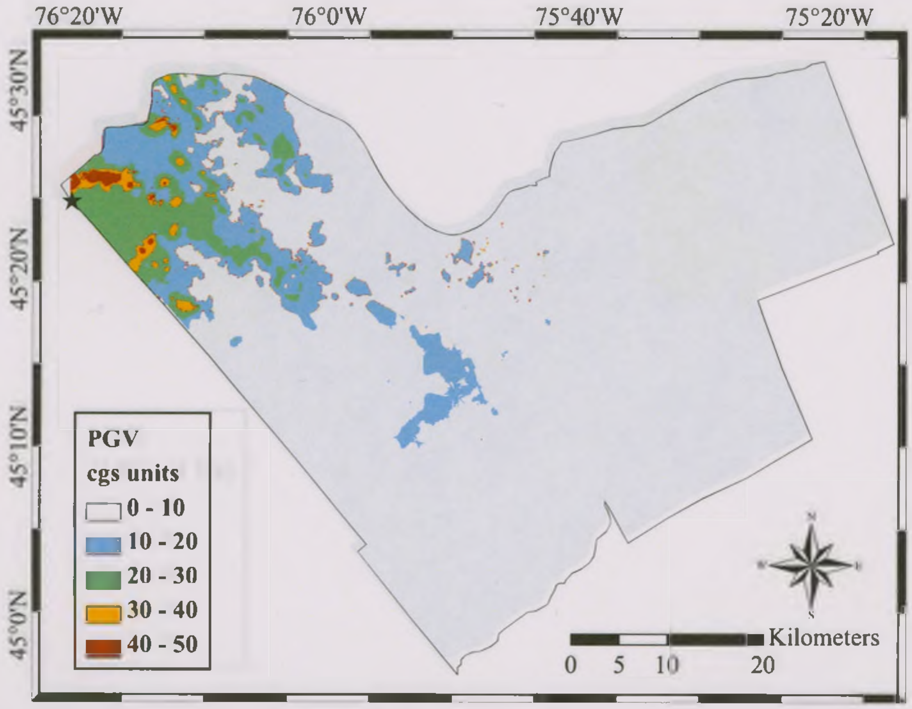

Figure A10.5. PGV for M6 event using amplification factors based on Quarter wavelength method for epicenter located in west.

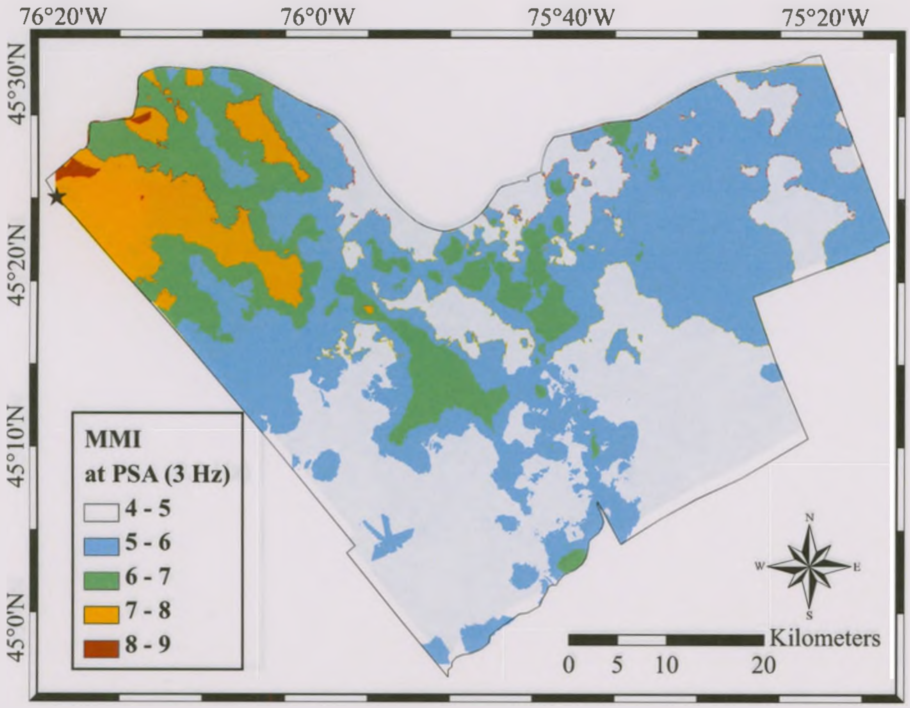

Figure A10.6. MMI based on PSA at 3 Hz for M6 event using amplification factors based on Quarter wavelength method for epicenter located in west.

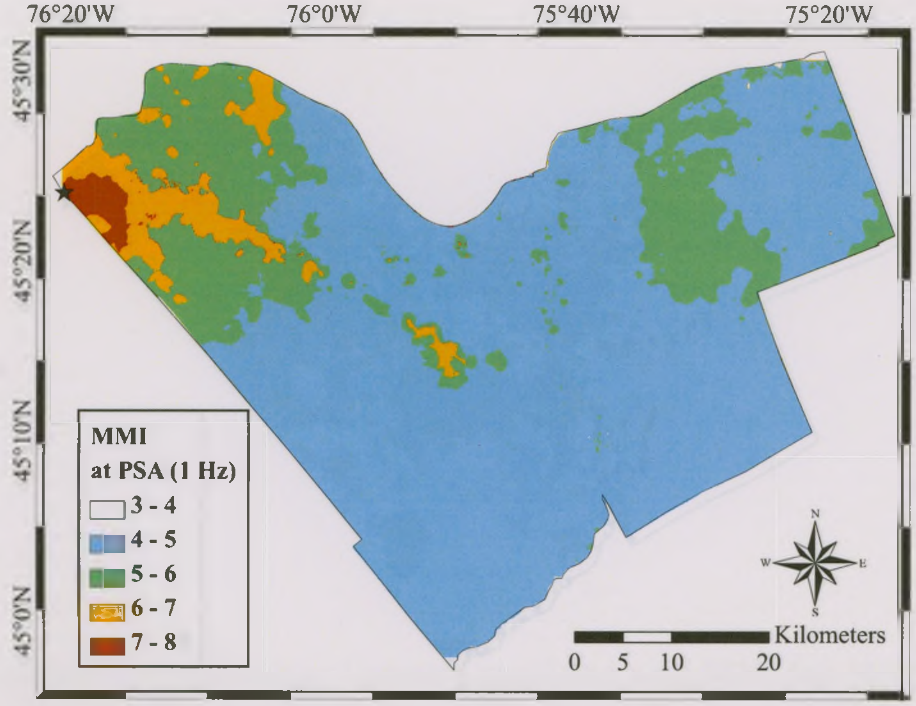

Figure A10.7. MMI based on PSA at 1 Hz for M6 event using amplification factors based on Quarter wavelength method for epicenter located in west.

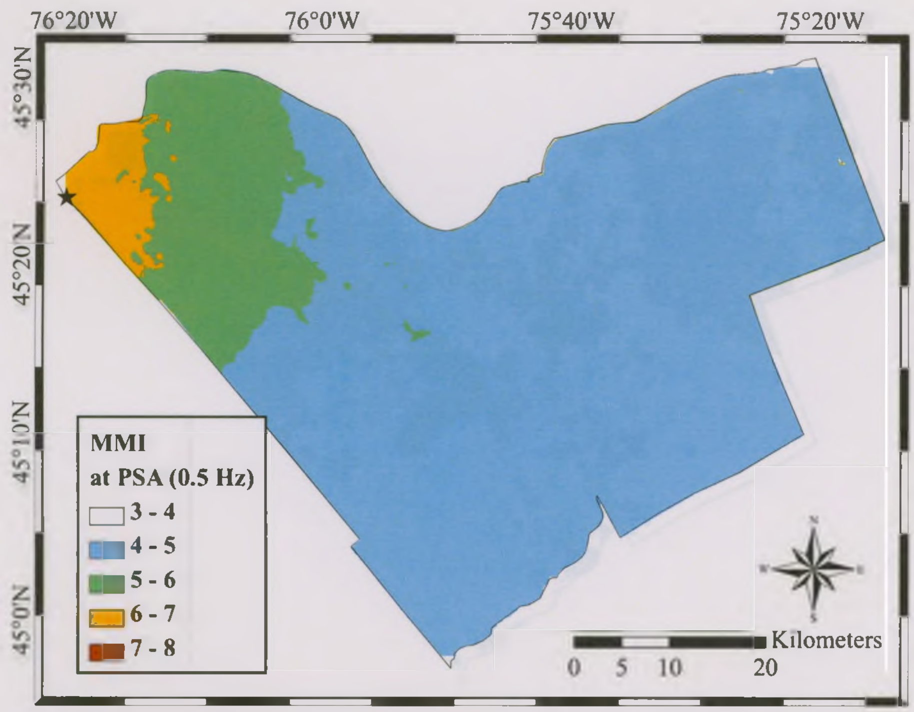

Figure A10.8. MMI based on PSA at 0.5 Hz for M6 event using amplification factors based on Quarter wavelength method for epicenter located in west.

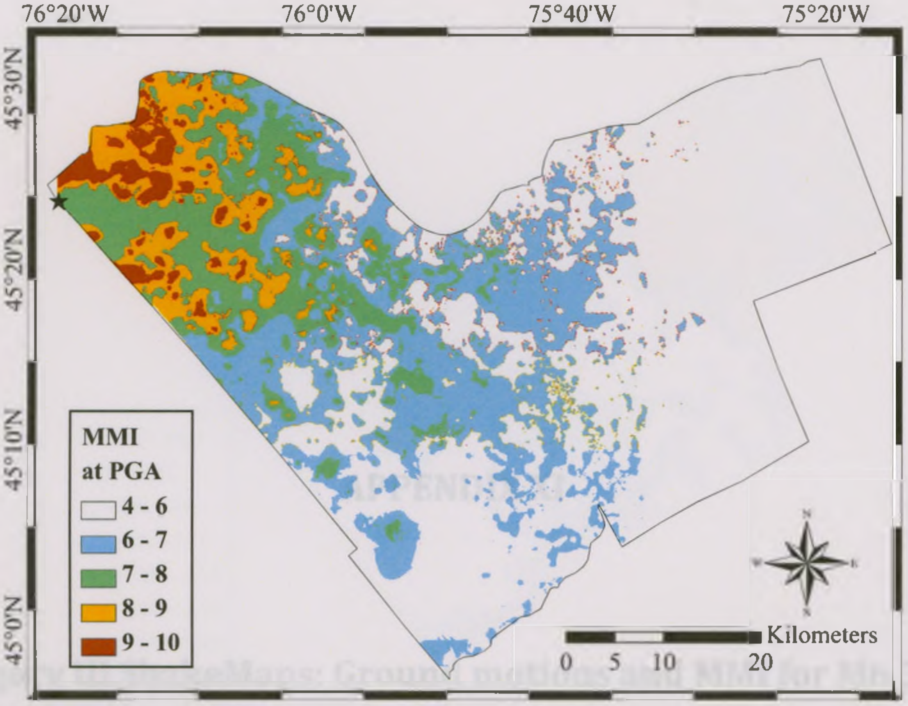

Figure A10.9. MMI based on PGA for M6 event using amplification factors based on Quarter wavelength method for epicenter located in west.

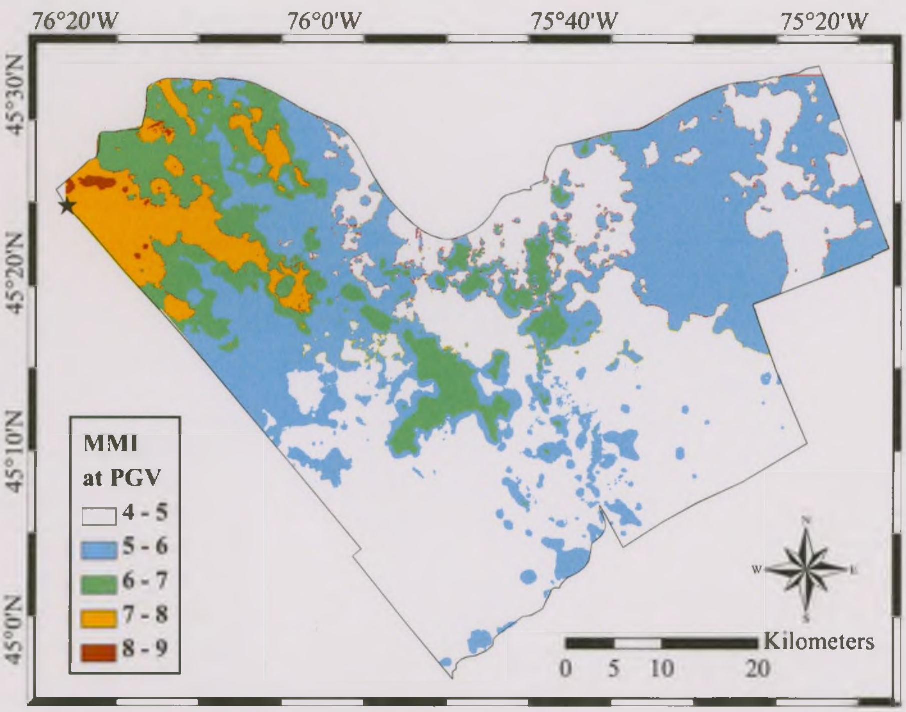

Figure A10.10. MMI based on PGV for M6 event using amplification factors based on Quarter wavelength method for epicenter located in west.

APPENDIX XI

Category III ShakeMaps: Ground motions and MMI for M6.5 and M7.5 Scenarios

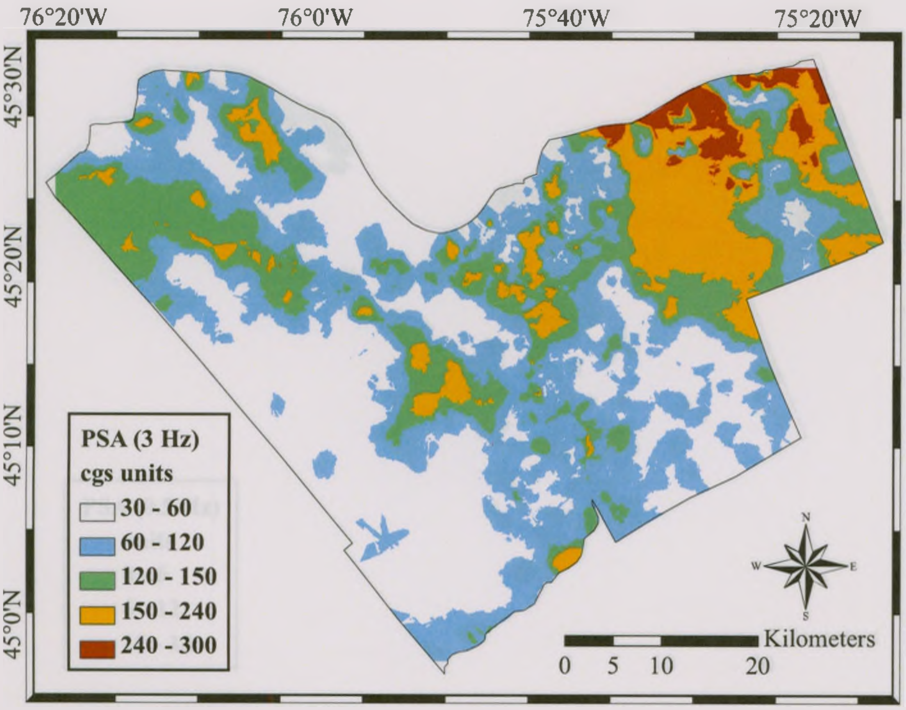

Figure A11.1. PSA at 3 Hz for M6.5 scenario using the profile-specific amplification factors, epicenter located 60 km North of Ottawa.

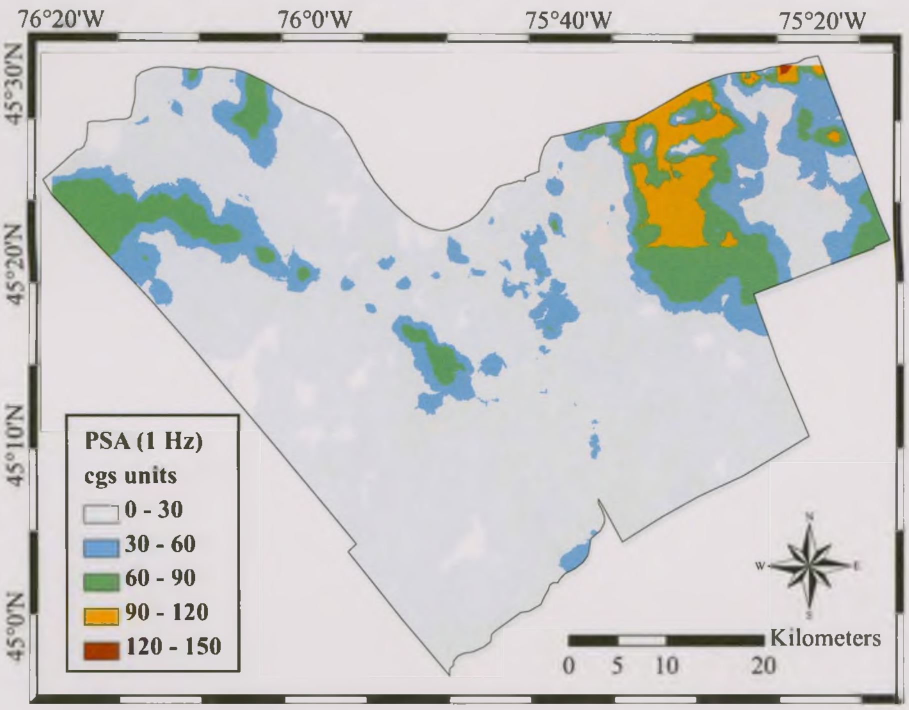

Figure A11.2. PSA at 1 Hz for M6.5 scenario using the profile-specific amplification factors, epicenter located 60 km North of Ottawa.

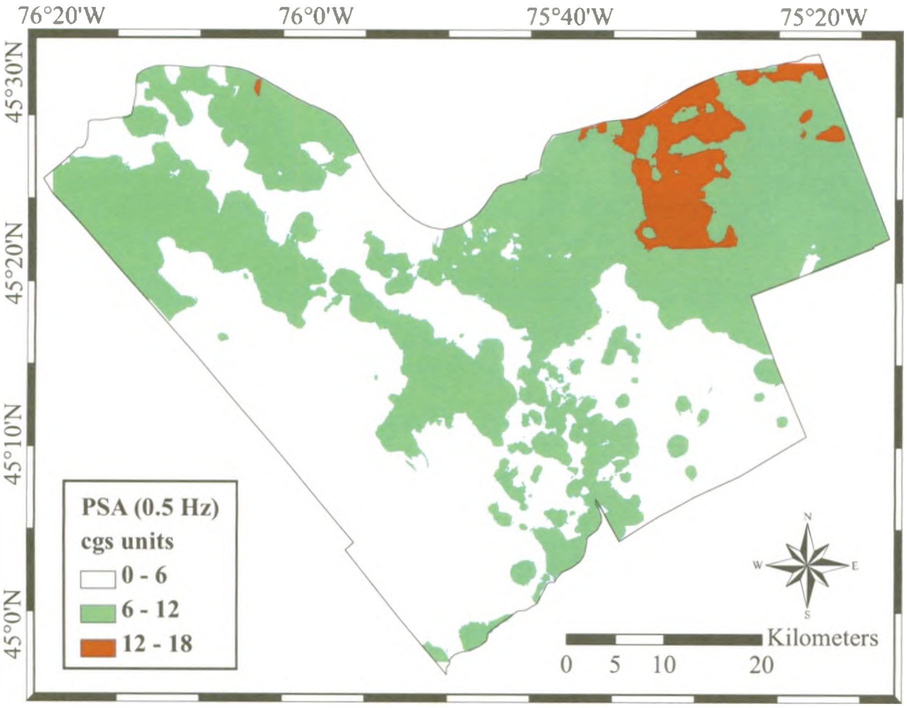

Figure A11.3. PSA at 0.5 Hz for M6.5 scenario using the profile-specific amplification factors, epicenter located 60 km North of Ottawa.

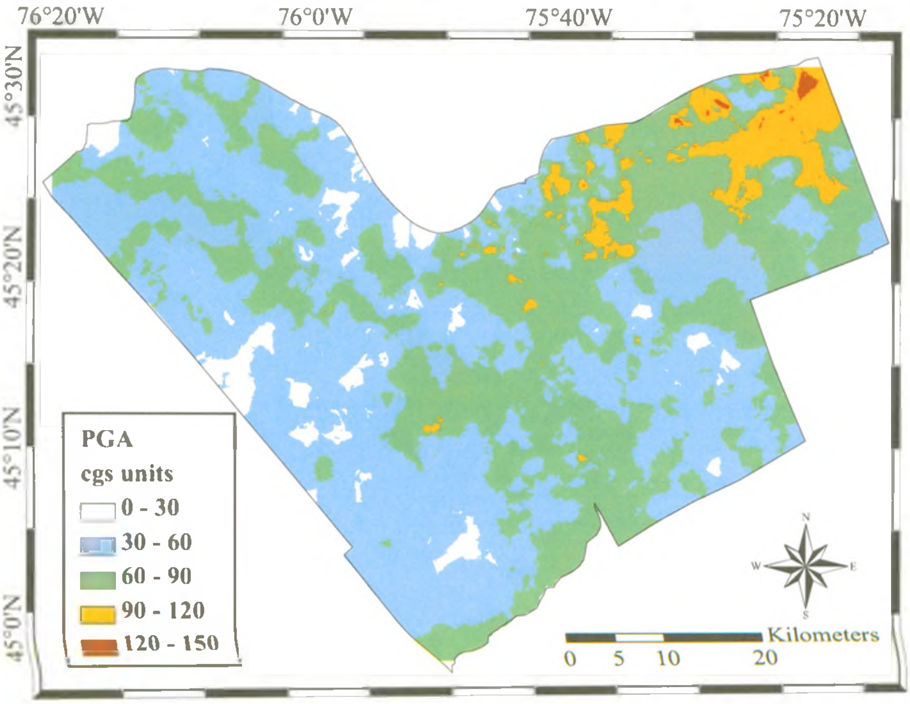

Figure A11.4. PGA for M6.5 scenario using the profile-specific amplification factors, epicenter located 60 km North of Ottawa.

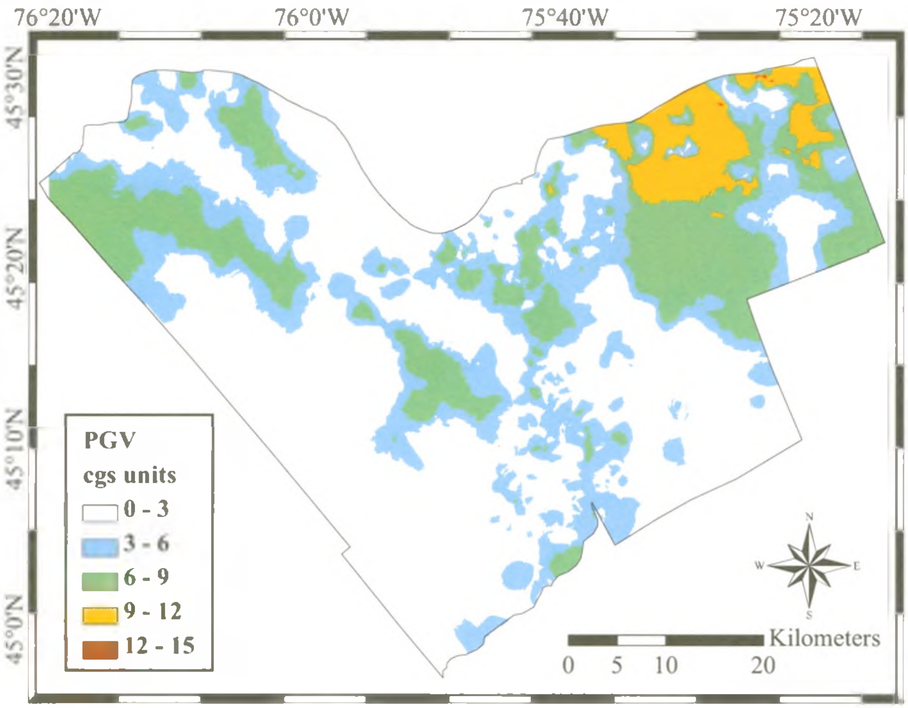

Figure A11.5. PGV for M6.5 scenario using the profile-specific amplification factors, epicenter located 60 km North of Ottawa.

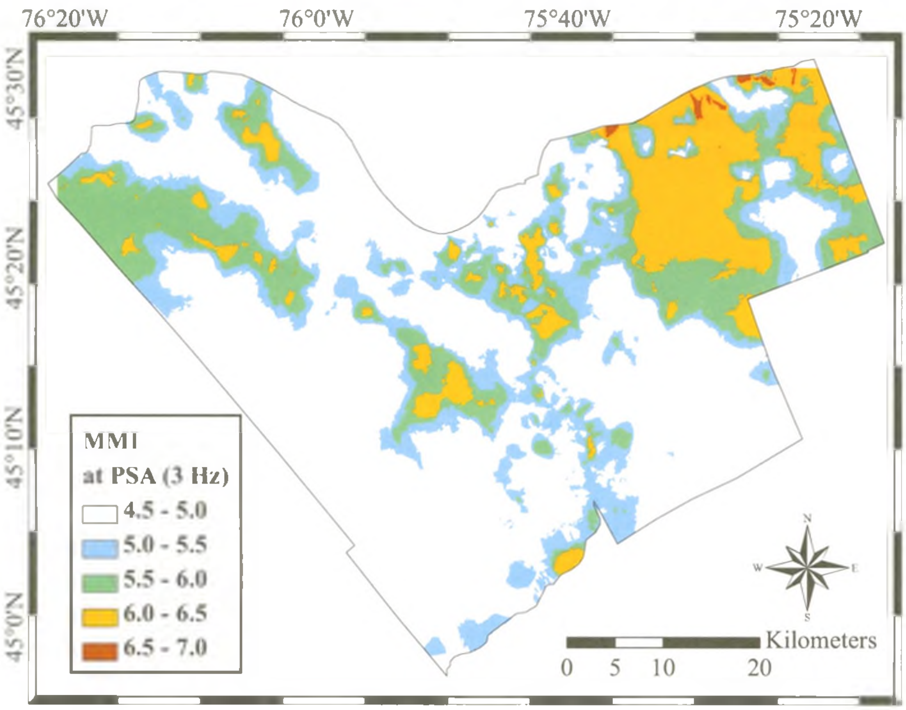

Figure A11.6. MMI based on PSA at 3 Hz for M6.5 scenario using the profile-specific amplification factors, epicenter located 60 km North of Ottawa.

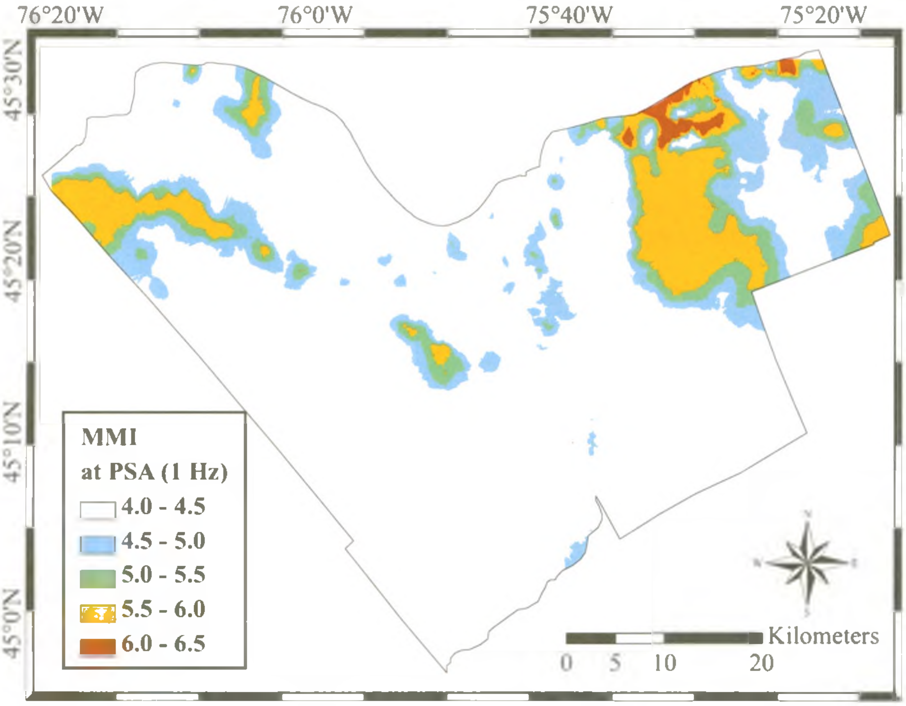

Figure A11.7. MMI based on PSA at 1 Hz for M6.5 scenario using the profile-specific amplification factors, epicenter located 60 km North of Ottawa.

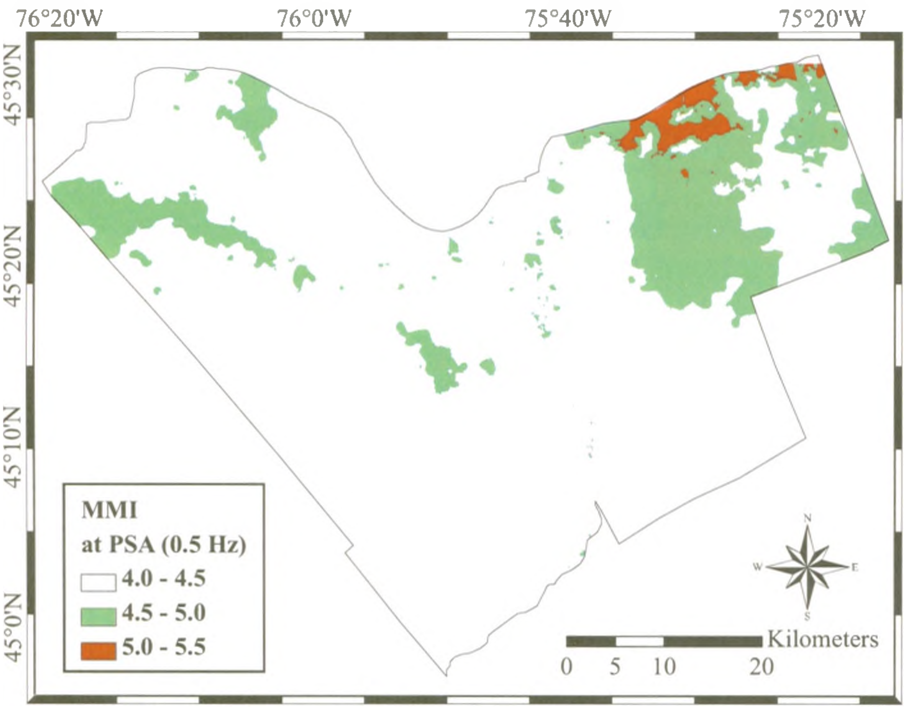

Figure A11.8. MMI based on PSA at 0.5 Hz for M6.5 scenario using the profile-specific amplification factors, epicenter located 60 km North of Ottawa.

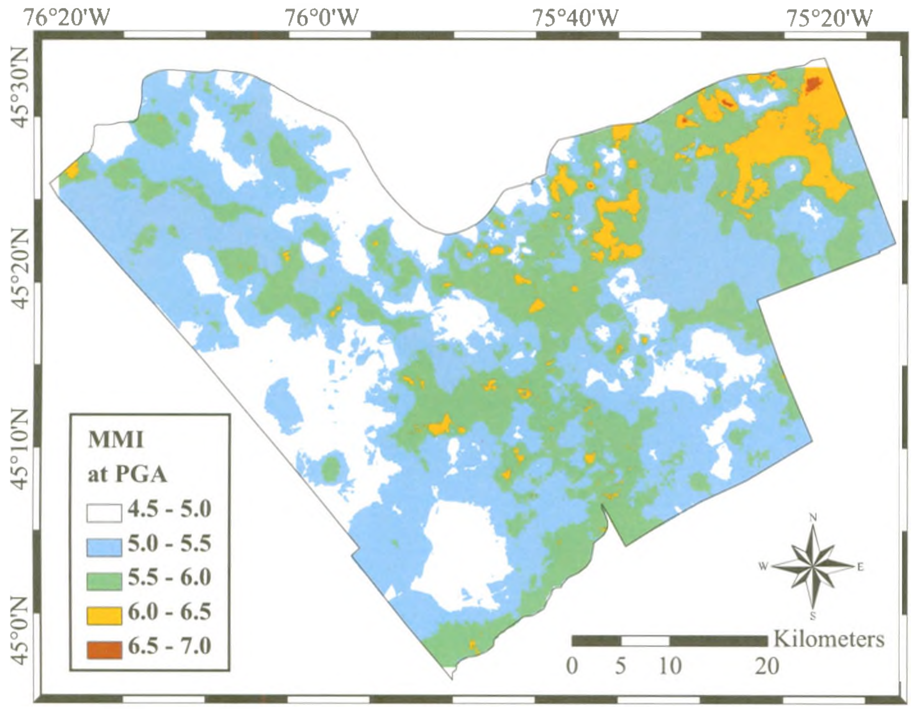

Figure A11.9. MMI based on PGA for M6.5 scenario using the profile-specific amplification factors, epicenter located 60 km North of Ottawa.

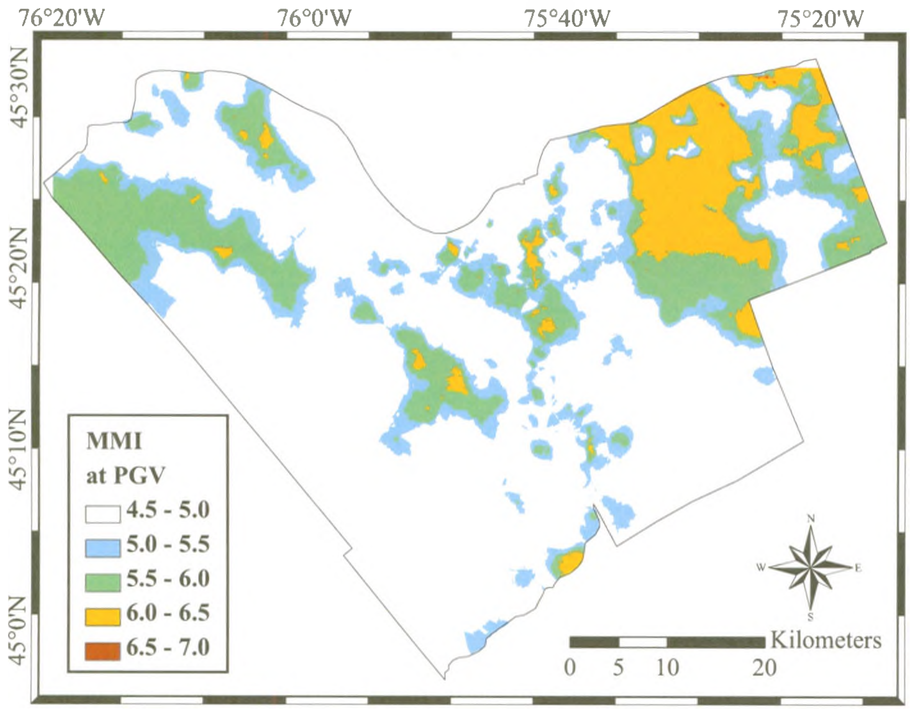

Figure A11.10. MMI based on PGV for M6.5 scenario using the profile-specific amplification factors, epicenter located 60 km North of Ottawa.

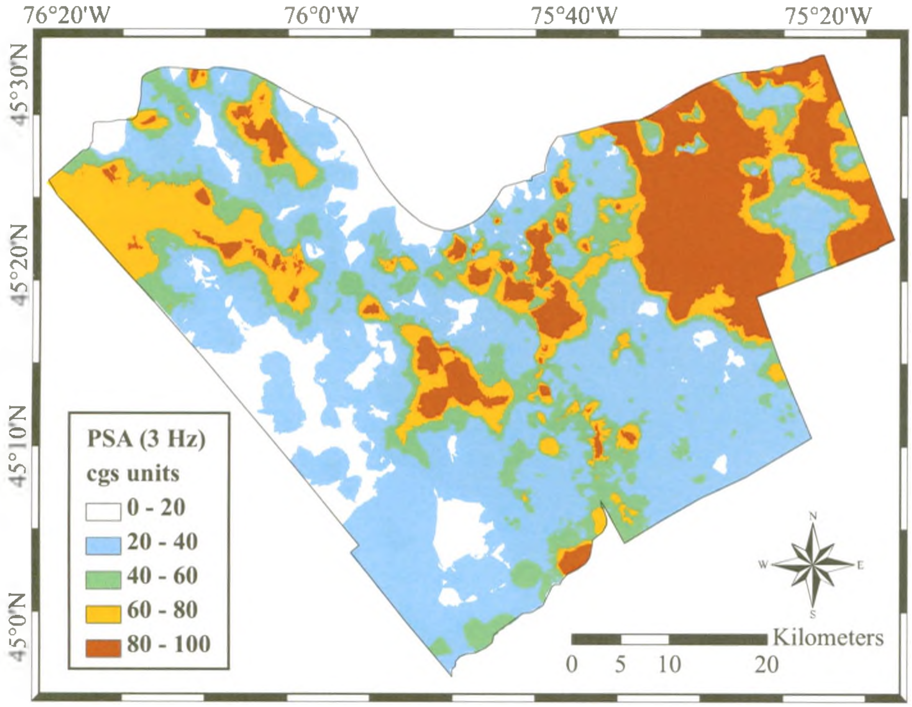

Figure A11.11. PSA at 3 Hz for M7.5 scenario using the profile-specific amplification factors, epicenter located ~460 km North-East of Ottawa.

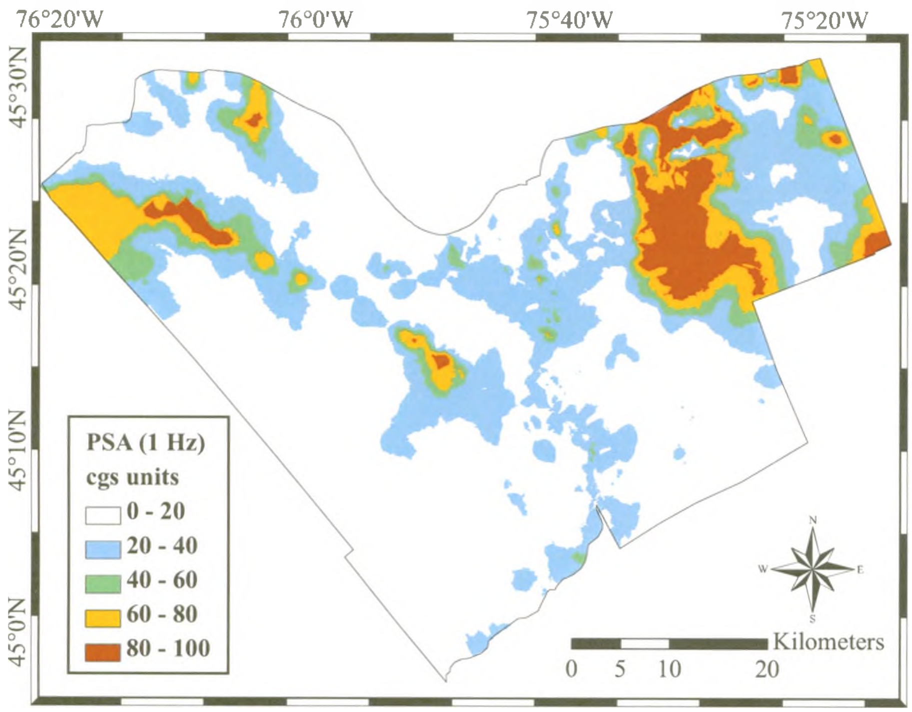

Figure A11.12. PSA at 1 Hz for M7.5 scenario using the profile-specific amplification factors, epicenter located ~460 km North-East of Ottawa.

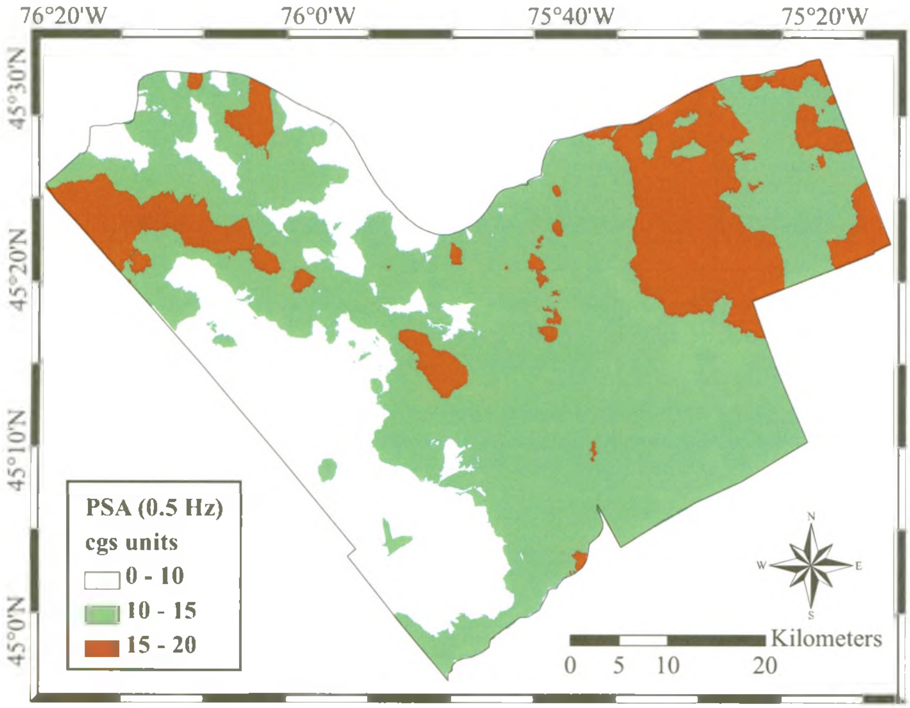

Figure A11.13. PSA at 0.5 Hz for M7.5 scenario using the profile-specific amplification factors, epicenter located ~460 km North-East of Ottawa.

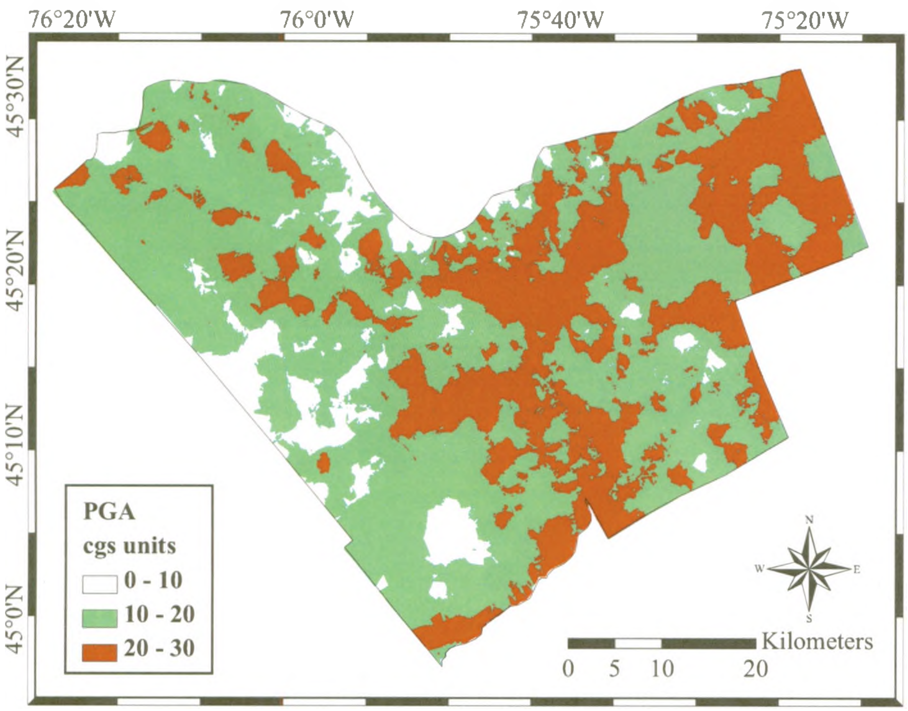

Figure A11.14. PGA for M7.5 scenario using the profile-specific amplification factors, epicenter located ~460 km North-East of Ottawa.

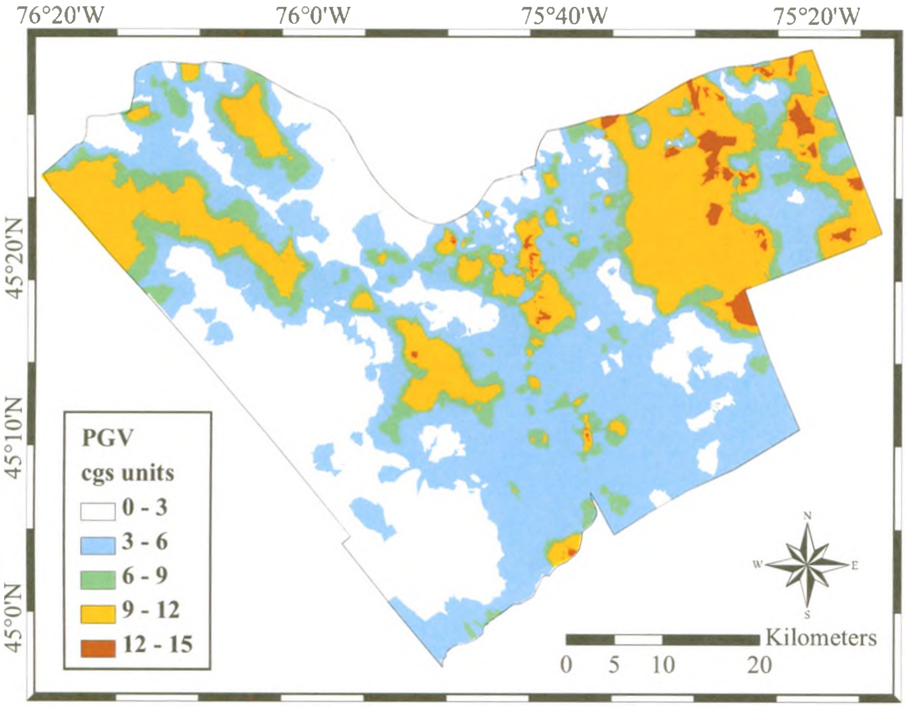

Figure A11.15. PGV for M7.5 scenario using the profile-specific amplification factors, epicenter located ~460 km North-East of Ottawa.

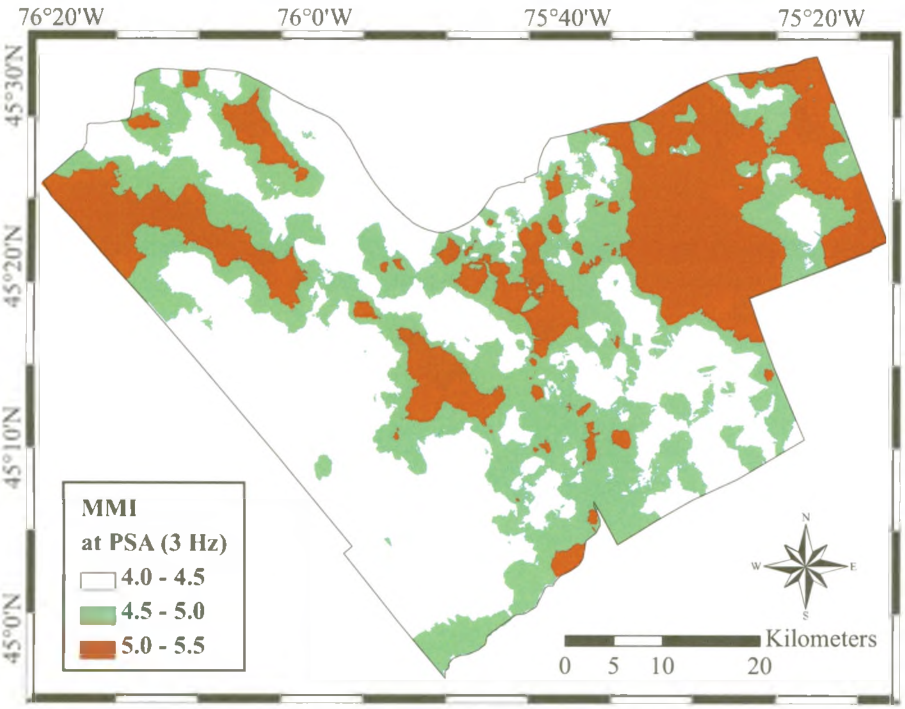

Figure A11.16. MMI based on PSA at 3 Hz for M7.5 scenario using the profile-specific amplification factors, epicenter located ~460 km North-East of Ottawa.

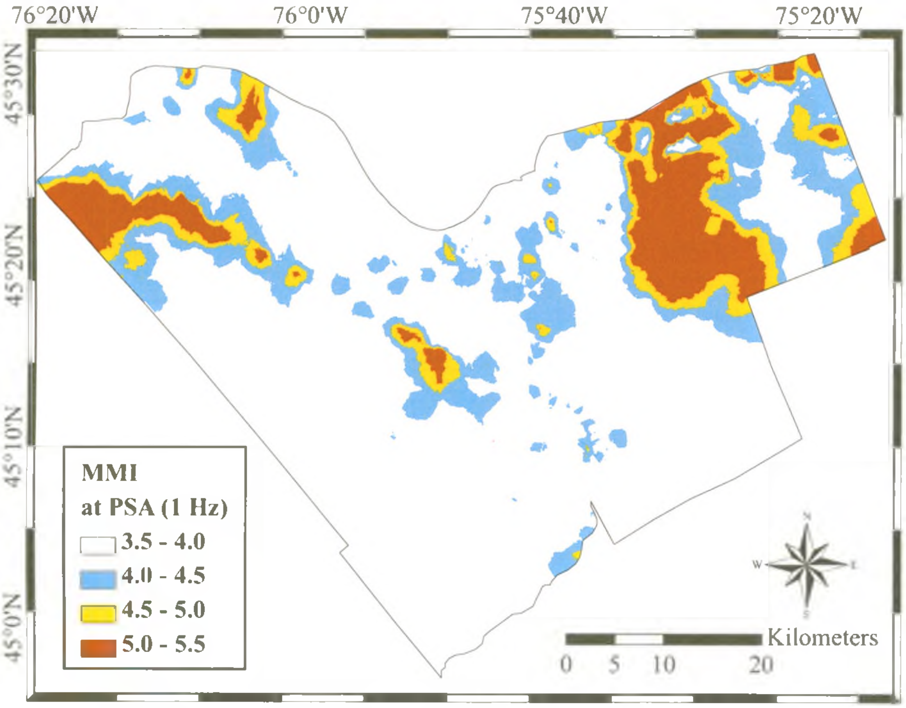

Figure A11.17. MMI based on PSA at 1 Hz for M7.5 scenario using the profile-specific amplification factors, epicenter located ~460 km North-East of Ottawa.

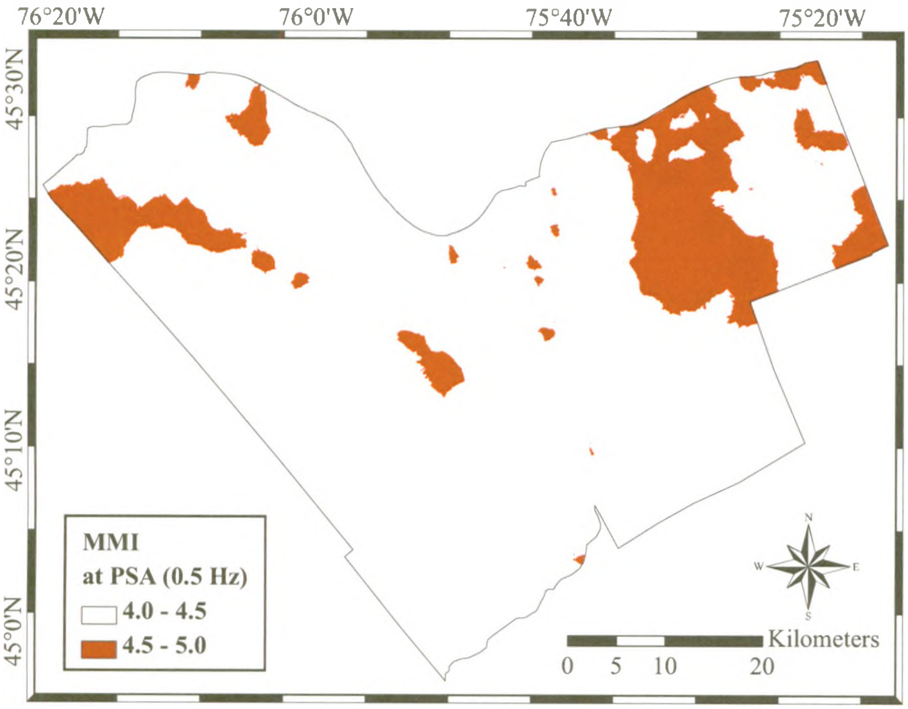

Figure A11.18. MMI based on PSA at 0.5 Hz for M7.5 scenario using the profile-specific amplification factors, epicenter located ~460 km North-East of Ottawa.

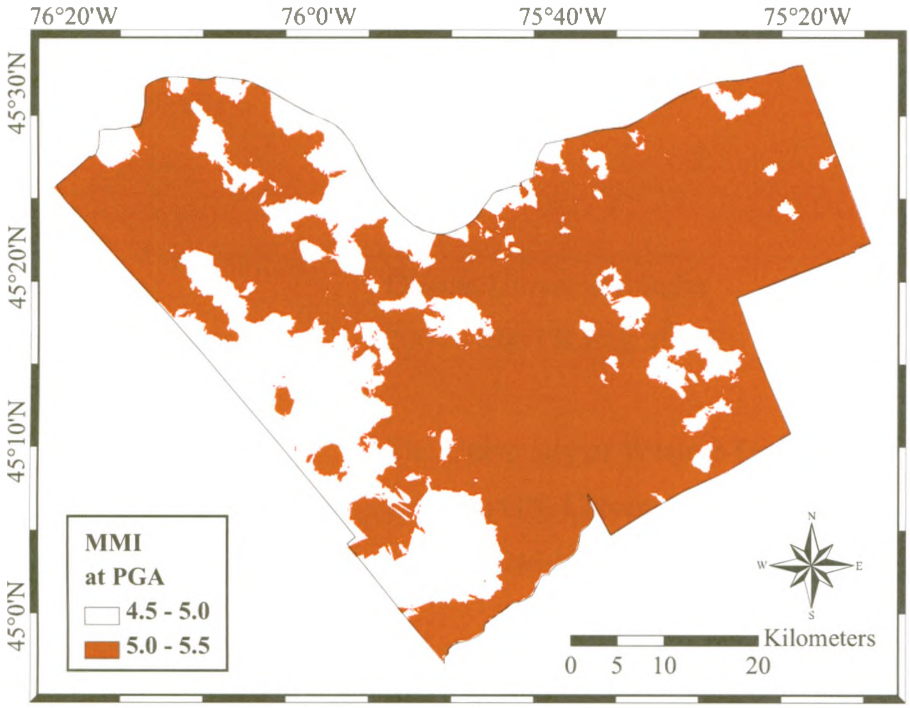

Figure A11.19. MMI based on PGA for M7.5 scenario using the profile-specific amplification factors, epicenter located ~460 km North-East of Ottawa.

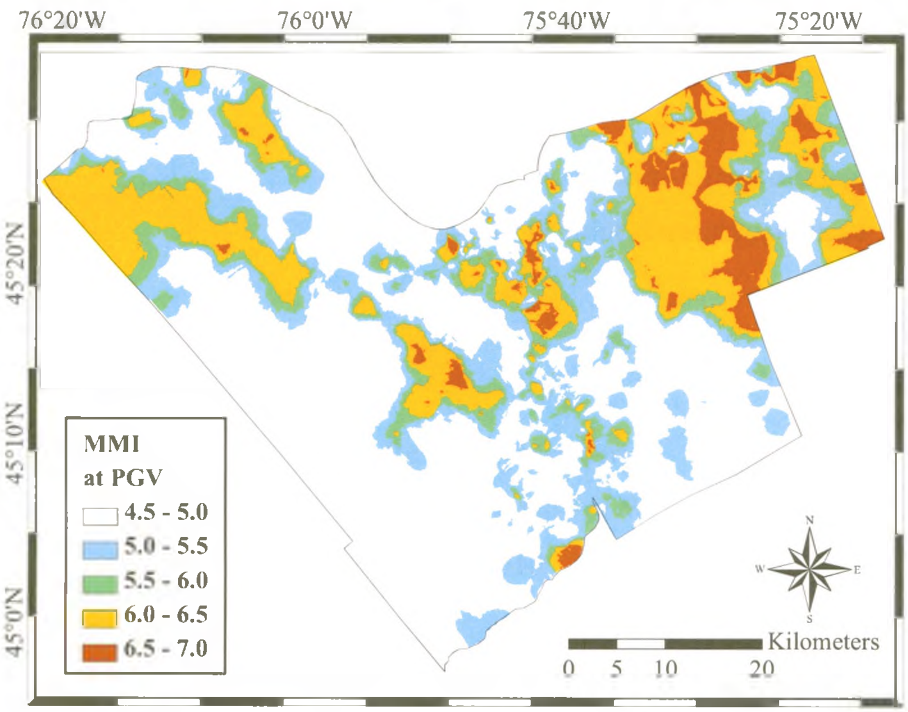

Figure A11.20. MMI based on PGV for M7.5 scenario using the profile-specific amplification factors, epicenter located ~460 km North-East of Ottawa.